Pôle de Morphologie

Unité de Radiobiologie

Microvascular activation by iodine deficiency and X-radiation in non-thyroidal NIS-expressing organs

Jessica Vanderstraeten

Thèse présentée en vue de l'obtention du grade de Docteur en Sciences Biomédicales et Pharmaceutiques

Director : Pr. M.C. Many

Co-directors : Dr. A.C. Gérard et Dr. H. Derradji

2018

We live on an island surrounded by a sea of ignorance. As our island of knowledge grows, so does the shore of our ignorance.

John Archibald Wheeler

Jury Composition

Thesis director:

Pr. Marie-Christine Many
Pôle de Morphologie (MORF), Institut de Recherche Expérimentale et Clinique (IREC),
Université catholique de Louvain (UCL), Bruxelles, Belgique.

Thesis co-directors:

Dr. Anne-Catherine Gérard
Service d'Endocrino-Diabétologie, Centre Hospitalier Régional (CHR), Mons-Hainaut, Belgique.
Institut des sciences de la vie (ISV), Université catholique de Louvain (UCL), Bruxelles, Belgique.

Dr. Hanane Derradji
Unité de Radiobiologie, Centre d'Etude de l'Energie Nucléaire (SCK•CEN), Mol, Belgium.

President of the Jury:

Pr. Etienne Marbaix
Biologie Cellulaire (Cell), Institut de Duve (DDUV), Université catholique de Louvain (UCL), Bruxelles, Belgique.

Jury Members:

Pr. Sarah Baatout
Unité de Radiobiologie, Centre d'Etude de l'Energie Nucléaire (SCK•CEN), Mol, Belgium.

Pr. Ides Colin
Service d'Endocrino-Diabétologie, Centre Hospitalier Régional (CHR), Mons-Hainaut, Belgique.

Pr. Bernard Knoops
Ecole de Biologie (BIOL), Institut des sciences de la vie (ISV), Université catholique de Louvain (UCL), Louvain-la-Neuve, Belgique.

Pr. Olivier Feron
Pole de Pharmacologie et Thérapeutique (FATH), Institut de Recherche Expérimentale et Clinique (IREC), Université catholique de Louvain (UCL), Bruxelles, Belgique.

External Jury Members:

Pr. Marian Ludgate
Division of Infection and Immunity, School of Medicine, Cardiff University, Cardiff, Wales, United Kingdom.

Dr. Xavier De Deken
Institut de Recherche Interdisciplinaire en Biologie Humaine et Moléculaire (IRIBHM), Université Libre de Bruxelles (ULB), Bruxelles, Belgique.

Acknowledgments

Je voudrais remercier ma promotrice, le Pr. Marie-christine Many ainsi que mes co-promotrices, les Dr. Anne-Catherine Gérard et Hanane Derradji, qui ont suivi ma recherche durant 6 ans, et n'ont cessé de s'impliquer dans ce travail afin qu'il aboutisse à la thèse présentée dans ce manuscrit.

Je voudrais également adresser ma reconnaissance aux professeurs Benoît Lengelé, Catherine Behets et Sarah Baatout, pour leur chaleureux accueil au sein de leur unité.

Mes remerciements vont aussi au Pr. Ides Colin, qui, en compagnie du Dr Gérard, a encadré une partie considérable de ce projet. Leurs nombreux conseils et leur enthousiasme ont solidement contribué à l'aboutissement de cette thèse.

Ik zou graag Jasmine Buset hartelijk bedanken voor haar waardevolle bijdrage aan de verwezenlijking van mijn werk bij de SCK-CEN. Pareillement, j'adresse mes remerciements à Christine de Ville de Goyet pour son aide précieuse au sein de notre laboratoire de Morphologie, ainsi qu'aux étudiants L. Nae, G. da Silva, A. Tessalli et N. Ben Said.

Je remercie aussi les membres du jury et du comité d'accompagnement, les professeurs E. Marbaix, B. Knoops, S. Baatout, O. Feron, X. de Deken et M. Ludgate, pour le suivi de ce travail et pour l'intérêt qu'ils y ont porté, ainsi que pour leurs conseils concernant la finalisation du présent manuscrit. Merci également à Michelle Parisi pour son aide pour la mise en page de ce manuscrit.

Tout au long de ces 6 années de thèse, j'ai eu le plaisir d'encadrer les travaux pratiques en biologie générale et moléculaire et en histologie au sein d'une merveilleuse équipe d'assistants dynamiques, et je désirerais remercier ces assistants avec qui j'ai travaillé pour la convivialité qui a régné lors de nos tâches d'enseignement. Je remercie également le Pr. Many pour son chaleureux encadrement pour la réalisation mes fonctions didactiques.

Enfin, je tiens à remercier ma famille pour son support, et tout particulièrement mon mari, Xavier, qui a toujours été présent pour me soutenir et m'encourager, aussi bien lors des découvertes scientifiques enthousiasmantes que lors des épreuves plus pénibles de cette thèse. Merci d'avoir cru en moi du début jusqu'à la fin de ce projet.

Summary

Iodine is an essential element required for diverse physiological functions, including thyroid hormone production. Beside thyroid, other organs take up iodide via the sodium/iodide symporter (NIS), such as stomach and salivary and mammary glands. In addition to its secretion into milk, iodide has been suggested to offer an antioxidant protection in the three mentioned tissues, along with a recycling role via salivary glands and stomach secretion of iodide into their respective fluids to avoid kidney clearance. Several studies have linked iodine deficiency (ID), which is still a global problem, to functional alterations and pathologies of those organs. In thyroid, ID is known to activate a TSH-independent microvascular response. We have thus hypothesized that those organs could also activate a vascular response when facing ID. In this work, we show that acute ID increases vascular endothelial factor (VEGF) expression in salivary glands, stomach, and lactating and virgin mammary glands, transiently leading to increased blood perfusion in salivary and mammary glands. This VEGF up-regulation was shown to depend on non-mitochondrial ROS and the mechanistic target of rapamycin (mTOR) in two breast cell lines: MCF7 and MCF12A. Because X-rays are able to activate angiogenic processes, we hypothesized that they could further increase ID-induced response. The combined exposure to ID and to 3 Gy of X-rays indeed led to additive effects on ROS production and *VEGF* mRNA expression, but in MCF12A cells only. Our results suggest that ROS induced by radiations with or without iodide come at least partly from mitochondria in this cell line. In conclusion, ID induces a transient microvascular response in all three organs studied as it does in thyroid. This microvascular response might be a common reaction of NIS-expressing organs to try to improve iodide supply, but, in the case of stomach and salivary glands, might also be a mechanism to increase iodide recycling and spare it for the thyroid. The increase in VEGF expression, along with mTOR activation and ROS formation in breast, could also provide new insight in the research on the link between ID and NIS-expressing organs pathologies. Furthermore, as radiations increase ID-induced oxidative stress and VEGF mRNA up-regulation in one of the two breast cell lines studied, iodide intake should not be overlooked in radiation prevention policies.

List of Abbreviations

4E-BP1	Translation initiation factor 4E-binding protein
AMPK	AMP activated protein kinase
AKT/PKB	Protein kinase B
bFGF	basic fibroblast growth factor
cAMP	cyclic adenosine monophosphate
cDNA	complementary deoxyribonucleic acid
CFTR	Cystic fibrosis transmembrane conductance regulator
ClC5	Chloride channel- 5
ClO_4^-	Perchlorate
CEP	w-carboxyethylpyrrole
CT-scan	Computed tomography scan
CYP1	Cytochrome P450 family 1
DEPTOR	DEP-domain containing mTOR-interacting protein
DNA	Deoxyribonucleic acid
DNA-PK	DNA-dependent protein kinase
DPI	Diphenyleneiodonium
DSB	Double strand break
DUOX	Dual oxidase
EC	Endothelial cell
Egr-1	Early growth response protein-1
eIF-4E	eukaryotic translation factor 4E
ER	Endoplasmic reticulum
Erk	Extracellular signal-regulated kinases
FIH	Factor inhibiting HIF-1
FRB	FKBP12-rapamycin binding domain
GSH	Glutathione
Gy	Gray
H_2O_2	Hydrogen peroxide
HIF	Hypoxia-inducible factor
HR	Homologous recombination
HRE	Hypoxia response element
Hsp	Heat shock protein
I^-	Iodide
I_2	Iodine
ID	Iodine deficiency
IGF	Insulin-like growth factor

IR	Ionizing radiation
KCNQ1	Potassium voltage-gated channel subfamily KQT member 1
KCNE2	Potassium voltage-gated channel subfamily E member 2
KO	Knockout
LCFA	Long chain fatty acid
LET	Linear energy transfer
MAPK	Mitogen-activated protein kinases
MCT8	Monocarboxylate transporter 8
MEK	Mitogen-activated protein kinase kinase
MNK	MAPK-interacting kinase
mRNA	messenger Ribonucleic acid
mTOR	mechanistic target of rapamycin (former “mammalian target of rapamycin”)
mTORC	mTOR complex
Na+/K+ATPase	Sodium/potassium ATPase
NAC	N-acetylcysteine
NADPH	Nicotinamide adenine dinucleotide phosphate
NHEJ	Non-homologous end-joining
NIS	Sodium-iodide symporter
NO	Nitric oxide
NO3-	Nitrate
NOS	Nitric oxide synthase
NOX	NADPH oxidase
NTF-1	NIS TSH-responsive factor 1
NUE	NIS upstream enhancer
O_2	Oxygen
$O_2^{\circ-}$	Superoxide anion
ODD	Oxygen-dependent degradation domain
OH°	Hydroxyl radical
$ONOO^-$	Peroxynitrite
OS	Oxidative stress
P70S6K	P70 ribosomal S6 Kinase
PDK1	Phosphoinositol-dependent protein kinase 1
PHD	Prolyl 4-hydroxylase domain
PI3K	Phosphoinositide 3-kinase
PKA	Protein kinase A
PKB	Protein kinase B also AKT
PKC	Protein kinase C
PRE	Progesterone response element
Protor	Protein observed with Rictor

PTEN	Phosphatase and tensin homologue
pVHL	Hippel-Lindau tumor suppressor protein
R°	Free radical
Rac1	Ras-related C3 botulinum toxin substrate 1
Raptor	Regulatory-associated protein of mTOR
RAS	Renin-angiotensin system
RBE	Relative biological effectiveness
RHEB	Ras homolog enriched in brain
Rictor	Rapamycin-insensitive companion of mTOR
RNA	Ribonucleic acid
RNS	Reactive nitrogen species
ROS	Reactive oxygen species
RTK	Receptor tyrosine kinase
RyRs	Ryanodine receptors
SCN-	Thiocyanate
SLC26	Solute carrier family 26
SOD	Superoxide dismutase
SP1/3	Specific protein 1/3
Src	Proto-oncogene tyrosine-protein kinase
SSB	Single strand break
STAT3	Signal transducer and activator of transcription 3
T3	triiodothyronine
T4	thyroxine
TH	Thyroid hormone
TPO	Thyroperoxidase
TR	TH receptor
TRβ1	TH receptor b1
TRH	Thyrotropin-releasing hormone
TSH	Thyroid stimulating hormone
TTF1	Thyroid transcription factor 1
UIC	Urinary iodide concentration
UPR	Unfolded protein response
UV	Ultraviolet
VEGF	Vascular endothelial growth factor
VEGFR	Vascular endothelial growth factor receptor
WHO	World health organization

Table of content

Introduction

1.1 Iodine

Iodine is a ubiquitous trace element. It was discovered by accident by the chemist Bernard Courtois, who used to extract sodium carbonate from seaweed by boiling it. Courtois once added too much sulfuric acid to destroy the leftover debris, and observed purple vapors which then condensed into purple crystals. Courtois then gave the crystals to a few known chemists, among which Gay-Lussac, who further analyzed the crystals and named the new element "iode", from the Greek word for violet: iodes. Iodine is the least abundant of stable halogens and forms species such as iodide (I^-) or I_2, to reach a stable octet. The anion iodide is easily oxidized and is thus a strong reducing agent compared to other halogens such as chlorine or brome, which is partly due to a higher number of electrons, implying that the outer electrons are located farther from the nucleus and are more shielded from its attractive force. Its reducing potential was demonstrated by Winkler and colleagues among others (451; 452). They induced free radicals formation by UV exposure in an aqueous system and measured free radical-induced hyaluronic acid depolymerization, which was inhibited in presence of iodide. I^- can thus act as an electron donor and neutralize free radicals: $R° + I^- \rightarrow R: + I$

It can serve as an intermediate specie in the detoxification of several common free radicals such as hydroxyl radical: $2\ OH° + 2\ I^- \rightarrow 2\ OH^- + I_2$ (418; 451). Iodine is usually not found in nature as a crystal but rather as salts, such as sodium iodide (NaI) or potassium iodide (KI), or as molecular iodine (I_2) or diverse iodate minerals (78; 229).

Iodine was originally dispersed throughout earth during rock formation, but was later leached out of soil and rocks towards oceans as a consequence of phenomena such as erosion or glaciers movement. Iodine can enter the atmosphere through water evaporation and then slowly be redistributed by rains. This cycle leads to differences in iodine concentration in soils according to the distance to sea and ocean or to the intensity of erosion, with regions such as mountains or ancient glaciers being more iodine deficient. Iodine concentration in soil can thus vary from 0.09 to 80 mg/kg (178; 229; 392).

1.1.1 Iodine in evolution

Three billions years ago, blue-green algae prokaryotes developed a new mechanism, the photosynthesis, which led to the production of oxygen (433).

Oxidative stress associated to this potent oxidant accumulation imposed a selective pressure on early life, which needed to develop protective antioxidant systems; and iodide was suggested to be one of the most ancient of those systems (212; 434). It was indeed shown that photosynthetic prokaryotic algae had developed a primitive iodide pump that allow them to concentrate it up to 20 000 times the level found in ocean and that they express a peroxidase system enabling them to synthesize iodo-compounds (32; 66; 213). It was suggested by several authors that the formation of iodo-compounds by marine algae was a consequence of photosynthesis and cellular respiration to reduce the amount of ROS produced during those processes (212; 213; 309).

Venturi and Venturi (434) therefore proposed the following antioxidant mechanism:

$2\ I^- + \text{peroxidase} + H_2O_2 + \text{tyrosine/histidine/lipids/carbons} \rightarrow \text{iodo-compounds} + H_2O + 2e^-$

500-600 million years ago, cells from primitive gut in Vertebrates migrated to form a new structure comparable to the endostyle of lampreys, which is specialized in iodine and iodo-compounds concentration and storage. After invasion of freshwater by early Vertebrates, this new structure evolved then in thyroid, an efficient reservoir to store iodine in the new environment where its concentration is considerably inferior to that of seas and oceans. The role of thyroid hormones (TH) evolved and they became active agents in the metamorphosis and thermogenesis of Vertebrates 300 to 400 million years ago, when amphibians and reptiles colonized the lands, helping their evolution and adaptation to land (322; 364; 467). In the course of evolution, TH acquired crucial functions in Vertebrates. They are essential in the growth and development of embryos and young offspring, especially for central nervous system and skeleton. They regulate basal metabolic rate throughout the life, acting on protein, glucose and lipid metabolism, heart rate... (322). TH consist of triiodothyronine (T3) and thyroxine (T4); they enter the cells through transporters where they exert their effects primarily through genomic but also non-genomic actions. As T3 is the main effector, T4 is deiodinated by iodothyronine deiodinase to generate T3. The classical mechanism triggered by TH involves their interaction with TH receptors (TR) to act as a transcription factor that will recognize a specific DNA region: the thyroid hormone response element. The interaction between TH and TRs will displace the interaction between TRs and their co-repressors and facilitate the recruitment of co-activators, eventually leading to chromatin remodeling, histone acetylation and RNA polymerase recruitment in

order to initiate target gene transcription (45; 142; 480). However, other non-genomic mechanisms have been described. TH were for instance shown to mediate signaling cascades through interaction with integrin $\alpha_v\beta_3$ (45; 234), to regulate ion channels/pumps either through direct interaction or indirectly via the activation of pathways such as the mitogen-activated protein kinases (MAPK) pathway (160; 224; 302), or activate central cellular pathways such as the phosphoinositide 3-kinase (PI3K)/ protein kinase B (AKT) pathway or the MAPK/ extracellular signal-regulated kinases (ERK)1/2 pathway via different mechanisms (148; 234; 235; 244; 265). For instance, direct interaction between the PI3K regulatory subunit p85 and the T3/TR complex, or the activation of Src consequently to the binding of T3 on integrin $\alpha_v\beta_3$ binding site activate PI3K/AKT pathway (148; 234; 265), while the interaction between the T4/TRβ1 complex and MAPK or the binding of T3 or T4 on other binding sites of integrin $\alpha_v\beta_3$ activate ERK1/2 (234; 235).

1.1.2 Iodine requirement

In order to ensure optimal TH formation, an adult human thyroid needs at least 60 µg iodide per day (204). It is thus recommended to consume 100 to 299 µg iodide daily to ensure that intake. However, iodine sources can be scarce depending on the environment. Sea algae and animals are a good source of iodine/iodide. Plants, though they are not known to require iodine for physiological purposes, can take it up from soils and accumulate it; therefore, plants form a rich or poor source of iodine for animal life depending on the soil they grow on. Since iodide is secreted in the milk, dairy products can be a source of iodide according to the iodide intake of dairy cows (229; 322).

1.1.2.1 Iodine deficiency

Due to the importance of iodide in thyroid hormone synthesis, ID is associated to several disorders related to thyroid or thyroid hormones. In adults, ID induces goiter and is linked to hypothyroidism prevalence and to thyroid cancer aggressiveness and prevalence (63; 239; 322). ID is also associated to increased pregnancy loss and infant mortality. Moreover, thyroid hormones have a fundamental role in the growth and neurodevelopment in utero and in early life; severe ID is thus a cause of cretinism as well as growth and intellectual impairment (88; 477).

Since the 90', considerable efforts were made worldwide to improve populations' iodide intake and iodine status of the member states of the World Health Organization (WHO) was recurrently assessed since the early 2000'. Iodide intake of the populations was estimated by measuring urinary iodide concentration (UIC) of school aged children because school-based surveys are easy to organize. Iodine intake in population was categorized following the WHO criteria (table 1). (14)

Before the 90', very few countries (Switzerland, some of the Scandinavian countries, Australia, the United States and Canada) were considered iodine sufficient (14). Thanks to implementation of various programs to improve access to iodine, remarkable improvement in iodine status was observed. The total number of iodine deficient countries declined from 54 out of 126 in 2003 to 25 out of 153 countries studied in 2014 (table 1, fig. 1 and 2) (165). It was estimated that around 70% of households had access to iodized salt in 2012 while only less than 10% had this access in 1990. Moreover, no countries were considered severely deficient in iodine for more than 10 years (308).

Iodine intake	WHO median/ range of UIC in SAC (μg/L)	2003	2007	2011	2014
Insufficient iodine intake					
Severe deficieny	<20	1	0	0	0
Moderate deficiency	20-49	13	10	9	7
Mild deficiency	50-99	40	37	23	18
Sufficient[1]	100-299	67	76	105	116
Excessive	≥300	5	7	11	12
Countries with data		126	130	148	153
Total number of countries		**192**	**193**	**193**	**194**

Table 1. WHO criteria to evaluate iodine intake based on median/range of UIC in school-aged children and WHO-evaluated countries from 2003 to 2014 (165).

Fig. 1 Iodine intake estimation worldwide in 2003 (456).

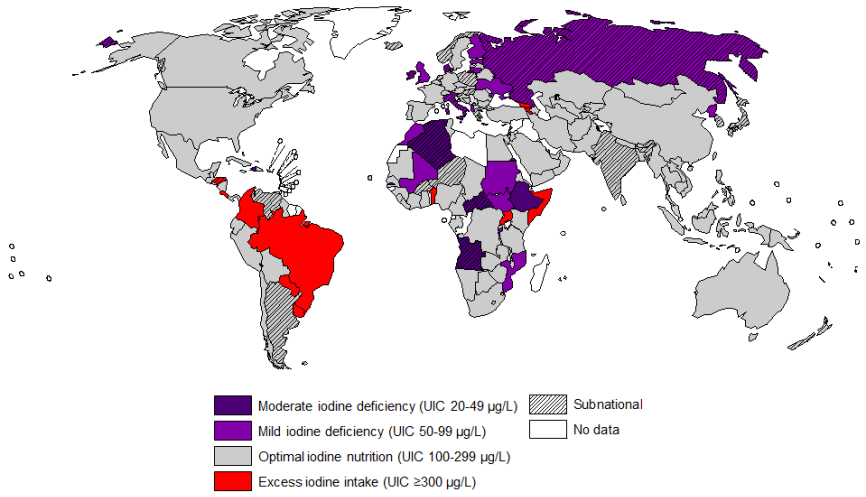

Fig. 2 Iodine intake estimation worldwide in 2014-2015 (457).

However, in countries where iodine intake is essentially coming from the consumption of dairy products such as in the USA or the UK, the intake of the adult population may be overestimated since their consumption of dairy products is lower than that of children (48; 308).

Furthermore, in a country considered iodine sufficient, subpopulations may still be iodine deficient. It was for instance shown that iodine intake was below

recommendation in southern regions of Saudi Arabia although national surveys indicate that the median intake in the country is sufficient (8). Besides, dietary habits may also influence iodine intake and it was suggested that vegans or vegetarians could be more at risk of iodine deficiency (229). Conversely, Jiang et al (2016) showed in Beijing a high prevalence of thyroid nodules, which is known to be associated to ID, but the incidence was lower in subgroups reporting increased frequency of seafood intake (176). UIC was also shown to be influenced by seasons in Switzerland and Belgium (11; 270). Besides, daily variation of iodine intake in iodine sufficient and deficient countries can be very important, potentially leading to important drop of iodine plasma concentration according to the ingested meal. Moreover, since iodine requirements increase during pregnancy and lactation, there is an important proportion of pregnant/lactating women considered iodine-deficient, even in iodine-sufficient countries (48; 308).

1.1.2.2 ID in Belgium

Various surveys during the last half-century showed that the Belgian population is mildly iodine deficient. A program aiming at progressive supplementation was thus elaborated in 2005. The strategy was to use iodized salt in bread because bread was demonstrated to be one of the main contributors to salt intake in the Belgian population (164). An agreement was signed on voluntary basis in 2009 between the bakeries and the Ministry of Health (272) and the percentage of bakers using iodized salt increased from 11% in 2001 to 41% in 2010 (269). The different surveys conducted during the last 17 years showed that UIC in school-aged children increased from ~80µg/L (2000 to 2011) to ~113µg/L in 2012 (14; 164; 165; 308) and the status of the country switched from iodine deficient to iodine sufficient. However, a cross-sectional study compared UIC of children and their mother and showed that, though children presented a sufficient UIC (median: 113µg/L), their mother had an insufficient median UIC (84µg/L) (428). The incidence of school-aged children with an insufficient UIC (< 100 µg/L) was only 39 % but reached 64 % among the mothers. They concluded UIC should also be monitored in women of child-bearing age. Besides, the same author conducted a survey among pregnant women in their first and third trimester. Though 60.8% of those women declared an intake of iodine-containing supplements, the median UIC of women in their first trimester was 118,3 µg/l and UIC of women in the third trimester was 131.0 µg/l, below the 150µg/L recommendation for pregnant women (427). Likewise, Moreno-Reyes et

al (2013) observed a high prevalence of hypothyroidism and abnormal values of TSH concentration among pregnant women (271).

1.1.3 Iodide transporters

Due to the importance of iodide in thyroid function, iodide transport was best characterized in this organ.

1.1.3.1 Basolateral transport

In thyroid, iodide enters the cells via the sodium/iodide symporter (NIS) expressed at the basolateral membrane, and it is concentrated to 20 to 40 times inside the cells *in vivo* and up to 60 times *in vitro* (183; 334). Iodide transport into the thyroid was observed in 1896 but the symporter NIS was identified only a century later (83). It was cloned and characterized by Dai, Levy and Carrasco in 1996 (73). NIS is an integral membrane protein of 643 amino acids with 13 transmembrane segments (fig. 3). NIS is conserved between species since the human protein shares high sequence identity with rat, mouse and pig NIS. It belongs to the solute carrier family 5 and, as for most members of this carrier family, its transport capacity relies on a Na^+ chemical gradient. The latter is provided by a sodium/potassium ATPase pump (Na^+/K^+ ATPase) (311; 378). However, though other members of the solute carrier family 5 can use H^+ or Li^+ chemical gradient as driving force, iodide transport by NIS cannot be driven by H^+ and only 10 to 20% transport capacity is observed with a Li^+ gradient. On the other hand, the anion transport is not specific. Anions transported by NIS include $SeCN^-$, SCN^-, $ClO3^-$, $NO3^-$, $ClO4^-$ and to a lesser extent Br^-, $BF4^-$, $IO4^-$ and $BrO3^-$. These anions can thus act as competitive inhibitors of NIS activity (94; 311; 322). Of note, NIS transport is electrogenic since it transports two Na^+ for one I^-. Dohan proposed an ordered simultaneous transport where Na^+ binding to NIS occurs before that of I^-. The stoichiometry is respected for all the cited anions transported by NIS except for $ClO4^-$ for which only one Na^+ is required for the transport. This is quite unusual for transporters to display different stoichiometries with different substrates (84).

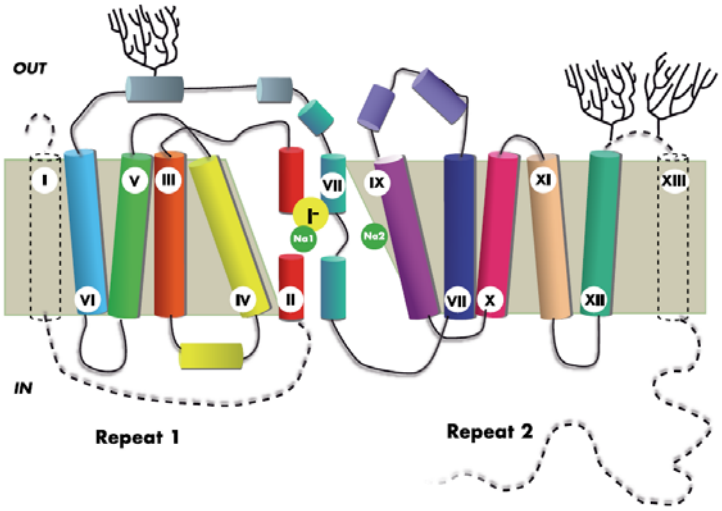

Fig. 3. Representation of NIS protein domains (322).

NIS is a glycosylated and phosphorylated protein. However, the function and stability of the protein seem not to be affected by the replacement of the three Asn sites of glycosylation, by three Gln. The phosphorylations mostly occur at the intracellular C-terminal end. Because the C-terminal end is thought to be important for NIS localization at the basolateral membrane, and because phosphorylation is known to have a role in the cellular localization of other transporters, it was suggested that the targeting of NIS could be dependent on its phosphorylation state. This hypothesis was supported by the fact that phosphorylation profile is not the same in presence or absence of TSH, which is known to regulate NIS expression but also its trafficking (34; 83; 337). However, Vadysirisack et al. (2007) showed that NIS stability and its kinetics were modulated according to its phosphorylated status, but did not find any influence of the latter on its subcellular localization (421).

In thyroid, NIS is mainly regulated by TSH and iodide. TSH regulates its localization and increases its transcription and expression whereas high concentration of iodide is associated with a decreased NIS expression (337). TSH upregulates NIS transcription via cyclic adenosine monophosphate (cAMP). Indeed, a TSH-responsive element is located in the proximal promoter of NIS gene, which is recognized by a putative transcription factor: NIS TSH-responsive factor 1 (NTF-1). This cis-element is required to mediate TSH/cAMP transcriptional regulation (297). The proximal promoter also contains a thyroid transcription factor 1 (TTF1, or NKx2 homeobox 1) binding site. Interestingly, mutation in NTF-1 binding site leads to a loss of TSH response, but also to a decrease in the transcriptional activity induced

by TTF-1, suggesting that TTF-1 response is at least partially controlled by TSH/cAMP (91). NIS promoter also contains a NIS upstream enhancer (NUE) region, which is recognized by the Paired-Domain Transcription Factor Pax8 and which contains cAMP responsive element sequence (CRE), important for full TSH-cAMP-dependent transcription. Though TTF1 also binds to 2 sequences located in the NUE, the NUE-dependent transcriptional stimulation by TSH/cAMP occurs through Pax8 and not TTF1, (9; 298; 405). Regarding NIS subcellular localization, TSH deprivation was shown to inhibit iodide uptake in FRTL-5 cells, a non-cancerous thyroid cell line, while isolated vesicles from those cells retained NIS activity (183). It was then further shown that TSH increases NIS synthesis but also increases its half-life and that NIS was predominantly located at the plasma membrane in presence of TSH and was redistributed in intracellular compartments in TSH-deprived cells (337).

On the other hand, excess iodide decreases NIS expression and activity. It has been long observed that iodide excess inhibits thyroid function. Indeed, iodide excess is associated with a dose-dependent decreased iodide organification and hormone synthesis, a phenomenon called the Wolff-Chaikoff effect (322). However, this effect is transient and thyrocytes can adapt to this excess of iodide by decreasing its uptake to escape the Wolff-Chaikoff effect and restore TH synthesis. Several groups have shown that iodide excess decreases NIS mRNA and/or protein expression in thyrocyte, but the mechanism involved is not yet perfectly elucidated (92; 227; 366; 420). The decrease in NIS mRNA is thought to be regulated at post-transcriptional level, since no NIS promoter change of activity is observed upon exposure to excess of iodide in thyrocytes (227). Moreover, it was demonstrated in rats that acute iodide exposure was associated with a shortened NIS mRNA poly-A tail (366). The authors proposed that this effect was responsible for the decreased NIS mRNA content, as poly-A tail length is associated with mRNA stability regulation and translation, and that it is dependent on iodide intracellular concentration. However, other regulatory mechanisms have been suggested such as increased NIS protein turnover or inhibition of NIS activity at the plasma membrane by iodide through a redox effect (92; 227).

Other factors may also contribute to NIS regulation, such as the ion channel KCNQ1/KCNE2 (potassium voltage-gated channel subfamily KQT member 1/ potassium voltage-gated channel subfamily E member 2), insulin, retinoids, cytokines such as TNF-α or TGF-β, or external factors such as lipopolysaccharides of Gram- bacteria (147; 205; 288; 341).

Functional NIS is also expressed in other organs, though its affinity for I^- is lower than in thyroid. Cloning NIS cDNA from stomach, salivary glands and mammary glands revealed identical sequences to that of thyroid. However, NIS expression regulation is not the same in the different organs. It is for instance not influenced by TSH in extrathyroidal tissues. Interestingly, regarding NIS basolateral expression, enterocytes in the intestine are an exception as they take up iodide from the diet through NIS, which is expressed at their apical membrane (287). NIS expression in extrathyroidal tissues will be developed in the following sections (83; 322).

1.1.3.2 Apical transport

Iodide crosses the thyrocyte and is excreted in the colloid through apical transporters. The main candidate for this apical efflux is pendrin, or Slc26a4, an anion antiporter located at the apical membrane of thyrocytes. It is a transmembrane protein of 780 amino acids with 12 trans-membrane domains that belongs to the solute carrier family 26 (SLC26). This antiporter mediates the electroneutral exchange of Cl^- for I^-, SCN^-, $HCOO^-$ or $HCO3^-$. Pendrin is also found in the inner ear, where it could be important for endocochlear potential generation and in the kidney, where it has a role in anion balance regulation (98; 328; 383). It is also expressed in mammary glands, where it probably is involved in iodide secretion into the milk for the progeny (339), in airway epithelium (328) and salivary ducts (370). In thyrocytes, TSH induces an increase in iodide apical efflux (289). TSH was also shown to induce pendrin translocation to the plasma membrane which was accompanied by iodide efflux (312).

Pendrin KO mice do not always develop goiter, and many patients with Pendred syndrome, a syndrome due to a mutation in pendrin gene, are euthyroid. Therefore, it was suggested that iodide apical efflux is also mediated by other apical transporters. Several transporters permeable to iodide and expressed at the apical membrane of thyrocytes are candidates for iodide efflux: the chloride channel cystic fibrosis transmembrane conductance regulator or CFTR, H^+/Cl^- antiporter ClC-5 and anoctamin 1 (166; 230; 322; 365; 424).

1.1.4 Iodine and extrathyroidal tissues

It is estimated that around 30 to 50 mg of iodine is concentrated in human tissues. However, only 20 to 40% of this amount is incorporated in thyroid hormones. While

the rest of it is mainly stored in the colloid, it is also found in extrathyroidal tissues (64).

Beside thyroid, there are several organs that express the Na^+/I^- symporter NIS. NIS mRNA was detected in various tissues such as brain, ovary, placenta, prostate, testis, spleen, kidney, heart, intestine, etc. However, NIS protein expression and its functionality have not yet been established in several of those tissues. Efficient iodide accumulation was reported in salivary glands, gastric mucosa, lactating mammary gland, placenta, airway mucosa, choroid plexus, the ciliary body of the eye, and the small intestine (44; 59; 83; 180; 287; 322; 389). This work focuses on three of those organs: the stomach, the salivary glands and the mammary glands.

1.1.4.1 Stomach

The stomach is divided in 4 anatomical regions: the cardia, the fundus, the body of the stomach and the pylorus. The cardia is the small zone that receives the content of the esophagus and its mucosa mostly contains mucus secreting ramified tubular glands. The fundus is the upper curvature of the stomach and its mucosa is histologically comparable to that of the body of the stomach. The latter is the central main region of the organ. Its mucosa is covered by a surface epithelium made of mucin-secreting cells. The surface epithelium sinks to form a pit in the underneath mucosa, the foveola, leading to the gastric tubular glands. Gastric glands release proteases (chief cells) and hydrochloric acid (parietal cells), responsible for chemical degradation of food. These glands are divided in three parts: the isthmus, with parietal cells, the neck with numerous mucous cells and parietal cells and the base of the gland with chief cells, parietal cells, mucous cells and neuroendocrine cells (fig. 4). Finally, the pylorus is the stomach section that connects it to the intestine and that facilitates the transit of the chyme into the small intestine. Its mucosa mainly contains mucus secreting ramified tubular glands. Endocrine cells are also present in the pylorus; they secrete the “gastrin” hormone (146; 419).

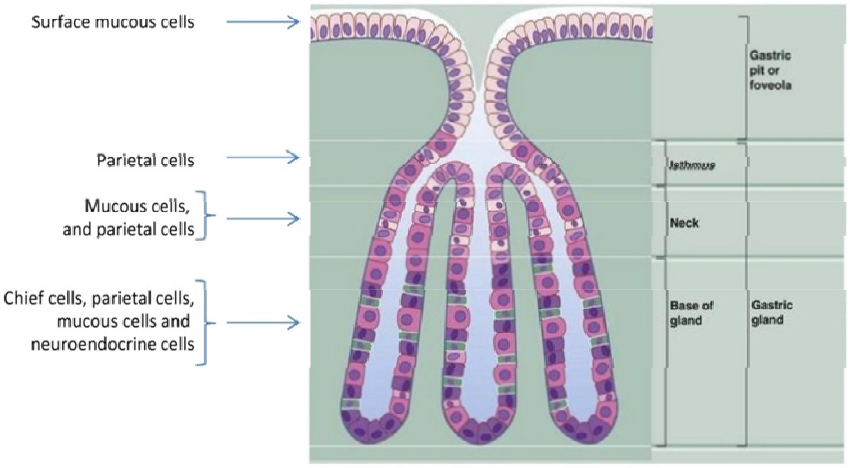

Fig. 4 Schematic representation of the stomach fundus and body histology (146).

Whole body scintigraphy using the isotopes I^{131} or technetium-99m to detect thyroid cancer or metastasis led to the finding that other tissues, among which stomach, were also capable of iodide uptake (263; 399). Since then, constitutive NIS expression was observed in the stomach by several groups and iodide uptake through NIS was confirmed (12; 100; 180; 389). Altorjay et al. detected NIS expression in human gastric tissue, only in the basolateral plasma membrane of mucin-secreting cells of the surface epithelium, but not the mucin-secreting cells of the foveolar (12). Farnedi et al. (2009) detected NIS in the basolateral cytoplasmic portion of foveolar mucous cells in human normal mucosa (100). However, Spitzweg et al. (1999) also detected NIS in parietal and chief cells at the base of gastric glands in human tissues (389). Furthermore, Josefsson et al. (2006) demonstrated, by using an *in vitro* chamber system, a significant transport of iodide from the serosal side of the gastric mucosa to the lumen. This transport was inhibited by perchlorate, a NIS inhibitor, and by an inhibitor of the Na^+/K^+-ATPase, suggesting that this transport is at least partially dependent on NIS. Moreover, the transport was not affected by TSH or TRH, nor by vasoactive intestinal peptide (VIP), histamine, or nitric oxide donor S-nitroso-N-acetyl-D,L-penicillamine (SNAP) (180).

1.1.4.2 Salivary glands

Salivary glands are exocrine glands that consist of 3 pairs of major glands and numerous minor glands. The glands are divided in lobules which contain the secretory units of the glands, the acini. The latter are made of serous or mucous

cells or a mix of both types of cells. In most major and minor glands, each secretory unit drains the saliva in an excreting duct called intercalated duct in one lobule. These ducts will join and finally connect with larger interlobular ducts, called striated ducts, which will drain saliva in a larger excretory duct (fig. 5). Striations in striated ducts are actually basal plasma membrane infoldings. These membrane segments contain many ion pumps to ensure saliva hypotonicity, and the necessary energy is provided by numerous mitochondria located between the membrane foldings.

The three major pairs of glands are:

-The parotid glands: These glands mainly contain serous acini. They secrete amylases containing saliva via the parotid duct, or Stenon duct.

-The submandibular glands: Situated beneath the lower jaws, they contain serous, mucous and mucoserous acini and excrete their secretion through the submandibular duct or Wharton duct.

-The sublingual glands: The prevailing acini found in the sublingual glands are the mucous acini and secrete a predominantly mucous secretion. The ductal system in these glands is different from the other glands, since it usually does not exhibit intercalated nor striated duct and the secretion is drained into the oral cavity through various ducts, the Rivinus ducts; the largest of them is the Bartholin duct.

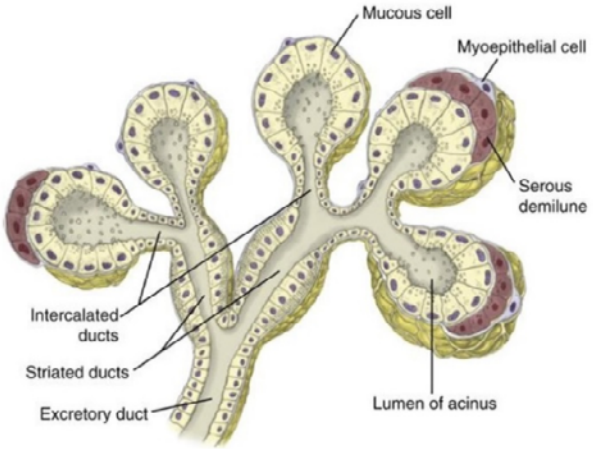

Fig. 5 Salivary acini schematic representation with their different excretory canals (318).

According to the species, varying number of minor salivary glands can be found in the oral cavity mucosa and submucosa. These glands are surrounded by connective tissue but the latter does not form a capsule around the glands like in major salivary glands. Their acini produce mostly mucous secretion, except for Von Ebner's glands, located around the circumvallate papillae on the dorsal surface of the tongue, which produce a serous secretion involved in the beginning of lipid hydrolysis and in the perception of taste (146; 419).

As for stomach, radioiodide uptake is often observed after whole body scintigraphy of differentiated thyroid cancer patients (263; 399). It was also observed that radioiodide therapy for such cancers induces dose-related damages in salivary glands such as swelling, pain or secondary sialoadenitis, which are often worse in parotid than in submandibular glands(247; 249). After NIS identification in thyroid, several groups detected NIS expression in salivary gland ducts but not, or only faintly, in acinar cells (175; 216; 389; 430). NIS is constitutively expressed at the basolateral membrane of duct cells (175; 216) in the majority of striated ducts, but a weaker staining was also observed in fewer intercalated and excretory duct cells, with a higher number of NIS expressing cells in the regions of these ducts nearer to the striated ducts (216). La Perle et al. (2013) observed more-or-less the same NIS expression pattern in parotid and submandibular gland, with the exception that the proportion of striated duct and the proportion of striated duct cells expressing NIS were a bit higher in submandibular glands than parotid and minor glands. Yet, the ^{123}I accumulation ratio between parotid and submandibular glands normalized to the volume was 1.19+/-0.06. They proposed that a highest saliva clearance in submandibular glands might be responsible for a lower iodide accumulation.

Iodide efflux at the apical membrane of salivary ducts is not perfectly clarified. Nevertheless, Shcheynikov et al. (2008) observed Slc26a4 protein expression at the luminal membrane of ducts but not of acinar cells in submandibular and parotid glands. They further studied the activity of the transporter only in parotid and determined that it is able to mediate 1:1 Cl^-/I^-, $HCO3^-/I^-$ and $Cl^-/HCO3^-$ exchange but mainly mediates I^- secretion while $HCO3^-$ secretion is marginal. While CFTR channel was proposed to potentially have a role in iodide efflux in thyroid, its silencing in salivary ducts does not affect iodide apical efflux, which suggests that it is not involved in iodide efflux in salivary glands (370).

1.1.4.3 Mammary glands

Mammary glands are merocrine and microapocrine glands that produce proteins- and lipids-containing secretions. Mammary glands consist of 15 to 25 independent secretory units called lobes. These lobes are tubular acinar glands that are embedded in adipose tissue. Each lobe is made up of lobules, which consist of multiple acini that are surrounded by myoepithelial cells, and separated from each other by semi-dense connective tissue (fig. 6). Of note, the intralobular connective tissue found around the acini in a lobule is less dense and more vascularized than that around the lobule. The ducts of each lobule end in the lactiferous duct of the lobe it belongs to. Each lactiferous duct ends at the surface of the nipple where it drains the secretions of the lobe. During pregnancy, alveolar duct epithelium proliferation, vascular expansion and milk production will be stimulated under the influence of different hormones such as estrogen, progesterone, prolactin... Numerous secretory acini will thus be formed while interlobular and intralobular connective tissue will decrease. At the end of pregnancy, the acini will produce a protein- and lipid-rich secretion called colostrum and after delivery, due to a drop in estrogens and progesterone concentration, milk production is stimulated by prolactin and other hormones (146; 419).

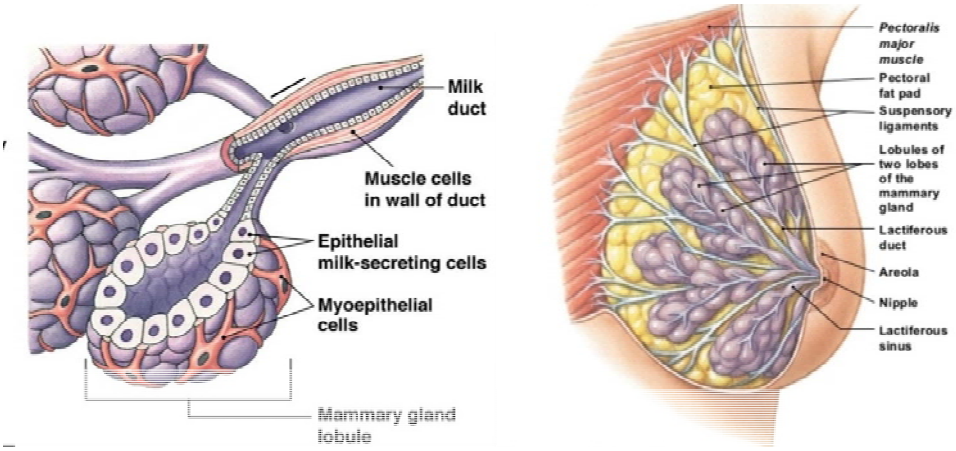

Fig.6 Schematic representation of mammary lobules and their excretory ducts (left) and of mammary architecture (right) (20).

To face the progeny's iodide need, lactating mammary gland must take up iodide and secrete it into the milk. For this purpose, NIS expression, at the basolateral membrane of alveolar and small ductal cells, and its activity are increased at the end of pregnancy and during lactation. A significant increase in iodide uptake that

is dependent on this NIS upregulation is then observed (4; 59; 311; 406). NIS expression and iodide uptake then decrease during involution (406). NIS expression was shown not to be regulated by TSH as in thyroid (83; 322). However, NIS regulation was found to be dependent on three hormones involved in lactation-induced mammary changes: oxytocin, prolactin and estrogens. Oxytocin alone is able to increase NIS expression and iodide uptake (406) and on the contrary, the use of an oxytocin antagonist decreases it in lactating mammary glands in animal models (59). However, contradicting results were obtained with prolactin. While Tazebay (2000) showed no effect of prolactin alone in mice, Rillema and colleagues showed a prolactin-induced increase in I^- accumulation and NIS expression in mice mammary tissue culture (340), and Cho (2000) showed that prolactin increases NIS mRNA expression and that its inhibition decreases milk iodide content in rat. However, prolactin was shown to have antagonist effects on NIS upregulation by oxytocin and prolactin inhibitory effect on estrogen synthesis was hypothesized to be responsible for this observation (59; 406). Indeed, though estrogens alone had only modest or no effects on iodide uptake or NIS expression in different breast models (58; 97), it was shown to be necessary for oxytocin-induced NIS up-regulation in ovariectomized mice (406). Of note, the highest NIS upregulation was observed when ovariectomized mice were treated with the three hormones together. During pregnancy and early lactation, iodide is partly organified in mammary cells and iodocompounds are secreted in milk along with unorganified iodide (322; 369). This organification could explain why after thyroid, lactating mammary gland is the organ that most retains iodide (77).

While NIS-dependent iodide uptake was observed in lactating mammary glands by many groups, it is still debated in resting mammary gland. Aceves et al. (2013) and Cho et al. (2000) both showed in virgin rat mammary glands only a weak iodide uptake of respectively around 2.5 times that of liver and 2.3 that of spleen, liver and spleen being two organs known not to take up iodide. Hammami and Bakheet detected iodide uptake in 6% of the non-lactating human breast tissue samples, and Vayre et al (1999) detected a weak NIS staining by immunohistochemistry in human virgin mammary glands (136; 430). However, Tazebay et al. (2000) did not see iodide uptake nor did they observe NIS expression in virgin rat and in non-lactating human tissues. Interestingly, NIS expression was detected in the majority of breast cancer tissues in animal and human models (33; 195; 406), though part of it was mislocalized leading to only modest I^- uptake (33; 268; 447).

In mammary glands, pendrin expression is highly increased by prolactin during lactation (339), which suggests a role in providing necessary iodide for the progeny, maybe through apical secretion of iodide, similarly to thyroid, from the mammary cell to the milk. However, iodide transport in mammary glands by pendrin is not well understood yet. While pendrin expression was demonstrated, its cellular localization has not been elucidated yet. Moreover, in MCF7 breast cancer cells, pendrin inhibition induced a decrease in iodide uptake, and the authors suggested that NIS might not have an important role in iodide uptake in those cells (338).

Iodide is not the only chemical form absorbed by mammary cells; iodine (I_2) was indeed shown to be taken up in resting cells, in lactating cells and in cancerous cells and its uptake was suggested to relate on facilitated diffusion in cancerous cells (19; 108).

1.1.5 Role of NIS and iodide/ iodine in extrathyroidal tissues homeostasis

Except for iodide supply for the progeny during lactation, the role of iodide and iodine in extrathyroidal tissues is not ascertained yet. As above-mentioned, iodide was suggested by various authors to have an ancestral protective antioxidant role (434). Studies in more evolved species support this notion. For instance, Berking et al. (2005) demonstrated an antioxidant action of iodide in Aurelia Aurita polyps (31). Moreover, it was shown that the total protection against ROS attacks in human serum was increased by the addition of exogenous iodide (452). It was thus suggested by various authors that iodide uptake could increase the cellular antioxidant defenses in NIS-expressing tissues.

In human breast milk, an inverse correlation was observed between iodide concentration and the activity of three antioxidant enzymes: superoxide dismutase, catalase and glutathione peroxidase, leading the authors to suggest that iodide might also be involved in the regulation of oxidative stress in breast milk (130). In breast, it was even put forward that I^- and I_2 were necessary to maintain normal tissue architecture after several animal studies had shown ID-induced atypia in non-lactating mammary glands (95; 432). Moreover, iodine supplementation was shown to reduce ID-induced lobular hyperplasia (96) and cyclic mastalgia (191). Iodine and, to a lesser extent, iodide also reduce fibrocystic diseases symptoms (114) and seaweed consumption, known for their high iodine/iodide content, was shown to delay breast adenocarcinoma in rats (407). Likewise, seaweed consumption reduced the incidence, weight and growth of DMBA-induced

mammary tumors in rats (24; 104). Accordingly, numerous studies showed antineoplastic molecular effects of iodine in breast. Soriano et al. (2011) demonstrated that iodine and iodide induced a caspase-dependent apoptosis through PPARγ in cancer tissue of DMBA-induced cancer in rat, but not in surrounding normal tissues (386). Furthermore, in MCF7 cancer cell line, iodine increases iodine-containing lipids such as 6-iodo-5-hydroxy-eicosatrienoic acid and 6-iodolactone that are able to decrease cell proliferation through caspase-dependent apoptosis (295). The same group further showed that 6-iodolactone can activate peroxisome proliferator response element and increase PPARγ and decrease PPARα. On the other hand, Shrivestarra et al. (2006) observed a caspase-independent apoptosis triggered by I_2 in MCF7 and showed I_2-induced increase in Bax and decrease in Bcl2, and a translocation of apoptotis factor from the mitochondria to the nucleus (374). Furthermore, iodide increases the antiproliferative effect of iodine in MCF7 cancer cells (345). The author suggested that a mitochondrial-mediated apoptosis was responsible for this effect. Further supporting the hypothesis that iodine is involved in cell cycle regulation, Stoddard et al. (2008) showed that lugol solution (a mixture of I_2 and KI in water) regulates various genes involved in cell cycle such as CYP1A1, CYP1B1, AR1C1 (393).

Though the mechanisms of action of iodide and iodine are not thoroughly unraveled yet, these reports support the hypothesis that iodine/iodide is necessary for mammary gland health.

In stomach and salivary glands, beside antioxidant protection, other functions for iodide were also proposed. It was for instance proposed that the secretion of iodide in saliva and in gastric fluid could have antimicrobial function. Moreover, an H_2O_2/peroxidase system was identified and DUOX2 mRNA was detected in salivary glands. A bactericidal mechanism was thus proposed where H_2O_2, produced by DUOX2, could be used by a secreted peroxidase in saliva to oxidize I^- and SCN^-, both NIS substrates, to HOI^- and $OSCN^-$ respectively. I^-/HOI^- and $OSCN^-$ were shown to have complementary antiviral and bactericidal properties in the airways, and could thus play a similar role in saliva (109; 181; 322; 450). Likewise, NIS was suggested to be involved in stomach bactericidal defense because of iodide secretion and because of $NO3^-$ and SCN^- secretion, two other NIS substrates. $NO3^-$ can indeed be transported by NIS and can be reduced to NO_2^- by facultative anaerobic bacteria once secreted in the stomach, where it can be acidified and produce NO, a robust bactericide. The bactericidal effect of acidified NO_2^- against H. pylori can moreover be augmented by SCN^- (12; 90; 101).

Besides, NIS expression in salivary glands and in stomach was hypothesized to have an iodide recycling role (fig. 7). Those two organs were indeed shown to secrete iodide in their respective fluids and are not involved in iodide uptake from the diet. On the contrary, NIS is expressed at the apical membrane of enterocytes in the small intestine and is responsible for iodide absorption (287). A recycling role of iodide was thus proposed for stomach and salivary glands iodide secretion. Iodide secreted by salivary glands and stomach, can thus be reabsorbed by the small intestine. It was therefore suggested that iodide not used by thyrocyte could avoid kidney clearance by reentering the gastroenteric system and being reabsorbed by enterocytes, creating a cycling circulation of iodide to spare it when facing iodide scarcity. This recycling system was first highlighted in cows and was then proposed for other mammals when iodide secretion in the stomach was demonstrated in various species (181; 262; 322).

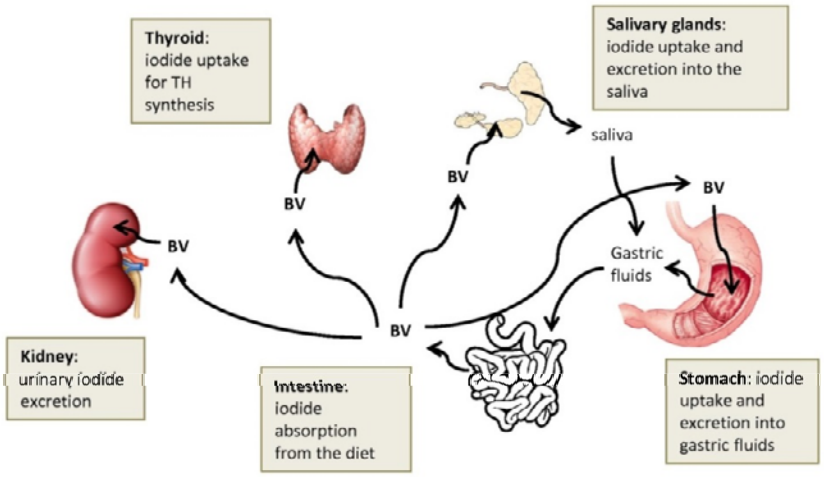

Fig.7 Iodide body fluxes illustrating the gastroenteric iodide recycling hypothesis. BV: blood vessels.

1.1.6 Iodine deficiency in extrathyroidal NIS-expressing organs

In mammary glands, some reports showed an association between ID and breast pathologies such as fibrosis or cancer (78; 95; 307). The prevalence of some breast pathologies is associated with some thyroid conditions which can be influenced by ID such as goiter, hypothyroidism or thyroid cancers (56; 211; 380; 381; 417). However, it remains to be determined whether these associations are due to ID or to impaired thyroid function.

Furthermore, the prevalence of breast cancer in Japan, where iodine intake is very high, is lower than in other parts of the world (78; 307; 316). This observation was not associated to a genetic advantage, as Japanese women lost their protection against breast pathologies when moving to Western countries and adopting their diet (476). The prevalence of breast cancer was particularly increased not in the generation that migrated who did not change much its habits, but in the next generations, to reach the prevalence of the host country (78). Lund and Bonaa (1993) also reported a lower breast cancer mortality among fisherman wives, which further supports the hypothesis that an iodide-rich diet offers a protection against breast cancer (241). Iceland is another example of ID influence on breast cancer which was analyzed and described by Dr. D. M. Derry. Fishing industry is well developed in Iceland and during the first half of the 20th century, the leftovers fish parts were used to feed dairy cows, leading to high iodide concentration in their milk. The iodide intake of the population was then high and their thyroid gland was smaller than thyroid gland in most countries of the world. Interestingly, their breast cancer rate was as low as the Japanese's but rose by 10 times after the fishing industry processes were optimized in the 50's and 60's and that all parts of fish received a destination, dramatically decreasing the amount of iodide given to dairy cows (78). Moreover, the fact that iodine level in breast cancer tissues is lower than that in normal tissues also endorses a hypothetic protective role of iodine in the breast (195).

Though these associations raised debates among scientists, interesting experimental studies have described ID effects in mammary glands. Eskin and colleagues observed mild atrophy, dysplasia and even neoplasia induced by ID in rat breast parenchyma (95). The same group observed similar changes induced by perchlorate (97), a NIS inhibitor. Perchlorate- and ID-induced atypia were not abrogated by the addition of thyroxine, suggesting that the effects were due to the lack of iodide itself, and not to the consequent decrease in thyroid hormones. Likewise, atrophy, but also necrosis, were observed in iodide-deficient rat mammary glands by Strum (396). Other researchers showed that perchlorate induced intralobular fibrosis in 16 week old rat. But the observed changes were different in older rats (52 week old) and included papillomatosis, sclerosing adenosis, dysplastic histology…(209).

Regarding the digestive tract, ID was linked to poorer digestion. This might partly be due to ID-induced low acid production, or achlorhydria, which is associated with acid reflux. More concerning are the epidemiological correlations made between

stomach pathologies and ID. Higher gastric cancer rate were indeed often reported in areas of endemic ID such as in Poland, China and in Anatolia (Turkey) (3; 120; 128). Regarding Poland, a higher incidence of goiter was observed in patients with gastric cancer. Interestingly, the prevalence of both gastric cancer and goiter decreased after the implementation of a national program of iodine supplementation (120). Similar correlations were reported in other countries with ID endemic regions such as in Iran, where a higher prevalence of low urinary iodide level was detected in gastric cancer patients (30) or in Turkey, where a higher prevalence of goiter in gastric cancer patients was reported (184). Moreover, a poorer iodine tissue content and NIS expression were observed in gastric cancer tissue than in surrounding healthy tissue and a protective role of iodide based on its antioxidant properties was thus proposed (12; 128). Other studies also correlated stomach conditions such as atrophic body gastritis (52) or cancer to thyroid dysfunctions (400). However, those studies did not address the causative link of those correlations, whether it is due to ID or to the subsequent TH dysregulation.

Because iodide is taken up in salivary ducts and then excreted in saliva, it was hypothesized that iodine-deficient diets could result in dry mouth, which is in agreement with some epidemiological observations. Moreover, the incidence of dental caries was associated to ID (436). However, the molecular explanation of these correlations is not elucidated yet. Unlike for stomach and breast, no epidemiological studies addressed a possible association between ID and salivary gland cancer to our knowledge. However, it was suggested that iodide could have a protective effect against salivary pathologies due to its antioxidant properties because oxidized DNA and proteins are often found in oral cancers and because NIS expression is decreased in inflammatory tissues and in salivary tumors (23; 216).

1.2 Vascular modifications as a mechanism to cope with ID in thyroid

Thyroid is the organ that most needs iodide for its function. However, it has to cope with highly fluctuating daily iodide intake and sometimes, iodide inadequacy. It is thus not surprising that thyroid has developed diverse mechanisms to cope with insufficient iodide intake. One of the thyroid reactions to ID has been extensively studied: the goiter formation. When thyroid hormones level drops, a negative feedback mechanism induces a rise in TSH hormone which will upregulate/activate

enzymes involved in TH synthesis as TPO and DUOX1-2 respectively, or increase iodide uptake through NIS expression increase, or VEGF secretion by the thyrocytes,… eventually leading to thyroid hypertrophy and vascular expansion (67; 251; 437). However, TSH intervenes late in the process, when TH level drops, which is observed after one week of ID diet in mice (113). There are other mechanisms activated by ID that take place well before TH level decreases and that are TSH-independent. For instance, intracellular iodide recycling, preferential synthesis of T3 over T4 or the regulation of the surrounding microvasculature in order to adapt iodide availability. The latter has been well described in our research group (fig. 8). Upon ID, a transient increase in thyroid blood flow is observed in mice after one day of ID diet, which is accompanied by endothelial cell (EC) proliferation and pericyte activation. The proposed molecular pathway leading to this microvascular activation is the following: ID induces an increased ROS content in thyrocyte which will stabilize the alpha subunit of the transcription factor HIF-1. The latter will enter the nucleus and, together with HIF-1β, will activate VEGF mRNA transcription. VEGF protein will be translated and secreted to act on adjacent blood vessels (112; 113). Though the type of ROS involved in this pathway is not entirely elucidated yet, a role for NO was evidenced. Craps et al. (2015) showed that ryanodine receptors, calcium and NO synthase 3 were involved in ID-mediated VEGF mRNA up-regulation and proposed that ID could activate ryanodine receptors, leading to an intracellular calcium leak, which activates NO synthase 3, increasing NO level. The latter was shown to stabilize HIF-1α (70). Interestingly, the increase in HIF-1α protein level is also dependent on mTOR. Though the exact mechanism of mTOR involvement is not known yet, the transient nature of this tightly controlled microvascular activation in mice and the transient increase in VEGF mRNA in non-cancerous thyroid cell line could be explained by a negative mTOR regulation by AMPK (69).

In a mice model of thyroid cancer, the ID-induced increase in blood flow was not transient (or at least lasted longer). Moreover, VEGF mRNA and HIF-1α protein expression increase were not down-regulated at the studied time points in cancerous cells as in non-cancerous cells. In malignant thyroid cell lines, ROS does not seem to have a role in VEGF mRNA transcription activation and HIF-1 seems to only have a minimal function. It seems thus that ID-induced response is affected in malignant cells, which lose their ability to closely regulate the activated angiogenic pathway (111).

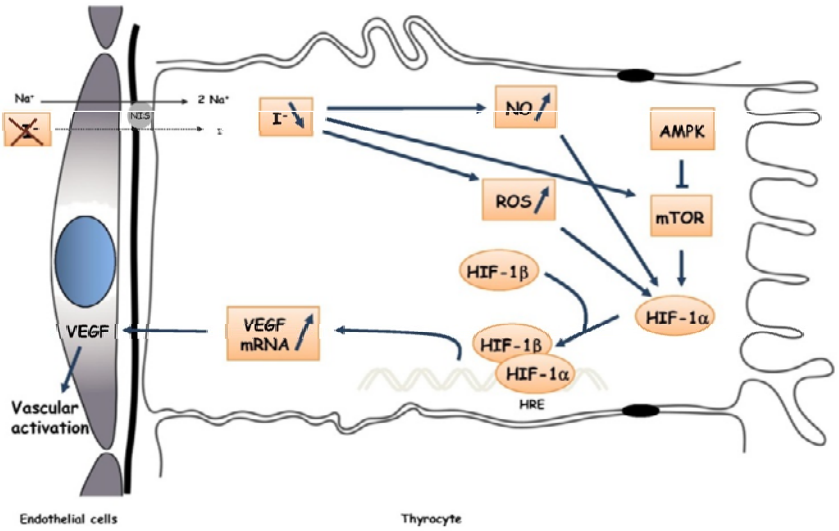

Fig. 8 Molecular mechanisms activated by ID in thyrocytes, leading to VEGF up-regulation and secretion. Adapted from Gérard et al., 2009 (112).

1.2.1 Key players involved in ID-induced macrovascular changes

The vascular compartment is under the tight control of various molecular stimulators and inhibitors which will transduce physiological and pathological signals. Vascular expansion is a normal process in growth and development, wound healing, and other physiological processes, but is also important in the development of several diseases. It may occur through vasodilation, the blood vessel broadening resulting from smooth muscle cell relaxation, angiogenesis, the formation of new blood vessels from preexisting ones, or vasculogenesis, the formation of new blood vessels from ECs that differentiate from mesoderm cell precursors. Some authors also distinguish vasculogenesis from neovascularization, the former being used for prenatal development, while other authors consider them as synonyms (62; 86; 362). One of the main effectors of vascular activation, the Vascular Endothelial Growth Factor (VEGF), is the focus of this work. A myriad of signals are involved in VEGF regulation, but key signaling pathways leading to VEGF up-regulation involve reactive oxygen species (ROS) signaling, the transcription factor hypoxia inducible factor 1 (HIF-1) and the mammalian Target of Rapamycin (mTOR) activation. Those factors will be studied in this work, and their function and regulation will thus be addressed in the following paragraphs, along with that of VEGF.

1.2.1.1 Vascular endothelial growth factor

The human VEGF family comprises 5 members: VEGF-A, B, C, D and placental growth factor. They are growth factors involved in vasculogenesis and angiogenesis in embryological development, proliferation of vascular bed in placenta, lymphangiogenesis, wound healing, cyclic changes within the endometrium, muscle growth, ischemia, tumor growth,... Each of them exhibits different biological function, time and tissue expression and receptor affinity (62).

The principal, dominant member of the VEGF family, VEGF-A, referred as VEGF in this manuscript, is one of the most potent stimuli of angiogenesis and vasculogenesis among the proangiogenic factors identified so far, but is also a vasodilator and permeability factor (62; 200; 359). It is up-regulated in many diseases including cancer, arthritis, cardiovascular diseases, proliferative retinopathy… thereby contributing to their progression. VEGF was therefore the focus of many studies. It is also involved in various physiological processes, as for instance in the induction of neovascularization of female organs linked to reproduction, such as mammary glands.

VEGF is a specific growth and permeability factor for EC. Through its binding to specific receptors, it will activate signaling cascades leading to EC proliferation and migration, increased matrix metalloproteinase activity, blood vessels fenestration, NO release and thereby vasodilation... (200; 443; 445). However, it does not only act on EC; it is hypothesized to have a role in maintaining various cells including lymphocytes, Schwann cells and retinal pigmental cells; it was also observed that VEGF induces autocrine signals in various tumors cell types that express VEGF receptors, potentially leading to cell proliferation and motility (187; 194; 228; 276; 304; 384). High VEGF expression was correlated to tumor malignancy in several tissues, among which breast, and increasing evidence suggest a role of VEGF through paracrine signaling in breast tumor cell motility, invasion, survival and metastasis (6; 86; 169; 282; 325; 350).

1.2.1.1.1 VEGF receptors

VEGF binds to VEGFR1 and VEGFR2, which are tyrosine kinase receptors (RTK), and to neuropilin 1 and 2, two non-enzymatic co-receptors. The binding of VEGF to RTKs induces their dimerization and subsequent tyrosine trans-auto phosphorylation on their intracellular domain. This phosphorylation leads to the recruitment of SH2 or PTB domain containing proteins which will induce a reaction cascade that will

mediate VEGF effects in the target cell (225). VEGF effects are mainly mediated through VEGFR2 binding (260). Indeed, VEGFR2 exhibit a strong kinase activity that induces cascades involving among others PI3K/AKT/NOS/NO, PI3K/S6K, PLCγ/PKC/MEK/ERK, PLCγ/NOS/NO, p38 MAPK signaling (188; 376; 397). Though VEGF affinity is much stronger for VEGFR1 than for VEGFR2, the kinase activity of VEGFR1 is weak and its signaling is still unclear (441). It has an important role in the organization of vascular network during embryonic development, and is thought to be involved in hematopoiesis and migration of monocytes (25; 102; 143). However, due to the strong binding of VEGF, a ligand sequestration function has also been hypothesized. Moreover, VEGF binding to VEGFR1 was shown to negatively modulate VEGFR2 signaling (293; 397).

Neuropilins have a very small cytoplasmic domain with no catalytic activity but that binds other receptors. They were shown to potentiate VEGFR2 signaling (188; 382). Nrp1 is particularly active during embryological vascular development and Nrp2, during lymphatic development (201; 469).

1.2.1.1.2 VEGF isoforms

The VEGF gene comprises 8 exons and 7 introns. Alternative splicing of this gene leads to different VEGF isoforms. So far, 14 different isoforms have been identified, which are differentially regulated according to the stimulus and pathophysiological conditions.

The most abundant isoforms are VEGF165 and VEGF121. VEGF165, the first discovered isoform, is considered to be the main contributor of VEGF angiogenic effects and was thus extensively studied. Other important isoforms include VEGF145, VEGF189, and VEGF206 (304; 454).

Each isoform exhibits different properties. VEGF165 and VEGF121 were for instance described as a strong EC mitogenic agent while VEGF189 is a weak one and VEGF206 has no mitogenic properties (152; 454). Moreover, the exclusion or retention of exons 6 or 7, that contain the heparin-binding domains, will affect the diffusibility of the isoform (57; 152), and thereby, their site of action. VEGF121 for instance does not bind to heparin, which makes it freely diffusible. VEGF165 moderately binds to heparin, which partially impairs its diffusion and cause 50 to 70% of it to be associated to cells and ECM. VEGF189 and VEGF206 however strongly bind to heparin which limits their bioavailability. Their affinity towards receptors is also different. VEGF121 for instance binds to both VEGFR1 and 2 but

has a low affinity for neuropilin 1, which is not sufficient to enhance transduction signals from RTKs, while VEGF165 binds the three receptors (188).

However, certain isoforms have been described to prevent growth of microvessels and it was suggested that the balance between pro-angiogenic (termed as VEGFxxx) and anti-angiogenic (termed as VEGFxxxb) isoforms expression controls angiogenesis in tissues. This sub-family of VEGF isoforms is generated by differential splice-acceptor site selection in the exon 8 (3'UTR) and they differ from the pro-angiogenic forms by their six C' terminal amino acids. VEGFxxxb isoforms are described as competitive inhibitor of VEGFxxx subfamily (26; 455). Binding of VEGF165b to VEGFR2 (455) was shown to induce a phosphorylation on different tyrosine residues that significantly reduces the activation of the downstream cascade and leads to only weak transient ERK phosphorylation (50; 189). Vegf165b does not bind to neuropilin 1 (50; 51; 189).

Proportion of pro-angiogenic and anti-angiogenic forms are tissue-dependent. Certain tissues such as placenta express very low amount of VEGFxxxb isoforms (1 %) while the proportion of VEGFxxxb isoforms in others reach significant amounts, such as 65% in eye vitreous body for instance. However, VEGFxxxb are usually down-regulated in cancer tissues (27; 454; 455).

1.2.1.1.3 VEGF regulation

VEGF expression is regulated at different levels. mRNA transcription is controlled by different transcription factors, mRNA stability through the binding of regulatory proteins at specific 3'UTR sites, and mRNA translation through IRES sequences at the 5'UTR (fig. 9).

1.2.1.1.4 Transcriptional regulation

Regarding mRNA transcription, various transcription factor consensus sites were described in the VEGF promoter. Consensus sites for Sp1/Sp3, AP-2, Egr-1, STAT-3 and HIF-1 were detected in many species, including human.

Signaling molecules that lead to VEGF transcriptional up-regulation are numerous and include EGF, insulin, IGF, HER2, HGF, PDGF. They activate tyrosine kinase receptors and usually transduce the signal through two main pathways: the MEK/Erk and the PI3K/AKT pathways (145; 177; 221; 254; 403; 462; 473). However, other signals can induce VEGF up-regulation, as for instance oxidative stress, which

can activate the Erk pathway and induce VEGF transcription through an increase in Sp1 levels (206; 359). Increased ROS content can also directly act on HIF-1α stability, thereby increasing VEGF transcription (*cfr*. section 1.2.1.4).

A crucial VEGF transcription factor is HIF-1 (103). Its importance is mainly due to its activation by hypoxia, and thereby, its role in hypoxic tumor progression. Hypoxia was shown to stabilize the HIF-1α subunit, subsequently leading to increased VEGF transcription. However, other cytokines including EGF, heregulin, insulin, and IGF1 and 2 were also shown to increase HIF-1α level in non-hypoxic conditions (174; 221; 415). HIF-1 regulation will be described in the section 3.2.

Sp1 is an essential transcription factor for many genes, among which, VEGF (371). Though conflicting data exist, the main regulation of Sp1 genes induction is assumed to be the Sp1/Sp3 ratio, as both compete for the same DNA response element. Interestingly, it was shown that hypoxia could decrease Sp3 level, thereby providing an HIF-1 independent VEGF regulatory mechanism (82). Moreover, pVHL, which is inhibited by hypoxia, was shown to interact with Sp1 and is considered as a permanent inhibitor of Sp1 (275). However, Sp1 can also be phosphorylated in response to the activation of Erk pathway to enhance its activity and it was observed that its phosphorylation was required for full VEGF induction (259).

DNA response elements for STAT-3 and AP-2 are also described in many species. AP-2 has been shown to activate VEGF transcription in various cell types and is thought to be regulated by Sp3, though this regulation seems highly cell specific (115; 348). STAT-3 induction of VEGF transcription occurs in response to diverse growth factors, cytokines, and hormones signaling (291).

In addition to these well-known ubiquitous pathways, some organ-specific pathways can also regulate VEGF transcription. Interestingly, ovarian sex steroids are involved in neovascularization occurring in tissues linked to reproduction and lactation such as uterus, ovaries or breast and are able to up-regulate VEGF during physiological and pathological processes. Estrogens were shown to modulate VEGF transcription via the binding of estrogen receptors α and β to an estrogen response element, but also via the interaction of ERα with Sp1 and Sp3 (46; 394). In uterine endometrial epithelium and breast cancer, 17β-estradiol (E2) was shown to induce VEGF expression *in vivo* and *in vitro* via the recruitment of ERα, but also via interplay between HIF-1 signaling and estrogen signaling (39; 46; 266). Moreover, it was suggested that both estrogen and androgen induce VEGF overexpression via both transcriptional activation and increased mRNA stability (349).

Progestins were also shown to increase VEGF transcription through 3 response elements identified in VEGF promoter (273). Progestins were shown to induce VEGF up-regulation through phosphatidyl inositol 3 (PI3)-kinase and MAP-kinase pathways. However, the inhibition of MAP-kinase did not inhibit VEGF transcription in certain cells, but inhibited protein secretion, suggesting that progestins could also regulate VEGF at a post-transcriptional level (232; 458).

Finally, VEGF is up-regulated by prolactin in mammary glands to prepare the glands for lactation. Prolactin induces VEGF transcription via a Jak2/MAP kinase-dependent activation of the transcription factor Egr-1 (119).

1.2.1.1.5 mRNA stabilization

VEGF can also be induced through the stabilization of its mRNA. This effect is mediated by the stabilizing mRNA binding protein HuR. The presence of AU-rich element (AREs) in the 3'UTR is associated to rapid mRNA degradation. But HuR binding to the mRNA increases mRNA stability (99). It was hypothesized that stabilizing mRNA binding proteins bind to destabilizing sequences which renders them inaccessible to endonucleases. Another hypothesis is that stabilizing mRNA binding proteins change secondary and tertiary mRNA structures and that specific endonuclease sites are not available as a consequence (118).

VEGF mRNA is labile in normoxia. Indeed, VEGF mRNA half-life was estimated to last 30 to 45 min (372) while the average half-life of eukaryotic mRNA is more than 10 h. Hypoxia was shown to increase its stability through HuR binding to VEGF mRNA (99; 118). Thus, hypoxia lengthens its half-life by 2 to 3 times, providing an additional mechanism in VEGF up-regulation (158; 372). (Levy, 1996, 1999)

1.2.1.1.6 Translational regulation

VEGF expression can also be modulated at the translational level. The eukaryotic initiation factor 4E (eIF4E), which binds the mRNA cap located at the 5'UTR and mediate ribosome recruitment, is involved in the translation of VEGF mRNA (Kevil 1996) (459). eIF4E binding is a rate-limiting factor in the events leading to ribosome loading on mRNA and increased VEGF expression was linked to increased eIF4E expression in several tumors (76; 248; 459). However, some mRNA can bypass the eIF4E, and directly recruit ribosomes to the start codon. Most of these mRNA show the presence of internal ribosome-entry sites (IRESs), which allow eIF4E-independent ribosome recruitment. Hypoxia usually increase eIF4E binding to 4E-

BP1, which globally decreases protein synthesis. VEGF mRNA, though, possesses IRES sequences and can undergo IRES-mediated translation under hypoxia (156).

Thus, VEGF translational regulation is likely to be different in normal and transformed cells.

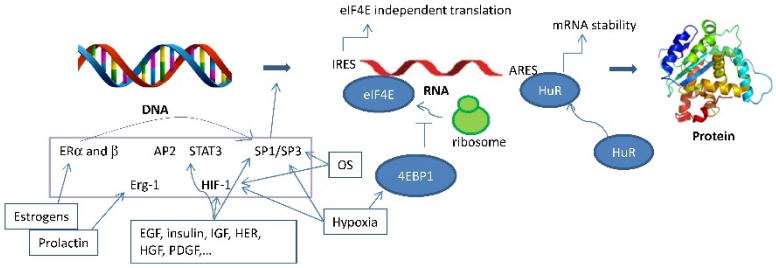

Fig. 9 Schematic representation of some mechanisms involved in VEGF regulation at the transcriptional level via transcription factor activation, and post-transcriptional level via eIF4E independent translation or via HuR-dependent mRNA stability increase.

1.2.1.2 Reactive oxygen species

Reactive oxygen species (ROS) include free radicals and non-radical molecules. Free radicals possess at least one unpaired electron in an orbital that renders them unstable, very reactive and short-lived. Free radicals derived from oxygen mainly include superoxide ($O_2^{\bullet -}$), hydroxyl (OH°), alkoxyl radical (RO°), peroxyl radical (ROO**°**). Frequent non-radicals include hypochlorous acid, (HOCl), ozone (O_3), singlet oxygen ($^1O_2$), hydrogen peroxide (H_2O_2), hypobromous acid (HOBr) and organic peroxide (ROOH). Non-radical ROS are oxidizing agents or precursor of free radicals. Among ROS radicals, peroxyl radicals are the more stable, with a half-life of 17 s, while the others have a half-life of 10^{-6} to 10^{-10} s. Except for ozone and singlet oxygen, non-radical ROS are more stable and have a half-life longer than a minute. Of note, reactive derivatives of oxygen containing nitrogen are classified as reactive nitrogen species (RNS); they include radical molecules such as nitric oxide (NO°) and nitrogen dioxide ($^{\bullet}NO_2$) and non-radicals such as dinitrogen trioxide (N_2O_3), peroxynitrite ($ONOO^-$), N-nitrosamines, S-nitrosothiols, nitrosated fatty acids,... (28; 80; 323).

1.2.1.2.1 ROS sources

ROS are continuously produced in cells, either to fulfill a physiological role, or as byproducts of cell metabolism. They can be produced in organelles where the oxygen consumption is often high, or by different enzymes located in the cytoplasm, at the plasmic membrane, the nuclear membranes, etc. There are also exogenous sources of ROS such as pollution, alcohol, tobacco smoke, heavy metals, high energy radiations, chemicals agents,... (80; 150; 323). The main cellular sources of ROS are schematically represented in fig. 10.

1.2.1.2.1.1 Cellular enzymes

Diverse cellular enzymes have been identified as ROS generating enzymes. They include among other the 7 identified NADPH oxidases, xanthine oxidase, lipoxygenase, monoamine oxidase, cyclooxygenase, cytochrome P450 system... (80).

As one of the main sources of cellular ROS, NADPH oxidases, NOXs, received large attention in the literature. These are transmembrane proteins that transport electrons from an electron donor, NADPH and sometimes NADH, across the membrane it is located to, and use them to reduce oxygen to superoxide. These enzymes are found in cell membrane, mitochondria, peroxisomes and endoplasmic reticulum. Superoxide is then converted to H_2O_2 either spontaneously or by superoxide dismutase catalysis (28; 323). This system was initially discovered as a defense system in cells capable of phagocytosis, such as neutrophils and macrophages (202), but NADPH oxidases were later discovered in a variety of cell types exercising a variety of functions such as posttranslational processing of proteins, cellular signaling, cell differentiation, host defense in airways, thyroid hormone synthesis, transcription regulation,... They comprise 7 homologues: NOX1, NOX2, NOX3, NOX4, NOX5, DUOX1 and DUOX2. NOX2 was the first described isoform, and NOX4 is the most widely distributed one in different tissues (28). A particularity of NOX4 is that the main product detected is H_2O_2 instead of $O_2^{\bullet -}$. It was suggested that $O_2^{\bullet -}$ is an intermediate in the formation of H_2O_2 by NOX4 that can occasionally leak and be detected too (290).

Other enzymes are involved in RNS generation, including the nitric oxide synthases (NOSs). The 3 main NOS isoforms oxidize the amino-acid L-arginine in a two-step reaction that requires NADPH. This reaction leads to the formation of L-citrulline

and NO. In addition, a bacterial form exists and a mitochondrial NOS variant was suggested, though this last form is controversial (80; 217; 409).

1.2.1.2.1.2 Cellular compartments that produce ROS

Mitochondria

Mitochondria is a major contributor to intracellular ROS production in many cell types. The main source of ROS in mitochondria is the respiratory chain, mostly the complexes I and III. A small percentage of electrons prematurely leak from the electron chain transport and combine with oxygen. Hence, less than 4% of oxygen used by mitochondria is converted to $O_2^{\bullet -}$ instead of water. The production of $O_2^{\bullet -}$ is directly proportional to the metabolic rate as the electron transfer to oxygen is not enzymatic. Superoxide radicals are then converted to H_2O_2, which is more stable, by the manganese superoxide dismutase (MnSOD). However, both H_2O_2 and $O_2^{\bullet -}$ were observed to leave the mitochondria and gain the cytoplasm. (40; 150; 277).

Other sources of mitochondrial ROS include monoamine oxidase, α-ketoglutarate dehydrogenase, glycerol phosphate dehydrogenase and the cytochrome P450 system located at the outer membrane (137; 192; 391).

Endoplasmic reticulum (ER)

Production of H_2O_2 is required for disulfide bond formation in endoplasmic reticulum. Disulfide bonds are produced by protein disulfide isomerase, which is regenerated by factors including ER oxidoreductin (EroP1). EroP1 catalyzes protein disulfide isomerase oxidation via H_2O_2 production through oxygen reduction. Excessive H_2O_2 production can be neutralized by peroxiredoxin 4, located in the endoplasmic reticulum. However, H_2O_2 not used can sometimes be released from the ER. Besides, NOX4 and cytochrome P450 also largely contribute to ER ROS formation (150; 471).

Peroxisome

One of the major functions of peroxisomes is the catabolism of long-chain fatty acids through the β-oxidation. The acetyl CoA-oxidases use oxygen for that purpose and produce H_2O_2 in the process. Other enzymes including D-amino acid oxidase,

uric acid oxidase, L-α-hydroxy oxidase and xanthine oxidase, are other oxidases that produce ROS. While H_2O_2 is the main ROS produced in peroxisomes, oxidation reactions also lead to the production of $O_2^{\circ-}$, OH° and NO°. H_2O_2 is used by catalase to oxidize substrates, such as phenols, formic acid, formaldehyde and alcohol (150; 361).

Nucleus

Although nuclear compartments are more reducing through redox couples such as GSH-GSSG that are maintained in their reduced state in order to protect the genome against ROS-induced damages (117), several NOXs were detected in the nucleus of various cell types, where they can contribute to redox signaling. For instance, NOX4 was detected in human umbilical vein endothelial cells, where its ROS production was suggested to regulate gene expression (215). It was also found in leukemia cells nucleus, where it was suggested to influence the disease progression towards acute myeloid leukemia through gene expression regulation (127). NOX2 was detected in human umbilical vein endothelial cells nuclei, and was hypothesized to play a role in some cardio-vascular diseases (377). Nuclei can therefore also be considered as a cellular ROS source.

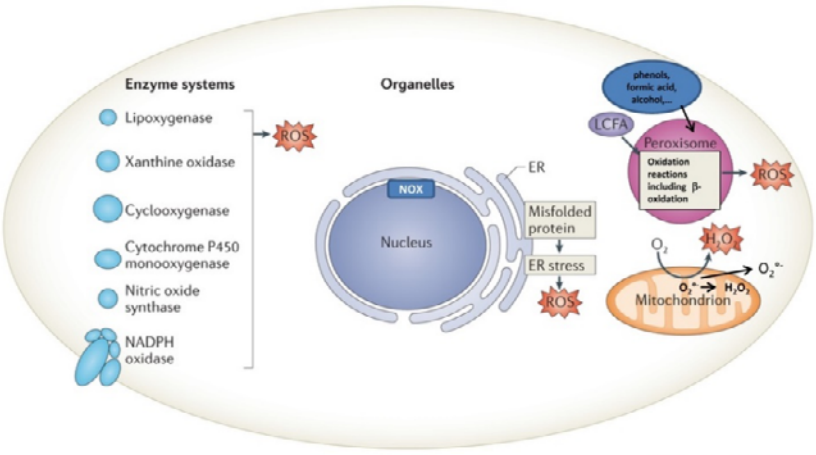

Fig. 10. Schematic representation of the main cellular ROS sources: enzymes systems, mitochondria, ER and peroxisome. Adapted from Holmström and Finkel (2014) (150).

1.2.1.3 Properties of some common endogenous ROS and RNS

$O_2^{\circ-}$ is the most important ROS produced endogenously. Its main source is the mitochondria, but it is also produced enzymatically by xanthine oxidase, lipooxygenase, cyclooxygenase and NOXs (fig. 11 (1)) (28; 208; 214; 277). It is not highly reactive towards biomolecules (333). Through a dismutation reaction, either spontaneously or catalyzed by a superoxide dismutase, $O_2^{\circ-}$ will be converted to H_2O_2 and O_2 (fig. 11 (2)). H_2O_2 is more stable than $O_2^{\circ-}$, and can easily diffuse through membranes. Elimination of H_2O_2 is predominantly achieved through the activity of catalase, glutathione peroxidase and peroxiredoxin enzymes. H_2O_2 cannot oxidize DNA itself, but it leads to OH° formation via the Fenton reaction in presence of transition metal ions (fig. 11 (3)) or via Haber-Weiss reaction where H_2O_2 reacts with $O_2^{\circ-}$ (fig. 11 (4)) (28; 135). By contrast, OH° has a high reactivity with DNA, proteins, lipids, carbohydrates and other molecules and cause severe cellular damage (135).

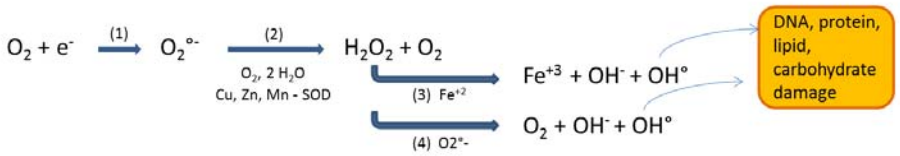

Fig. 3 Chemical reactions involving superoxide anion, hydroxide peroxide and hydroxyl radical.

$^1O_2$ is oxygen in a highly electronically excited state that renders it very reactive and damaging. It is mostly produced by the activation of neutrophils and eosinophils, but is also formed by some reactions involving lipoxygenases, dioxygenases and lactoperoxidase (185; 186; 301; 331).

Ozone is mostly formed in pathways involved in inflammation processes. It can cause lipid peroxidation and chromosomal aberrations through direct or indirect (via secondly generated free radicals) attacks to the DNA (301).

HOCl is predominantly converted from H_2O_2 and chloride by myeloperoxidase in activated neutrophils during inflammation (453).

NO° is produced by NOSs (fig. 12 (5)) and is involved in many biological processes acting as a second messenger that stimulates guanylate cyclase and protein kinases but also through other mechanisms such as redox regulation. It has the particularity to be soluble in water and lipids, and therefore readily diffuses through

cytoplasm and membranes. NO° can react with $O_2^{\circ-}$ and form highly toxic peroxynitrite ($OONO^-$) (fig. 12 (6)). $OONO^-$ can oxidize lipids, methionine and tyrosine residues in proteins and DNA guanines. It can also react with CO_2 to form other RNS which can eventually lead to OH°, NO_2 and NO_3 production (fig. 12 (7)) (72; 157; 168; 409).

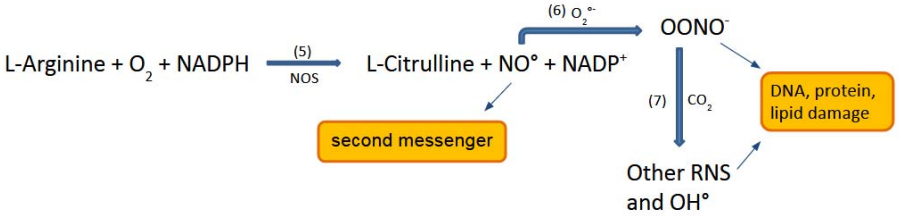

Fig. 4 Chemical reactions involving nitric oxide and peroxynitrite.

1.2.1.3.1 Role and consequences of ROS signaling

1.2.1.3.1.1 ROS cellular signaling in physiological situations

At moderate or low level, ROS contribute to several physiological processes and are thus beneficial. Here are a few examples of ROS physiological functions.

NOX2 has a key function in host defense. However, $O_2^{\circ-}$ is neither very reactive nor very efficient at killing bacteria. It was thus suggested that superoxide could exercise these functions in phagosomes where the pH is low or in the vicinity of cell membranes where the environment is nonpolar, enhancing its reactivity through its conversion into its protonated form, HO_2°. Moreover, H_2O_2 production from superoxide was suggested to intervene in host defense in phagocytes. $O_2^{\circ-}$ also reacts with NO° to form peroxynitrite and other RNS which might be involved in host defense. Likewise, HOCl found in phagosomes could also play a role in those processes. NOX2 could also be involved in host defense by changing pH and ions concentration in phagosomes. (28; 333; 357)

Beside host defense, ROS are also involved in various signaling pathways. For instance, tyrosine phosphatases, which regulate the phosphorylation of proteins involved in cell proliferation, differentiation, motility and metabolism, are inactivated by oxidation (223). ROS are also thought to regulate the activity of various ion channels, such as K^+ channel, plasma membrane Ca^{2+} channel or

ryanodine receptor, thereby influencing a series of reactions that depend on the intracellular concentration of the concerned ion (28). They are involved in oxygen sensing, thereby influencing hypoxia responses, including angiogenesis, through HIF-1α stabilization (*cfr* paragraph 1.2.1.4.1.).

ROS were shown to regulate gene expression through various mechanisms. Several transcription factors such as NFκB, Ap-1, HIF-1α, and p53 display redox-sensitive residues and ROS were shown to influence gene expression through their effects on those transcription factors (250; 358; 431). Moreover, ROS are known to activate mitogen-activated protein (MAP) kinases, subsequently influencing the expression of genes controlled by MAP kinases (442). Lastly, ROS were suggested to influence gene expression acting on mRNA stability (475).

As a consequence, ROS act as mediators of different cellular pathways such as apoptosis or senescence (via DNA damages and p53 for instance), or prosurvival pathways and cellular growth (via the activation of NFκB- or HIF-1-dependent pathways for instance). These apparently contradictory effects are thought to depend on ROS type, subcellular localization, signal duration, and cell type (28).

An interesting example of a physiological role of ROS is the one played in thyrocytes. Thyrocytes are known to produce a high amount of ROS, not only as a result of common physiological processes such as ATP production in mitochondria among others, but also for hormone synthesis. Thyrocytes are thus constantly exposed to ROS, which are detoxified by strong antioxidant systems and during the process of hormone synthesis. However, ROS production is essential to thyroid function since the addition of ROS scavenger leads to a down-regulation of several enzymes involved in thyroid hormones production such as DUOX, TPO, and pendrin (319).

1.2.1.3.1.2 ROS in pathological situations

However, at higher concentration ROS and RNS can induce oxidative and nitrosative stress. They can disrupt molecular pathways and cause damages to biomolecules. ROS and RNS are highly reactive and can attack biomolecules, and transfer unpaired electron in the case of free radicals, sometimes initiating a chain reaction cascade, inducing heavier damages to the cells (21; 257; 323). ROS, particularly OH°, can induce DNA damages at different levels: among other effects, they react with

purine and pyrimidine bases leading to purine and pyrimidine adducts, they damage deoxyribose structure and induce single and double strand breaks (193; 315). According to the DNA region or gene affected, these damages can lead to diverse complications including carcinogenesis. RNA is more susceptible to ROS damages due to its closer localization to ROS production sites, but also due to a lesser protection by proteins, a lack of repair mechanism and to its single stranded nature (149). Lipids, particularly polyunsaturated lipids, are affected by ROS. In membranes, lipid peroxidation can affect their stability and interaction with membrane proteins, thereby losing membrane functions. Moreover, lipid radicals can react with oxygen, producing lipid peroxyl radicals that can in turn affect other molecules such as DNA and proteins (21). Proteins can be oxidized by most radical and non-radical ROS, leading to their denaturation, cross linkage and loss of activity (375; 387).

Such damages to biomolecules were associated with the progression of various pathologies, such as diabetes via mechanisms including an increased redox imbalance due to increased glycolysis; several neurodegenerative diseases where high lipid, DNA and RNA oxidation were observed; cancer, where a high level of intracellular ROS is observed due to tumor suppressor loss or oncogenes activation, and higher metabolic rates linked to higher mitochondrial dysfunction; cardiovascular diseases; cataract; asthma,... (5; 29; 193; 375; 387; 401)

In the thyroid, ROS intervene in various situations. For instance, intracellular ROS are increased during goiter formation. This increase does not appear to harm the cell and is accompanied by an up-regulation of antioxidant defenses (320). It is even necessary for cell proliferation during goiter formation since ROS scavengers hamper this phenomenon (321). Of note, however, when ROS production is pathological such as the ROS increase observed during iodide-induced goiter involution, it is accompanied by an inflammatory reaction (320). The type and origin of ROS in those different situations are thus likely to influence thyrocytes response.

1.2.1.3.2 ROS and angiogenesis

Angiogenesis occurs in physiological situations such as tissue repair, embryogenesis,... and in pathological situation, and ROS are implicated in both physiological and pathological angiogenesis (fig. 13) (62; 206; 257; 362). Angiogenesis is one of the main responses to hypoxia, to face the tissue demands for oxygen and nutrients. It was suggested by various authors that hypoxia leads to

increased mitochondrial ROS involved in HIF-1α stabilization (*cfr* paragraph 1.2.1.4.1). Besides, hypoxia/reoxygenation cycle in turn promotes ROS formation, either through mitochondrial electron transport or through NOXs activation. However, angiogenesis can be triggered by ROS from other origin than hypoxia, as shown by Schaafhausen et al. 2013. They revealed a role of ROS-induced NFκB signaling in melanoma cells in a fish model (358).

Several experiments demonstrated that ROS increase VEGF expression in different cell types and *in vivo* and *in vitro* models support those results by showing that the lack of NOX1 or NOX2, or that of $p22^{phox}$, a protein that stabilizes some NOXs isoforms, prevents VEGF up-regulation and/or impairs VEGF-mediated angiogenesis (206; 231; 413). ROS can act on HIF-1α both directly, preventing its proteasomal degradation, or indirectly, via the activation of AKT/mTOR or MEK/ERK pathway, increasing HIF-1α translation (231; 238; 442).

There is a double role for ROS in angiogenesis, as ROS were shown to be able to regulate VEGF expression, but also because VEGF-downstream effects in EC such as cell migration, permeability and proliferation, are primarily mediated through ROS increase. EC NOX, mitochondrial-derived ROS and NO° were shown to have an important role in transducing VEGF signals (18; 200; 200; 446). Moreover, NOX1, a NOX isoform expressed in EC and various other cell types, increases VEGFR2 expression in EC, offering another mechanism for ROS-mediated angiogenic effects (18). This result was confirmed by various teams using different ROS types. Of note, though VEGF is the major angiogenic factor, ROS can induce angiogenesis through the regulation of other angiogenic factors such as angiopoietin 1 or angiogenin (358).

While many reports showed HIF-1/VEGF pathway induction by various types of ROS, some authors showed VEGF overexpression via mRNA stabilization.

Interestingly, ROS can activate angiogenesis in VEGF-independent ways. Indeed, ROS were shown to produce oxidized lipids with proangiogenic properties. Oxidized polyunsaturated phospholipids can lead to w-carboxyalkylpyrrol (CAP) protein modifications, further leading to w-carboxyethylpyrrole (CEP) protein adducts formation after a series of reactions. CEP was shown to promote angiogenesis and its neutralization decreases tissue healing and tumor angiogenesis. CEP effects were proved to be VEGF/VEGFR2 independent and are currently thought to rely on a Toll-like receptor (TLR)2/ MyD88/Rac1 pathway. Several TLR ligands other than CEP were found to be generated by oxidative stress and play a role in ROS- induced

angiogenesis (351; 448). Of note, TLR pathways were shown to modulate the HIF-1/VEGF pathway in certain conditions, and both pathways can thus be interconnected (388).

Moreover, ataxia-telangiectasia mutated (ATM) kinase facilitates angiogenic responses in pathological situation after activation by increased ROS in immature blood vessels also in a VEGF-independent fashion (300).

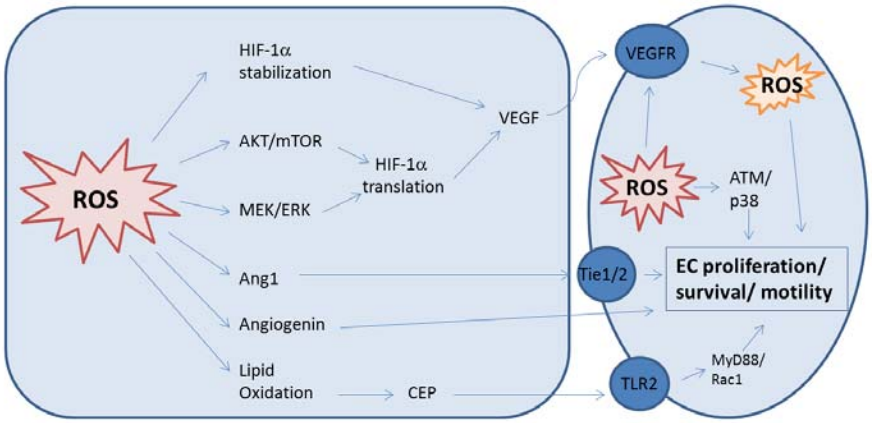

Fig. 5 Schematic representation of some angiogenic pathways in which ROS are involved.

Though angiogenic signal cascades are usually similar in physiological and pathological situations, pathological angiogenesis is often uncontrolled, leading to abnormal vascular morphology. In many pathological conditions, such as atherosclerosis or cancer, the presence of inflammatory cells accounts for an important source of ROS. Moreover, cancer cells were shown to produce ROS in excess compared to respective non-cancerous cells (401). This excess of ROS is caused by an imbalance between ROS production and antioxidative defense. ROS excess was linked to increased angiogenesis, mainly through VEGF signaling, which plays an important role in the progression of the diseases. NADPH oxidases and mitochondria are frequently the main origin of this excess of ROS, causing intracellular HIF-1α content to increase and thereby VEGF overexpression (62; 257).

1.2.1.4 Hypoxia inducible factor 1: HIF-1

HIFs, or hypoxia inducible factors, are heterodimeric transcription factors displaying a basic helix-loop-helix DNA binding domain. As indicated by their name, they can be activated by low oxygen, but other signals can also activate them (329).

HIF-1 was the first of the 3 HIFs to be characterized. It regulates the expression of more than a hundred genes that control processes related to glucose uptake and metabolism, angiogenesis, erythropoiesis, cell proliferation and apoptosis. It is a key regulator of the molecular response to adapt to reduced oxygen supply (190). Regarding the focus of this manuscript, HIF-1 is an important transcription factor controlling VEGF expression (103; 190). Unlike HIF-2 and HIF-3, HIF-1 is ubiquitously expressed. It is made of two subunits, HIF-1α and HIF-1β or ARNT. Both subunits are constitutively expressed but the alpha subunit is continuously degraded by ubiquitin-proteasome pathway, preventing HIF-1 activity (155).

1.2.1.4.1 Oxygen-dependent regulation of HIF-1

HIF-1α possesses an O_2-dependent degradation domain (ODD) that is hydroxylated by prolyl-4-hydroxylase domain-containing proteins (PHD) on proline residues under normoxia (fig. 14 a). ODD hydroxylation allows the von Hippel-Lindau tumor suppressor protein (pVHL) binding and recognition by E3 ubiquitin ligase, consequently leading to HIF-1α degradation by 26S proteasome (155; 170; 246). Under hypoxia, HIF-1α is stabilized. It migrates to the nucleus where it can interact with ARNT and then bind to hypoxia response elements (HREs) in HIF-1 target gene regulatory elements. A second O_2-dependent regulatory mechanism of HIF-1 activity is achieved by the protein factor inhibiting HIF-1 (FIH). This protein hydroxylates aspartate residues in the C-terminal transactivation domain of HIF-1α in normoxia, which will prevent the binding of the transcriptional activators p300/CBP that are necessary for HIF-1 activity (17; 246).

Regarding O_2 sensing, a role was attributed to ROS signaling. Indeed, several groups demonstrated that HIF-1α was primarily stabilized by an increased ROS content (43; 131; 154; 250). It was observed that the addition of H_2O_2 in culture medium induces HIF-1α stabilization in normoxia (250) and that hypoxia-induced stabilization of HIF-1α was essentially dependent on ROS (154). Several groups further demonstrated that hypoxia induced an increase in mitochondrial ROS that is essential for O_2 sensing and HIF-1α stabilization (43; 131; 250). It was further shown that hypoxia

induces an increase in $O_2^{-\circ}$ in the mitochondrial inter-membrane space leading to an increase in H_2O_2 in cytosol that was responsible for HIF-1α stabilization (43; 250). Furthermore, oxidant signal was shown to inhibit PHD activity. However, hypoxia only decreases HIF-1α hydroxylation and degradation while anoxia leads to a complete inhibition of HIF-1α hydroxylation and degradation (131). Moreover, it was shown that anoxia induced HIF-1α stabilization even in absence of mitochondrial ROS (250). It was thus proposed that hypoxia-induced stabilization is mainly triggered through ROS signaling, while anoxia response is mainly due to PHD and FIH inactivity since they require oxygen as substrate (329).

Besides, p53 was shown to bind HIF-1α in normoxia, thereby inducing mdm2 mediated ubiquitination (332).

1.2.1.4.2 Oxygen-independent regulation of HIF-1

Various hormones, cytokines and growth factors can regulate HIF-1 in an oxygen-independent way (fig. 14 b). Factors such as insulin, angiotensin II, EGF, HER2, … were shown to regulate HIF-1α translation and activity via two main pathways: the MAP kinase pathway and PI3K/AKT/mTOR pathway (174; 221; 415). Regarding PI3K/AKT/mTOR pathway, once activated, mTOR induces protein synthesis through either the phosphorylation of the translation initiation factor (eIF-4E) binding protein 4E-BP1, thereby releasing eIF4E and inducing protein translation; or the phosphorylation of the Ribosomal protein S6 kinase (P70S6K), which will phosphorylate the ribosomal protein S6. The MAPK pathway involves the Ras/Raf/MEK/ERK cascade. ERK induces protein synthesis through 4E-BPI, P70S6K and MNK phosphorylation. pMNK then phosphorylates eIF-4E (252). Moreover, MEK1/MAPK signaling facilitates the interaction between CBP/p300, a transcriptional activator, and HIF-1α possibly through HIF-1α phosphorylation by ERK, thereby increasing HIF-1 activity (353). Besides, Hsp90 is known to bind HIF-1α and its inhibition prevents HIF-1 downstream effects, in a pVHL- and oxygen-independent way (167). Moreover, it was shown that PHD activity was regulated by NO, thereby leading to HIF-1α protein increase in normoxia (258). However, NO modulates HIF-1α stability through different mechanisms and can have opposite effects depending on its concentration (200).

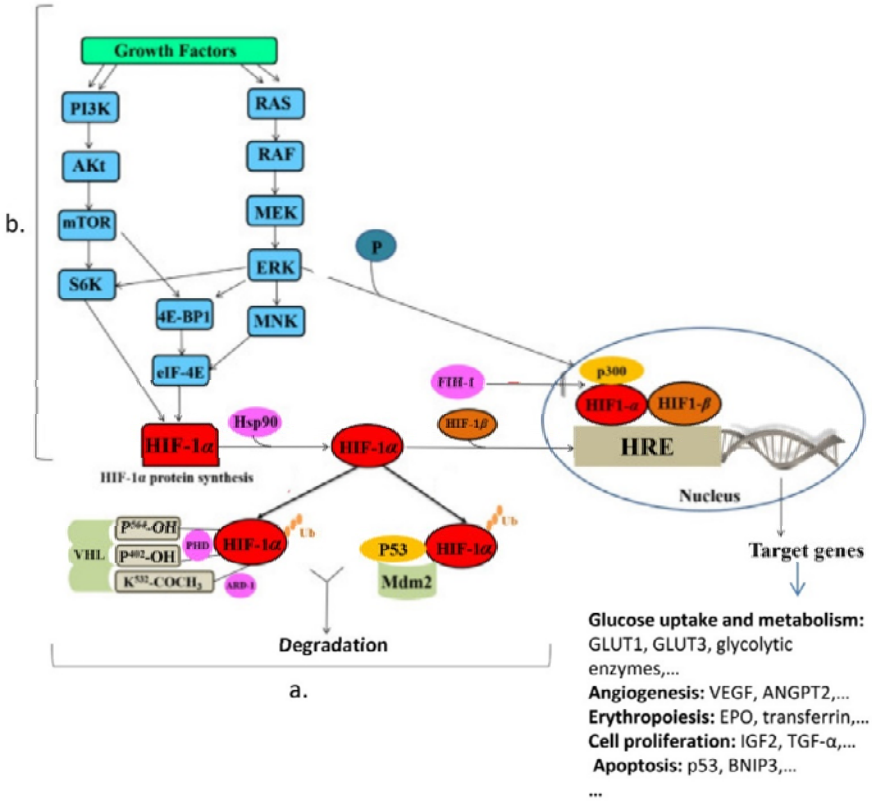

Fig.6 HIF-1 oxygen-dependent (a) and -independent regulation (b) (adapted from Masoud & Li 2015) (252).

1.2.1.5 Mammalian Target of Rapamycin, mTOR

The mammalian or mechanistic target of rapamycin, mTOR, is a key regulator of several cellular processes such as metabolism, growth, proliferation and survival. mTOR is a serine-threonine kinase that associates to different proteins to form two complexes, namely mTOR complex 1 and 2 (mTORC1 and mTORC2).

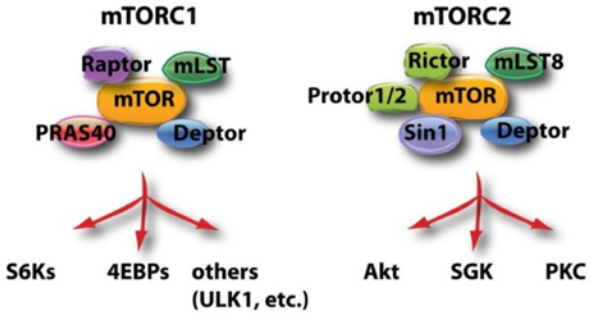

Fig. 7 mTOR complexes 1 and 2 (233).

1.2.1.5.1 mTORC1

This complex consists of 6 protein components (fig. 15 left): the catalytic subunit mTOR, the regulatory-associated protein of mTOR (Raptor), the proline-rich AKT substrate 40 kDA (PRA S40), the mammalian lethal with Sec13 protein 8 (mLST8 or GbL), the Tti1/Tel2 complex and the DEP-domain-containing mTOR-interacting protein (Deptor). Raptor was proposed to regulate the complex assembly and to recruit mTOR target substrates (138). PRA S40 inhibits mTOR substrate binding, thereby negatively regulating the kinase activity of the complex (444). Deptor was also described as negative regulator of mTORC1 (313). However, mLST8 function is not elucidated yet as its deletion does not seem to affect the complex activity (126). The Tti1/Tel2 complex is described as a scaffold that regulates mTORC1 assembly and stability (182).

1.2.1.5.2 mTORC1 regulation

The small Ras-related GTPase Rheb is an mTORC1 activator. Its interaction with mTORC1 is inhibited by the tuberous sclerosis complex (TSC) 1 and 2 heterodimer, which is a GTPase-activating protein (GAP) for Rheb that converts it to its inactive GDP-bound form (408). Interestingly, many of the signals activating mTORC1 are integrated through the modulation of TSC1/2 inhibitory activity. Those signals are mainly growth factors, energy status, cellular stress, oxygen and amino acids. For instance, growth factors involving insulin and Ras signaling pathways will induce TSC2 phosphorylation by protein kinase B (PKB or AKT), ERK, or ribosomal S6 kinase 1 (RSK1), inactivating TSC2 (243; 347). However, AKT can also phosphorylate and thereby dissociate the PRA S40 inhibitor of mTORC1 (444). AKT is inhibited by PTEN

(474). Interestingly, an auto-regulatory pathway was suggested, where activation of mTORC1 diminishes PI3K/AKT pathway in a P70S6K-dependent fashion (141).

AMP-activated protein kinase (AMPK) is a negative regulator of mTORC1 (fig. 16). In response to energy depletion, it can increase TSC2 activity or phosphorylate the inhibitor Raptor to inhibit mTORC1 (132; 161). Hypoxia can activate TSC1/2 complex via both AMPK and transcriptional regulation of DNA damage response 1 (REDD1) activation (79; 220; 237). Though the two described mechanisms are the main response to hypoxia, other mechanisms were also described to reduce mTORC1 activity during hypoxia. Amino acids, particularly leucine and arginine, were shown to activate mTORC1. Interestingly, their presence is necessary for growth factor signaling (286). Among other mechanisms, amino acids were shown to induce the recruitment of mTORC1 to lysosome membranes, where its interaction with Rheb is facilitated (352). Stress signals such as inflammation, Wnt ligand or DNA damage were shown to activate mTORC1 by inactivating TSC1/2 through different mechanisms. The signals regulating mTOR activity can be modulated by different types of ROS, including NO, acting for instance on AKT or AMPK pathways (240; 474).

1.2.1.5.3 mTORC1 downstream effects

mTORC1 was shown to positively control various anabolic processes (fig. 16). It promotes protein synthesis either by phosphorylating 4E-BP1, hindering its inhibitory interaction with the cap-dependent translation promoter eIF4E; or by phosphorylating P70S6K, which will phosphorylate its targets, among which the ribosomal protein S6, leading to increased mRNA synthesis, cap-dependent translation and elongation and the translation of ribosomal proteins (220). Interestingly, the release of eIF4E leads to HIF-1α up-regulation, and thereby, to VEGF transcription. P70S6K activation is another potential positive regulator of HIF-1α (174; 238). PI3K pathway was also shown to increase VEGF in an HIF-1 independent fashion. Of note, the PI3K/AKT pathway is also involved in the regulation of other angiogenic factors such as angiopoietins and NO° and Ras was shown to induce VEGF, PGF and angiopoietin 2, partially depending on AKT signaling. mTOR also promote protein synthesis via the activation of regulatory element tripartite motif-containing protein-24 and its subsequent interaction with RNA polymerase I or via the inhibition of a RNA polymerase III repressor, Maf1 (256; 373).

Along protein synthesis up-regulation, mTORC1 was also shown to induce lipid synthesis that is necessary for membrane formation in proliferating cells. mTORC1 was proposed to mediate this effect through the up-regulation of two transcription factors that control genes involved in lipid synthesis: the sterol regulatory element binding protein 1/2 (SREBP1/2), possibly through lipin-1 regulation, consequently preventing it from repressing SREBP (89; 314); and the peroxisome proliferator-activated receptor-γ (PPARγ) (196).

mTORC1 was also shown to positively regulate mitochondrial metabolism, oxygen consumption, and subsequently, cellular ATP levels (360). Mitochondrial expression of several protein involved in oxidative metabolism were linked to mTORC1 activity (71). mTORC1 up-regulates many glycolytic enzymes through HIF-1α up-regulation, and is thereby involved in the metabolic switch that often occurs in cancers (89).

On the other hand, mTORC1 can also inhibit certain catabolic processes promoting turnover such as autophagy (151). In this regard, it also negatively regulates lysosome formation, as lysosomes are involved in the catabolism of many cellular components (368).

1.2.1.5.4 mTORC2

mTORC2 comprises 7 proteins (fig. 15, right): mTOR, rapamycin-insensitive companion of mTOR (Rictor), mammalian stress-activated protein kinase interacting protein (mSIN1), protein observed with Rictor-1 (Protor-1), mLST8, the Tti1/Tel2 complex and Deptor. As what is observed in mTORC1, Deptor was described as a mTORC2 negative regulator (313). Contrasting to its deletion in mTORC1, mLST8 deletion drastically decreases mTORC2 activity and stability (126). mSIN1 were proposed to stabilize mTORC2/rictor interaction and both mSIN1 and rictor are necessary for mTORC2 phosphorylation activity (171). Likewise, Tti1/Tel2 complex is a scaffold that regulates mTORC2 assembly and stability (182). Protor-1 was described to interact with Rictor and increases mTORC2-mediated activation of one of its targets: glucocorticoid-induced protein kinase 1 (SGK1) (220).

mTORC2 biology is much less understood than that of mTORC1 (fig. 16). Nevertheless, it is known to regulate processes such as cell survival, metabolism, proliferation and cytoskeleton organization. It is insensitive to nutrient status but reacts to various growth factors. Regarding cell survival, metabolism and proliferation, mTORC2 was shown to contribute to AKT activation, a key regulator of these processes. Indeed, to be fully activated, AKT must be phosphorylated at

two different sites, one of which by mTORC2 (356). Consequently, mTORC2 inhibition leads to decreased AKT activity and, thereafter, the activation of the forkhead box protein O 1 and 3 (FoxO1 and 3) transcription factors that control genes involved in metabolism, stress resistance, cell cycle arrest and apoptosis (253). Regarding vascularization, mTORC2-induced activation of AKT can lead to eNOS activation and thereby, to NO production, a potent vasodilator (200). mTORC2 also activates SGK1, which is involved in ion transport and growth regulation (107). Regarding cytoskeleton, mTORC2 is thought to affect actin polymerization and cell morphology through phosphorylation of protein kinase C alpha (354).

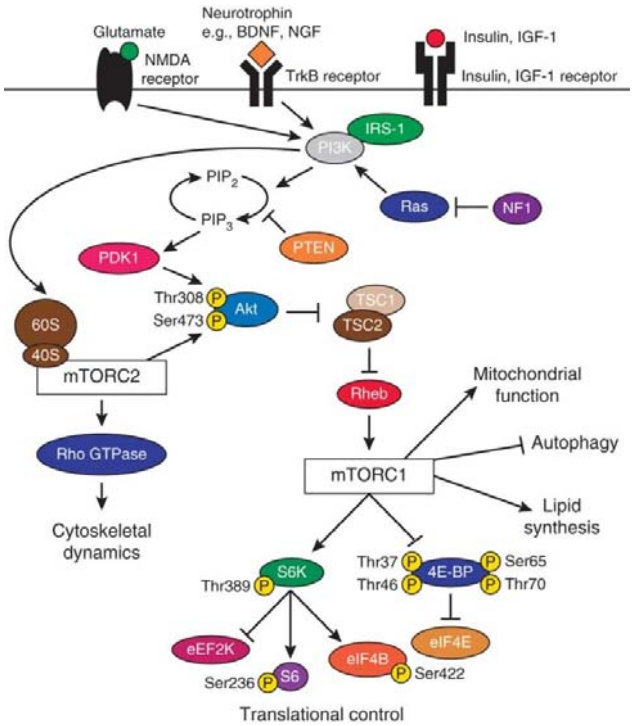

Fig.8 mTORC1 and mTORC2 regulation and downstream effects (478).

1.2.1.5.5 Rapamycin

Rapamycin is a molecule produced by *Streptomyces hygroscopicus* bacteria. Once it binds to FK506-binding protein of 12 kDa (FKBP12), it can interact with FKBP12-

rapamycin binding domain (FRB) of mTOR. This interaction inhibits mTORC1 activity (463). By contrast, the FKBP12-rapamycin does not interact with mTOR when it is part of mTORC2. Therefore, mTORC1 and 2 were initially described respectively as rapamycin sensitive and insensitive complexes. However, it appears that chronic exposure to rapamycin can sometimes inhibit mTORC2 function, but this effect is cell-dependent (355). Moreover some mTORC1 effects are not sensitive to rapamycin, suggesting that rapamycin inhibition is more complex than previously thought (61; 410).

1.3 Radiation

Every organism on earth is daily exposed to low doses of different types of radiation from natural sources, via UV, terrestrial sources such as radon, cosmic rays... and recently, from man-made radiation mainly through medical exposure in human populations.

However, according to the type of the radiation and to its dose, it can interact with organic matter and cause damages that the cells will be able to handle and repair, or not.

1.3.1 Types of radiations

Radiation can be first categorized according to their nature: particles, electromagnetic, acoustic or gravitational radiation. Particles and electromagnetic radiations can then be subdivided into ionizing and non-ionizing radiations, depending on their energy, and thereby, their capacity to ionize atoms (163).

1.3.1.1 Particle radiations

Particle radiations comprise charged elementary particles such as protons, α and β particles, ions and uncharged particles such as neutrons. When passing through matter, their energy will be transferred to the molecules they interact with. All particle radiations are able to cause excitation or ionization of atoms. However, charged particles and ions cause more damage than neutrons because of stronger electrostatic interactions. Conversely, neutrons are more penetrating than charged particles. The energy deposition pattern strongly differs among particle radiations because it is proportional to the charge squared and inversely proportional to the

velocity. These physical properties are extensively studied in the framework of radiation therapy, where ion particles receive increasing attention due to their ballistic effect. Indeed, ions release the maximum of their energy at the end of their track path, thereby leading to an accurate irradiation of cancer tissues while sparing the surrounding healthy tissues (134; 163).

1.3.1.2 Electromagnetic radiations

Electromagnetic radiations include radiowaves, microwaves, visible light, ultraviolet (UV) light, X-rays and γ-rays. Their quantum energy, called photon, varies inversely with their wavelength, radiowaves having the smallest energy and γ-rays the strongest. While x-rays and γ-rays are clearly ionizing, this demarcation is not as clear for UV radiation. Some molecules can indeed be ionized with electromagnetic radiations carrying less energy than that of X- and γ-rays, and far UV with a wavelength close to that of X-rays are thus able to ionize these molecules. For example, when they reach the atmosphere, they can ionize air molecules but they are then strongly absorbed by the latter, preventing them from reaching living organisms on the earth's surface. (134; 163).

When a high energy electromagnetic photon moves through matter, the consequent energy deposition will induce, in the molecule it interacts with, the ejection of an electron from its orbital. Depending on the energy of the incident photon and the atomic weight of the absorbing atom, this energy transfer takes place through different processes. Electromagnetic photons can thus excite or ionize matter. Ionized and excited molecules can fragment into free radicals, or return to their original state. While lower energy electromagnetic radiations are not able to ionize matter, they can still induce damage through heating effects. (163)

1.3.2 Linear energy transfer (LET)

The LET of a radiation beam is its average energy transfer per unit of track and is expressed in keV/μm. Charged particles tend to have a higher LET than photon radiations because they interact more with matter, which slows them and leads to a higher energy deposition density that reaches a peak when the particles stop (the Bragg peak) (285). Among particles, larger ones have a higher LET and deposit more energy at the same dose (122; 163; 425).

Moreover, photon beams tend to scatter when they penetrate matter whereas particle beams follow a straighter path. Therefore, though protons have a low LET that is comparable to that of photon radiations due to their small size, their effects and the induced biological response in tissue will be very different to that of photon radiations (122; 163).

1.3.3 Radiation doses

In physics, the radiation exposure is expressed in Coulombs/kg of air and it measures the physical capacity of a radiation beam to ionize air under standard temperature and pressure. However, this unit is not applicable in tissues. Therefore, other units of measures have been developed. The absorbed dose is expressed in Grays (Gy) and represents the energy absorbed in a given tissue mass (1 Gy = 1 J/kg). But the biological effects of radiations will vary according to the radiation type and its LET. Therefore, the notion of "equivalent dose" was introduced to facilitate the comparison of the effects of different radiation types in tissues. The equivalent dose is expressed in Sievert (Sv). It is the product of the absorbed dose in the tissue multiplied by a weighting factor that depends on the radiation type. For X-rays, this weighting factor is 1. To estimate radiation risk in humans, the effective dose was introduced. It is the product of the equivalent dose received in each tissue or organ multiplied by a weighting tissue factor, as the sensitivity of the different tissues and organs towards radiation is different. In parallel, the relative biological effectiveness (RBE) is used to compare the biological effects produced by different types of radiation given the same absorbed dose. For a given biological effect, the RBE is usually expressed as the ratio of a dose of a standard radiation (γ-rays of Co60) to the dose of test radiation that triggers the same biological effect (134; 163; 425)

1.3.4 Biological effects of ionizing radiations (IR)

1.3.4.1 Free radicals and ROS generation following IR exposure

1.3.4.1.1 Direct effects of IR

Radiation damage in biological tissues are due to either direct or indirect effects. Radiations can directly ionize key molecules, such as DNA, protein or lipids (**1**) causing functional alterations or inactivating them (134). Both electromagnetic and

particle radiations are able to induce direct ionization of such molecules, but direct effects are predominant only with high LET radiations. Directs effects account for only approximately one third of photon radiation biological effects. The radical formed can then react with another molecule to stabilize itself, leading to the formation of a new radical (**2**), or can react with another radical in a cross-linking process (**3**). Moreover, interaction of organic radicals with oxygen can lead to less unstable organic peroxy free radical (**4**) (163; 425).

(1) IR + RH → R° + H°
(2) R° + R'H → R'° + RH
(3) R° + R° → R-R
(4) $R° + O_2 \rightarrow RO_2°$

1.3.4.1.2 Indirect effects of IR

Biological damages also arise from indirect effects of radiations that involve the production of reactive free radicals. Because 80% of the cell weight is water, the latter is commonly the free radical formation and propagation intermediary. This process is called water radiolysis. The interaction of radiation with water can lead to electronically excited water molecules (**1**), which can then emit a photon to lose its energy (**2**), or can fragment into OH° and H° radicals (**3**). Radiation can also produce highly reactive $H2O^+$ radical and an ejected electron (**4**). $H2O^+$ cation radical will lead to the formation of $H3O^+$ and hydroxyl radical in an aqueous environment (**5**).

The ejected electron can interact with water to form a temporary anion radical $H2O^{°-}$ leading to the formation of hydroxyl and hydrogen radicals (**6**), or, can lose its energy by interactions with the medium (**7**) and can interact with a proton to give an atom of hydrogen or, in the presence of oxygen, it can then interact with it to form superoxide anion.

Besides, in the presence of oxygen, hydrogen radicals can lead to the formation of hydroperoxyl free radicals (**8**). (22; 163)

(1) $IR + H_2O \rightarrow H_2O^*$

(2) $H_2O^* \rightarrow H_2O + photon$

(3) $H_2O^* \rightarrow OH^\circ + H^\circ$

(4) $IR + H_2O \rightarrow H_2O^+ + e^-$

(5) $H_2O^+ + H_2O \rightarrow H_3O^+ + OH^\circ$

(6) $e^- + H_2O \rightarrow H_2O^{\circ -} \rightarrow OH^- + H^\circ$

(7) $e^- \rightarrow aq\ e^-$

$aq\ e^- + H^+ \rightarrow H$

$aq\ e^- + O_2 \rightarrow O_2^{\circ -}$

(8) $H^\circ + O_2 \rightarrow HO_2^\circ$

1.3.4.1.3 Reactive nitrogen species

IR exposure was shown to stimulate nitric oxide synthases and thus increase intracellular NO (199; 222). NO exhibits signaling properties and this increase can influence diverse molecular pathways. Moreover, as mentioned before (see section 2.2.2.), NO can interact with $O_2^{\circ -}$ to generate peroxynitrite anion, a radical that can induce damage in various biomolecules in its immediate vicinity due to its high reactivity (22).

1.3.4.1.4 Mitochondria

Mitochondria can also be the target of IR. As one of the main intracellular ROS source, IR-induced damage in mitochondria often leads to significant redox perturbation (22; 41). It was shown that radiation leads to excessive $O_2^{\circ -}$ radical generation from the oxidative phosphorylation complexes in the mitochondrial inner membrane (460; 464). This ROS excess causes damage to mitochondrial biomolecules, but also to biomolecules in the rest of the cell (22).

1.3.4.1.5 NOX enzymes

Recently, several studies have enlightened a role of NADPH oxidases in radiation-induced biological effects through ROS production, such as DNA damage, or collagen deposition in radiation-induced fibrosis. NADPH oxidases are another important cellular source of ROS along with mitochondria, and, according to the

tissue/cell type, different members of the NADPH oxidase family were activated or up-regulated and were shown to be involved in radiation effects (13; 60; 449).

1.3.4.2 Biological consequences of free radicals and ROS

Generated free radicals can recombine to return to their initial state (**9**), can dimerize (**10**) or can be transferred to an organic molecule, causing bond breakage or inactivation of function. This will contribute to biological damages of which the extent depends on the target molecules and the ability of the cells to repair the induced damages (134).

(9) $H^\circ + OH^\circ \rightarrow H_2O$

(10) $H^\circ + H^\circ \rightarrow H_2$

$OH^\circ + OH^\circ \rightarrow H_2O_2$

The lifetime of the first generated radicals (OH° and H°) is very short, preventing them from migrating to the nucleus if they are generated in the cytoplasm. But their interaction with oxygen leads to the formation of less unstable radicals (hydroperoxyl and organic peroxy free radicals) which will be able to migrate further in the cells, perpetrating damages in other cell compartments, and possibly leading to more serious damages (163; 425). Particularly in the case of lipids, free radicals can be transferred from molecule to molecule damaging each of them, and sometimes elicit chain reactions, leading to cumulative effects (163).

IR-induced cellular damages, especially DNA damage, but also membrane lipid damage will induce a stress response. Checkpoints during the cell cycle to evaluate DNA damage will lead to cell cycle arrest and, according to the extent of DNA damage, to DNA repair or cell death. Key mediators involved in this response are p53, DNA-PK (DNA-dependent protein kinase), PARP, and ATM (179; 425). According to the type of DNA damage, different repair mechanisms can be triggered(134; 425). In the case of double strand breaks (DSB), two major repair pathways can be activated: homologous recombination (HR) and non-homologous end-joining (NHEJ). HR needs an undamaged DNA copy as template and therefore predominates in cell in the late S phase or in the G2 phase of the cell cycle. The process starts by resecting the blunt damaged ends to obtain single stranded ends which will then pair to the equivalent sequence from the undamaged DNA, leading to an error-free synthesis of the missing nucleotides based on the sequence of the undamaged DNA copy. NHEJ, the predominant repair system of DSB after IR

exposure, on the contrary, will directly act on the blunt ends of the DNA fragment. After processing damaged nucleotides, or mismatched nucleotides, the DNA blunt ends will be ligated without the need of a homologous sequence and is thus error-prone. This mechanism functions throughout the cell cycles, but predominates during G1 phase and the beginning of S phase. Other types of DNA damage such as alkylation, base oxidation or strand intercalation will induce other repair responses. For instance, base damages can induce the base excision repair mechanism (BER), where the base is removed, leaving a DNA site lacking a purine or pyrimidine. This apurinic/ apyrimidic site is then excised and is replaced by the resynthesis of a new complementary nucleotide, or strand of nucleotides in the case of long-patch BER, where more than one base was excised. Other DNA repair mechanisms include the mismatch repair induced by inaccurate nucleotides insertion or deletion, and nucleotide excision repair, induced by pyrimidine dimers and other DNA-adducts formation. IR damage at the membrane can also initiate a stress response through the oxidation of polyunsaturated fatty acids or activation of cell surface receptors/ion channels and sphingomyelinases. The latter degrade sphingomyelin to produce ceramide-enriched lipid rafts platforms that can act as a second messenger to mediate apoptosis (10; 133). Moreover, ROS produced by IR can also trigger apoptosis, or when in smaller amount, influence different molecular pathways due to their role as second messengers, disrupting cellular behavior which can then influence the progression of diseases such as cancers. Altogether, heavily damaged cells overwhelmed by ROS production will undergo cell death which accounts for acute syndrome of radiation and will not induce cancer. Lighter damage though, if not properly repaired, can dysregulate pathways and lead to cancer formation depending on the gene affected by the mutation, or induce genomic instability that is associated to increased rate of mutation in future cell generation, potentially inducing neoplastic transformation (22; 245).

1.3.4.3 The effects of low doses of radiation

While the effects of high doses of radiation have been extensively studied, biological effects of low doses of radiations are still debated.

Several experiments and studies carried out during the first half of the 20th century, among which the experiments of Muller on fruit fly sperm, led to the dogma that the biological effects of IR exposure is directly proportional to the received dose (422). This dogma is illustrated by the linear-no-threshold model (fig. 17 curve B). According to this model, very small doses of radiation could induce a cancer, based

on the assumption that each radioactive photon can cause a DNA mutation. However, this model does not take defense mechanisms into account. Moreover, the effects of low doses of radiation are often extrapolated from studies using higher doses of radiation and more recent studies came to challenge this view. Other models were thus proposed, such as the supralinear model (fig. 17 curve A) which describes an hypersentivity of cells to radiations at low doses, the linear threshold model (fig. 17 curve C) where low doses of radiation below a given threshold were proposed to have no biological long-term effects; and the hormesis model (fig. 17 curve D) where low doses of radiation show protective effects.

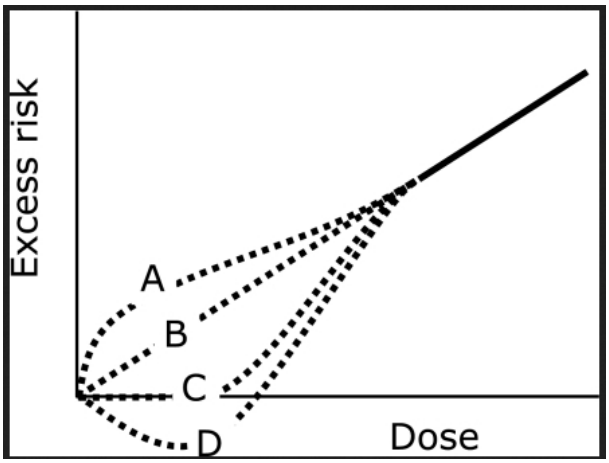

Fig. 9 Models of carcinogenic effects of photon radiations: the supralinear model (A), the linear-no-threshold model (B), the linear threshold model (C) and the hormesis model (D) (479).

The hormesis model assumes that adaptive and protective mechanisms can be triggered by low-dose radiation, increasing the organism protection against the carcinogenic effects of IR or other aggressors. This hypothesis is based on several studies showing that low doses of radiation stimulate DNA repair, while it is often inhibited with high doses (65; 284), decrease the number of double-strand breaks (DSB) in cell cultures compared to that of unirradiated cells (346), eliminate aberrant cells (210), increase antioxidant defenses, down-regulate oxidative metabolism, or stimulate different immune mechanisms (22; 54; 55; 292). Moreover, Scott et al. 2009 proposed that low-dose radiation can induce protective epigenetic mechanisms that could facilitate cellular response to future IR exposure

(363). In those studies, protective effects are generally accepted to arise below 100 mGy, though the response is highly tissue-dependent and the threshold can thus vary according to the tissue. However, epidemiological studies on the carcinogenic effects of low doses are contradictory (422; 422). Of note, the low dose induced protective mechanisms is not observed with high LET radiations and the hormesis hypothesis does not apply to this kind of radiation (22).

Interestingly, several studies have also shown a hypersensitivity to low doses of IR in different models, leading to the supralinear model hypothesis. Excess cell killing or DNA damage was indeed observed at low dose in different tissues adjacent to irradiated tumors or in cell lines (93; 125; 226; 283; 367). This hypersensitivity was proposed to result from a threshold dose-dependent trigger of the cell DNA repair mechanisms. Grudzenski et al. (2010) for instance showed in fibroblasts that "repair foci" loss, which reflects efficient DNA repair" was compromised after exposure to doses of γ-rays below 10 mGy, and absent under 2.5 mGy. Conversely, Nasonova et al. (2006) showed lymphocytes hypersensitivity after exposure to doses ranging from 10 to 50 mGy, which was accompanied by an increased chromosomal aberrations compared to cells exposed to higher doses. Other mechanisms potentially playing a role in low dose IR hypersensitivity were also highlighted, as an increased p53-dependent apoptosis induction (93).

However, this hypersensititvity is cell- and dose-specific. Enns et al. (2004) for instance showed hypersensitivity of lung cancer and glioma cell line to doses below 50 cGy, but not in breast cancer cell line (93). Bogdandi et al. (2010) also observed different apoptotic response and different resistance to low doses of γ-rays between blood cells such as lymphocytes T, B, regulatory T lymphocytes and natural killers (36).

Therefore, further research is needed to properly characterize the biological effects of low dose IR.

1.3.4.4 Radiations and cancer incidence

As mentioned before, radiation exposure is an established cancer risk factor. Several studies have linked radiotherapy for benign diseases such as tinea capitis, enlarged thymus or tonsils, or for malignant diseases as head and neck cancers for instance to a higher cancer prevalence in organs located near the irradiated sites such as the central nervous system, salivary glands, thyroid, exposed bones… (342; 395). Moreover, radiologists who started working before 1950, when no exposure

dose limit was defined for the medical staff yet, were also exposed to a greater cancer risk, particularly leukemia (466). Non-medical exposure to radiations as radon or after a nuclear catastrophe/bombing was also respectively linked to lung cancer or leukemia prevalence for instance (236; 326; 466).

Regarding NIS-expressing organs, a huge amount of data have shown increased risk of thyroid and breast cancers after IR exposure.

Long-term follow-up studies after nuclear catastrophe/bombing have shown increased risk of thyroid cancer, particularly from 5 to 10 years after exposure, but the increased risk persisted to more than 40 years after exposure. Increased prevalence of large thyroid nodules (>10 mm diameter), cysts, malignant nodules, and cancer was observed in cohorts of Nagasaki and Hiroshima atomic bomb survivors (105; 144; 159; 281; 335). Unlike other research groups, Nagataki et al. (1994) also found an increased risk of autoimmune hypothyroidism. But, contrasting to thyroid cancer, the excess risk did not show a linear dose-dependency but rather exhibited a concave dose response, with a peak at 0.7 Gy. Likewise, dose-dependent increase in large thyroid nodules, neoplastic nodules and cancer prevalence was observed in residents of contaminated areas after the Chernobyl catastrophe (47; 49; 326; 470). One year after Fukushima disaster, an increased prevalence of thyroid nodules and cysts could already be observed in children living near the plant (280). In most follow-up studies after atomic bombing or nuclear plant accidents, increased thyroid cancer prevalence was age-dependent, the risk being the highest for the youngest children, while usually not increased in exposed adults over the age of 20 at the moment of the exposure. However, a few studies have found an increased risk in adults, though much lower, but primarily in woman (144; 326; 335). Moreover, while it is generally admitted that the feminine gender is more susceptible to develop thyroid cancer after radiation exposure, some follow-up studies have shown that the gender did not influence thyroid cancer prevalence (159). Regarding the accident of Chernobyl, Cardis et al. (2005) have found that ID increased the risk of developing a thyroid cancer. Because the main radiation exposure after Chernobyl accident was through radioactive I^{131} fallout, this increased risk is probably due to an increased I^{131} uptake by the gland, and thereby, an increased intrathyroidal radiation exposure. However, other groups did not find any influence of iodine diet on thyroid cancer development after Chernobyl catastrophe (470). Interestingly, various studies have shown an increased risk in thyroid nodules or cancer after medical exposure to radiations, such as radiotherapy for central nervous system cancer (53; 299; 395),

for Hodgkin lymphoma (414) or fractionated radiotherapy before hematopoietic stem cell transplantation (438) in children or adolescents.

Numerous follow-up studies of people exposed to radiations for medical reason or by accident also established radiation as a breast cancer risk factor.

Early reports observing a link between breast cancer and radiation come from a study following women treated in Nova Scotia, Canada, with X-rays for tuberculosis 15 to 25 years after exposure, in which 60% of the women who developed breast cancer had received more than 175 fluoroscopies, which corresponded to a dose of about 1.5 Gy (calculated by myself from the data in the article) (279). A similar study by Boice and colleagues (1991) in Massachusetts led to comparable results (37). Several reports also observed increased breast cancer risk in Hodgkin's disease patients, years after exposure to high doses of radiation, especially in the case of mantle-field irradiation (68; 74; 87).

However, other studies revealed positive correlation between breast cancer risk and much lower doses of radiation. Women suffering from tuberculosis exposed to total X-rays doses from 0.1 Gy and above during fluoroscopic examinations were shown to have an increased risk of breast cancer (261), and a dose-dependent increase in breast cancer risk in women exposed to cumulative doses from 0.1 to 0.5 Gy following multiple radiographies of abnormal spinal curvature was observed, particularly in women with a family history of breast cancer (343; 344).

Many follow-up studies confirmed this association between breast cancer risk and cumulative exposure to radiations, including:

-Preston et al. (2016) studied this risk among radiologists, particularly among those who started working before 1950 when mean annual doses were estimated to 37 mGy, which was reduced the following year (1.3 mGy) due to growing concerns on the biological effects of radiations (324).

-Lundell et al. (1999) observed this association in women treated with radium-226 applicators during infancy for hemangioma (242).

-Inskip et al. (2009) found a linear relationship between secondary breast cancer risk and radiation dose received by cancer survivors during childhood (162).

-Adams and colleagues (2010) compared breast cancer occurrence in women treated during infancy for enlarged thymus whose breast received a mean dose of 0.71Gy with a control cohort and found a breast cancer rate ratio of 3.01 (7).

However, some studies have also shown inverse relationship, such as Strodbeck et al., who observed a lower risk of female breast and men prostate cancer after radiotherapy for multiform glioblastoma although this risk was increased for other types of induced secondary cancer. They did not observe that inverse relationship after radiotherapy for other types of central nervous system tumors (395).

1.3.4.5 Radiation and angiogenesis

1.3.4.5.1 Photon radiations and angiogenesis

1.3.4.5.1.1 Importance of vascularization in IR effects

The cell cytotoxicity potential of radiation has long been used in radiotherapy to kill tumor cells. While the high dose IR-induced DNA damage in tumor cells leading to cell death is widely admitted to be the main factor contributing to antitumor effect of radiotherapy, growing evidence shows an important contribution of IR-induced cytotoxicity to the vascular compartment (106). An important contribution supporting this view was brought by Paris et al. (2001). Though it was assumed that lethal gastrointestinal syndrome was primarily caused by IR damage to the epithelial stem cells in intestinal crypts, they showed that IR first induced microvascular damage and endothelial cell (EC) death (305). Stem cell and crypt cell dysfunction and death were shown to be secondary to microvascular damage. Since then, several groups have contributed to show the importance of cytotoxic effects in EC in IR antitumor effects, based on the fact that tumor cells rely on their vasculature for their survival.

Besides, tumor recurrence after radiotherapy mainly occurs near the irradiated site. It is widely thought that recurrence is due to radioresistant cells. However, growing attention has been brought to IR-induced changes in the environment of the tumor and to a possible role of IR-induced paracrine signals between the different cells present in the tumor and its environment (194), involving among others, endothelial cells and mediators of angiogenic pathways.

While damage induced to EC by high doses of radiations are believed to participate to IR antitumor effects, EC surrounding the irradiated area are exposed to lower doses of radiations, which can trigger opposite reaction in those cells (423). Vala and colleagues (2010) indeed showed *in vitro* that the DSB induced by X-rays under

0.8 Gy in EC could be repaired and did not impair EC proliferation. On the contrary, EC migration was enhanced after IR exposure consequent to IR-induced phosphorylation of VEGFR2. However, cell proliferation decreased at doses higher than 1 Gy and cell death increased at 10 Gy. They also showed that a local dose of 0.3 Gy increases angiogenesis in adult mice, accelerates embryonic angiogenic sprouting in zebrafish, increases lung metastasis in a xenograft model of breast cancer in a VEGFR2-dependent mechanism, and increases tumor growth in an *in vivo* model of leukemia, also in a VEGFR2-dependent manner. Likewise, other groups observed that sublethal X-radiation promotes EC migration and tube structure formation (404).

1.3.4.5.1.2 IR-induced VEGF and bFGF overexpression

Interestingly, several groups have shown that photon radiations could induce angiogenic factors overexpression and that their overexpression was linked to increased radioresistance. An increase in VEGF expression was for instance observed in 75% of rectal carcinoma biopsies taken after radiotherapy compared to biopsies before radiotherapy (294). Experimentally, VEGF IR-induction was shown in various models. For instance, high doses of X-rays and γ-rays induce a dose-dependent VEGF overproduction in various glioma cell lines (153; 194). Gorski et al. (1999) showed an increase in VEGF mRNA and a dose-dependent increase in its protein after exposure to 5, 10 and 20 Gy of X-rays in lung carcinoma and in glioblastoma and melanoma cell lines (121). A transient increase in VEGF and bFGF mRNA was also observed in prostate tumor cells after an exposure to 2Gy of X-rays (2). Yu et al. (2012) observed an increase in VEGF and bFGF mRNA and protein expression in breast cancer cells following exposure to 2Gy γ-rays (468).

1.3.4.5.1.3 Protection of EC and tumor cell invasion through VEGF and bFGF signaling

Supporting a role of angiogenic factors in radioresistance, exogenous bFGF prevented the IR-induced damage in crypt cells and consequent organ failure in the above-mentioned Paris and colleagues' experiments (2001) (305). Of note, bFGF receptors are only found in EC and not in stem or crypt cells. Furthermore, xenograft of $VEGF^{+/+}$ transformed fibrosarcoma cells were shown to be more radioresistant than xenograft of $VEGF^{-/-}$ cells (129).

Besides, Gorski et al. (1999) showed that the extent of IR-induced cells death in umbilical vein EC *in vitro* was lower when VEGF was added to the medium and the opposite effect was observed when VEGF was blocked by the addition of an antibody (121). Lung carcinoma cells, though, were not protected by the addition of VEGF in their experiment. Interestingly, different results were observed in other cell lines, such as in glioma cells (194). These cells, known to express VEGFR2, overexpress VEGF after irradiation. This VEGF overexpression was shown to induce cell migration and invasion in non-irradiated glioma cells, probably through a mechanism involving the phosphorylation of Src and FAK protein. Those experiments led to the concept that IR display antiangiogenic effects in tumor due to its cytotoxicity on EC and tumor cells at high dose, but also display proangiogenic effects via the release of angiogenic factors by the tumor cells to protect its vasculature at sublethal doses (2) and may induce metastasis among tumor cells if they express VEGF receptors, as it is the case in several tumor models (172; 411).

Accordingly, Abdollahi et al. (2003) showed that X-rays from 1 to 10 Gy decreased EC survival, proliferation and tube formation *in vitro* in a receptor tyrosine kinase (RTK)-dependent manner and that the addition of VEGF and bFGF attenuated this effect. Interestingly, they showed that IR induces the overexpression of VEGF and bFGF in prostate tumor cells and that of VEGFR2 in EC. They showed that the invasiveness of EC was increased when they were co-cultured with irradiated prostate tumors cells and this effect depended on RTK functionality (2). Yu et al. (2012) observed a 2Gy γ-rays VEGF and bFGF induction in breast cancer cells and an overexpression of their respective receptors accompanied by *in vitro* tube formation in EC co-cultured with irradiated breast cancer cells (468). Those studies enlighten a possible interplay between tumor cells and EC leading to IR-dependent increase in EC survival and invasiveness by tumor cell.

1.3.4.5.1.4 Radioresistance differences in vivo and in vitro

Several discrepancies between the observed radiosensitivity of certain tumor *in vivo* and that of their equivalent cell line *in vitro* were described in the literature (110; 110; 402). These discrepancies led some authors to hypothesize that the ability/inability of tumor cells to protect their vasculature through paracrine signaling might at least partly explain those differences *in vivo* and *in vitro* (2).

1.3.4.5.1.5 IR-induced molecular pathways

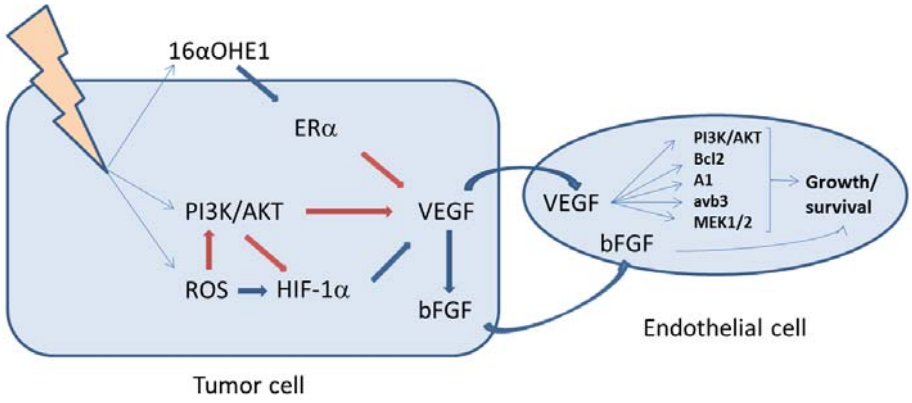

Fig. 10 Some of the pathways hypothetically involved in radiation-induced VEGF up-regulation and EC protection. Blue arrows: demonstrated in radiation research; red arrows: hypothetical.

Several pathways were proposed to be activated by VEGF and bFGF to enhance EC survival after irradiation, including the overexpression of Bcl2 and A1 antiapoptotic proteins, the activation of PI3K, AKT pathway thereby preventing apoptosis or via the interaction with integrins such as avb3, promoting EC survival (1; 2). A role of MAPK and MEK1/MEK2 pathways was proposed in vascular preservation via VEGF-induced EC growth and survival following radiation exposure (129). Sonveaux et al. (2003) revealed a role for NO in X-rays induced EC migration and sprouting (385).

Regarding IR-induced VEGF up-regulation in tumors cells, one possible mechanism is that the ROS increase following irradiation could stabilize HIF-1α, a known VEGF transcription factor. Accordingly, several studies showed IR-induced up-regulation of HIF-1α. For instance, 5 to 15 Gy of γ-rays were shown to induce a ROS-dependent increase in HIF-1 nuclear accumulation and increased HIF-1α translation following stress granule depolymerization in tumor tissues. This led to the overexpression of VEGF and bFGF, though the latter was probably increased via an indirect VEGF activation (264). The authors showed that HIF-1 inhibition increases tumor radiosensitivity due to enhanced vascular destruction. Interestingly, Lall and colleagues (2014) showed an increase of HIF-1α expression upon exposure to a low dose of X-rays (0.1Gy) and showed overexpression of HIF-1 targets, p21 and Glut3, with doses ranging from 0.025 to 1 Gy. Other pathways might also be involved in IR-induced VEGF up-regulation. It was for instance shown in a study on IR associated glioma cell invasiveness that the PI3K-AKT-mTOR pathway was activated

by γ-rays (306) and γ-irradiation of mice led to increased phosphorylation of AKT and mTOR in mammary glands (398). Because PI3K/AKT/mTOR pathway is known to increase VEGF expression (174), it is possible that it also has a role in IR-induced VEGF overexpression.

Of note, oxygen delivery in tumors may be very variable and tumors may present various hypoxic regions that will influence IR effects. Hypoxia in tumors was indeed associated with increased radioresistance, partly due to the fact that IR- induced free radical effects are prolonged in presence of oxygen, but also because of survival pathways induced by hypoxia (218; 465). It was shown that IR increased cellular ROS content and improved glucose and oxygen availability which in turn will increase HIF-1α expression, eventually leading to a metabolic switch from oxidative phosphorylation to glycolysis, increased invasion and metastasis of tumor cells or angiogenesis (139; 140; 218; 264; 465).

Suman et al. (2012) observed an activation of PI3K/AKT/mTOR pathway following a total body γ-irradiation of 2 Gy in mouse mammary glands (398). Interestingly, they also observed an increase in serum oncogenic estrogen metabolite (16αOHE1) accompanied by a long-term increase in nuclear ERα. As estrogen stimulation was shown to increase VEGF expression (394), IR effects on these hormones could play a role in IR-induced VEGF expression in breast.

1.3.4.5.2 Particle radiations and angiogenesis

The majority of studies on the effects of radiations on angiogenesis were carried out using photon beams. Few studies used particle beams and led to very different results. Several studies indeed showed an IR-induced decrease in angiogenic factors and an inhibition of vasculogenesis at low doses. For instance, Grabham and colleagues showed an IR-induced inhibition of vasculogenesis *in vitro* with doses from 40 to 80 cGy of proton and Fe ion radiation. They had to increase the dose up to 15 times to have the same cytotoxic effect with γ-rays (122; 123). Of note, though both radiation types were as effective at inhibiting vasculogenesis though through different mechanisms, high LET Fe ions caused more damage in vessel structure than low LET proton radiation. Likewise, Takahashi and colleagues (2003) compared the effects of high LET carbon ion and low LET X-ray irradiation on *in vitro* angiogenesis and observed that low doses (0.1 Gy) of carbon irradiation inhibited it while sublethal doses of X-rays had the opposite effect (404). Other studies showing proton IR-induced decrease in angiogenesis in zebrafish embryos, increase

in ROS-dependent *in vitro* EC deaths (173) and decrease in iris neovascularization (42) support those results. Moreover, co-culturing EC with proton-irradiated cancer or fibroblast cells inhibited EC survival and invasion (116), unlike what was observed with γ- and X-rays (2; 468). They also showed a proton IR-induced decrease in VEGF mRNA, HIF-1α protein and IL-6 and 8 at doses from 0.5 to 2 Gy.

2 Objectives

Mechanisms to cope with ID have abundantly been studied in thyroid. However, while the role of iodine/iodide is not perfectly understood in extrathyroidal NIS-expressing tissues, it is evident that it has its importance and NIS-expressing organs might have developed mechanisms to face sudden or prolonged iodide shortage due to variation in the diet, but nothing is known about it. Because the ID-induced microvascular reaction in thyroid is TSH-independent, we hypothesized that ID could trigger similar mechanisms in other NIS-expressing organs. Though there is not such a close relationship between the vascular network and mammary glands, salivary glands and stomach cells as in the thyroid, these organs may also try to increase iodide supply through increased blood supply. Therefore, the first objective of this work was to study ID impacts on stomach, salivary glands and mammary glands, focusing on vascular responses.

To achieve our objectives, *in vivo* and *in vitro* models were chosen. To study ID impact on stomach, salivary glands and mammary glands vascularization, NMRI mice were chosen because an outbred strain could better represent a heterogeneous population, and because the ID treatment had been applied to this particular strain of mice before and was known to be well accepted (113). The blood perfusion of those organs was first assessed in a pilot study using short ID exposure (1 and 2 days), which corresponds to the exposure timing where a TSH-independent ID-increased thyroid blood perfusion (113). Exposure timing was then prolonged to study the microvascular regulation in the different organs. To unravel the pathways involved in ID response in breast, the first steps were achieved *in vitro*, in two different cell lines, to avoid unnecessary sacrifice of mice since nothing is known about the molecular pathways activated by ID in this organ. A cancerous and a non-cancerous cell line were chosen, both known to express the iodide symporter NIS. A time- response curve focusing on VEGF mRNA regulation was first established from 2h to 24h of ID, and the rest of the pathway was then assessed at time points based on this time-response curve.

Iodide being an antioxidant in itself, such a response is likely to depend on ROS. Another factor known to increase cell ROS concentration is the exposure to IR. Moreover, electromagnetic radiations were shown to induce angiogenesis, mostly through VEGF up-regulation. So, if ID increases ROS and induces VEGF overexpression in other NIS-expressing organs as it does in thyroid, the combination of IR with ID could have additional effects on angiogenic pathways induction. However, though high dose IR angiogenic effects were abundantly studied, the effects of low doses are not so well understood. Therefore, the second

objective of this thesis was to compare IR high dose and low dose effects on ROS production and their implication in VEGF expression in iodide-sufficient and -deficient conditions in a NIS-expressing organ. Due to the importance of radiation in cancer research and therapy, and due to the health burden that breast cancer constitutes to societies, this part of the project only focused on breast response.

To study the combined effects of radiations and ID, X-rays were chosen because they largely contribute to medical radiation exposure at very variable doses via radiography, CT-scans, radiotherapy… As a start, we chose to work with one low dose and one high dose. 0.1 Gy was chosen as the low dose because biological response to radiation is generally not well understood from this dose and below. 3 Gy was chosen as a high dose because it is in the range of fractionated therapy doses. Because the two cell lines chosen for the study on ID microvascular effects were determined to be ID-sensitive in the first part of this project, they were used again in the study of the combined effects of radiations and ID.

3 Results

3.1 PAPER 1

Iodine deficiency induces a VEGF-dependent microvascular response in salivary glands and in the stomach

Jessica Vanderstraeten[1], Hanane Derradji[2], Julie Craps[1], Pierre Sonveaux[3], Ides. M. Colin[4], Marie-Christine Many[1], Anne-Catherine Gérard[1*]

Histology and Histopathology, 2016, 31(8):897-909.

Iodine deficiency induces a VEGF-dependent microvascular response in salivary glands and in the stomach

Jessica Vanderstraeten[1], Hanane Derradji[2], Julie Craps[1], Pierre Sonveaux[3], Ides. M. Colin[4], Marie-Christine Many[1], Anne-Catherine Gérard[1*]

[1]Pole of Experimental Morphology, Institute of Experimental and Clinical Research (IREC), Catholic University of Louvain (UCL), Brussels, Belgium; [2]Radiobiology Unit**,** Belgian Nuclear Research Centre (SCK-CEN), Mol, Belgium; [3]Pole of Pharmacology and Therapeutics, Institute of Experimental and Clinical Research (IREC), Catholic University of Louvain (UCL), Brussels, Belgium; [4]Department of Endocrinology and Diabetology, Regional Hospital Center (CHR) Mons-Hainaut, Belgium. *Present address: Department of Endocrinology and Diabetology, Regional Hospital Center (CHR) Mons-Hainaut, Belgium and Institute of life sciences (ISV), Catholic University of Louvain (UCL), Belgium

Address for correspondence: Marie-Christine Many, Pôle de Morphologie Expérimentale, Avenue Mounier 52, box B1.52.04, Brussels, 1200, Belgium (marie-christine.many@uclouvain.be)

Short title: Iodine deficiency in stomach and salivary gland

Abstract

Despite efforts to optimize iodine supply in iodine deficient countries, iodine deficiency (ID) remains a global problem worldwide. Activation of the local microvasculature by ID in the thyroid gland aims at improving the local supply of iodide. For this purpose, the thyrocytes secrete vascular endothelial growth factor (VEGF) that acts on adjacent capillaries, via a reactive oxygen species (ROS)/Hypoxia Inducible factor (HIF)-dependent pathway. Beside the thyroid, other organs including salivary glands and the stomach do express the sodium/iodide symporter (NIS) and are able to take iodide up, potentially rendering them sensitive to ID. To verify this hypothesis, ID-induced effects on the local microvasculature were studied in salivary glands and in the stomach. ID was induced by feeding young mice with an iodide-deficient diet and NIS inhibitor perchlorate in the drinking water. In salivary glands, ID induced a transient increase in HIF-1α protein expression accompanied by a transient, VEGF-dependent increase in blood flow. In the gastric mucosa, ID transiently increased VEGF expression in the mucin-secreting epithelium and in ghrelin-secreting endocrine cells. These observations suggest that microvascular changes in response to ID occur in NIS-expressing tissues other than the thyroid. NIS expressing cells could be viewed as iodide sensors that respond to ID by inducing vascular changes, probably to optimize iodide bioavailability at regional or systemic levels.

Keywords: Iodine deficiency, salivary glands, stomach, microvasculature, VEGF
Abbreviations: Iodine Deficiency (ID), Hypoxia Inducible Factor 1α (HIF-1α), Reactive oxygen species (ROS), Sodium Iodide Symporter (NIS), Vascular Endothelial Growth Factor A (VEGF), Low Iodide Diet (LID)

Introduction

Despite ongoing dietary efforts to improve iodine supply, almost 2 billion people still suffer from mild to moderate ID worldwide (Andersson & Zimmermann, 2012; Pearce et al., 2013; WHO, 2015). In order to face iodine scarcity, many mechanisms of adaptation are readily activated inside and outside the thyroid gland. While thyrotropin (TSH) intervenes after severe ID to avoid hormonal deficit by stimulating both thyroid cell function and proliferation (Zimmermann, 2009), the thyroid gland continuously copes with moderate ID through several TSH-independent mechanisms, including the preferential synthesis of T3 over T4, the recycling of intracellular iodide, and the peripheral conversion of T4 into T3 (Pedraza et al., 2006; Kopp, 2008). In addition, thyrocytes constantly react to fluctuations in iodide availability by regulating their surrounding microvasculature (Gerard et al., 2008). This TSH-independent increase in blood flow is mediated, at least in part, by reactive oxygen species (ROS)-dependent stabilization of the □ subunit of hypoxia inducible factor (HIF). This transcription factor up-regulates vascular endothelial growth factor (VEGF) expression, leading to an increase in VEGF protein secretion by the thyrocytes which results in a rise in the local blood flow, probably in order to adapt iodide delivery (Gerard et al. 2008; Gerard et al. 2009). Although this microvascular activation is tightly controlled in healthy tissues, thyrocytes in a cancerous environment would lose the ability to fine-tune blood flow upon ID, thereby promoting tumor progression (Gerard et al., 2012).

Beside the thyroid gland, other organs express the iodide/sodium symporter (NIS), including salivary glands and the stomach, and might therefore be sensitive to ID. Both organs are characterized by active iodide uptake (MIRD, 1975; Bruno et al., 2004) probably to benefit from its antioxidant properties (Venturi and Venturi, 2007). Iodide is taken up at the basolateral membrane of the ductal cells in salivary glands and of mucin-secreting cells in the stomach. It is then secreted along its concentration gradient into the saliva and gastric fluids respectively (Brown-Grant, 1961; Josefsson et al., 2006). The physiological role for this iodide secretion is still uncertain, but evidence suggests that iodide may act as an antimicrobial agent in the saliva and gastric juice (Thomas et al., 1980; Geiszt et al., 2003; Portulano et al., 2014). It was hypothesized that salivary glands and the stomach could also be involved in systemic iodide recycling (Miller et al., 1975; Josefsson et al., 2002). As orally ingested iodide is normally absorbed by enterocytes to be partially cleared by the kidneys (Nicola et al., 2009), iodide taken up by salivary glands and the stomach could therefore escape from kidney clearance to be spared as a reserve potentially usable by the thyroid during ID periods.

Since salivary glands and the stomach are able to actively transport iodide, it is possible that they are also affected by ID. Consistently, in addition to the potential link between ID and dental carries (Venturi and Venturi, 2009), NIS expression was reported to be decreased in salivary glands during inflammation and tumor formation (La Perle et al., 2013). Accordingly, oxidized DNA and proteins are often found in oral cancers, possibly because of ID-associated oxidative stress (Bahar et al., 2007; Maier et al., 2007). Several studies also reported that ID is associated with stomach disorders. For instance, a higher rate of stomach cancers has been reported in iodine deficient areas in Poland, in China, and in Anatolia (Turkey) (Gulaboglu et al., 2005; Abnet et al., 2006; Golkowski et al., 2007). Moreover, patients with stomach cancer in Poland were more often diagnosed with goiter compared to the rest of the population when the country was still iodine-deficient. After iodine supplementation, both disorder rates decreased (Golkowski et al., 2007). At the molecular level, iodine concentration and NIS expression were reported to be lower in cancer tissues compared to the normal surrounding tissue (Gulaboglu et al., 2005; Altorjay et al., 2007).

While it seems that ID plays a role in different pathologies of diverse NIS-expressing organs, underlying mechanisms are still largely unknown. In this study, we investigated the potential effects of ID on the regulation of the local microvasculature in two NIS-expressing organs, salivary glands and stomach, and compared their biological response to ID to that of the thyroid.

Materials and methods

Animals and treatments

To induce ID, 8 week-old NMRI mice (strain 008, Harlan, Boxmeer, The Netherlands) were fed with a low-iodine diet (LID) (0.1 µg iodide/day; Animalabo, Brussels, Belgium) supplemented or not with 1% sodium perchlorate (a NIS inhibitor) in tap water for 1 to 10 days, or with a normal diet (0.4 mg iodide/kg, AO3, Scientific Animal Food and Engineering, Augy, France). ID was induced using the exact same protocol as in Gérard et al. (2008), where LID was combined with perchlorate (Bianco et al. 2014) in order to compare the effects of ID in the thyroid, the salivary glands and the stomach. Control animals received normal diet and tap water.

To inhibit VEGF-A, animals were injected intraperitoneally with a saline solution of bevacizumab (10 mg/kg; Roche, Welwyn Garden City, UK). Control animals were injected with an equimolar solution of irrelevant human IgGs (Sigma, St.-Louis, MO,

USA). In both groups, animals were either fed a normal diet (controls) or LID supplemented with 1% sodium perchlorate in drinking water for 2 days.
Mice were housed and handled according to the Belgian regulation of Laboratory Animal Welfare. All *in vivo* experiments were performed with approval of UCL *Comité d'Ethique pour l'Expérimentation Animale* according to national and European animal care regulations.

Laser Doppler blood flow measurement and preparation of tissue samples

Mice were anesthetized with Ketamine (Anesketin, Eurovet, Belgium) and Xylasine (Rompun, Bayer HealthCare; Belgium) and placed on a heating pad (37°C). The skin was then incised and pulled aside to expose the submandibular glands, which are the most accessible salivary glands for blood flow measurements. Blood flow was measured using a Laser Doppler imager (Moor Instruments, Axminster, UK). Submandibular glands were identified and delineated based on anatomical images and blood flow was quantified based on corresponding colored histogram pixels. After measurements, mice were euthanized with an overdose of pentothal (Abbott, Louvain, Belgium). Stomach and submandibular salivary glands were collected. Emptied stomach and a portion of salivary glands were fixed in paraformaldehyde (4% in phosphate-buffered saline [PBS]) for 36 hours and embedded in paraffin. Thick sections (5 µm) were used for immunohistochemistry and immunofluorescence. The remaining submandibular salivary glands were directly frozen in liquid nitrogen and used for protein analysis.

Western blots

Samples of salivary gland were homogenized into Laemmli buffer (10ml Glycerol, 2g SDS, 0.756g Tris-hydroxymethylaminomethan, 0.19g EDTA (5mM) in a 100 ml distilled water solution) containing protease inhibitors (protease inhibitor cocktail tablets, Roche, Mannheim, Germany) and sonicated for 15 seconds. The protein content was measured using a BCA Protein assay kit (Pierce, Rockford, IL) according to manufacturer's protocol. Western blotting was performed as previously described (Gerard et al., 2012). Primary antibodies were incubated overnight at 4°C and secondary antibodies were incubated for one hour at room temperature (Table 1). Signal was detected using the Supersignal West Pico/Femto chemiluminescence kit from Thermo Scientific (Waltham, MA, USA). Western blots were scanned and the protein content of each sample was quantified by densitometry using NIH Scion ImageAnalysis Software (National Institutes of Health, Bethesda, MA). Protein levels were normalized to those of β-actin and GAPDH.

Protein	Primary Antibody	Primary antibody Dilution	Secondary antibody
HIF-1α	human/mouse/rat hif-1α, MAB-1536, R&D Systems	1:500	Biotinylated anti-Mouse, 1:200 (BA-9200, Labconsult)
NIS	NIS, SMC-391D, Stress Marq Biosciences Inc.	1:1000	Biotinylated anti-Mouse 1:200 (BA-9200, Labconsult)
β-Actin	β-Actin, A5060, Sigma	1:5000	Goat anti-Rabbit Poly-HRP 1:5000(32260, Pierce)
VEGFR1	VEGF R1/Flt-1, AF471, R&D systems	1/1000	Biotinylated anti-Goat, 1:200 (BA-9500, Labconsult)
VEGFR2	VEGFR2/Flk-1, sc-6251, Santa Cruz Biotechnology	1/800	Biotinylated anti-Mouse 1:200 (BA-9200, Labconsult)

Table 1: Western blot, primary and secondary antibody dilutions for HIF-1α, mNIS, β-actin, VEGFR1 and VEGFR2 proteins detection

Immunohistochemistry

Immunohistochemistry was performed as previously described (Gerard et al., 2012). For VEGF-A detection, antigen retrieval was carried out: tissue sections were treated in a microwave oven in citrate buffer (0.01 M, pH 6) for one cycle of 3 min at 750 W, followed by 4 cycles of 3.5 min at 350 W. Then, sections were blocked in 1:50 non-immune goat serum (Vector Laboratories, Burlingame, CA, USA) in PBS/BSA 5% (albumin fraction V from bovine serum, VWR) for 30 min at room temperature. Antibodies, incubation times and dilutions are listed in Table 2. Primary antibodies were omitted in negative controls. Peroxidase activity was revealed with 3,3'-diaminobenzidine (DakoCytomation, Heverlee, Belgium). Sections were counterstained with Mayer's hematoxylin. Images were captured on an Axio scope A.1 microscope (Zeiss, Zaventem, Belgium) equipped with a DS-5Mc Color Digital Camera Head (Nikon, Amsterdam, The Netherlands).

Protein	Primary antibody	Primary antibody dilution and incubation time	Secondary antibody	Secondary antibody dilution and incubation time
VEGF-A	VEGF-A, SC-53462, Santa Cruz Biotechnology	-Salivary glands 1:75, o/n -Stomach 1:50, o/n	Goat anti-mouse poly-HRP, 32230, Pierce	1/50, 1 hour
NIS	NIS, a gift from Nancy Carrasco, Yale University School of Medicine, USA (Levy *et al.* 1997)	-Salivary glands 1 :1500, 1 hour Stomach 1:4000, 1 hour	Goat anti-rabbit poly-HRP, 32260, Pierce	1/50, 1 hour

Table 2: Immunohistochemistry, primary and secondary antibody dilutions for VEGF-A and mNIS proteins detection

Immunofluorescence

Sections from paraffin-embedded tissues were dewaxed in toluene and rehydrated in a series of graded alcohols to distilled water. Sections were washed three times in PBS-Triton X-100 (Sigma-Aldrich, St.-Louis, MO, USA) between each of the following steps. Slices were first quenched with $NaBH_4$ (10 mg/ml H_2O; sodium borohydride, Sigma-Aldrich). Antigen retrieval was performed as described above. After cooling down for 15 min, slices were blocked for 1 h in PBS/BSA 5%, and incubated at 4ºC overnight with primary antibodies (VEGF-A, SC-152, Santa Cruz Biotechnology, 1/100; Ghrelin, SC-10368, Santa Cruz Biotechnology, 1/500) in PBS/BSA 2%. Primary antibodies were omitted in negative controls. Signals were revealed by 1-h incubation at room temperature in the dark with species-specific secondary antibodies conjugated to fluorophores (First: Alexa Fluor 488-conjugated donkey anti-goat, A-11055, Invitrogen, 1/300; second: Alexa Fluor 568-conjugated goat anti-rabbit, A11036, Invitrogen, 1/300) in PBS/BSA 1%. Nuclei were stained for 5 minutes with 4'-6'diamidino-2-phenylindole (DAPI, 1/10,000) and slides were mounted in Fluorescent Mounting Medium (Dako Cytomation). Images were captured on an AxioCam MRc5 fluorescence microscope using the Axio Vision 4.8 software (Zeiss).

Data analysis and statistics

All data are expressed as mean ± SEM. Experiments were conducted on groups of at least 3 mice and repeated independently 2 to 3 times (N=6-9), except for control experiment at days 20 and 30 (N=3). Statistical analysis was performed using one-way ANOVA with a Tukey-Kramer or a Dunnett multiple comparison or post hoc test or by using an unpaired Student *t* test when appropriate (GraphPad Instat, San Diego, CA, USA). $P < 0.05$ was considered as statistically significant.

Results

Salivary glands

ID increases blood flow in salivary glands

Differences in basal blood flow in submandibular salivary glands were observed between male and female mice (**fig. 1**). The results were therefore segregated by gender. A significant increase in blood flow was observed from day 1 to day 4 after ID induction in males and at day 2 in females (**fig. 1A**). Blood flow then decreased to reach control levels at days 10 and 4, respectively. Although both male and female mice showed a transient rise in blood flow, the increase was proportionally stronger in males. A second experiment, with longer monitoring time showed no further changes in submandibular salivary glands up to 30 days after ID induction (**fig. 1B**).

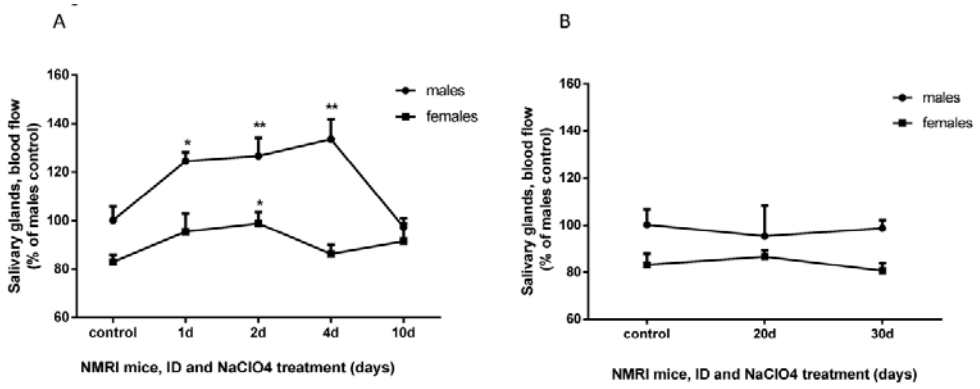

Fig. 1.*: NMRI mice salivary gland blood flow after 0, 1, 2, 4 and 10 days of ID (**1a**) or after 20 and 30 days (**1b**).* ***A****. Values are expressed as means ± SEM, N=9.* ***B****. Values are expressed as means ± SEM, N=3. *p value < 0,05, **p value <0,01.*

To discriminate between the LID-associated effects *versus* NIS inhibition by perchlorate and to eliminate the possibility that observed effects were due to an off-target effect of perchlorate, control experiments were carried out using either LID alone or perchlorate alone. In males, LID treatment without perchlorate induced a significant transient increase in submandibular salivary gland blood flow at day 2 (supplemental data, fig. 1A), but no significant increase was seen in females at day 2, despite a trend (supplemental data, fig. 1B). Conversely, perchlorate alone did not modulate blood flow significantly (supplemental data, fig. 1C and D). Thus, salivary glands respond to ID by increasing local blood flow with additive effects between LID and perchlorate, at least in females.

ID increases HIF-1α and VEGF protein expression in salivary glands

In male mice, HIF-1α protein level was significantly increased at days 1 and 2 following ID induction, and decreased back to basal levels at days 4 and 10 (**fig. 2A**). In females, HIF-1α protein expression increased at day 1 of ID to remain high up to day 10 (**fig. 2B**).

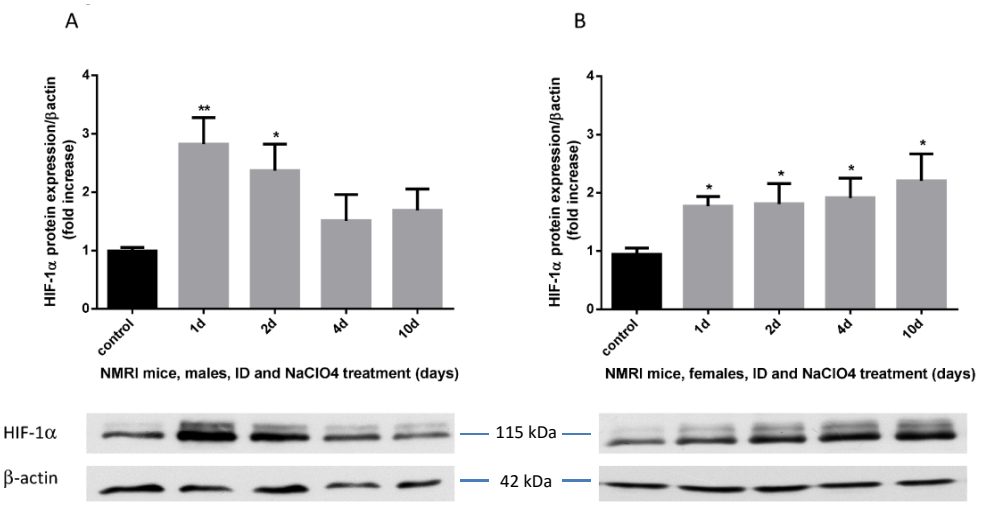

***Fig. 2**. HIF-1α protein expression in salivary glands of male (2a) and female (2b) NMRI mice after 0, 1, 2, 4 and 10 days of ID. Values are expressed as means ± SEM, N=9. *p value < 0,05, **p value <0,01.*

Low expression of VEGF was detected using immunohistochemistry in duct cells of the submandibular salivary glands of both male (**fig. 3A**) and female (f**ig. 3B**) control mice. From day 1 to day 4 of ID, VEGF immunostaining increased (**fig. 3C-D**), to

decrease thereafter and reach the control level at day 10 (**fig. 3E-F**) in both male and female mice. Weak VEGF staining was also observed in the stroma between acini from day 2 to day 4 (**fig. 3C-D**).

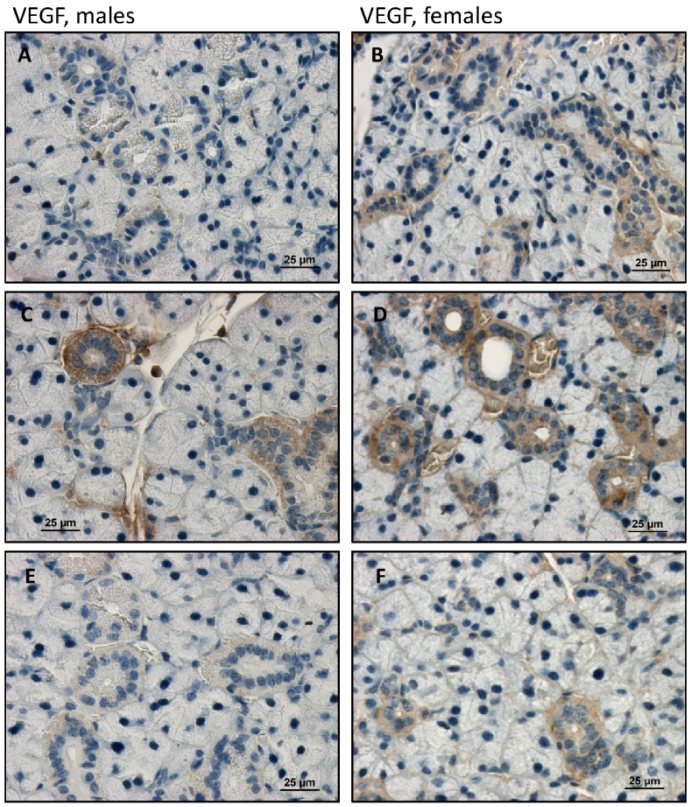

Fig. 3. *Analysis of VEGF expression by immunohistochemistry in salivary glands (serous acini and ducts):* ***A,B.*** *Control.* ***C,D.*** *ID 2 day.* ***E,F****. ID 10 days. Magnification: x40.*

In order to prove the role of VEGF in ID-induced increase in salivary gland blood flow, the experiment was repeated with and without VEGF blocking antibody bevacizumab (Bock et al. 2007). In both male (**fig. 4A**) and female (**fig.4B**) mice treated with irrelevant IgG, ID induced a significant rise in blood flow after 2 days of treatment, whereas blood flow was unchanged upon bevacizumab treatment. The blood flow was not affected by bevacizumab in control mice. Moreover, Western blot analyses of VEGF receptor 1 and 2 showed that their expression remained unchanged in mice treated with bevacizumab compared to control mice (supplemental data, fig. 2) indicating that the expression of VEGF receptors 1 and 2

was not influenced by bevacizumab treatment. Thus, VEGF is at least partly responsible for the observed increase in blood flow in submandibular salivary glands during ID.

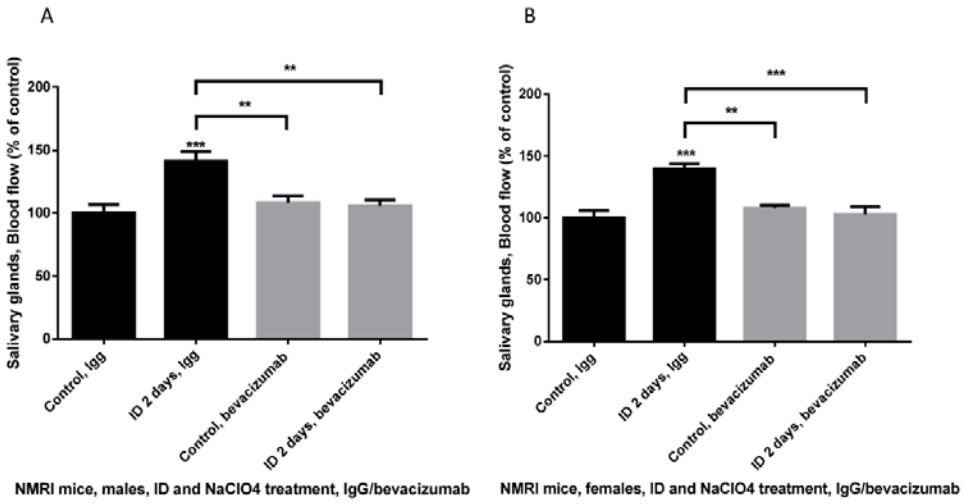

Fig. 4. *Salivary gland blood flow after 0 or 2 days of ID in male (4a) and female (4b) mice pre-injected with bevacizumab or IgG in order to assess VEGF involvement in blood flow levels. Values are expressed as means ± SEM, N=6. *p value < 0,05, **p value <0,01, ***p value < 0,001.*

ID promotes NIS protein expression in salivary glands

Because salivary glands express the sodium/iodide symporter NIS (MIRD, 1975; Bruno et al., 2004), we looked at NIS expression in condition of ID to check whether decreased iodide bioavailability triggers NIS expression to optimize cellular iodine uptake. The immunohistochemical analysis showed that NIS expression in submandibular salivary glands is restricted to basolateral membranes of ductal cells (**fig. 5A-B**). NIS expression increased in male and female mice over 2 days of ID (**fig. 5C-D**), to decrease down to basal expression between days 4 and 10 (**fig. 5E-F**). Changes were slightly more pronounced in males compared to females. ID-induced NIS protein expression increase was confirmed by Western blotting (supplemental data, fig. 3).

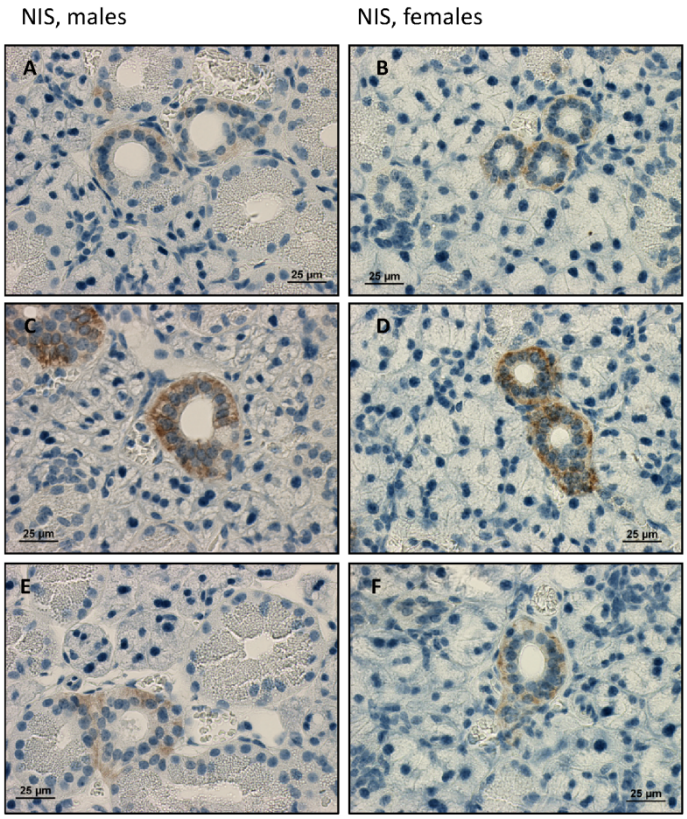

***Fig. 5**. Analysis of NIS expression by immunohistochemistry in salivary glands (serous acini and ducts). **A,B**. Control. **C,D**. ID 2 day. **E,F**. ID 10 days. Magnification: x40.*

Because NIS is the direct target of perchlorate, but perchlorate as a single treatment did not modify blood flow significantly in salivary glands, we compared NIS expression in animals treated with LID alone or perchlorate alone (Supplemental data fig. 4). In males, LID and perchlorate used separately increased NIS expression at days 4 and 2, respectively. Similar data were obtained in female mice. NIS expression increase due to LID was delayed by 2 days compared to perchlorate treatment alone or LID/perchlorate co-treatment, confirming that perchlorate is used at a bioactive dose in our *in vivo* assays.

Stomach

ID stimulates VEGF expression in the stomach

Immunohistochemical detection showed no VEGF expression in mucin-secreting cells of control mice, but few capillaries underneath the epithelial layer were positively stained (**fig. 6A**). Additionally, a few small cells located at the bottom of the tubular glands and surrounding the tubular glands showed positive cytoplasmic staining (**fig. 6B**). After 1 day of ID, more capillaries under the mucin-secreting epithelium and more cells in tubular glands were stained (**fig. 6D-E**). After 2 days of ID, increased VEGF staining was also observed inside the cytoplasm of most mucin-secreting cells, which are NIS-expressing cells (**fig. 6G**). The increase in VEGF expression lasted until day 4 of ID, after which it decreased up to day 10 (**fig. 6J-K**). Compared to control mice, VEGF signal at day 10 of ID was slightly stronger in the vessels underneath mucin-secreting cells, but not in the small cells located in the tubular glands. Additional experiments showed that LID and perchlorate as separate treatments did increase VEGF expression (supplemental data fig. 5A).

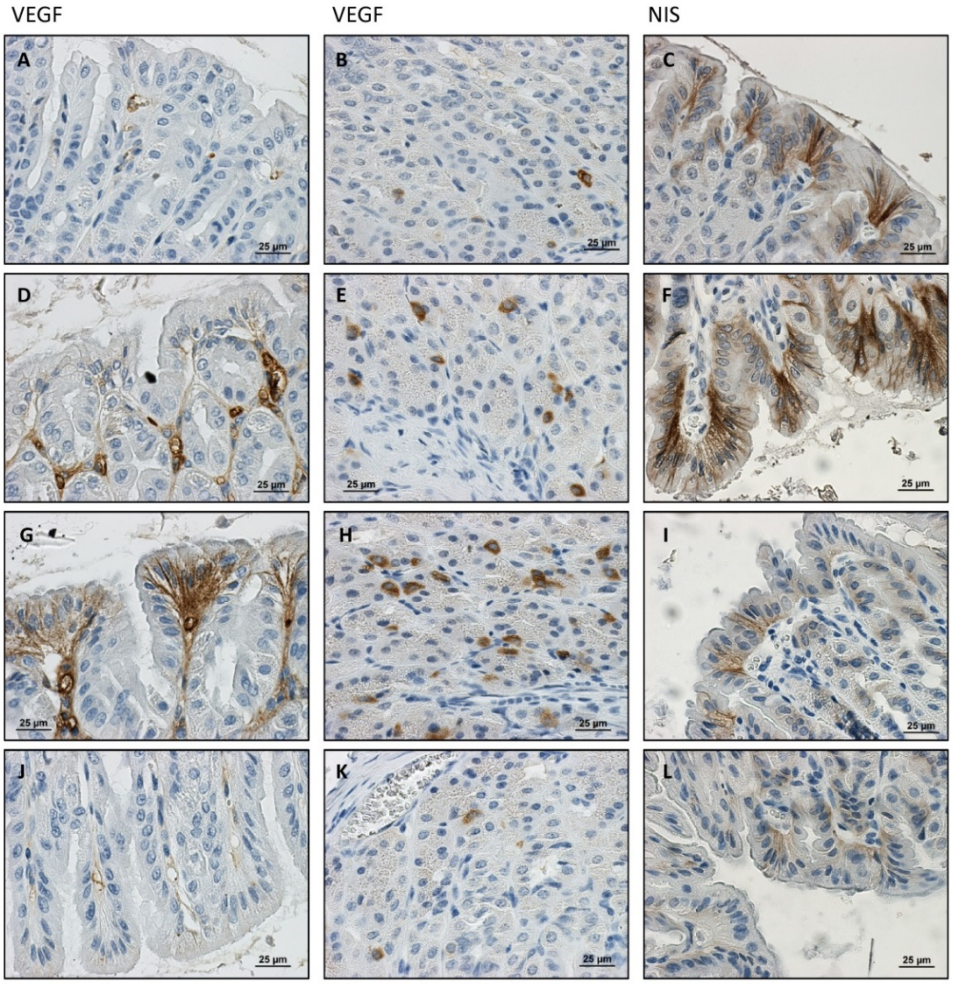

Fig. 6. *Analysis of VEGF and NIS expression by immunohistochemistry in stomach. :**A,B.** VEGF, control. **C.** NIS, control. **D,E.** VEGF, ID 1 day. **F.** NIS, ID 1 day. **G,H**. VEGF, ID 2 days. **I.** NIS, ID 2 days. **J,K.** VEGF, ID 10 days. **L.** NIS, ID 10 days. Magnification: x40.*

The cells expressing VEGF at the bottom of the tubular gland during ID were localized around the tubular glands and their size was smaller than that of parietal cells. As these characteristics are compatible with gastric endocrine cells, we performed a double immunofluorescence staining for both VEGF and a well expressed gastric hormone, ghrelin (**fig. 7**). In control mice, ghrelin-expressing cells (G-cells) did not express VEGF (**fig. 7A-C**), whereas the vast majority of G-cells were double stained with VEGF in ID mice (**fig. 7D-F**). Of note, a few cells expressed VEGF, but not ghrelin, in ID mice.

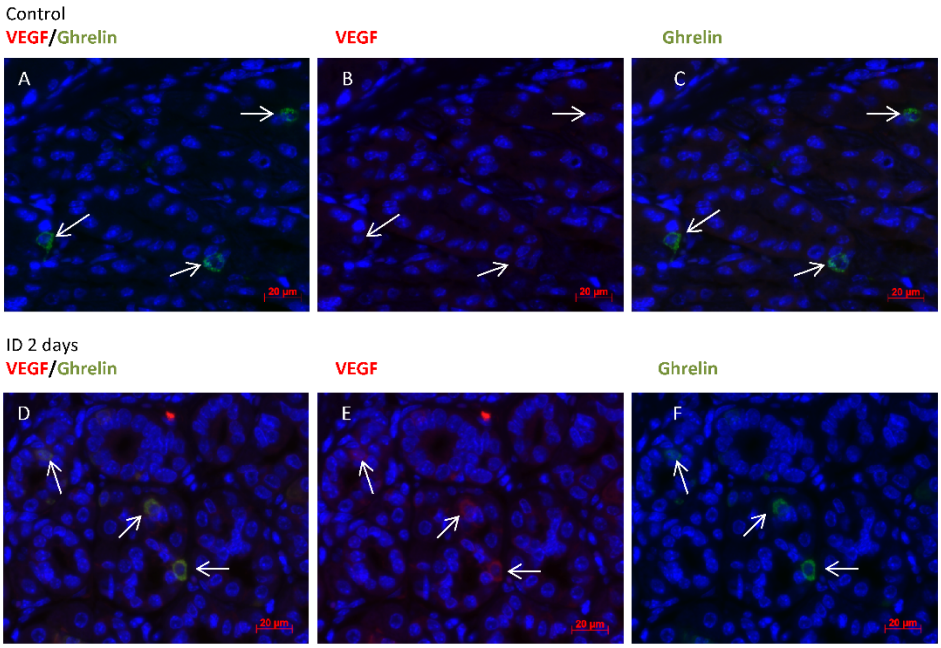

***Fig. 7**. Analysis of VEGF and ghrelin expression by immunofluorescence in stomach. **A, B, C**. Control. **D, E, F.** ID, 2 days. Red: VEGF. Green: Ghrelin. **A, D**. VEGF/Ghrelin double staining. **B, E**. VEGF staining. **C, F**. Ghrelin staining. Magnification: x40.*

ID induces a slight increase followed by a decrease in NIS expression.

NIS protein expression was also looked at in the stomach. In basal conditions, a positive immunohistochemical staining for NIS was visible only at the basolateral membrane of mucin-secreting cells (**fig. 6C**), but not in parietal cells. ID induced a weak increase in NIS staining at day 1 (**fig. 6F**), which was followed by a strong decrease from day 2 to 10 (**fig. 6I, L**). LID and perchlorate as separate agents both induced a decrease in NIS expression on day 2 (supplemental data, fig. 5B), confirming that NIS expression is controlled by ID rather than by any off-target effect of perchlorate. Thus, in contrast to the salivary glands, ID induced only a slight increase which was followed by a strong decrease in NIS expression in the stomach.

Discussion

While several epidemiological studies have associated ID to disorders in salivary glands and in the stomach (Gulaboglu et al., 2005; Abnet et al., 2006; Golkowski et al., 2007; Venturi and Venturi, 2009; La Perle et al., 2013), few studies have addressed the molecular effects of ID in these organs. Here, we report that, as already described in the thyroid (Gerard *et al.* 2008), salivary glands and the stomach respond to ID by inducing a microvascular response.

A striking similarity between these three NIS-expressing tissues is the rapid ID-induced increase in VEGF expression and in the local blood flow (at least in salivary glands and thyroid). In the thyroid, the microvascular response that occurs in response to ID to improve the local supply of iodide is biphasic (Gerard et al., 2008). An early transient TSH-independent response occurs already at day 1 of ID with thyrocytes releasing VEGF which directly acts on adjacent capillaries. A second delayed phase then takes place when ID-induced impaired thyroid hormone synthesis triggers TSH production from the pituitary gland which further stimulates VEGF secretion from thyrocytes. In salivary glands and in the stomach, a rapid, but only transient, ID-induced increase in VEGF expression was observed and it was associated with an increase in blood flow in the salivary glands. This may also occur in the stomach but this hypothesis cannot be verified because the gastric mucosa is not accessible for Laser Doppler measurements due to the presence of muscles. We therefore focused on VEGF as ID response effector and documented increased VEGF staining in small blood vessels close to mucin secreting epithelial cells, which are known to express NIS (Altorjay et al. 2007), while only few of them were positively stained in control mice, suggesting endothelial activation by VEGF during ID in the stomach. In contrast with the thyroid, the delayed TSH-dependent phase was not observed, which is in accordance with the fact that salivary glands and the stomach are not sensitive to TSH signaling (Viglietto et al., 1997; Josefsson et al., 2006; Gerard et al., 2008; Portulano et al., 2014).

In their early transient response to ID, the thyroid and salivary glands share a similar molecular pathway. In both organs ((Gerard et al., 2008; Gerard et al., 2009) and this study), increased blood flow is preceded by an increased expression of HIF-1 transcription factor subunit α. This subunit is known to bind to HIF-1β to form active HIF-1 and to stimulate the expression of target genes including VEGF. Accordingly, ID increases VEGF production by thyrocytes (Gerard et al., 2008; Gerard et al., 2009), and by ductal cells in serous acini of the salivary glands. The active contribution of VEGF to the increased microvascular perfusion was clearly

demonstrated in salivary glands where bevacizumab inhibited ID effects. This does not rule out the potential involvement of other pro-angiogenic factors such as FGF2 in response to ID, as already reported in the thyroid (Gerard et al., 2008; Gerard et al., 2009). Like thyrocytes and ductal cells of the salivary glands, mucin-secreting epithelial cells in the stomach are NIS expressing cells (Jhiang et al., 1998; Altorjay et al., 2007) and also responded to ID by increasing VEGF production. It is therefore reasonable to postulate that, as already reported in the thyroid gland, NIS-expressing cells in salivary glands and in the stomach are sensitive to ID. In addition to mucin-secreting cells, ghrelin positive endocrine cells also overexpressed VEGF when exposed to ID, even though NIS expression was not reported in gastric endocrine cells to our knowledge (Kotani et al., 1998; Vayre et al., 1999; Altorjay et al., 2007). Moreover, a few cells located at the bottom end of the tubular glands did overexpress VEGF but not ghrelin. Based on their localization and because they were of the same size as ghrelin-expressing cells, it is reasonable to propose that they correspond to another type of gastric endocrine cells. While it is also possible that among those cells, a few are mast cells, which are known to secrete VEGF (Ribatti and Crivellato, 2012), mast cells were too few in the stroma between the glands (unpublished results), to account for the population of cells expressing VEGF but not ghrelin. We cannot yet interpret the physiological relevance of this observation that obviously requires further investigations.

It is proposed that iodide exerts antioxidative effects, which may explain the early release of ROS and nitric oxide (NO) in response to ID in the thyroid gland. In this organ, ROS and NO can stabilize HIF-1α and activate HIF-1 during ID in thyroid cells (Gerard et al., 2008; Gerard et al., 2009; Craps et al., 2015). Thus, it is likely that redox stress initiates the HIF-1-VEGF response to ID in NIS-expressing cells, which will be addressed experimentally in further investigation. Similarly, it remains to be determined if the changes in NIS expression induced by ID in salivary glands and in stomach originates from a redox imbalance. *NIS* is not a HIF-1 target gene (Yeom et al., 2008), but its expression is sensitive to redox changes (Serrano-Nascimento et al., 2014). However, NIS expression is transiently increased in salivary glands and only slightly increased, then decreased in the stomach. Its regulation is thus influenced by iodide supply in both organs but may depend on different molecular pathways.

In the thyroid, salivary glands and stomach, functional consequences of the molecular responses to ID could represent strategies aimed at improving iodide supply. By increasing local perfusion, NIS-expressing cells would promote local iodide supply from blood. In salivary glands, a second strategy would be to increase NIS expression in duct cells, in order to optimize iodide uptake. Accordingly, cellular

responses were maximal when both iodine ingestion (LID) and NIS activity (perchlorate) were impaired. Although the role of iodide in salivary glands and the stomach has not yet been totally clarified, three possibilities have been evoked: an antioxidant, a bactericidal and a recycling function (Thomas et al., 1980; Josefsson et al., 2002; Geiszt et al., 2003; Venturi and Venturi, 2007, 2009; Portulano et al., 2014). Thus, when facing ID, salivary glands and the stomach might try to optimize iodide intake to benefit from its antioxidant and bactericidal properties. It is also possible that by recycling iodide into the blood circulation via the enteroenteric circulation, this would reduce its clearance through the kidneys, as suggested by Miller et al. (1975) and Josefsson et al. (2002), thereby optimizing iodide supply to the thyroid gland. This mechanism of iodide sparing should therefore be considered in addition to those activated by the thyroid, including the improved local supply of iodide through increased microvascular flow, the preferential synthesis of T3 over T4 and the internal recycling of unused mono- and di-iodotyrosines (Pedraza et al., 2006; Kopp, 2008). Further arguments are required to strengthen the validity of this hypothesis.

It is worth mentioning that a gender difference in the response to ID was observed. Gender-associated differences in salivary gland functions have already been reported in several studies (Ferguson and Stephen, 1972; Lazarus et al., 1974), but our observation that basal blood flow is higher in the submandibular salivary glands of male compared to female mice is, to our knowledge, unprecedented. In addition, male salivary glands showed a stronger response to ID. LID alone was sufficient to significantly enhance salivary gland blood flow while perchlorate alone had no significant effect in males. In females, maximal effects required combined treatment. Accordingly, while NIS is known to be expressed only in salivary ducts and iodide uptake has been observed in duct cells in both males and females (Ferguson and Stephen, 1972; Jhiang et al., 1998), a higher iodide concentration was reported in male compared to female ducts (Lazarus et al., 1974). Thus, the difference that we observed in the amplitude of salivary glands response to ID between males and females follows the same trend as the capacity of the glands to concentrate iodide. However, while a concordance was observed between changes in HIF-1α and VEGF levels and blood flow in males, HIF-1α levels remained elevated in females even after the end of the microvascular reaction, suggesting the existence of other molecular pathways that regulate ID-induced blood flow in a gender-specific manner.

In conclusion, our study reports that ID induces microvascular responses in salivary glands and in the stomach similar to those previously observed in the

thyroid. It is reasonable to postulate that this microvascular activation that occurs in response to ID in these two NIS-expressing tissues contributes to optimize as much as possible the local delivery of iodide in periods of iodide deprivation.

Acknowledgments

This study has been supported by grants from the *Fonds National de la Recherche Scientifique* (F.R.S.-FNRS) (project J.0112.13), the Belgian Federal Agency for Nuclear Control (AFCN-FANC) and FP7/2007-2013 ERC Independent Researcher Starting Grant 243188 TUMETABO to PS. PS is a Research Associate of the F.R.S.-FNRS. The authors thank Benoît Lengelé, head of the pole of Morphologie Expérimentale, for his support. Authors also thank Nancy Carrasco (Yale University School of Medicine, CT, USA) and Françoise Miot (ULB, Brussels, Belgium) for the kind gift of anti-NIS antibody, Christine de Ville de Goyet (UCL) and Luminita Nae (Institut Paul Lambin, Brussels) for expert technical support, and Quentin Binet (UCL) for technical assistance.

Disclosure statement

The authors declare that no conflict of interest exists.

Supplemental data

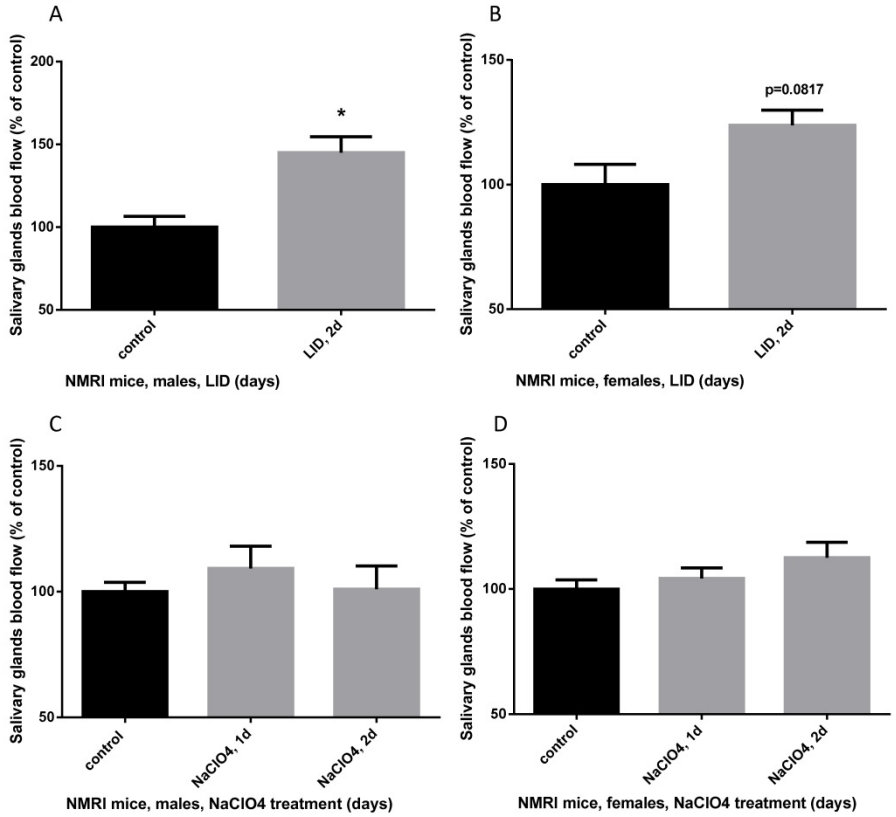

Fig. 1. LID treatment without perchlorate induces an increase in salivary glands blood flow in males but not in females while perchlorate alone had no effect. *Salivary glands blood flow after 0 or 2 days of LID in males (1a) and females (1b), N=4. Salivary glands blood flow after 0, 1 or 2 days of perchlorate treatment in males (1c) and females (1d), N=9. Values are expressed as means ± SEM. Statistical test: Unpaired Student's t test (A, B) or One-way ANOVA (C, D). *p value < 0,05.*

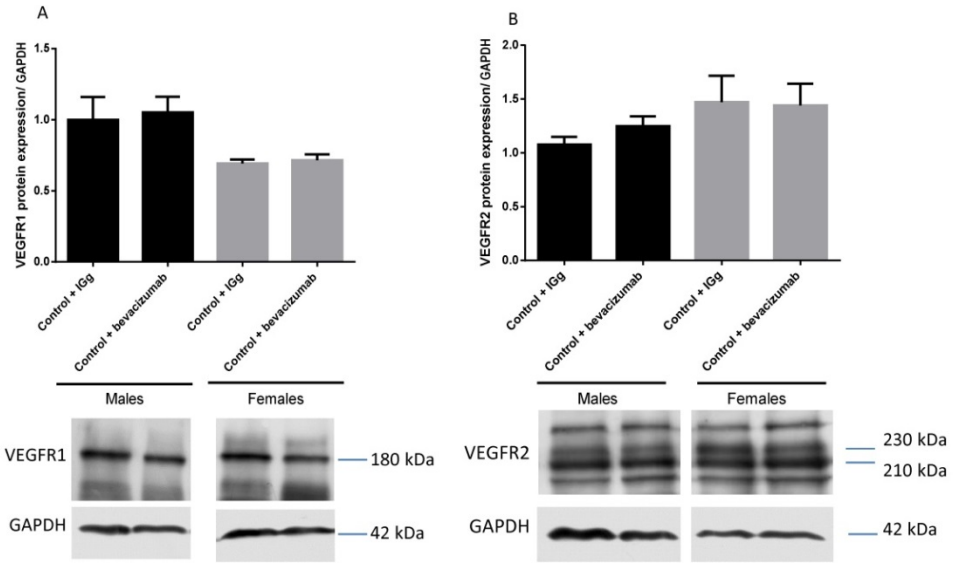

Fig. 2*. *Bevacizumab does not modify VEGF receptors expression in salivary glands. *VEGFR1,2 expression, western blot. A. VEGFR1 expression in males and females. B. VEGFR2 expression in males and females. Three different bands correspond to different glycosylation states. Statistical test: One-way ANOVA followed by a Bonferroni post-hoc test. Values are expressed as means ± SEM, N=6.*

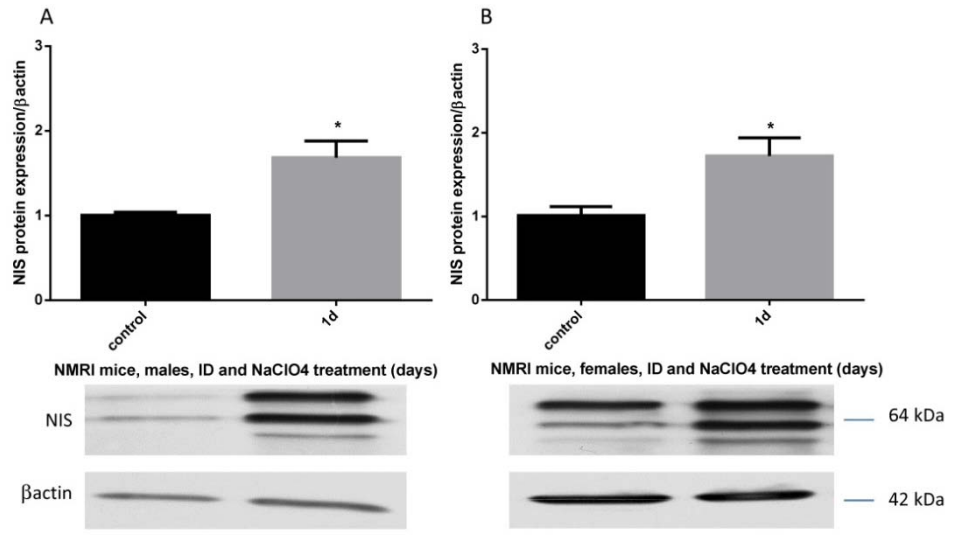

Fig. 3. NIS protein expression is increased by ID in salivary glands. *NMRI mice were exposed to ID and perchlorate for 1 day. NIS expression was studied by western blot in males (3A) and females (3B). Values are expressed as means ± SEM, N=8. *p value < 0,05.*

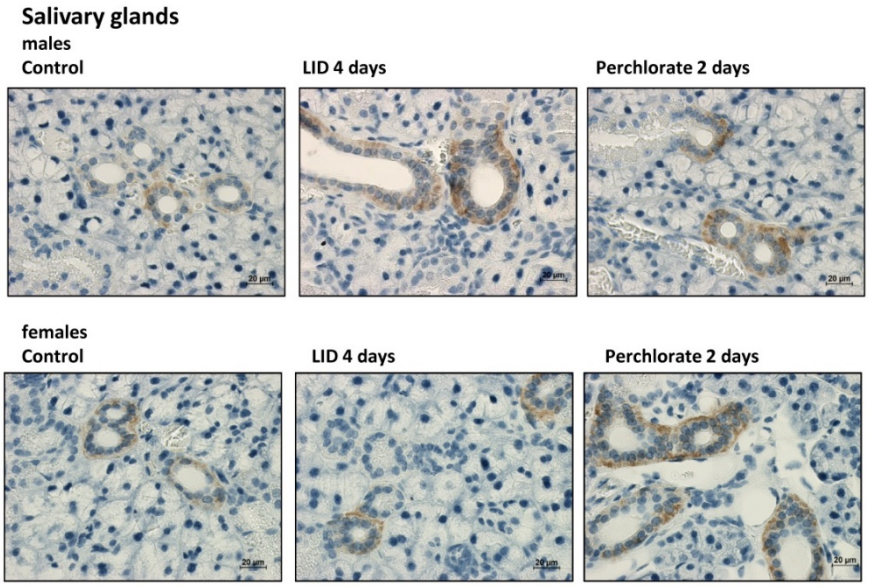

Fig. 4. LID and perchlorate treatment separately increase NIS expression in salivary glands. *Analysis of NIS expression by immunohistochemistry in salivary glands after LID (N=4) or perchlorate (N=9) treatment. Magnification: x40.*

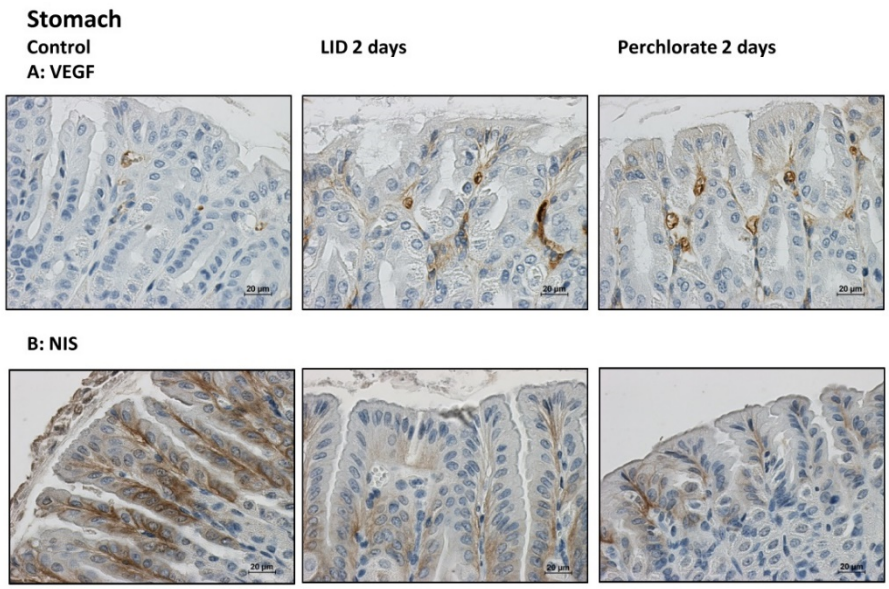

Fig. 5. LID and perchlorate treatment separately increase VEGF expression and decrease NIS expression in stomach. *Analysis of VEGF and NIS expression by immunohistochemistry in stomach after LID (N=4) or perchlorate (N=9) treatment. Magnification: x40.*

Reference List

Abnet C.C., Fan J.H., Kamangar F., Sun X.D., Taylor P.R., Ren J.S., Mark S.D., Zhao P., Fraumeni J.F., Jr., Qiao Y.L. and Dawsey S.M. (2006). Self-reported goiter is associated with a significantly increased risk of gastric noncardia adenocarcinoma in a large population-based Chinese cohort. Int. J. Cancer 119, 1508-1510.

Altorjay A., Dohan O., Szilagyi A., Paroder M., Wapnir I.L. and Carrasco N. (2007). Expression of the Na+/I- symporter (NIS) is markedly decreased or absent in gastric cancer and intestinal metaplastic mucosa of Barrett esophagus. BMC Cancer 7, 5.

Andersson M. and Zimmermann M., (2012). Global iodine nutrition: a remarkable leap forward in the past decade. IDD newsletter 40.

Bahar G., Feinmesser R., Shpitzer T., Popovtzer A. and Nagler R.M. (2007). Salivary analysis in oral cancer patients: DNA and protein oxidation, reactive nitrogen species, and antioxidant profile. Cancer 109, 54-59.

Bianco A.C., Anderson G., Forrest D., Galton V.A., Gereben B., Kim B.W., Kopp P.A., Liao X.H., Obregon M.J., Peeters R.P., Refetoff S., Sharlin D.S., Simonides W.S., Weiss R.E. and Williams G.R. (2014). American Thyroid Association Guide to investigating thyroid hormone economy and action in rodent and cell models. Thyroid 24, 88-168.

Bock F., Onderka J., Dietrich T., Bachmann B., Kruse F.E., Paschke M., Zahn G. and Cursiefen C. (2007). Bevacizumab as a potent inhibitor of inflammatory corneal angiogenesis and lymphangiogenesis. Invest. Ophthalmol. Vis. Sci. 48, 2545-2552.

Brown-Grant, K. (1961). Extrathyroidal iodide concentrating mechanisms. Physiol. Rev. 41, 189-213.

Bruno R., Giannasio P., Ronga G., Baudin E., Travagli J.P., Russo D., Filetti S. and Schlumberger M. (2004). Sodium iodide symporter expression and radioiodine distribution in extrathyroidal tissues. J. Endocrinol. Invest. 27, 1010-1014.

Craps J., Wilvers C., Joris V., De J.B., Vanderstraeten J., Lobysheva I., Balligand J.L., Sonveaux P., Gilon P., Many M.C., Gerard A.C. and Colin I.M. (2015). Involvement of nitric oxide in iodine deficiency-induced microvascular remodeling in the thyroid gland: role of nitric oxide synthase 3 and ryanodine receptors. Endocrinology 156, 707-720.

Ferguson M.M. and Stephen K.W. (1972). Sex differences in the autoradiographic pattern of (125 I)iodide uptake in mouse submandibular salivary gland. Arch. Oral Biol. 17, 1117-1119.

Geiszt M., Witta J., Baffi J., Lekstrom K. and Leto T.L. (2003). Dual oxidases represent novel hydrogen peroxide sources supporting mucosal surface host defense. FASEB J. 17, 1502-1504.

Gerard A.C., Humblet K., Wilvers C., Poncin S., Derradji H., de Ville de G.C., Abou-el-Ardat K., Baatout S., Sonveaux P., Denef J.F. and Colin I.M. (2012). Iodine-deficiency-induced long lasting angiogenic reaction in thyroid cancers occurs via a vascular endothelial growth

factor-hypoxia inducible factor-1-dependent, but not a reactive oxygen species-dependent, pathway. Thyroid 22, 699-708.

Gerard A.C., Poncin S., Audinot J.N., Denef J.F. and Colin I.M. (2009). Iodide deficiency-induced angiogenic stimulus in the thyroid occurs via HIF- and ROS-dependent VEGF-A secretion from thyrocytes. Am. J. Physiol. Endocrinol. Metab. 296, E1414-E1422.

Gerard A.C., Poncin S., Caetano B., Sonveaux P., Audinot J.N., Feron O., Colin I.M. and Soncin F. (2008). Iodine deficiency induces a thyroid stimulating hormone-independent early phase of microvascular reshaping in the thyroid. Am. J. Pathol. 172, 748-760.

Golkowski F., Szybinski Z., Rachtan J., Sokolowski A., Buziak-Bereza M., Trofimiuk M., Hubalewska-Dydejczyk A., Przybylik-Mazurek E. and Huszno B. (2007). Iodine prophylaxis--the protective factor against stomach cancer in iodine deficient areas. Eur. J. Nutr. 46, 251-256.

Gulaboglu M., Yildiz L., Celebi F., Gul M. and Peker K. (2005). Comparison of iodine contents in gastric cancer and surrounding normal tissues. Clin. Chem. Lab. Med. 43, 581-584.

Jhiang S.M., Cho J.Y., Ryu K.Y., DeYoung B.R., Smanik P.A., McGaughy V.R., Fischer A.H. and Mazzaferri E.L. (1998). An immunohistochemical study of Na+/I- symporter in human thyroid tissues and salivary gland tissues. Endocrinology 139, 4416-4419.

Josefsson M., Evilevitch L., Westrom B., Grunditz T. and Ekblad E. (2006). Sodium-iodide symporter mediates iodide secretion in rat gastric mucosa in vitro. Exp. Biol. Med.(Maywood.) 231, 277-281.

Josefsson M., Grunditz T., Ohlsson T. and Ekblad E. (2002). Sodium/iodide-symporter: distribution in different mammals and role in entero-thyroid circulation of iodide. Acta Physiol. Scand. 175, 129-137.

Kopp P.A. (2008). Reduce, recycle, reuse--iodotyrosine deiodinase in thyroid iodide metabolism. N. Engl. J. Med. 358, 1856-1859.

Kotani T., Ogata Y., Yamamoto I., Aratake Y., Kawano J.I., Suganuma T. and Ohtaki S (1998). Characterization of gastric Na+/I- symporter of the rat. Clin. Immunol. Immunopathol. 89, 271-278.

La Perle K.M., Kim D.C., Hall N.C., Bobbey A., Shen D.H., Nagy R.S., Wakely P.E., Jr., Lehman A., Jarjoura D. and Jhiang S.M. (2013). Modulation of sodium/iodide symporter expression in the salivary gland. Thyroid 23, 1029-1036.

Lazarus J.H., Harden R.M. and Robertson J.W. (1974). Quantitative studies of the inhibitory effect of perchlorate on the concentration of 36C1O minus 4 125I minus and 99mTcO minus 4 in salivary glands of male and female mice. Arch. Oral Biol. 19, 493-498.

Levy O., Dai G., Riedel C., Ginter C.S., Paul E.M., Lebowitz A.N. and Carrasco N. (1997). Characterization of the thyroid Na+/I- symporter with an anti-COOH terminus antibody. Proc. Natl. Acad. Sci. U.S.A 94, 5568-5573.

Maier J., van S.H., van O.C., Paschke R., Weiss R.E. and Krohn K. (2007). Iodine deficiency activates antioxidant genes and causes DNA damage in the thyroid gland of rats and mice. Biochim. Biophys. Acta 1773, 990-999.

Miller J.K., Swanson E.W. and Spalding G.E. (1975). Iodine absorption, excretion, recycling, and tissue distribution in the dairy cow. J. Dairy Sci. 58, 1578-1593.

MIRD (1975). Summary of current radiation dose estimates to humans from 123I, 124I, 125I, 126I, 130I, 131I, and 132I as sodium iodide. J. Nucl. Med. 16, 857-860.

Nicola J.P., Basquin C., Portulano C., Reyna-Neyra A., Paroder M. and Carrasco N. (2009). The Na+/I- symporter mediates active iodide uptake in the intestine. Am. J. Physiol. Cell Physiol. 296, C654-C662.

Pearce E.N., Andersson M. and Zimmermann M.B. (2013). Global iodine nutrition: Where do we stand in 2013? Thyroid 23, 523-528.

Pedraza P.E., Obregon M.J., Escobar-Morreale H.F., del Rey F.E. and de Escobar G.M. (2006). Mechanisms of adaptation to iodine deficiency in rats: thyroid status is tissue specific. Its relevance for man. Endocrinology 147, 2098-2108.

Portulano C., Paroder-Belenitsky M. and Carrasco N. (2014). The Na+/I- symporter (NIS): mechanism and medical impact. Endocr. Rev. 35, 106-149.

Ribatti D. and Crivellato E. (2012). Mast cells, angiogenesis, and tumour growth. Biochimica et Biophysica Acta (BBA) - Molecular Basis of Disease, 1822, 2-8.

Serrano-Nascimento C., da Silva T.S., Nicola J.P., Nachbar R.T., Masini-Repiso A.M. and Nunes M.T. (2014). The acute inhibitory effect of iodide excess on sodium/iodide symporter expression and activity involves the PI3K/Akt signaling pathway. Endocrinology 155, 1145-1156.

Thomas E.L., Bates K.P. and Jefferson M.M. (1980). Hypothiocyanite ion: detection of the antimicrobial agent in human saliva. J. Dent. Res. 59, 1466-1472.

Vayre L., Sabourin J.C., Caillou B., Ducreux M., Schlumberger M. and Bidart J.M. (1999). Immunohistochemical analysis of Na+/I- symporter distribution in human extra-thyroidal tissues. Eur. J. Endocrinol. 141, 382-386.

Venturi, S. and Venturi, M. (2007). Evolution of Dietary Antioxidant Defences. European Epi-Marker 11, 1-12.

Venturi S. and Venturi M. (2009). Iodine in evolution of salivary glands and in oral health. Nutr. Health 20, 119-134.

Viglietto G., Romano A., Manzo G., Chiappetta G., Paoletti I., Califano D., Galati M.G., Mauriello V., Bruni P., Lago C.T., Fusco A. and Persico M.G. (1997). Upregulation of the angiogenic factors PlGF, VEGF and their receptors (Flt-1, Flk-1/KDR) by TSH in cultured thyrocytes and in the thyroid gland of thiouracil-fed rats suggest a TSH-dependent paracrine mechanism for goiter hypervascularization. Oncogene 15, 2687-2698.

WHO: http://www.who.int/vmnis/database/iodine/iodine_data_status_summary/en/

Yeom C.J., Chung J.K., Kang J.H., Jeon Y.H., Kim K.I., Jin Y.N., Lee Y.M., Jeong J.M. and Lee D.S. (2008). Visualization of hypoxia-inducible factor-1 transcriptional activation in C6 glioma using luciferase and sodium iodide symporter genes. J. Nucl. Med. 49, 1489-1497.

Zimmermann M.B. (2009). Iodine deficiency. Endocr. Rev. 30, 376-408.

3.2 PAPER 2

Acute iodine deficiency induces a transient VEGF dependent microvascular response in mammary glands involving HIF-1, ROS and mTOR

Jessica Vanderstraeten[1], Hanane Derradji[2], Pierre Sonveaux[3],
Ides M. Colin[4], Marie-Christine Many[1], Anne-Catherine Gérard[4]

Submitted to the American Journal of Physiology, Cell Physiology

Under revision

Acute iodine deficiency induces a transient VEGF dependent microvascular response in mammary glands involving HIF-1, ROS and mTOR

Jessica Vanderstraeten[1], Hanane Derradji[2], Pierre Sonveaux[3], Ides M. Colin[4], Marie-Christine Many[1], Anne-Catherine Gérard[4]

Authors' affiliation

[1]Pole of Morphology, Institut de Recherche Expérimentale et Clinique (IREC), Université catholique de Louvain (UCL), Brussels, Belgium; [2]Radiobiology Unit**,** Belgian Nuclear Research Centre (SCK•CEN), Mol, Belgium; [3]Pole of Pharmacology and Therapeutics, Institut de Recherche Expérimentale et Clinique (IREC), Université catholique de Louvain (UCL), Brussels, Belgium; [4]Service d'Endocrino-Diabétologie, Centre Hospitalier Régional (CHR) Mons-Hainaut, Belgium.

Running head: Microvascular response to iodine deficiency in mammary glands

Corresponding Author: Jessica Vanderstraeten; jessica.vanderstraeten@uclouvain.be

Avenue Mounier 52, boîte B1.52.04, 1200 Woluwe-Saint-Lambert, Belgium Phone number: +32 2 764 52 59

Abstract

Iodine deficiency (ID), which affects almost two billion people worldwide, is associated with breast pathologies such as fibrosis in human and induces breast atypia in animal models. Because ID induces vascular activation in the thyroid, another iodide-uptaking organ, and as breast is also sensitive to ID, we aimed to characterize ID-induced effects on the breast microvasculature *in vivo* and in two different breast cell lines *in vitro*.

Virgin and lactating NMRI mice received an iodide-deficient diet and a Na^+/I^- symporter inhibitor for one to 20 days. Some virgin mice were treated with vascular endothelial growth factor A (VEGF) or VEGF receptors inhibitors. *In vitro*, ID was induced in MCF7 and MCF12A cells by replacing the iodide containing medium by an iodide-deficient medium.

In vivo, VEGF expression was increased following ID in mammary tissues. Consequently, ID induced a transient increase in mammary gland blood flow, measured after anesthesia, in virgin and lactating mice, which was repressed by VEGF or VEGF receptor inhibitors. In MCF7 cells, ID induced a transient increase in reactive oxygen species (ROS), followed by an increase in hypoxia-inducible factor-1α (HIF-1α) protein and *VEGF* mRNA expression. Antioxidant *N*-acetylcysteine and mammalian target of rapamycin (mTOR) inhibitor blocked ID-induced HIF-1α protein increase and *VEGF* transcription. However, mTOR activity was not inhibited by *N*-acetylcysteine. Similar responses were observed in MCF12A cells.

These data indicate that ID activates the canonical VEGF pathway and mTOR in breast tissues, which provides new insights to better understand the correlation between ID, vascular activation and breast pathologies.

Keywords:

Breast epithelial cells, mammalian target of rapamycin (mTOR), reactive oxygen species (ROS), vascular endothelial growth factor (VEGF), iodine deficiency.

Introduction

In mammals, iodine is an essential trace element required for several physiological purposes. Its supply must be ensured through adequate diet. However, a recent survey showed that still 25 countries out of 153 studied are considered iodine deficient (19). Beside the thyroid that processes iodide for hormone synthesis, the breast secretes iodide into the milk in order to meet the needs of the progeny and therefore increases iodide uptake at the end of pregnancy and during lactation through increased Na^+/I^- symporter (NIS) expression (4; 30). Because of increased needs in iodide, the population of pregnant or breast-feeding women suffering from iodine shortage is often higher compared to the normal population (29). While molecular iodine uptake by normal and cancerous virgin mammary gland is not dependent on NIS and seems to depend on facilitated diffusion in breast cancer cell line MCF7 (1; 11), iodide transport in non-lactating breast is debated due to low NIS expression (16; 22; 34; 41). However, iodine/iodide supply seems to be required for the maintenance of healthy mammary glands. Several studies have indeed highlighted changes induced by iodine deficiency (ID) in mammary glands and linked ID to mammary pathologies. For example, an acute drop in dietary iodide in rats caused atypia and dysplasia in the parenchyma as well as functional alteration in mammary glands (8). Similar alterations in breast morphology were seen in mice treated with NIS inhibitor perchlorate, although the implication of NIS in the transport of iodide in the mammary gland of non-lactating animals is still debated (9). Upon ID or perchlorate treatment, above mentioned changes in the breast were not abrogated when the animals were administered with prohormone thyroxin, suggesting that they were directly due to a lack of inorganic iodide and not to induced hypothyroidism (9).

Notably, perturbations in iodine/iodide supply have been linked to breast pathologies. Iodide was suggested to offer antioxidant protective effects in NIS expressing organs during reproductive and non-reproductive periods (36; 42) and several epidemiological and molecular studies have attributed to iodine/iodide a protective role against breast pathologies. It was indeed shown that iodine and to a lesser extent iodide are able to reduce fibrocystic diseases (15) and to induce apoptosis and a reduction in breast tumor size (35; 37; 39). Several epidemiological studies have also shown a lower prevalence of breast tumors in diverse populations known for their high iodine/iodide intake (7; 24; 28; 31; 45) and it was proposed that high seaweed consumption, which is a source of high iodine/iodide supply, could have a protective role against breast cancer (2). Likewise, the prevalence of

some breast pathologies is associated with some thyroid conditions known to be associated with ID such as enlarged thyroid (38). Moreover, the fact that iodine level in breast cancer tissues is lower than that in normal tissues also endorses a hypothetic protective role of iodine in the breast (21).

Because iodine/iodide seems to be important for mammary glands health, it is therefore worth investigating whether the breast has developed mechanisms to cope with iodine/iodide scarcity. Due to the primordial role of iodide in thyroid functions, thyroid pathologies associated with ID have largely been documented. The thyroid has different mechanisms to face ID that, in our opinion, are worth considering if relevant for the breast situation. One strategy consists in activating the microvasculature (14). We have previously shown *in vitro* and *in vivo* that, when facing short periods of acute ID, the level of reactive oxygen species (ROS) increases in thyrocytes, which increases local blood flow via a VEGF dependent pathway, independently of changes in thyroid-stimulating hormone production, probably in order to rapidly improve iodide supply (13; 14). As this effect does not depend on TSH but rather on the ability of thyrocytes to sense ID (13), we addressed the possibility that, similar to thyrocytes, mammary cells could activate the local microvascularization in response to iodide shortage and we report the existence of molecular pathways activated by acute ID in mammary glands.

Material and methods

Animal models

All *in vivo* experiments were conducted under approval of the Université catholique de Louvain (UCL) authorities (*Comité d'Ethique Facultaire pour l'Expérimentation Animale*) according to national animal care regulations (authorization # 2014/UCL/MD/011).

To induce acute ID, wild-type NMRI mice (Harlan, Boxmeer, The Netherlands) were fed with a low-iodine diet (LID; 0.1 µg iodide/kg; Animalabo, Brussels, Belgium) supplemented or not with 1% sodium perchlorate in tap water for 1 to 20 days, or with a LID and tap water. Control animals received a normal diet (0.4 mg iodide/kg, AO3, Scientific Animal Food and Engineering, Augy, France) and tap water. Virgin mice were eight week old and lactating mice 12 week old at the time of sacrifice; lactating mice were sacrificed in the third week of lactation and pups were separated from their mother 30 minutes before the blood flow measurement.

For inhibition of the VEGF pathway, wild-type NMRI mice (Harlan, Boxmeer, The Netherlands) were either fed with a normal diet (controls) or with a low-iodine diet supplemented with 1% sodium perchlorate in drinking water for 2 days. At the beginning of the ID treatment, half of the groups were injected intraperitoneally with a saline solution of bevacizumab (10 mg/kg; Roche, Welwyn Garden City, UK) or with a solution of SU5416 (25 mg/kg; VWR, Pennsylvania, United States) in dimethyl sulfoxide (DMSO) to inhibit VEGF-A and VEGF receptors 1 and 2, respectively. Control animals were injected with an equimolar solution of irrelevant human IgGs (Sigma, St.-Louis, MO, USA) as a control for bevacizumab or with DMSO as a control for SU5416 treatment.

Blood flow measurements and tissue sampling

Mice were anesthetized with Ketamine (Anesketin, Eurovet, Belgium) and Xylasine (Rompun, Bayer HealthCare, Belgium) and placed on a heating pad (35°C). The area around the second right mammary gland starting from the tail was shaved. Its blood flow was measured using a Laser Doppler imager (Moor Instruments, Axminster, UK). Glands were identified and delineated based on anatomical images, and blood flow was quantified in the areas of interest from colored histogram pixels. After measurements, mice were overdosed with Pentothal (Abbott, Louvain, Belgium). Mammary glands were excised, fixed in 4% of paraformaldehyde in PBS for 36 h, and embedded in paraffin. Thick sections (5 µm) were used for immunohistochemistry and immunofluorescence. A portion of mammary tissue of lactating mice was frozen in liquid nitrogen and used for RNA and protein analyses.

Cell models

MCF7 human mammary gland adenocarcinoma cells (ATCC, Manassas, USA) were routinely cultured in high glucose Dulbecco's Modified Eagle's Medium (DMEM, Invitrogen, Paisley, UK) supplemented with 10% of fetal bovine serum, 100 U/ml (50 µg/ml) penicillin-streptomycin (Invitrogen) and 2.5 µg/ml fungizone (Invitrogen). MCF12A human normal mammary gland cells (ATCC) were cultured in a 1:1 mixture of DMEM and Ham's F12 medium, supplemented with 20 ng/ml human epidermal growth factor, 100 ng/ml cholera toxin, 0.01 mg/ml bovine insulin, 500 ng/ml hydrocortisone, 5% horse serum, 100 U/ml (50 µg/ml) penicillin-streptomycin and 2.5 µg/ml fungizone. HDF human dermal fibroblasts (PromoCell, Heidelberg, Germany) were cultured in DMEM (Invitrogen) supplemented with 2% fetal calf serum (Invitrogen), 1% L-glutamine (Sigma), 100 U/ml (50 µg/ml) penicillin-streptomycin and 2.5 µg/ml fungizone. Cells were cultured at 5% CO_2,

37°C in a humidified atmosphere, as previously described (13). Seven days before the experiments, 10^{-8} M NaI was added to the medium. For the experiment with trans-retinoic acid (tRA), 1µM tRA (Sigma) was added 24 h before acute ID induction. On the day of the experiment, 0.75 mM of antioxidant *N*-acetylcysteine (NAC, Sigma) was added to the medium for 1 h before medium change where indicated. After washing with PBS, culture medium was replaced by fresh medium containing NaI (controls) or not (ID) with or without 10 nM of mTOR inhibitor rapamycin (LC Laboratories, Woburn, USA), 0.75mM of NAC or 100 nM of echinomycin (Alexis Biochemicals, California, USA) where indicated. Cells were harvested at different time points after medium renewal.

Western blotting

Cell and tissue samples were homogenized in Laemmli buffer (10% glycerol, 2% SDS, 50 mM Tris-hydroxymethylaminomethane, 5 mM EDTA in 100 ml distilled water) containing a protease inhibitor cocktail (Roche, Mannheim, Germany), and sonicated for 15 s. Protein content was determined using a BCA protein assay kit (Pierce, Rockford, IL). Western blots were performed as previously described (Gérard 2012). Primary antibodies were incubated overnight at 4°C and secondary antibodies for 1 h at room temperature (**table 1**). Staining was visualized using the Supersignal West Pico/Femto chemiluminescence kit of Thermo Scientific (Waltham, MA). Exposure times are given in **table 1**. Protein expression was quantified by densitometry using NIH Scion Image Analysis Software (National Institutes of Health, Bethesda, MA). Data were normalized to β-actin.

Target protein	Primary Antibody	Dilution	Secondary antibody	Exposure time
β-Actin	Monoclonal antibody, raised in mouse (Sigma #A5441)	1:5,000	Goat anti-mouse poly-HRP 1:5,000 (ThermosFisher Scientific #32230)	30" to 1'
HIF-1α	Monoclonal antibody, raised in mouse (BD transduction #610959)	1:500	Goat biotinylated anti-mouse, 1:200 (Labconsult #BA-9200)	4 to 5'
NIS	Monoclonal antibody, raised in mouse (Antibodies online #ABIN863184)	1:1,000	Goat biotinylated anti-mouse, 1:200 (Labconsult #BA-9200)	1 to 3'
P70S6K	Monoclonal antibody, raised in rabbit (Cell Signaling/Bioké #2708S)	1:1,000	Goat anti-rabbit poly-HRP 1:5,000 (ThermosFisher Scientific #31460)	2 to 4'
p(T389)P70S6K	Monoclonal antibody, raised in rabbit (Cell Signaling/Bioké #9234L)	1:1,000	Goat anti-rabbit poly-HRP 1:5,000 (ThermosFisher Scientific #31460)	2 to 4'

Table 1: Primary and secondary antibodies and their dilution for western blot.

Immunohistochemistry

Immunohistochemistry was performed as previously described (12). Antigen retrieval was necessary for VEGF-A and CD31 detection. To that aim, tissue sections were microwaved in citrate buffer (0.01 M, pH 6.0) for one cycle of 3 min at 750 W, followed by 4 cycles of 3.5 min each at 350 W. Nonspecific staining was prevented by incubating sections with non-immune goat serum (1:50; Vector Laboratories, Burlingame, CA) in PBS/BSA 5% for 30 min at room temperature. Primary antibodies were incubated overnight at 4°C and secondary antibodies for 1 h at room temperature (**table 2**). Primary antibodies were omitted in negative controls. Peroxidase activity was revealed using 3,3'-diaminobenzidine (Dako). Sections were counterstained with Mayer's hematoxylin. Tissues were imaged on an Axio scope A.1 microscope (Zeiss) equipped with a DS-5Mc color digital camera head (Nikon, Amsterdam, The Netherlands). Anti-VEGF antibody specificity was assessed as described before (14). Stained surface was quantified with a brightfield immunohistochemistry image analysis program (Leica Biosystems, Wetzlar, Germany).

For staining quantification, sections were digitalized at a 20x magnification using an SCN400 slide scanner (Leica, Wetzlar, Germany). The tissue in each section was delineated manually and care was taken to exclude tissue folds, bubbles and artefacts from the analysis. Scanned slides were then quantified using Tissue IA

(Leica Biosystems, Dublin, Ireland).Color deconvolution was applied to each pixel using hematoxylin and DAB matrices of the software. On the DAB matrice, a threshold was adjusted for DAB detection according to intensity (grey values from 0 to 255) on representative stained versus not stained tissue areas. In a similar way, a threshold was also adjusted for tissue detection. These parameters were kept constant throughout the study for each immunostaining. Results were expressed as stained area /tissue area.

Protein	**Primary antibody**	**Dilution**	**Secondary antibody**
VEGF-A	Monoclonal mouse anti-VEGF-A (Santa Cruz #SC-53462)	1:100	Goat anti-mouse poly-HRP, 1:50 (ThermosFisher Scientific #32230)
CD31	Polyclonal rabbit anti-CD31 (Abcam #ab28364)	1:100	Goat anti-rabbit poly-HRP, 1:50 (thermosFisher Scientific #32260)

Table 2: Primary and secondary antibodies and their dilution for immunohistochemistry.

Quantitative polymerase chain reaction

For quantitative polymerase chain reaction (RT-qPCR), cell and tissue samples were homogenized in 1 ml TriPure isolation reagent (Roche), and total RNA was extracted according to the manufacturer's protocol and resuspended in RNase-free water. Reverse transcription was performed as previously described (13). cDNAs (0.04 µg of cDNA template in 2 µL) were admixed with 10 µM of each selected primer pair (**table 3**) and Perfecta SYBR green reaction mix (VWR) in a final volume of 15 µL. Reactions were performed with an IQ5 iCycler (Bio-Rad, Herts, UK) as previously described (13). Annealing temperatures are given in **table 3**. Amplification levels were normalized to those of β-actin. All samples were measured in duplicate.

RNA	Forward primer	Reverse primer	Annealing temp.
β-actin	5'CATCCTGCGTCTGGACCT3'	5'AGGAGGAGCAATGATCTTGAT3'	62°C
VEGF-A mouse	5'GAGTATATCTTCAAGCCGTCCTGT3'	5'TTTTCTGGCTTTGTTCTATCTTTC3'	55°C
NIS mouse	5'TGCGGGATGCACCAATGCCT3'	5'GGCGGCCCGAGTCCATTCCA3'	59°C
VEGF-A human	5'GCAGATGTCCCGGCGAAGAGAAGA3'	5'CGGGGAGGGCAGAGCTGAGTGTTA3'	62°C
NIS human	5'CCCCCTCCTGATTCTGCTTGTTG3'	5'ACCGCGCCCCACCTCTTTCTTATT3'	62°C

Table 3: Primer sequences and their annealing temperature for qRT-PCR.

ROS measurements

ROS production was measured using fluorescent dye Carboxy-DCFDA (5-(and-6)-Carboxy-2',7'-Dichlorofluorescein Diacetate) (DCFDA, Invitrogen). Cells were plated in multichamber glass slides (Sigma) in medium containing 10^{-8} M of NaI until they reached 80% confluence. After washing with PBS, medium was replaced by fresh medium containing NaI or not. After 2, 4 or 6 h, cells were washed with PBS and incubated in a Krebs-Ringer HEPES (pH 7.4) solution without albumin and containing DCFDA (25 mM) for 1 h at 37°C, 5% CO_2. Slides were washed 3X3 min with PBS, and nuclei were stained with Hoechst dye (ThermoFisher; 1/5000). Excess dye was removed with PBS, and slides were mounted in fluorescent mounting medium (Dako, Heverlee, Belgium). ROS production was visualized on a fluorescence microscope (Zeiss, Axio scope A.1, Zaventem, Belgium).

Immunofluorescence

Cells were plated in multichamber glass slides (Sigma) in medium containing 10^{-8} M of NaI until they reached 80% confluence. After washing with PBS, medium was replaced by fresh medium containing NaI or not. After 4 h, cells were washed with PBS and fixed with paraformaldehyde 4% for 10 minutes. Cells were washed and then quenched with NH4Cl 50mM in water (ammonium chloride, Sigma-Aldrich) for

5 minutes, twice. After washing, cells were blocked for 1 h in PBS/BSA 5%/saponin 0.1%, and incubated at 4ºC overnight with primary antibodies (4-HNE, 393207-100, VWR, 1/500) in PBS/BSA 1%/saponin 0.1%. Primary antibodies were omitted in negative controls. Signals were revealed after 1h incubation at room temperature in the dark with species-specific secondary antibodies conjugated to fluorophores (Alexa Fluor 488-conjugated goat anti-rabbit, A11034, Invitrogen, 1/300) in PBS/BSA 1%/saponin 0.1%. Nuclei were stained for 5 minutes with 4'-6'diamidino-2-phenylindole (DAPI, 1/10,000) and slides were mounted in Fluorescent Mounting Medium (Dako Cytomation). Images were captured on an AxioCam MRc5 fluorescence microscope using the Axio Vision 4.8 software (Zeiss).

Statistics

All data are expressed as means ± SEM. *In vivo* experiments were independently repeated 2 or 3 times with 3 animals in each group. *In vitro* experiments were independently conducted 3 to 11 times with 3 to 6 replicates for each condition. Unpaired Student's *t* test and one-way ANOVA with Dunnett, Tukey-Kramer or Bonferroni post-hoc test were used where indicated (GraphPad Instat, San Diego, CA). $P < 0.05$ was considered to be statistically significant.

Results

Acute ID induces a transient increase in blood flow and VEGF expression in lactating mammary glands

Iodide uptake and NIS expression by the mammary gland are strongly enhanced during lactation (4). Therefore, we initially studied the effects of acute ID in lactating mice. We first investigated the impact of ID on mammary gland blood flow and microvasculature. Compared to control, ID increased blood flow from day 1 to day 10 of the treatment (**fig. 1a**). This increase was maximal after 10 days and then decreased to reach back control level after 15 days of treatment. To rule out the potential toxic or off-target effects of perchlorate in this response, a group of mice received LID food without perchlorate for 4 days, which also induced a significant increase in blood flow (**fig. 1b**).

VEGF has been involved in the response of the thyroid vasculature to ID (14). In the mammary gland, RT-qPCR analyses detected a significant increase in *VEGF* mRNA expression at day 1 of ID (**fig. 1c**). It went along with increased VEGF protein expression detected by immunohistochemistry around some blood vessels

and in the stroma (**fig. 1d-g**). This staining was strongly enhanced from day one (**fig. 1e-f**) to day 10 of the treatment. Increased staining was also observed in the lumen of the glands and at the apical membrane of the mammary epithelial cells (**fig. 1g**).

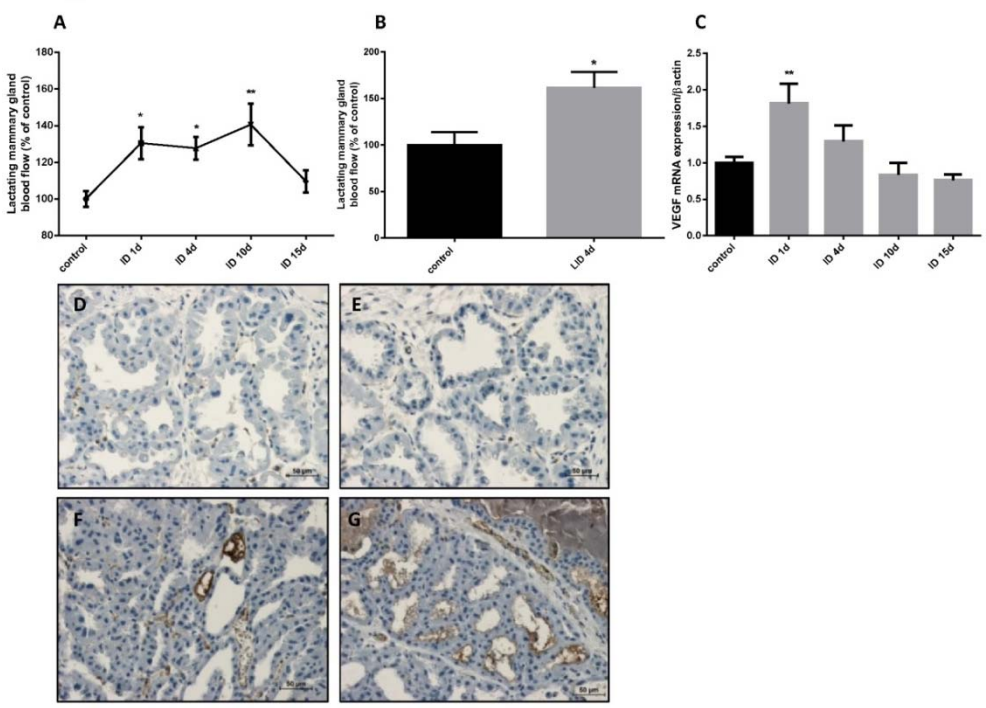

Figure 1. Acute iodine deficiency triggers perfusion and VEGF expression in lactating mammary glands in mice. *Lactating NMRI mice received an iodine containing diet (control) or iodine-deficient diet with 1% sodium perchlorate (ID) or without perchlorate (LID) in the drinking water for 1 to 15 days (d). (**A-B**) Blood flow in mammary glands was measured with a Laser Doppler flowmeter (A: control: N=10, ID 1 and 15 days: N=8, ID 4 and 10 days: N=9; B: N=3). (**C**) VEGF mRNA expression was determined using RT-qPCR on tissue samples (control and ID 15 days: N=8, ID 1, 4 and 10 days: N=7). (**D-G**) VEGF protein was detected using immunohistochemistry on mammary glands collected 1 day after ID or control treatment. Representative pictures of N = 8 are shown for control mice (**D-E**) and iodine-deprived mice (**F-G**). Scale bars = 50 µm. Data are expressed as means ± SEM. Statistical test: one-way ANOVA with Dunnett post-hoc test (**A, C**) or unpaired Student's t test (**B**). * P < 0.05, ** P < 0.01 versus control (**A-C**).*

Acute ID induces a transient VEGF-dependent increase in blood flow in virgin mammary glands

Although iodide uptake is very low in non-lactating mammary glands compared to lactating glands (4), acute ID also induced an increase in blood flow in the mammary

glands of virgin mice (**fig. 2a**). Increased perfusion was detected only at day 1 of treatment. Blood flow then progressively declined to basal level from day 2 to day 10 (**fig. 2a**). A second experiment with longer treatment times revealed no increase in blood flow after ID exposure up to 20 days (**fig. 2b**). Mice that received LID food without perchlorate for 2 days also experienced increased mammary gland blood flow (**fig. 2c**).

To investigate the effects of acute ID on vascularization, blood vessels were labelled with an anti-CD31 antibody. An increase in total stained surface was observed at day 2, showing that the total vascular surface was increased upon ID (**fig. 2d**). However, ID did not induce an increase in the number of vessel sections per unit of surface (**fig. 2e**), indicating that vasodilation, not angiogenesis, could be responsible for increased blood flow in the mammary gland upon acute ID. This was associated to changes in VEGF expression. In control mice, weak VEGF staining, studied by immunohistochemistry, was observed in few mammary epithelial and endothelial cells and in the stroma (**fig. 2f-g**). Comparatively, VEGF expression was enhanced on days 1 and 2 of ID at all 3 locations (**fig. 2h-i**). After 4 days of ID, VEGF expression decreased but was still higher than in controls. At day 10, VEGF expression was similar to the expression in controls.

To determine whether VEGF is responsible for ID-induced increase in blood flow, mice were injected either with VEGFR2/1 inhibitor SU5416 or with DMSO as a control. SU5416 inhibited the increased blood flow in response to acute ID, whereas basal blood flow in iodine-replenished mice was not affected (**fig. 2j**). Similar data were obtained when using VEGF-blocking antibody bevacizumab at a high dose instead of SU5416 (**fig. 2k**), thus indicating that VEGF is at least involved in the increased mammary gland perfusion in iodine-deprived virgin mice.

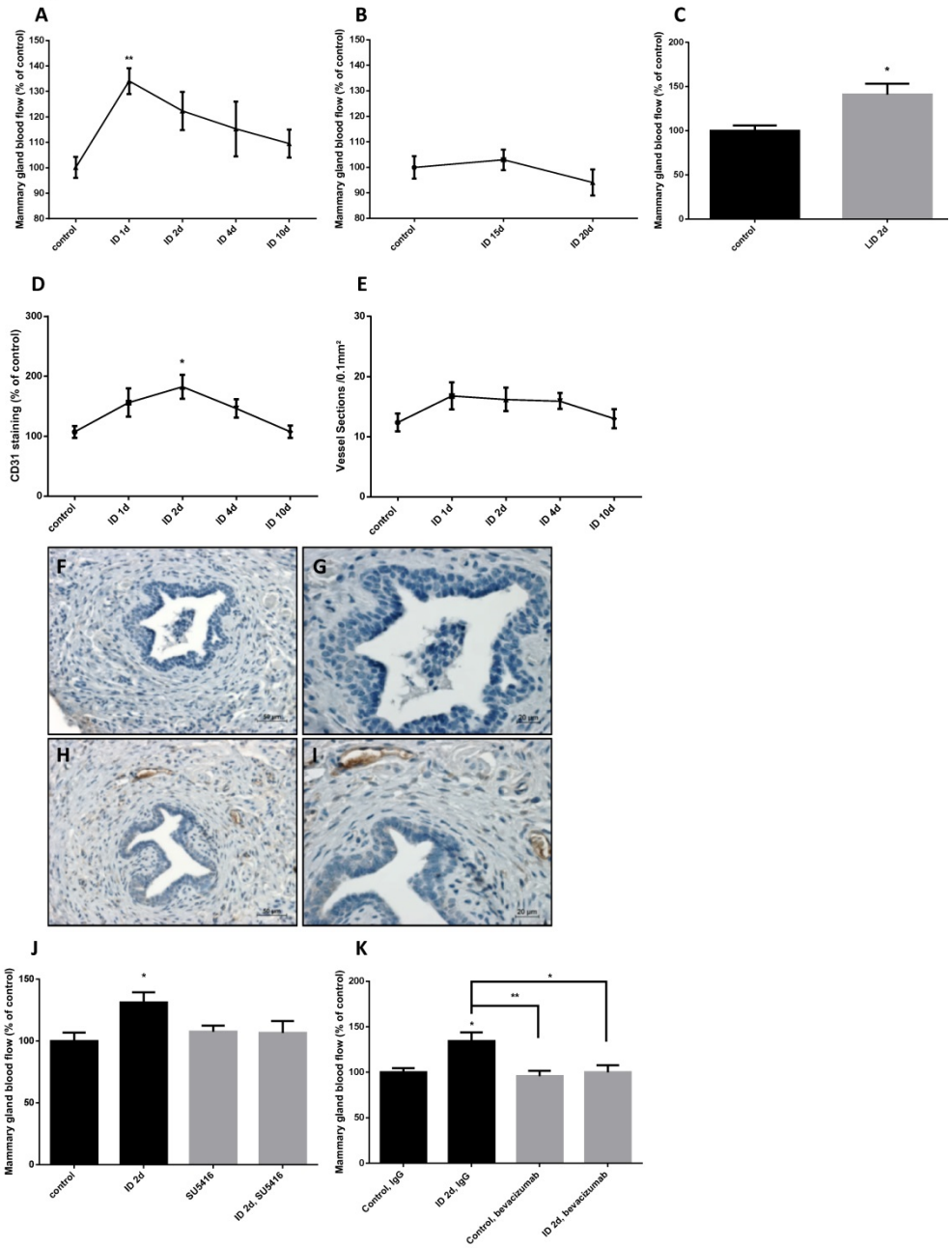
A
Mammary gland blood flow (% of control)
control
ID 1d
ID 2d
ID 4d
ID 10d
B
Mammary gland blood flow (% of control)
control
ID 15d
ID 20d
C
Mammary gland blood flow (% of control)
control
LID 2d
D
CD31 staining (% of control)
control
ID 1d
ID 2d
ID 4d
ID 10d
E
Vessel Sections /0.1mm²
control
ID 1d
ID 2d
ID 4d
ID 10d
F
G
H
I
J
Mammary gland blood flow (% of control)
control
ID 2d
SU5416
ID 2d, SU5416
K
Mammary gland blood flow (% of control)
Control, IgG
ID 2d, IgG
Control, bevacizumab
ID 2d, bevacizumab

Figure 2. Acute iodine deficiency triggers VEGF expression that induces perfusion in mammary glands of virgin mice. *Virgin mice received an iodine containing diet (control) or iodine-deficient diet with 1% sodium perchlorate (ID) in the drinking water or without perchlorate (LID) for 1 to 10 days or from 15 to 20 days (d). (**A-C**) Blood flow in mammary glands was measured with a Laser Doppler flowmeter (A: control: N=9, ID 1, 2, 4 and 10 days: N=8; B: control: N = 7, ID 15 and 20 days: N=6; C: N=3). (**D-E**) CD31 immunostaining on mammary glands collected 1 to 10 days after ID or control treatment was quantified from scanned slides (**D**) and sections into vessels were counted (**E**) (D: control and ID 10 days: N=5, ID 1 day: N=7, ID 2 and 4 days: N=6; E: control: N=6, ID 1, 2 and 4 days: N=7, ID 10 days: N=5). (**F-I**) VEGF protein was detected using immunohistochemistry on mammary glands collected 1 day after ID or control treatment. Representative pictures of N = 8 are shown for control mice (**F-G**) and iodine-deprived mice (**H-I**). Scale bars = 20 (G, I) or 50 µm (F, H). (**J**) Virgin mice exposed to ID or control treatment were injected with either DMSO or SU5416 diluted in DMSO (control and ID 2 days: N=6, SU5416 and SU5416 ID 2 days: N=5). (**K**) Virgin mice exposed to ID or control treatment were injected with either IgG or bevacizumab (control IgG and control bevacizumab: N=6, ID 2 days IgG: N=5, ID 2 days, bevacizumab: N=7). (**J-K**) Blood flow in mammary glands was measured with a Laser Doppler flowmeter. Data are expressed as means ± SEM. Statistical test: one-way ANOVA with Dunnett post-hoc test (**A, B, D, E, J, K**) or unpaired Student's t test (**C**). * P < 0.05, ** P < 0.01 (**A-E, J-K**).*

Acute ID induces a ROS and mTOR-dependent increase in HIF-1α protein and VEGF mRNA expression in MCF7 cells

VEGF expression was increased during acute ID in both lactating and virgin glands. We therefore aimed to elucidate the underlying molecular pathway. To do so, we used two NIS expressing cell lines: MCF7, a breast cancer cell line, and MCF12A, a non-cancerous cell line. NIS expression was compared in MCF12A and in MCF7 cell lines in control experiments. NIS mRNA expression was considerably higher in MCF7 cells than in MCF12A cells while NIS protein expression was not significantly different in both cell lines (*supplemental data, Fig. 1*).

In MCF7 cells, acute ID induced a transient increase in *VEGF* mRNA expression at 6 h (**fig. 3a**). Of note, VEGF mRNA expression assessment at several time points from 2 to 24 h are shown in supplemental data, Fig. 2. Iodide uptake and NIS expression were shown to increase with trans-retinoic acid (tRA) treatment (22). Cells were thus treated with tRA to see whether NIS and iodide uptake induction could influence the response to ID. However, though the addition of tRA increased *NIS* and *VEGF* mRNA expression, it did not influence the amplitude of the increase in VEGF mRNA induced by acute ID (*supplemental data, Fig.3)*. Because iodide is an antioxidant (43) and ROS are able to influence VEGF expression (25; 44), we analyzed ROS content and found that iodine-deprived cells had increased ROS levels 4 h after ID (**fig. 3b-e**). Oxidative damage was then assessed through 4-HNE adducts measurement by immunofluorescence. An increase in 4-HNE staining was observed at 4 h of ID (**fig. 3f-g**). A causative link between increased ROS and *VEGF*

mRNA expression in the context of acute ID was established by showing that antioxidant NAC prevented the increase in *VEGF* mRNA levels in cells exposed to ID (**fig. 3h**). NAC had no effect on basal *VEGF* mRNA expression in control cells. Further, *VEGF* is a HIF-1-target gene (10), and transcription factor HIF-1 is activated by ROS that increase the expression of its α subunit (18). In line with an involvement of HIF-1 in the response to ID, we observed a significant increase in HIF-1α expression 4 h after ID (**fig. 3i**). HIF-1α protein expression was studied at time points from 2 to 24 h but no increase was observed at 2 h and 24 h of ID (supplemental data, Fig. 4). NAC prevented ID-induced HIF-1α protein overexpression (**fig. 3j**), which revealed that HIF-1 can act downstream of ROS in the response of breast cancer cells to ID. Of note, NAC did not influence basal HIF-1α protein expression in iodide-replenished cells.

The activity of the transcription factor HIF-1 was then inhibited by echinomycin. As a consequence, the ID-induced effect on VEGF mRNA overexpression was not observed (**fig. 3k**).

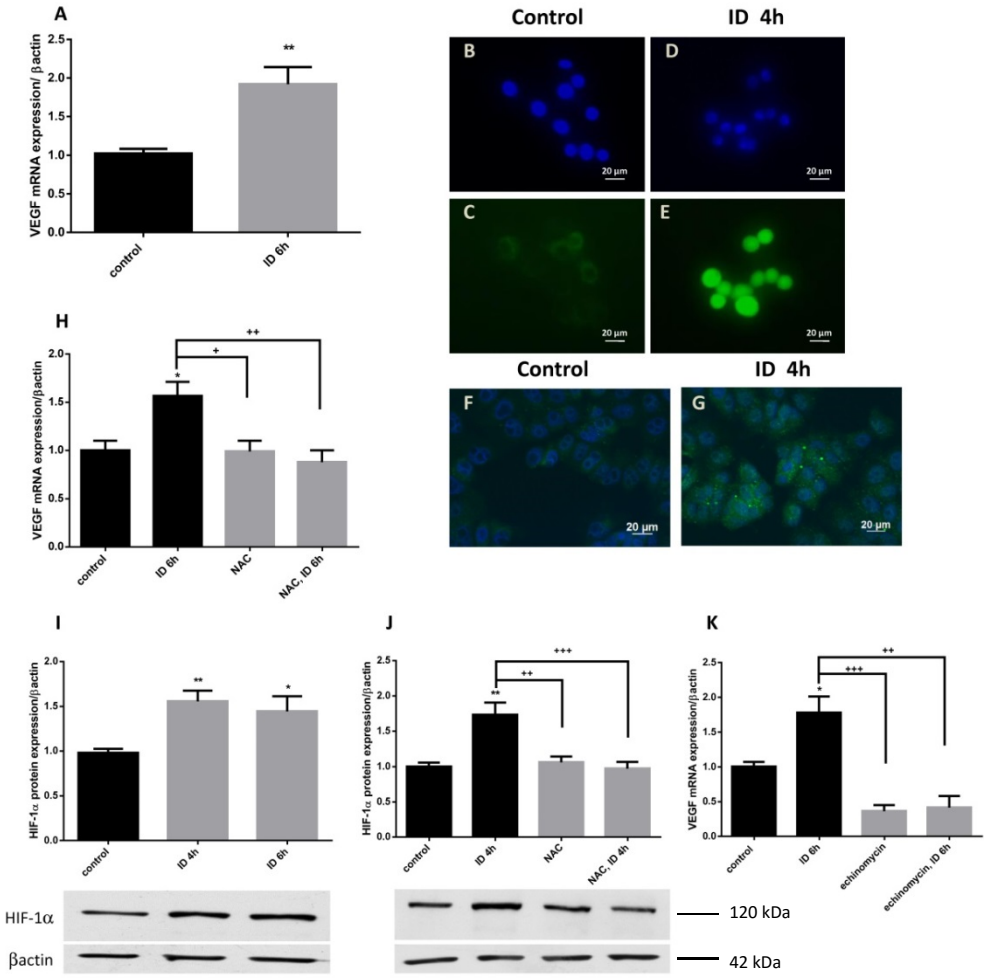

Figure 3. Acute iodine deficiency induces a ROS/HIF-1-dependent increase in VEGF mRNA expression in MCF7 breast cells. *MCF7 cells were cultured in iodine-containing medium for 7 days. Medium was replaced by iodine-containing (control) or iodine deficient (ID) medium with or without the antioxidant NAC. Cells were harvested 4 or 6 hours (h) after medium change. (**A**) VEGF mRNA expression was determined using RT-qPCR (N=11). (**B-E**) ROS content was visualized with DCFDA and nuclei were stained with Hoechst fluorescent dye in control (B-C) and iodine deficient (D-E) cells (N=3). (**F-G**) 4-HNE adducts were detected using immunofluorescence after 4 h of ID (G) or control (F) treatment (N = 3). Representative pictures are shown. Scale bars = 20 µm. (**H**) The involvement of ROS in ID-induced VEGF mRNA expression was studied by RT-qPCR thanks to the use of NAC (N=4). (**I**) HIF-1α protein expression was studied by western blotting (N=7). (**J**) The involvement of ROS in ID-induced HIF-1α protein expression was studied by western blotting thanks to the use of NAC (N=5). (**K**) The involvement of HIF-1α in ID-induced VEGF mRNA expression was studied by RT-qPCR thanks to the use of echinomycin (N=3). Data are expressed as means ± SEM. Statistical test: Unpaired Student's t test (**A**) or one-way ANOVA with Dunnett (**I**) or Tukey-Kramer (**H, J, K**) post-hoc test. */+ P < 0.05, **/++ P < 0.01, ***/+++P<0.001 *versus control; + versus ID 4/6h (**A, H-K**).*

In thyrocytes, mTOR promotes HIF-1α and VEGF expression during ID (6), and mTOR activity can be increased by ROS (3). We therefore reasoned that mTOR could be involved in the response of breast cancer cells to ID. Accordingly, phosphorylation of P70S6K on threonine 389, an established target of mTOR (33), significantly increased in MCF7 cells following acute ID (**fig. 4a**). P70S6K phosphorylation was increased as soon as 2 hours after ID induction (**fig.4d**), indicating that mTOR activity is enhanced before the HIF-1α rise. This response was not reduced by NAC (**fig. 4b**) which suggests that mTOR activation by ID is not dependent on ROS production. Downstream, the mTOR inhibitor rapamycin inhibited ID-induced HIF-1α protein (**fig. 4c**) and *VEGF* mRNA (**fig. 4d**) expression, thereby showing the involvement of mTOR in ID-induced pathway that leads to VEGF overexpression. Rapamycin did not modify the basal levels of the HIF-1α protein and *VEGF* mRNA in iodine-replenished MCF7 cells (**fig. 4c-d**).

Altogether, our results strongly suggest that acute ID induces a ROS and mTOR-dependent rise in HIF-1α protein that promotes *VEGF* mRNA overexpression.

Figure 4. Increase in VEGF mRNA and HIF-1α protein expression depends on mTOR in MCF7 breast cells. *MCF7 cells were cultured in iodine-containing medium for 7 days. Medium was replaced by iodine-containing (control) or iodine deficient (ID) medium with or without the inhibitor of mTOR, rapamycin. Cells were harvested 2 or 4 hours (h) after medium change. (**A**) P70S6K phosphorylation on threonine 389 was determined by western blotting (N=5). (**B**) The involvement of ROS in ID-induced P70S6K phosphorylation on threonine 389 was studied through the use of rapamycin (N=3). (**C**) The involvement of mTOR in ID-induced HIF-1α protein expression was studied by western blotting thanks to the use of rapamycin (N=5). (**D**) The involvement of mTOR in ID-induced VEGF mRNA expression was studied by RT-qPCR thanks to the use of rapamycin (N=4). Data are expressed as means ± SEM. Statistical test: one-way ANOVA with Dunnett (**A**), Bonferroni (**B**: comparing "control" to "ID 4h" and "NAC" to "NAC, ID 4h") or Tukey-Kramer (**C, D**) post-hoc test. * P < 0.05, **/++ P < 0.01, +++ P<0.001. *versus control, +versus ID 4h.*

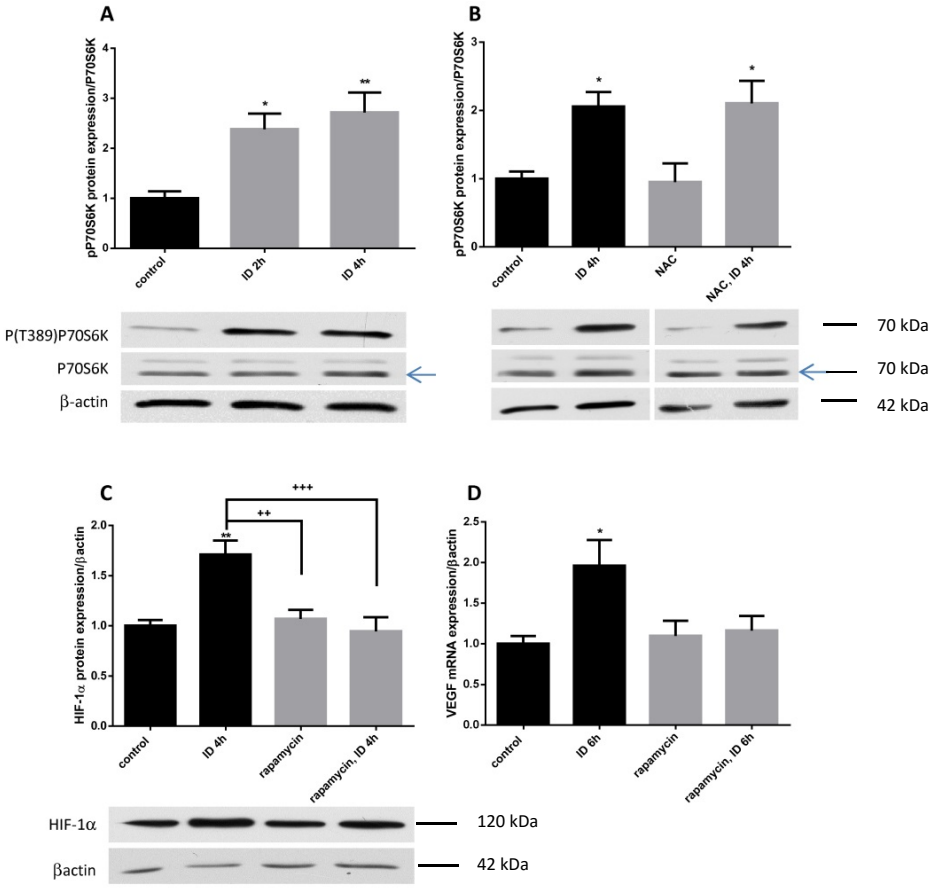

Acute ID induces a ROS and mTOR-dependent increase in *VEGF* mRNA expression MCF12A cells

We next verified whether acute ID could induce a rise in VEGF mRNA in another NIS-expressing breast cell line. Intracellular ROS content of MCF12A cells was increased after 2 h of ID, compared to controls (**fig. 5a-d**) and 4-HNE staining was also more pronounced after 3 h of ID (**fig. 5e-f**). It was followed by an increase in *VEGF* mRNA expression that was significant at 3 h (**fig. 5g**) and could be repressed by NAC (**fig. 5h**) and rapamycin (**fig. 5i**). Similar to what was seen in MCF7 cells, neither NAC nor rapamycin influenced basal *VEGF* mRNA expression in MCF12A cells supplied with iodine (**fig. 5h-i**). Our data suggest that the same molecular

pathways are activated in MCF12A and in MCF7 cells during acute ID. *VEGF* mRNA expression was assessed at shorter and longer time points to prove the transient nature of its induction by ID (*supplemental data, fig*. 5).

In order to assess whether ID-induced effects are specific to cells capable of iodide uptake, a control experiment was carried out with human dermal fibroblast (HDF) cells which do not express NIS. HDF cells exposed to ID for 4 or 6 h did not increase *VEGF* mRNA expression (*supplemental data, fig. 6*).

Acute ID increases NIS expression *in vitro* and *in vivo*

Finally, NIS expression was investigated in mammary cells *in vivo* and *in vitro* in order to know whether these cells try to adapt their iodide uptake *via* increased expression in NIS. *In vivo*, in lactating mammary glands, NIS mRNA expression, studied by qPCR, appeared to be non-significantly increased at the first and 4th day of ID treatment, and gradually decreased back to control level (**fig. 6a**). NIS protein expression, studied by western blot, was significantly enhanced at day 10 of ID treatment (**fig. 6b**). *In vitro*, in MCF7 cells, NIS mRNA expression increased after 4 hours of ID (**fig. 6c**) and its protein expression transiently increased after 4h of ID (**fig. 6d**). Nevertheless, in MCF12A cells, ID did not induce an increase in NIS mRNA and protein expression at the studied time points (**fig. 6e, f**).

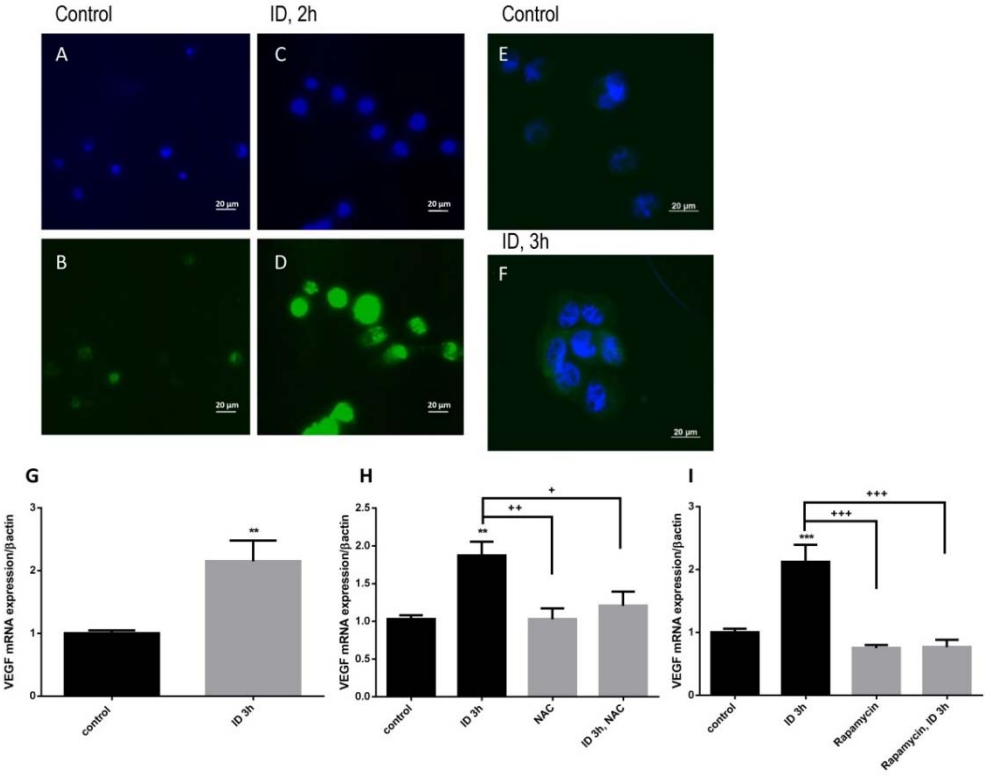

Figure 5. Acute iodine deficiency induces a ROS/ mTOR-dependent increase in VEGF mRNA expression in MCF12A breast cells. *MCF12A cells were cultured in iodine-containing medium for 7 days. Medium was replaced by iodine-containing (control) or iodine deficient (ID) medium with or without the antioxidant NAC or the inhibitor of mTOR, rapamycin. Cells were harvested 2 or 3 hours (h) after medium change. (**A-D**) ROS content was visualized with DCFDA and nuclei were stained with Hoechst fluorescent dye in control (A-B) and iodine deficient (C-D) cells (N=3). (**E-F**) 4-HNE adducts were detected using immunofluorescence after 3 h of ID (G) or control (F) treatment (N = 3). Representative pictures are shown. Scale bars = 20 µm. (**G**) VEGF mRNA expression was determined using RT-qPCR (N=6). (**H**) The involvement of ROS in ID-induced VEGF mRNA expression was studied by RT-qPCR thanks to the use of NAC (N=4). (**I**) The involvement of mTOR in ID-induced VEGF mRNA expression was studied by RT-qPCR thanks to the use of rapamycin (N=5). Data are expressed as means ± SEM. Statistical test: Unpaired Student's t test (**G**) or one-way ANOVA with Tukey-Kramer post-hoc test (**H-I**). + P < 0.05, **/++ P < 0.01, ***/+++ P<0.001; *versus control, +versus ID 3h (**G-I**).*

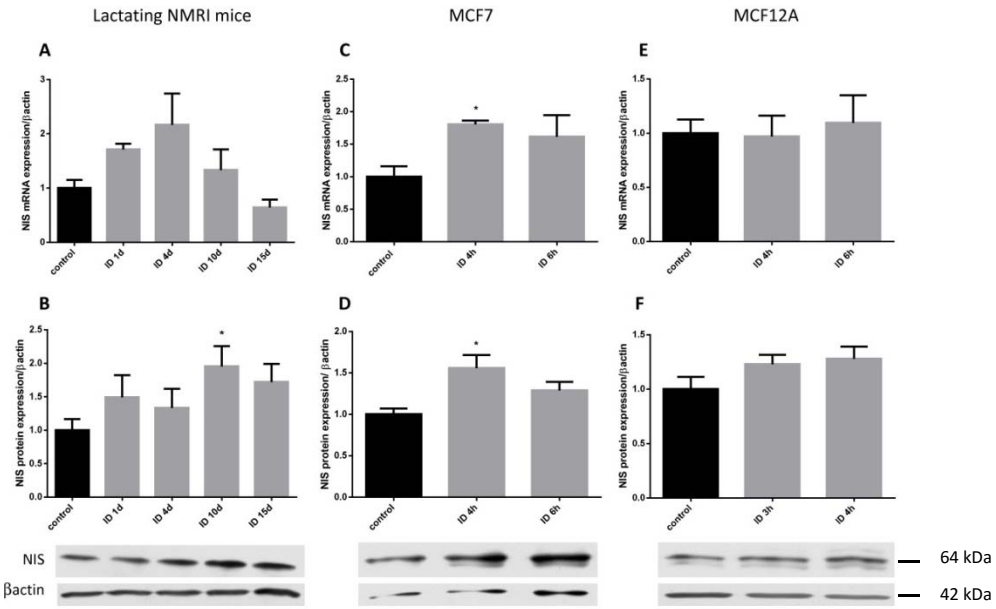

Figure 6. Acute iodine deficiency influences NIS expression in MCF7 cells and in lactating mammary glands. *Lactating NMRI mice received an iodine containing diet (control) or iodine-deficient diet with 1% sodium perchlorate (ID) in the drinking water for 1 to 15 days (d) (**A-B**). MCF7 (**C-D**) and MCF12A (**E-F**) cells were cultured in iodine-containing medium for 7 days. Medium was replaced by iodine-containing (control) or iodine deficient (ID) medium. Cells were harvested 4 and 6 (MCF7) or 3 and 4 (MCF12A) hours (h) after medium change. (**A, C, E**) NIS mRNA expression was determined using RT-qPCR (A: control, ID 10 and 15 days: N=6, ID 1 and 4 days: N=5; C: N=4; E: N=3). (**B, D, F**) NIS protein expression was determined by western blotting (B: control, ID 1 and 4 days: N=5, ID 10 and 15 days: N=6; D: N=4; F: N=3). Data are expressed as means ± SEM. Statistical test: one-way ANOVA with Dunnett post-hoc test. * P < 0.05, versus control.*

Discussion

Several studies have reported functional and histological changes in the breast tissues induced by ID and have suggested links between iodine supply and breast health (8; 9; 38; 40); but, unlike the molecular pathways activated by iodide/iodine supplementation that are well characterized (27; 37; 39), little is known about the pathways activated by an acute drop in iodide supply. Here, we report that acute ID activates a ROS/mTOR-HIF-1-VEGF pathway in the mammary cells, which induces vasodilation in the mammary gland.

We first observed that transient microvascular activation occurred when iodide intake dropped in virgin and lactating mouse mammary glands, *i.e.*, two models with different iodide requirements (4). ID significantly increased local perfusion in the two models, which was shown to be dependent on VEGF in virgin mice. This finding does not rule out the possible involvement of other factors. Although VEGF inhibition was not carried out in lactating mice, VEGF could also be involved in ID-induced lactating mammary gland perfusion because increased VEGF mRNA and protein expression was detected after ID along with the transient increase in the blood flow. The response was independent of angiogenesis and could thus be explained by the vasodilatory activity of VEGF (17; 23).

Several factors triggering VEGF expression and microvascular activation were assessed *in vitro* in two different NIS-expressing cell lines: MCF7 breast cancer cells and MCF12A breast non-cancer cells. In both models, ID increased *VEGF* mRNA expression, which is in good agreement with the VEGF-dependent vascular activation detected *in vivo*. Increased *VEGF* mRNA expression in the two cell lines in the absence of thyroid hormones and perchlorate indicate that breast cells are directly sensitive to ID alone and that the vascular activation observed in mice is not due to perchlorate itself or to changes in thyroid hormone levels. Furthermore, the increase in blood flow *in vivo* occurred 1 day after ID, before any changes in thyroid hormone levels (14). Moreover, there were no more changes in the blood flow in hypothyroid condition after 15, 20 or 30 days. Likewise, a control experiment where mice only received a low iodide diet without perchlorate lefts out the possibility that vascular activation is an off-target effect of perchlorate.

In MCF7 cells, the expression of both *VEGF* mRNA and the α subunit of transcription factor HIF-1 was induced by acute ID. In this cell line, ROS, mTOR and HIF-1 were required to induce VEGF transcription, as the inhibition of ROS and mTOR prevented both HIF-1α and *VEGF* overexpression and the inhibition of HIF-1 prevented *VEGF* overexpression. However, mTOR activation was not dependent on ROS. It is thus possible that two different pathways leading to *VEGF* overexpression

are activated by acute ID. Thus, we propose that acute ID triggered ROS production, activated mTOR, and that both ROS and mTOR increased HIF-1α expression that triggered *VEGF* transcription in these cells. We do not exclude the possibility that other transcription factors are also involved in the pathway. Although the initial aim of our study was not to focus on ROS, a likely explanation for increased ROS content upon acute ID could be related to unrestricted production of ROS associated with the cellular respiration (46). A drop in the level of available iodide might reduce antioxidant mammary cell defenses against their own metabolic production of ROS. This of course does not exclude other possibilities, such as for example an ID-associated activation of ROS generating NADPH oxidases.

While VEGF induction upon acute ID was observed in virgin and lactating mice as well as in two cell line models, the kinetics of its expression varied in the different models. In mice, blood flow induction, though transient in both models, lasted longer in lactating breasts. This might reflect the increased requirement of iodide in breast during lactation, both for the mother and the progeny (29). However, it is also possible that estrogens, which are known to be able to stimulate angiogenesis (20; 26), might reinforce the effects of ID. Mammary glands could therefore react to ID through microvascular activation, the extent of which depending on the physiological state. In our assays, microvascular activation was accompanied by an increased expression of NIS, which was detected in lactating mice and in MCF7 cells, but not in MCF12A cells. This does not exclude a possible regulation of NIS in these cells after longer exposure time. Taken together, these data suggest that mammary cells are sensitive to ID and attempt to increase their iodide intake by increasing their surrounding blood flow and, in MCF7 cells and lactating mice, their transport activity. Of note, this reaction occurred only when cells faced a sudden decrease in iodide supply, as *VEGF* mRNA expression did not change in cells constantly exposed to ID and in cells constantly exposed to sodium iodide (*supplemental data, fig. 7*).

In MCF12A cells, the same pathways are activated by acute ID as in MCF7 cells, though basal iodide uptake is low in both cell lines (22). VEGF transcription was induced by acute ID and it was also dependent on both ROS and mTOR. In MCF7 cells, the amplitude of ID-induced *VEGF* mRNA overexpression was not influenced by tRA, which is known to increase NIS expression and iodide uptake in those cells (22). Furthermore, virgin mice, which are known to have a very low iodide intake (4), also reacted to ID by increasing mammary gland blood flow and VEGF expression. Conversely, a control experiment suggests that acute ID in fibroblasts, which are not known to require iodide, did not induce a rise in *VEGF* mRNA expression. Thus, this effect seems to be specific to cells that physiologically require

iodide. The initial amount of intracellular iodide does not seem to affect the trigger of the reaction, but might influence the regulation of the reaction since it lasted longer in lactating females than in virgin females.

However, while the increase in VEGF expression and in blood flow was transient and therefore regulated, VEGF overexpression is generally of bad prognosis in breast cancers due to its potent angiogenic activity (Mercurio, 2005). Moreover, ROS are known to be involved in the initiation of many cancers, and mTOR is a key regulator of the cell cycle (5; 32). Therefore, it is worth questioning whether ID could influence breast cancer progression through a modification of the cell environment. In this regard, this work illustrates how acute ID may alter the cellular microenvironment, thereby influencing breast pathologies.

Conclusion

In conclusion, our results show that acute ID induces a VEGF-dependent microvascular activation in mammary glands. ID-induced HIF-1/VEGF pathway is dependent on mTOR signaling and on increased ROS content (fig. 7). This local vascular activation leading to a vasodilation and an increased blood flow could be viewed as a rapid response to ID that aims at improving iodide bioavailability to the breast tissue when facing iodide shortage, similar to what is described in the thyroid (13).

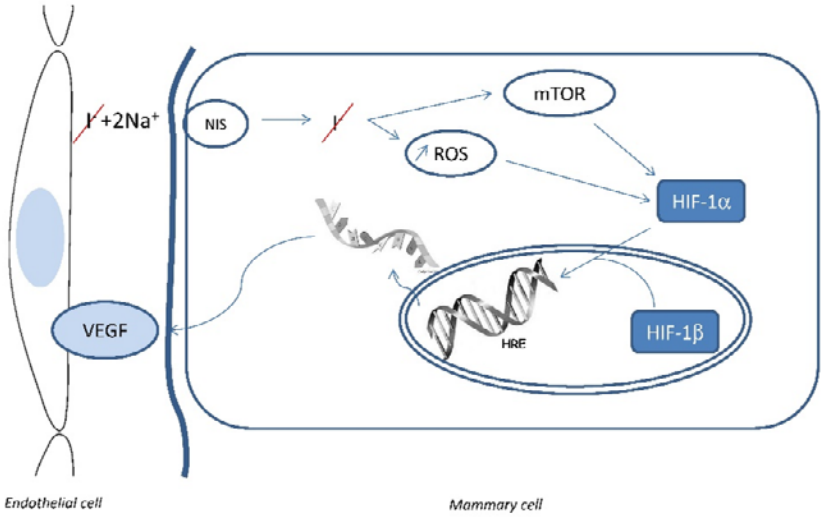

Figure 7. *Molecular pathways activated by ID in cancerous and non-cancerous breast cells.*

List of abbreviations

Hypoxia-inducible factor-1α (HIF-1α), iodine deficiency (ID), low iodide diet (LID), mammalian target of rapamycin (mTOR), *N*-acetylcysteine (NAC), quantitative polymerase chain reaction (qPCR), reactive oxygen species (ROS), sodium-iodide symporter (NIS), trans-retinoic acid (tRA), vascular endothelial growth factor A (VEGF).

Acknowledgements

The authors thank Christine de Ville de Goyet (UCL) and Gaelle Da Silva for expert technical support.

Funding

This study was supported by the *Fonds National de la Recherche Scientifique* (F.R.S.-FNRS) (grant J.0112.13).

Competing interests

The authors declare that they have no conflict of interest.

Supplemental data

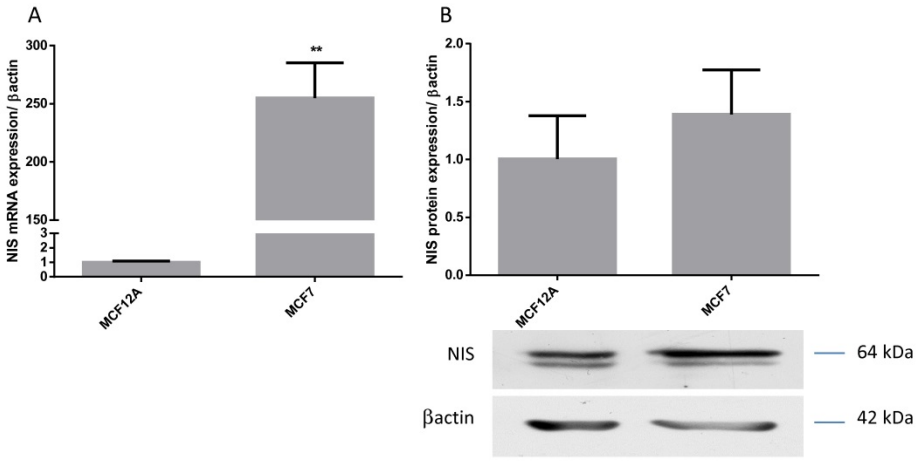

Figure 1. NIS mRNA expression is higher in breast cancer cells than in non-cancer cells. *(**A**) NIS mRNA expression was determined using RT-qPCR (N=2, one representative experiment). (**B**) NIS protein expression was determined by western blotting (N=2, one representative experiment). Data are expressed as means ± SEM. Statistical test: Unpaired Student's t test. ** P < 0.001.*

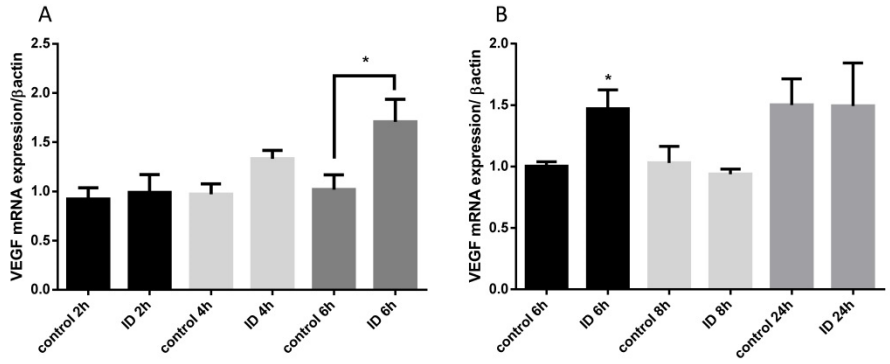

Figure 2. Iodine deficiency transiently increases VEGF mRNA expression in breast cancer cells. *MCF7 cells were cultured in iodine-containing medium for 7 days. Medium was replaced by iodine-containing (control) or iodine deficient (ID) medium for 2 to 6 or 6 to 24 hours. VEGF mRNA expression was determined using RT-qPCR (A: N=5; B: N=2, one representative experiment). Data are expressed as means ± SEM. Statistical test: one-way ANOVA with Bonferroni (comparing pairs of columns with corresponding timing) post-hoc test. *P < 0.05.*

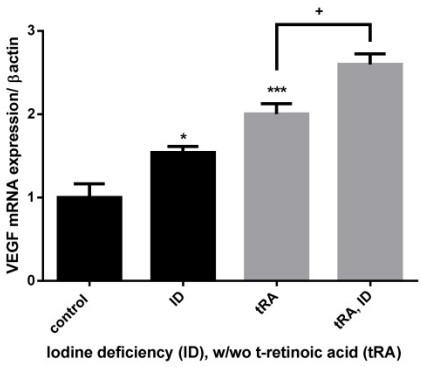

Figure 3. Iodine deficiency increases VEGF mRNA expression in breast cancer cells in presence of trans-retinoic acid. *MCF7 cells were cultured in iodine-containing medium for 7 days. Part of the cells was treated with tRA 24 hours before ID induction. Medium was replaced by iodine-containing (control) or iodine deficient (ID) medium. Cells were harvested 6 hours after medium change. VEGF mRNA expression was determined using RT-qPCR (N=3, one representative experiment). Data are expressed as means ± SEM. Statistical test: one-way ANOVA with Bonferroni (comparing "control" to "ID", "control" to "tRA" and "tRA" to "tRA, ID") post-hoc test. */+ P < 0.05, *** P<0.001, *versus control, +versus tRA.*

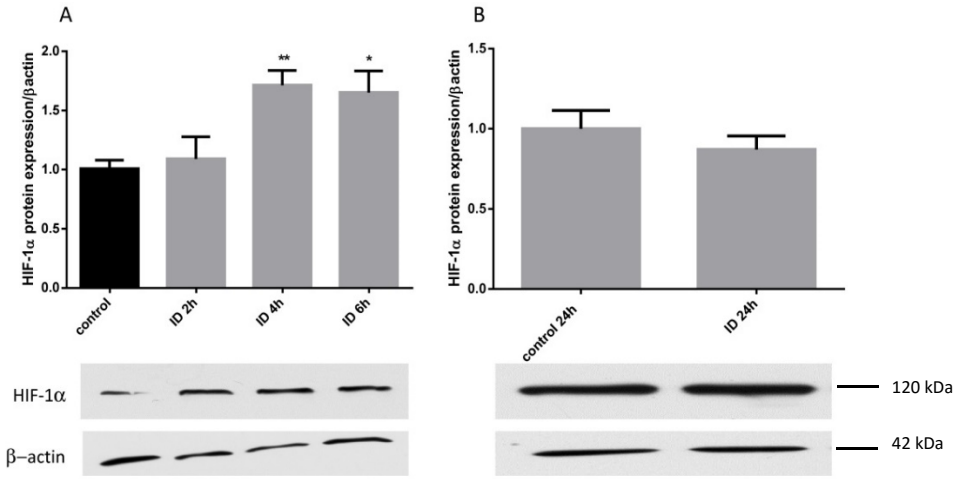

Figure 4. Iodine deficiency transiently increases HIF-1α protein expression in breast cancer cells. *MCF7 cells were cultured in iodine-containing medium for 7 days. Medium was replaced by iodine-containing (control) or iodine deficient (ID) medium for 2 to 6 or for 24 hours. HIF-1α protein expression was determined by western blot (A: N=5, B: N=3). Data are expressed as means ± SEM. Statistical test: one-way ANOVA with Dunnett post-hoc test. *P < 0.05, **p < 0.01.*

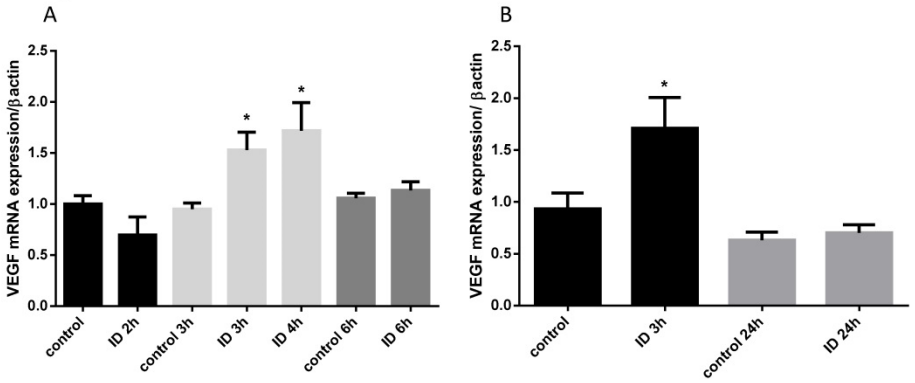

Figure 5. Iodine deficiency transiently increases VEGF mRNA expression in breast non-cancerous cells. *MCF12A cells were cultured in iodine-containing medium for 7 days. Medium was replaced by iodine-containing (control) or iodine deficient (ID) medium for 2 to 6 or 3 to 24 hours. VEGF mRNA expression was determined using RT-qPCR (A: N=3, B: N=2, one representative experiment). Data are expressed as means ± SEM. Statistical test: one-way ANOVA with Bonferroni (comparing pairs of columns with corresponding timing) post-hoc test. *P < 0.05.*

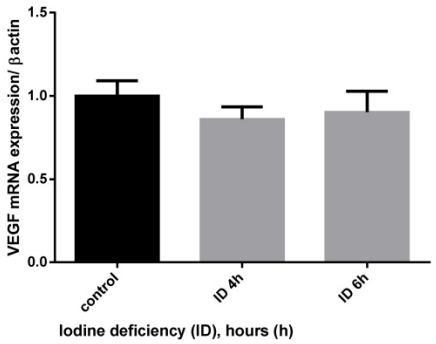

Figure 6. Iodine deficiency does not influence VEGF mRNA expression in human dermal fibroblasts. *HDF cells were cultured in iodine-containing medium for 7 days. Medium was replaced by iodine-containing (control) or iodine deficient (ID) medium. Cells were harvested 4 and 6 hours after medium change. VEGF mRNA expression was determined using RT-qPCR (N=2, one representative experiment). Data are expressed as means ± SEM. Statistical test: one-way ANOVA.*

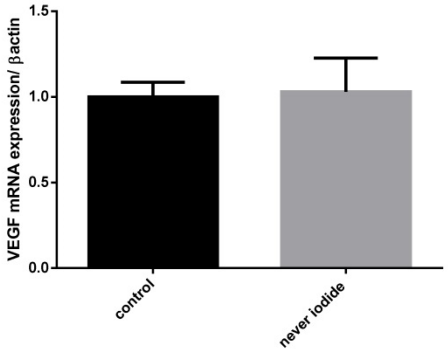

Figure 7. VEGF mRNA expression does not differ in breast cancer cells exposed or never exposed to iodine. *MCF7 cells were cultured in iodine-containing or iodine-deficient medium for 7 days. VEGF mRNA expression was determined using RT-qPCR (N=3). Statistical test: Unpaired Student's t test.*

References

1. **Arroyo-Helguera O, Anguiano B, Delgado G and Aceves C**. Uptake and antiproliferative effect of molecular iodine in the MCF-7 breast cancer cell line. *Endocr Relat Cancer* 13: 1147-1158, 2006.
2. **Cann SA, van Netten JP and van NC**. Hypothesis: iodine, selenium and the development of breast cancer. *Cancer Causes Control* 11: 121-127, 2000.
3. **Chen L, Xu B, Liu L, Luo Y, Zhou H, Chen W, Shen T, Han X, Kontos CD and Huang S**. Cadmium induction of reactive oxygen species activates the mTOR pathway, leading to neuronal cell death. *Free Radic Biol Med* 50: 624-632, 2011.
4. **Cho JY, Leveille R, Kao R, Rousset B, Parlow AF, Burak WE, Jr., Mazzaferri EL and Jhiang SM**. Hormonal regulation of radioiodide uptake activity and Na+/I- symporter expression in mammary glands. *J Clin Endocrinol Metab* 85: 2936-2943, 2000.
5. **Ciruelos Gil EM**. Targeting the PI3K/AKT/mTOR pathway in estrogen receptor-positive breast cancer. *Cancer Treat Rev* 40: 862-871, 2014.
6. **Craps J, Joris V, De JB, Sonveaux P, Horman S, Lengele B, Bertrand L, Many MC, Colin IM and Gerard AC**. Involvement of mTOR and Regulation by AMPK in Early Iodine Deficiency-Induced Thyroid Microvascular Activation. *Endocrinology* 157: 2545-2559, 2016.
7. **Derry DM**. *Breast Cancer and Iodine*. Trafford Publishing, 2001,
8. **Eskin BA, Bartuska DG, Dunn MR, Jacob G and Dratman MB**. Mammary gland dysplasia in iodine deficiency. Studies in rats. *JAMA* 200: 691-695, 1967.
9. **Eskin BA, Shuman R, Krouse T and Merion JA**. Rat mammary gland atypia produced by iodine blockade with perchlorate. *Cancer Res* 35: 2332-2339, 1975.
10. **Forsythe JA, Jiang BH, Iyer NV, Agani F, Leung SW, Koos RD and Semenza GL**. Activation of vascular endothelial growth factor gene transcription by hypoxia-inducible factor 1. *Mol Cell Biol* 16: 4604-4613, 1996.

11. **Garcia-Solis P, Alfaro Y, Anguiano B, Delgado G, Guzman RC, Nandi S, Diaz-Munoz M, Vazquez-Martinez O and Aceves C**. Inhibition of N-methyl-N-nitrosourea-induced mammary carcinogenesis by molecular iodine (I2) but not by iodide (I-) treatment Evidence that I2 prevents cancer promotion. *Mol Cell Endocrinol* 236: 49-57, 2005.
12. **Gerard AC, Humblet K, Wilvers C, Poncin S, Derradji H, de Ville de GC, Abou-el-Ardat K, Baatout S, Sonveaux P, Denef JF and Colin IM**. Iodine-deficiency-induced long lasting angiogenic reaction in thyroid cancers occurs via a vascular endothelial growth factor-hypoxia inducible factor-1-dependent, but not a reactive oxygen species-dependent, pathway. *Thyroid* 22: 699-708, 2012.
13. **Gerard AC, Poncin S, Audinot JN, Denef JF and Colin IM**. Iodide deficiency-induced angiogenic stimulus in the thyroid occurs via HIF- and ROS-dependent VEGF-A secretion from thyrocytes. *Am J Physiol Endocrinol Metab* 296: E1414-E1422, 2009.
14. **Gerard AC, Poncin S, Caetano B, Sonveaux P, Audinot JN, Feron O, Colin IM and Soncin F**. Iodine deficiency induces a thyroid stimulating hormone-independent early phase of microvascular reshaping in the thyroid. *Am J Pathol* 172: 748-760, 2008.
15. **Ghent WR, Eskin BA, Low DA and Hill LP**. Iodine replacement in fibrocystic disease of the breast. *Can J Surg* 36: 453-460, 1993.
16. **Hammami MM and Bakheet S**. Radioiodine breast uptake in nonbreastfeeding women: clinical and scintigraphic characteristics. *J Nucl Med* 37: 26-31, 1996.
17. **He H, Venema VJ, Gu X, Venema RC, Marrero MB and Caldwell RB**. Vascular endothelial growth factor signals endothelial cell production of nitric oxide and prostacyclin through flk-1/KDR activation of c-Src. *J Biol Chem* 274: 25130-25135, 1999.
18. **Huang LE, Arany Z, Livingston DM and Bunn HF**. Activation of hypoxia-inducible transcription factor depends primarily upon redox-sensitive stabilization of its alpha subunit. *J Biol Chem* 271: 32253-32259, 1996.
19. Iodine Global Network. Global Scorecard 2014: Number of iodine deficient countries more than halved in past decade. IDD newsletter . 2015.
20. **Johns A, Freay AD, Fraser W, Korach KS and Rubanyi GM**. Disruption of estrogen receptor gene prevents 17 beta estradiol-induced angiogenesis in transgenic mice. *Endocrinology* 137: 4511-4513, 1996.
21. **Kilbane MT, Ajjan RA, Weetman AP, Dwyer R, McDermott EW, O'Higgins NJ and Smyth PP**. Tissue iodine content and serum-mediated 125I uptake-blocking activity in breast cancer. *J Clin Endocrinol Metab* 85: 1245-1250, 2000.
22. **Kogai T, Schultz JJ, Johnson LS, Huang M and Brent GA**. Retinoic acid induces sodium/iodide symporter gene expression and radioiodide uptake in the MCF-7 breast cancer cell line. *Proc Natl Acad Sci U S A* 97: 8519-8524, 2000.
23. **Ku DD, Zaleski JK, Liu S and Brock TA**. Vascular endothelial growth factor induces EDRF-dependent relaxation in coronary arteries. *Am J Physiol* 265: H586-H592, 1993.
24. **Lund E and Bonaa KH**. Reduced breast cancer mortality among fishermen's wives in Norway. *Cancer Causes Control* 4: 283-287, 1993.
25. **Ma J, Zhang Q, Chen S, Fang B, Yang Q, Chen C, Miele L, Sarkar FH, Xia J and Wang Z**. Mitochondrial dysfunction promotes breast cancer cell migration and invasion

through HIF1alpha accumulation via increased production of reactive oxygen species. *PLoS One* 8: e69485, 2013.

26. **Nakamura J, Savinov A, Lu Q and Brodie A**. Estrogen regulates vascular endothelial growth/permeability factor expression in 7,12-dimethylbenz(a)anthracene-induced rat mammary tumors. *Endocrinology* 137: 5589-5596, 1996.
27. **Nava-Villalba M, Nunez-Anita RE, Bontempo A and Aceves C**. Activation of peroxisome proliferator-activated receptor gamma is crucial for antitumoral effects of 6-iodolactone. *Mol Cancer* 14: 168, 2015.
28. **Patrick L**. Iodine: deficiency and therapeutic considerations. *Altern Med Rev* 13: 116-127, 2008.
29. **Pearce EN, Andersson M and Zimmermann MB**. Global iodine nutrition: Where do we stand in 2013? *Thyroid* 23: 523-528, 2013.
30. **Perron B, Rodriguez AM, Leblanc G and Pourcher T**. Cloning of the mouse sodium iodide symporter and its expression in the mammary gland and other tissues. *J Endocrinol* 170: 185-196, 2001.
31. **Pisani P, Parkin DM, Bray F and Ferlay J**. Estimates of the worldwide mortality from 25 cancers in 1990. *Int J Cancer* 83: 18-29, 1999.
32. **Prasad S, Gupta SC and Tyagi AK**. Reactive oxygen species (ROS) and cancer: Role of antioxidative nutraceuticals. *Cancer Lett* 2016.
33. **Price DJ, Grove JR, Calvo V, Avruch J and Bierer BE**. Rapamycin-induced inhibition of the 70-kilodalton S6 protein kinase. *Science* 257: 973-977, 1992.
34. **Rillema JA and Hill MA**. Prolactin regulation of the pendrin-iodide transporter in the mammary gland. *Am J Physiol Endocrinol Metab* 284: E25-E28, 2003.
35. **Rosner H, Moller W, Groebner S and Torremante P**. Antiproliferative/cytotoxic effects of molecular iodine, povidone-iodine and Lugol's solution in different human carcinoma cell lines. *Oncol Lett* 12: 2159-2162, 2016.
36. **Sebastiano Venturi**. **Evolutionary Significance of Iodine**. *Current Chemical Biology* 5: 2011.
37. **Shrivastava A, Tiwari M, Sinha RA, Kumar A, Balapure AK, Bajpai VK, Sharma R, Mitra K, Tandon A and Godbole MM**. Molecular iodine induces caspase-independent apoptosis in human breast carcinoma cells involving the mitochondria-mediated pathway. *J Biol Chem* 281: 19762-19771, 2006.
38. **Smyth PP, Smith DF, McDermott EW, Murray MJ, Geraghty JG and O'Higgins NJ**. A direct relationship between thyroid enlargement and breast cancer. *J Clin Endocrinol Metab* 81: 937-941, 1996.
39. **Soriano O, Delgado G, Anguiano B, Petrosyan P, Molina-Servin ED, Gonsebatt ME and Aceves C**. Antineoplastic effect of iodine and iodide in dimethylbenz[a]anthracene-induced mammary tumors: association between lactoperoxidase and estrogen-adduct production. *Endocr Relat Cancer* 18: 529-539, 2011.
40. **Stoddard FR, Brooks AD, Eskin BA and Johannes GJ**. Iodine alters gene expression in the MCF7 breast cancer cell line: evidence for an anti-estrogen effect of iodine. *Int J Med Sci* 5: 189-196, 2008.

41. **Vayre L, Sabourin JC, Caillou B, Ducreux M, Schlumberger M and Bidart JM**. Immunohistochemical analysis of Na+/I- symporter distribution in human extra-thyroidal tissues. *Eur J Endocrinol* 141: 382-386, 1999.
42. **Venturi S**. Is there a role for iodine in breast diseases? *Breast* 10: 379-382, 2001.
43. **Venturi S and Venturi M**. Evolution of Dietary Antioxidant Defences. *European Epi-Marker* 11: 1-12, 2007.
44. **Zhu D, Shen Z, Liu J, Chen J, Liu Y, Hu C, Li Z and Li Y**. The ROS-mediated activation of STAT-3/VEGF signaling is involved in the 27-hydroxycholesterol-induced angiogenesis in human breast cancer cells. *Toxicol Lett* 264: 79-86, 2016.
45. **Ziegler RG, Hoover RN, Pike MC, Hildesheim A, Nomura AM, West DW, Wu-Williams AH, Kolonel LN, Horn-Ross PL, Rosenthal JF and Hyer MB**. Migration patterns and breast cancer risk in Asian-American women. *J Natl Cancer Inst* 85: 1819-1827, 1993.
46. **Zorov DB, Juhaszova M and Sollott SJ**. Mitochondrial reactive oxygen species (ROS) and ROS-induced ROS release. *Physiol Rev* 94: 909-950, 2014.

3.3 PAPER 3

Differential VEGF expression post-irradiation is modulated by iodine deficiency in cancerous and non-cancerous breast cells

Jessica Vanderstraeten[1], Bjorn Baselet[2], Jasmine Buset[2], Naziha Ben Said[1], Marie-Christine Many[1], Anne-Catherine Gérard[3]* and Hanane Derradji[2]*

The work presented in this manuscript is still in progress

Differential VEGF expression post-irradiation is modulated by iodine deficiency in cancerous and non-cancerous breast cells

Jessica Vanderstraeten[1], Bjorn Baselet[2], Jasmine Buset[2], Naziha Ben Said[1], Marie-Christine Many[1], Anne-Catherine Gérard[3]* and Hanane Derradji[2]*

Authors' affiliation

[1]Pole of Morphology, Institut de Recherche Expérimentale et Clinique (IREC), Université catholique de Louvain (UCL), Brussels, Belgium; [2]Radiobiology Unit**,** Belgian Nuclear Research Centre (SCK•CEN), Mol, Belgium; [3]Service d'Endocrino-Diabétologie, Centre Hospitalier Régional (CHR) Mons-Hainaut, Belgium.

*these authors equally contributed to the present manuscript

Abstract

Breast is an organ that is sensitive to radiation and iodine deficiency (ID). Indeed, several studies showed increased breast cancer risk after radiation treatment for benign conditions. Besides, ID was shown to induce structural and functional breast alterations and is linked to breast pathologies. In addition, radiations and ID are both able to induce oxidative stress and VEGF (vascular endothelial growth factor)-dependent microvascular responses in breast and other organs. Therefore, we hypothesized that the combination of radiation-induced ROS overproduction and VEGF up-regulation could be amplified in ID conditions. Radiations and ID combined and separate effects on ROS production and VEGF expression were thus compared in two breast cell lines: MCF7 and MCF12A. ID was induced by medium change and cells were then X-irradiated with doses of 0.1 or 3 Gy. In MCF7, ID alone or combined with both doses of radiation significantly increased VEGF mRNA expression to a similar extent, but radiations alone had no effect. ROS other than mitochondrial superoxide and alkyl radicals were involved in VEGF up-regulation. In MCF12A cells, ID and both radiation doses separately increased VEGF mRNA and an additive effect on VEGF up-regulation was observed when a dose of 3 Gy of X-rays was combined to ID. ROS excluding mitochondrial superoxide and alkyl radicals were involved in ID-induced VEGF up-regulation while mitochondrial superoxide and alkyl radicals were involved in VEGF up-regulation induced by radiations alone and combined with ID.

In conclusion, radiations induce a different regulation of VEGF in different breast cell lines, which is further enhanced by ID in MCF12A cells. Since VEGF is related to a bad prognosis in breast cancer, iodine status should not be ignored before exposure to high radiation doses as in the case of radiotherapy and even in the context of exposure to lower doses such as 0.1 Gy.

Key words

Radiation, Iodine Deficiency, Breast, VEGF, ROS, vascularization

Introduction

Human populations are constantly exposed to diverse types of radiation through natural sources such as UV, radioactive materials from earth or cosmic rays; or through man-made sources from medical exposure and in some cases from usually small quantities of radioactive materials released from coal and nuclear power plants activities (18). Breast is a radiation-sensitive organ, as demonstrated by several epidemiological studies showing a link between radiation exposure and breast cancer risk (17; 34). For a better understanding of breast cancer risks associated with radiation exposure, studies on the molecular targets of radiations are essential and a myriad of genes were shown to be down- or up-regulated by radiations. Some genes often up-regulated by radiations, such as *VEGF,* are involved in vascularization and angiogenesis. Indeed, several studies demonstrated radiation-induced increase in VEGF expression *in vivo* and *in vitro* in diverse organs and cell lines, among which breast cell lines (21; 44). Due to the important role of angiogenesis in tumor progression, several authors have hypothesized a role for VEGF in radiation resistance (38). A likely explanation for this VEGF up-regulation involves radiation-induced ROS increase. Indeed, radiations are known to induce radiolysis of water, which is followed by the formation of diverse ROS, potentially leading to oxidative stress according to the dose and type of radiation used (3; 18). Besides, VEGF expression is known to be regulated by ROS content and oxidative stress (OS) via, for instance, ROS- and OS-sensitive transcription factors as HIF-1 and Sp1 (28; 35).

Another factor that can influence breast pathologies is iodine deficiency (ID). ID was shown to induce breast atypia (10; 11; 22), and a lower breast cancer rate was observed in various populations known for their high iodine intake (8; 26; 32). Moreover, acute ID was shown to transiently increase VEGF expression *in vivo* and *in vitro* in different organs capable of iodine uptake such as thyroid, salivary glands, stomach and mammary glands (39; 40). This VEGF increase was further demonstrated to be dependent on an increase in ROS content in thyroid and mammary cells (12; 40).

Because ID is still a major health problem worldwide (19), its potential interference with the radiation response is an interesting question. In this regard, the combination of ID and an exposure to 4 Gy of X-rays was shown to induce additive effects on thyroid carcinogenesis in rats (6).

Thus, because radiations and ID are able to increase ROS content and up-regulate VEGF expression, we hypothesized that the combination of both factors could lead

to an additive effect regarding ROS production and VEGF regulation in breast cells, thereby influencing breast response to radiations.

In this study, the effects of radiation alone or as combined with ID were studied in two I^-/Na^+ symporter (NIS)-expressing breast cell lines, a cancerous (MCF7) and a non-cancerous (MCF12A) cell line. Currently, the biological effects of low doses of radiation are mostly extrapolated from the effects of high doses of radiations, based on the linear non-threshold model. However, increasing results tend to disagree with this model, and fundamental research is thus needed to assess low dose radiation effects (23; 31; 37). Therefore, two doses of X-rays were used in this project: a low dose (0,1 Gy) and a high dose (3 Gy) for comparison purposes.

Material and methods

Cell models

MCF7 human mammary gland adenocarcinoma cell line (Sigma, St.-Louis, MO, USA) and MCF12A human normal mammary gland cell line (ATCC, Manassas, USA) were routinely cultured at 5% CO2, 37°C in a humidified atmosphere, as previously described [...]. Seven days before the experiments, 10^{-8} M NaI was added to the medium. On the day of the experiment, 10 µM of diphenyleneiodonium (Sigma), a NADPH oxidase inhibitor, or 0.75mM of N-acetylcysteine (NAC, Sigma) was added to the medium 1 h before replacing the medium where indicated. After washing with PBS, culture medium was replaced by fresh medium containing NaI (controls) or not (ID) with or without 10µM of DPI 0.75mM of NAC, or 10 µM (MCF7 cells) or 2 µM (MCF12A cells) mitoTEMPO (Sigma) where indicated. Cells were harvested at different time points after medium renewal.

Irradiation

30 min after medium change, cells were X-irradiated once with a dose of 0,1 or 3 Gy, using an Xstrahl RX generator (operating at 250 kV and12 mA, 3.8 mm Al- and 1.4 mm Cu-filtered X-rays).

Quantitative polymerase chain reaction

Cell were harvested and homogenized in 1 ml TriPure isolation reagent (Roche, Mannheim, Germany), and total RNA was extracted according to the

manufacturer's protocol and resuspended in RNase-free water. Reverse transcription was performed as previously described [...]. cDNAs (0.04 µg of cDNA template in 2 µL) were mixed with 10 µM of selected primer pair (**table 1**) and Perfecta SYBR green reaction mix (VWR, Pennsylvania, United States) in a final volume of 15 µL. Reactions were performed with an IQ5 iCycler (Bio-Rad, Herts, UK) as previously described (7). Annealing temperatures are given in **table 1**. Amplification levels were normalized to those of β-actin. All samples were measured in duplicate.

RNA	Forward primer	Reverse primer	Annealing temp.
ß-actin	5'CATCCTGCGTCTGGACCT3'	5'AGGAGGAGCAATGATCTTGAT3'	62°C
VEGF-A	5'GCAGATGTCCCGGCGAAGAGAAGA3'	5'CGGGGAGGGCAGAGCTGAGTGTTA3'	62°C
VEGF165a	*5'GAGCAAGACAAGAAAATCCC3'*	*5'CCTCGGCTTGTCACATCTG3'*	58.5°C
VEGF165b	*5'GAGCAAGACAAGAAAATCCC3'*	*5'GTGAGAGATCTGCAAGTACG3'*	59°C

Table 3: Primer sequences and their annealing temperature for qRT-PCR.

Immunofluorescence

Immunofluorescence was performed as previously described (40). Plates were incubated at 4ºC overnight with primary antibody (4-hydroxynonenal (4-HNE), 393207-100, VWR) at a concentration of 1/1000. Primary antibody was omitted in negative controls. Signals were revealed after 1h incubation at room temperature in the dark with species-specific secondary antibodies conjugated to fluorophores (Alexa Fluor 488-conjugated goat anti-rabbit, A11034, 1/300, Invitrogen, Ghent, Belgium). Nuclei were stained for 5 minutes with 4'-6'diamidino-2-phenylindole (DAPI, 1/10,000) and slides were mounted in Fluorescent Mounting Medium (Dako Cytomation, Heverlee, Belgium). Images were captured on an AxioCam MRc5 fluorescence microscope using the Axio Vision 4.8 software (Zeiss, Zaventem, Belgium).

ROS measurement using flow cytometry

On the day of the experiment, medium change was executed with phenol red free medium. ROS production was measured with a fluorescent dye Carboxy-DCFDA (5-(and-6)-Carboxy-2',7'-Dichlorofluorescein Diacetate) (DCF-DA, Invitrogen). Cells were washed with PBS and incubated at 37°C, 5% CO2 during 45 min with the DCF-DA dye at a final concentration of 10µM in HEPES/HBSS with Ca2+/Mg2+ (Thermo Scientific, Ghent, Belgium). Cells were washed and trypsinized. Harvested cells were centrifuged at 200g for 5 min and supernatant was discarded. Pellets were washed and resuspended in HBSS without Ca2+/Mg2+. Cells were filtered to avoid aggregates and propidium iodide was added at a final concentration of 1µg/ml to eliminate dead cells from the measurements. Positive ROS control was obtained by adding a ROS inducer, tert-butyl hydroxide, at 25 or 50 µM in untreated cells. DCFDA and propidium iodide fluorescence were measured with a BD Accuri C6 flow cytometer (BD biosciences, New Jersey, USA) at 525 and 620 nm respectively. Maximum flow speed was 300 events/s and a total of 10 000 events per sample were analyzed.

Statistics

All data are expressed as means ± SEM. Experiments were independently conducted 3 to 8 times with 3 to 5 replicates for each condition. Student T-test or one-way ANOVA with Tukey-Kramer or Bonferroni post-hoc test were used where appropriate (GraphPad Instat, San Diego, CA). $P < 0.05$ was considered to be statistically significant.

Results

Additive effect of radiation and ID on VEGF mRNA up-regulation in MCF12A but not in MCF7 cells

Two cell lines known to express the iodide/sodium symporter NIS and to be influenced by acute ID (40) were used. Acute ID induced VEGF mRNA up-regulation after 4 h in MCF12A (fig. 1a and 1c) and after 6 hours in MCF7 cells (Fig. 1b and 1d), which is in agreement with previous results (40). Radiations alone (3 Gy and 0.1 Gy) also increased VEGF mRNA in MCF12A cells (fig. 1a and 1c) but not in MCF7 cells (fig. 1b and 1d). Interestingly, the combination of ID with 3 Gy X-irradiation had an additive effect on VEGF mRNA in MCF12A cells (fig. 1a) but showed a similar VEGF mRNA induction to that induced by ID alone in MCF7 cells (fig. 1b). In MCF12A cells,

the response induced by the exposure to a low dose of X-rays alone was similar to the response induced by a high dose, but the combination of 0.1 Gy of X-rays with ID did not have an additive effect on VEGF mRNA expression (fig. 1c). In MCF7 cells, exposure to the low dose of X-rays combined or not with ID induced a similar response as the high dose (fig. 1d).

Because an additive effect on VEGF mRNA expression was observed when ID was combined with an exposure to the high dose and not to the low dose in MCF12A, the rest of the analyses were carried out only with the high dose.

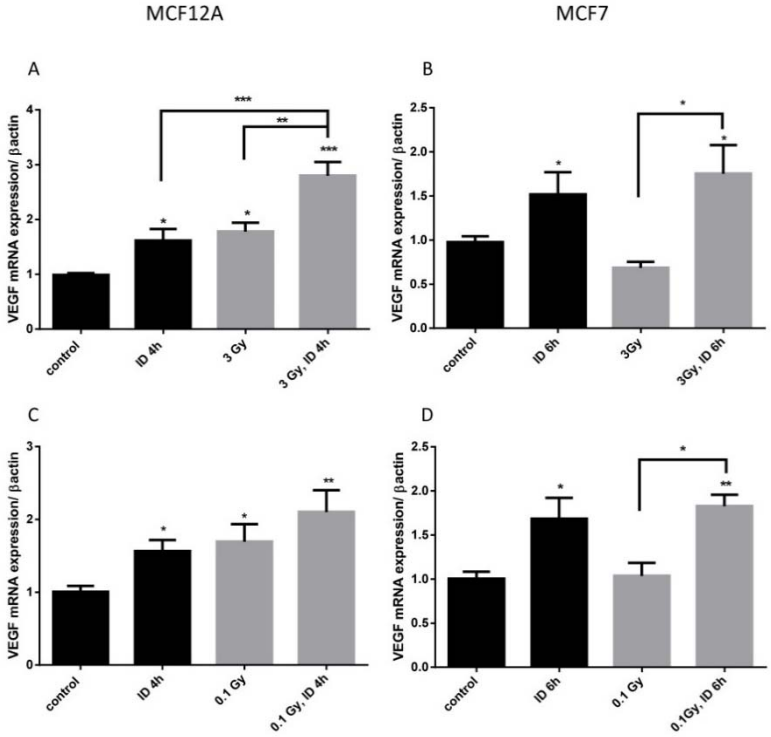

Figure 1. Acute ID and radiation at a high dose induce an additive VEGF mRNA up-regulation in MCF12A but not in MCF7 breast cells. *Cells were cultured in iodine-containing medium for 7 days. Thereafter, the medium was replaced by iodine-containing (control) or iodine deficient (ID) medium and cells were then irradiated with a dose of 3 Gy (**A, B**) or 0.1 Gy (**C, D**). Cells were harvested 4 or 6 hours (h) after medium change. (**A-D**) VEGF mRNA expression in MCF12A (**A, C**) and MCF7 cells (**B, D**) was determined using RT-qPCR. N= 7 (A), 5 (B, C) or 4 (D). Data are expressed as means ± SEM. Statistical test: one-way ANOVA with Tukey-Kramer post-hoc test. P-values < 0.05 were considered as statistically significant.:*P < 0.05, **P < 0.01, ***P<0.001.*

High dose of radiation and/or ID have similar effects on VEGF165a splice variant mRNA expression than on total VEGF mRNA, but not on VEGF165b mRNA expression

VEGF pre-RNA is known to be alternatively spliced and splice variants have different angiogenic capacities (42). One of the principal splice variants involved in pro-angiogenic response is VEGF165a (15). We have therefore looked at its mRNA expression and observed that 3 Gy X-irradiation with/without ID induced a similar response in VEGF165a mRNA regulation to that of global VEGF mRNA regulation in both cell lines, with an additive effect on mRNA induction in the presence of radiation and ID together (fig. 2a-b). The alternate splicing of VEGF exon 8 leads to splice variants that do not have pro-angiogenic activity and that are considered as competitive inhibitors of the pro-angiogenic forms. They are termed as VEGFxxxb (43). We have therefore looked at the negative splice variant VEGF165b to see whether it is also up-regulated. ID and high-dose X-rays separately or combined did not significantly modulate VEGF165b mRNA in both cell lines (fig. 2 c-d).

Radiation and ID induced an increase in ROS production in MCF12A and MCF7 cells

Because VEGF is known to be regulated by ROS and because ROS were previously shown to be involved in ID-induced VEGF up-regulation in breast cells (25; 40), ROS production was indirectly assessed through 4-HNE staining, a product of lipid peroxidation and a marker of oxidative stress, and directly via the use of DCF-DA dye. 4-HNE staining revealed an increase in ROS-induced damages 2 h and 4 h after ID or radiation in MCF12A (fig. 3a-c) and MCF7 cells (fig. 3e-g) respectively. However, the increase in HNE staining was visually stronger in MCF12A cells exposed to both factors simultaneously (fig. 3d), but not in MCF7 cells (fig. 3h).

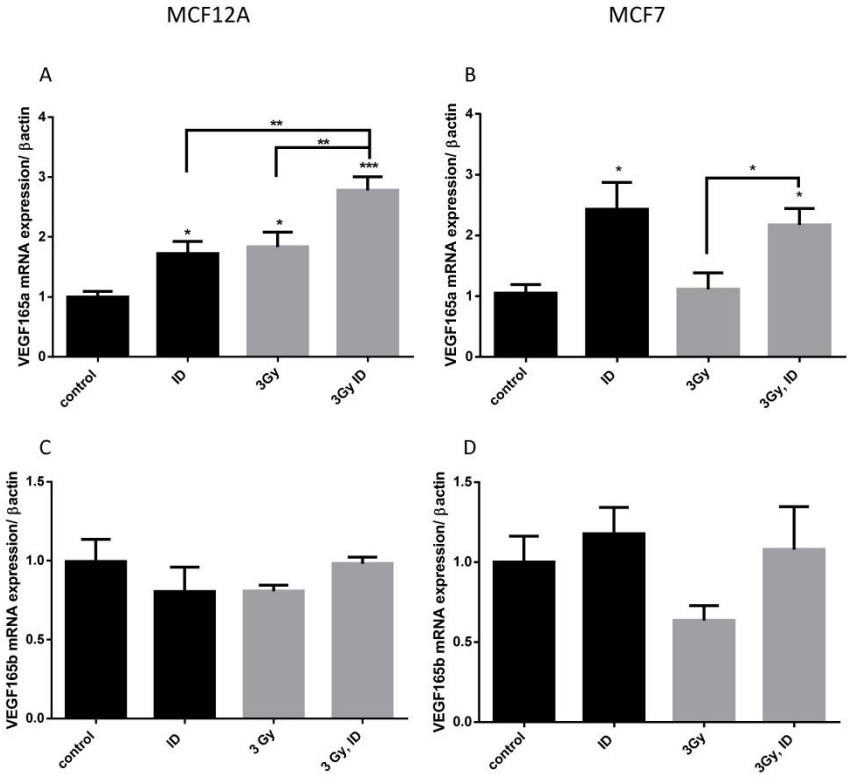

Figure 2. Acute ID and 3 Gy irradiation do not influence VEGF165b mRNA expression but induce an additive VEGF165a mRNA up-regulation in MCF12A but not in MCF7 breast cells. *Cells were cultured in iodine-containing medium for 7 days. Thereafter, the medium was replaced by iodine-containing (control) or iodine deficient (ID) medium and cells were then irradiated with a dose of 3 Gy. Cells were harvested 4 (A, C) or 6 hours (B,D) (h) after medium change. mRNA expression in MCF12A (**A, C**) and MCF7 cells (**B, D**) was determined using RT-qPCR. N= 5 (A), 4(B) or 3 (C, D). Data are expressed as means ± SEM. Statistical test: one-way ANOVA with Tukey-Kramer post-hoc test. P-values < 0.05 were considered as statistically significant.:*P < 0.05, **P < 0.01, ***P<0.001.*

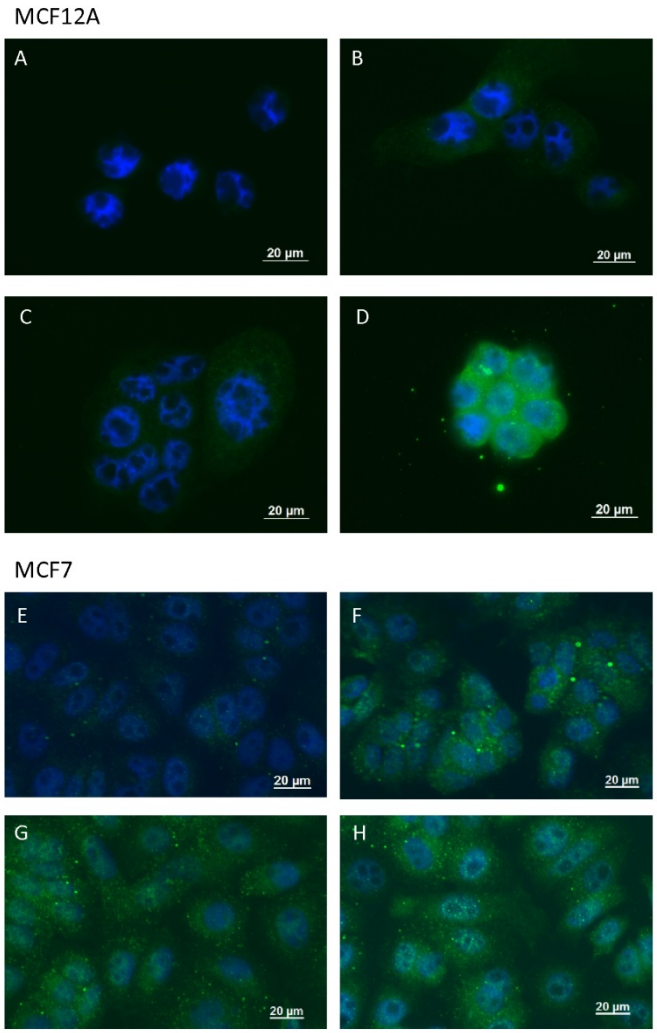

Figure 3. Acute ID and 3 Gy irradiation separately increase OS in both breast cell lines and OS induced by ID combined with radiation is more important in MCF12A cells. *Cells were cultured in iodine-containing medium for 7 days. Thereafter, the medium was replaced by iodine-containing (control) or iodine deficient (ID) medium and cells were then irradiated with a dose of 3 Gy. 4-HNE adducts were detected using immunofluorescence after 2 or 4 h in MCF12A (**A-D**) and MCF7 (**E-H**) cells respectively. Control (A, E), ID (B, F), 3 Gy X-rays (C, G) and ID + 3 Gy X-rays (D, H). N=3. Representative pictures are shown. Scale bars = 20 µm.*

Since an additive effect of ID and 3 Gy of X-rays on VEGF mRNA and HNE staining was only observed in MCF12A, ROS induction was further assessed in those cells. ROS content was detected with DCF-DA dye and quantified by flow cytometry. ID was induced by medium change and lasted 1 or 2 h. ID alone induced a moderate increase in ROS at both time points (fig. 4a). Control and ID cells were irradiated after medium change and cells were exposed to the dye 10 min before irradiation (fig. 4b), 10 min after the end of irradiation (fig. 4c) or 25 min after the end of irradiation (fig. 4d). When the dye was added before irradiation, a huge increase in ROS content was observed, probably mostly due to water radiolysis, but no significant difference in ROS content between iodine-sufficient and iodine-deprived cells was observed, though the difference between iodine-sufficient and iodine-deprived cells was significant in non-irradiated cells (fig. 4b). When the dye was added 10 min after the irradiation, X-rays alone induced a non-significant increase in ROS (fig. 4c), which is consistent with observations in the literature describing a short burst of ROS following irradiation that disappear within seconds. However, the ROS content of irradiated ID cells was still significantly higher than that of ID cells (fig. 4c). But, when the dye was added 25 min after irradiation, the ROS production in ID cells and in ID irradiated cells was increased to a similar extent (fig.4d).

To summarize, our data suggest that ID induces a modest increase in ROS that lasted until two hours of treatment, which is in agreement with previous observations (40) while 3 Gy X-rays only induced a short burst of ROS. However, the increase in ROS content induced by radiations lasted longer in iodide-deficient cells.

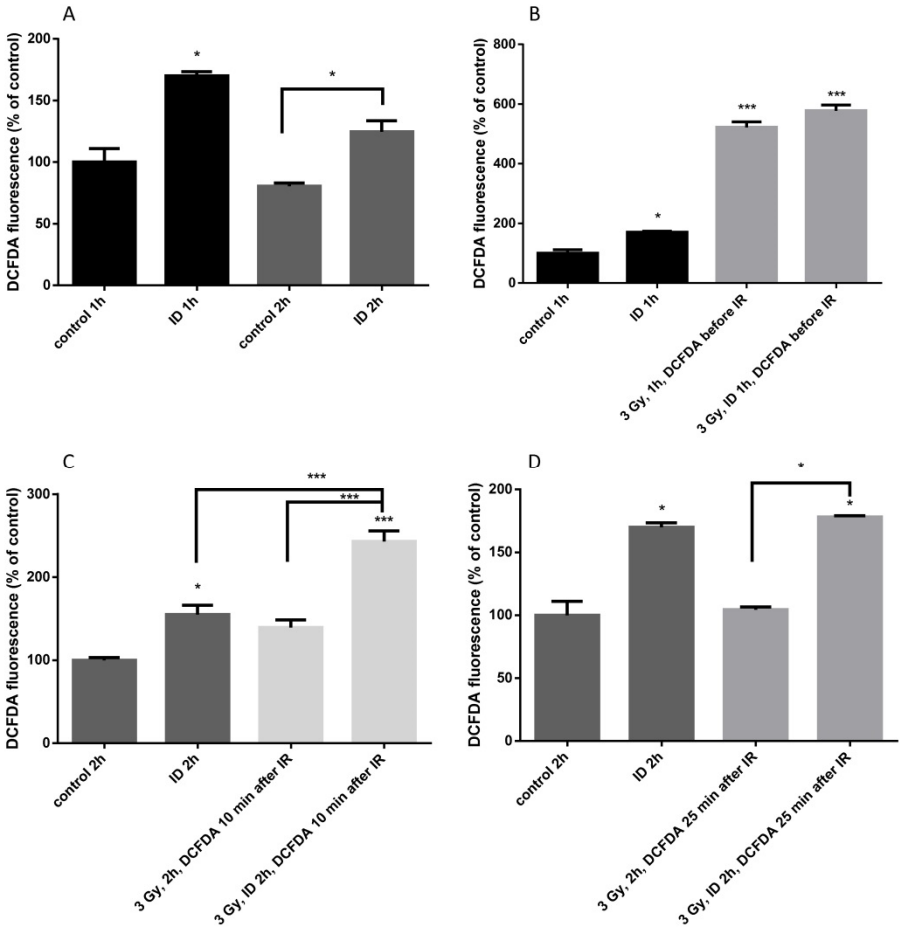

Figure 4. Acute ID increases ROS production and prolongs radiation-induced ROS increase in MCF12A cells. *Cells were cultured in iodine-containing medium for 7 days. Thereafter, the medium was replaced by iodine-containing (control) or iodine deficient (ID) medium and cells were then irradiated with a dose of 3 Gy. Cells were harvested 1 (**A** (two first columns), **B**) or 2 hours (h) (**A** (two last columns)**, C, D**) after medium change. Cellular ROS content was visualized with DCF-DA and measured by flow cytometry. In irradiated cells, DCF-DA was added 10 min before exposure to radiation (**B**), 10 min after the irradiation (**C**) or 25 min after irradiation (**D**). DCF-DA was added at corresponding timing in non-irradiated cells. N=3, one representative experiment. Data are expressed as means ± SEM. Statistical test: one-way ANOVA with Tukey-Kramer post-hoc test. P-values < 0.05 were considered as statistically significant.:*P < 0.05, ***P<0.001.*

ID and radiation-induced increase in VEGF mRNA depends on cellular ROS

To verify the hypothesis that ROS could be implicated in ID- and radiation-induced VEGF up-regulation, cells were treated with NAC, a general antioxidant (supplemental data, fig. 1). VEGF up-regulation was no longer observed after exposure to ID and/or radiation in presence of NAC, in both cell lines.
Two distinct inhibitors of cellular ROS were then used to shed some light on the origin of ROS in our model. Firstly, to know whether ROS from cellular production are involved in VEGF mRNA regulation, its expression was assessed in presence of DPI, an inhibitor that targets flavoenzymes, a major cellular source of ROS, and that partially targets mitochondrial ROS, another major source of ROS (5; 30). VEGF mRNA increase induced by ID and radiations alone or combined in MCF12A cells was totally inhibited by DPI (fig. 5a). Likewise, VEGF mRNA increase induced by ID and by ID and radiations was not observed in MCF7 cells treated with DPI (fig. 5b).

Involvement of mitochondrial ROS in VEGF mRNA up-regulation

Another important source of ROS is the mitochondria, particularly through mitochondrial electron transport superoxide leakage (30). Therefore, VEGF mRNA was studied in presence of mitoTEMPO, a mitochondrial superoxide and alkyl radical scavenger. In MCF12A cells, mitoTEMPO did not prevent the ID-induced increase in VEGF mRNA (fig. 5c). However, it prevented the one induced by radiation with or without ID (fig. 5c). Likewise, the presence of mitoTEMPO did not prevent ID-induced VEGF mRNA increase in MCF7 (fig. 5d). MitoTEMPO did not block the increase induced by both treatments together either (fig. 5d).

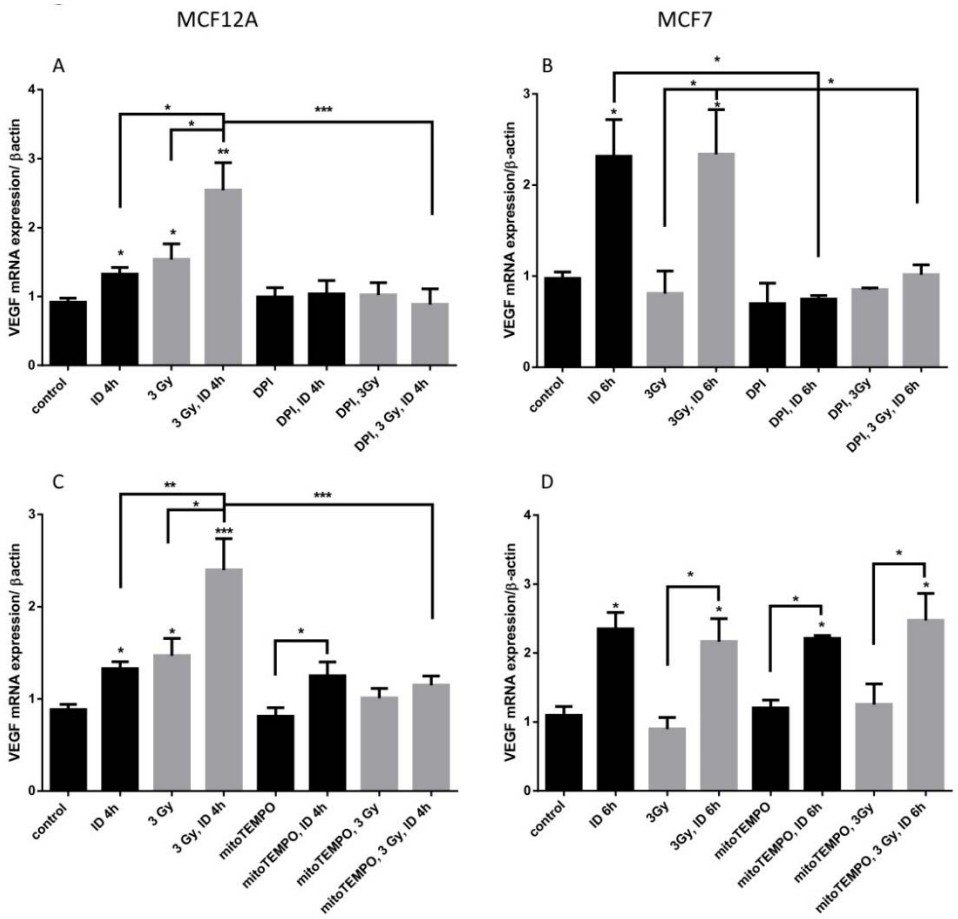

Figure 5. Acute ID and radiations-induced VEGF mRNA up-regulation depends on cellular ROS production in both cell lines but mitochondrial ROS is only involved in radiation-induced VEGF mRNA up-regulation in ID and iodide-sufficient MCF12A cells . *Cells were cultured in iodine-containing medium for 7 days. Medium was replaced by iodine-containing (control) or iodine deficient (ID) medium and were then irradiated with a dose of 3 Gy. Part of the cells were treated with DPI (**A, B**) or mitoTEMPO (**C, D**). Cells were harvested 4 or 6 hours (h) after medium change. VEGF mRNA expression in MCF12A (**A, C**) and MCF7 cells (**B, D**) was determined using RT-qPCR. N= 4(A, C) or 3 (B, D). Data are expressed as means ± SEM. Statistical test: one-way ANOVA with Bonferroni post-hoc test. P-value < 0,05 were considered as statistically significant.:*P < 0.05, **P < 0.01, ***P<0.001.*

ROS induced by ID and/or radiation are partially dependent on flavoenzymes activity and partially originate from mitochondria

ROS content was assessed in the presence of DPI and mitoTEMPO in MCF12A cells after exposure to 3 Gy of X-rays with or without acute ID. The basic experimental

design used here was the same as in fig. 4c : medium was changed to induce ID for two hours, thereafter, cells were irradiated with 3 Gy X-rays and the DCF-DA dye was added 10 min after the end of irradiation. These conditions were repeated in presence of either DPI (fig. 6a) or mitoTEMPO (fig. 6b).

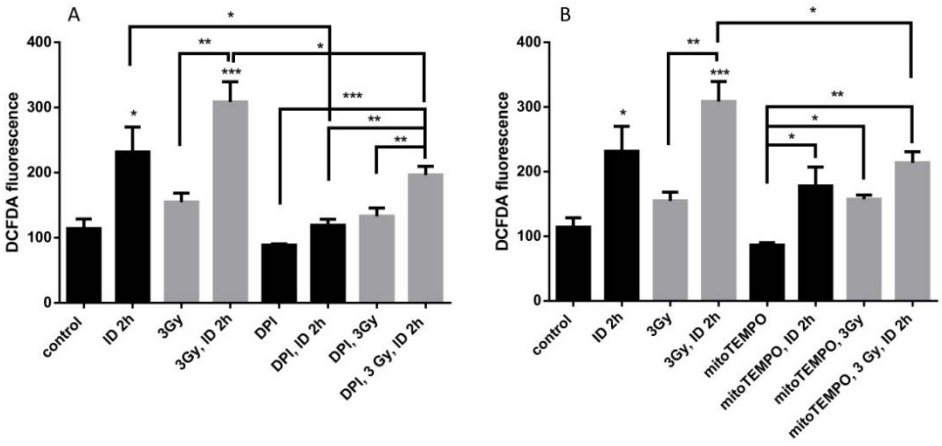

Figure 6. Acute ID-induced ROS increase does not depend on mitochondria and radiation-dependent ROS increase in ID depends on cellular ROS production, including at least mitochondrial ROS in MCF12A cells. *Cells were cultured in iodine-containing medium for 7 days. Thereafter, the medium was replaced by iodine-containing (control) or iodine deficient (ID) medium and cells were then irradiated with a dose of 3 Gy. Part of the cells were treated with DPI (**A**) or mitoTEMPO (**B**). Cells were harvested 2 hours (h) after medium change. Cellular ROS content was visualized with DCF-DA and measured by flow cytometry. DCF-DA was added 10 min after the irradiation. N=1, 3 technical replicates. Data are expressed as means ± SEM. Statistical test: one-way ANOVA with Bonferroni post-hoc test. P-values < 0,05 were considered as statistically significant.:*P < 0.05, **P<0,001, ***P<0.001.*

Though this experiment was carried out only once so far and must be interpreted with caution, the results suggest that mitochondrial superoxide and alkyl radicals are not induced by ID, since mitoTEMPO failed to decrease ID-induced increase in ROS, but are part of the ROS induced by irradiation in ID cells, since mitoTEMPO decreased ROS content but the latter is still significantly higher than in non-irradiated cells exposed to mitoTEMPO (fig. 6b). However, ROS induced by ID depend on flavoenzymes activity since DPI inhibits ID-induced ROS increase. Moreover, ROS induced by the combination of acute ID with radiation are partially dependent on flavoenzymes activity since DPI decreased their level but not to the level of non-irradiated cells exposed to DPI (fig. 6a). These results are consistent with the effects of mitoTEMPO and DPI on VEGF mRNA induction by acute ID with or without radiation.

Discussion

Radiations and ID are both known to influence breast pathologies and to elicit changes in molecular pathways, such as the activation of pathways regulating VEGF expression (8; 21; 34; 38; 40). Here, we report that, in some conditions, the combination of these two factors may induce greater VEGF mRNA up-regulation than when applied separately. In this research, two breast cell lines known for their sensitivity to ID were used. However, both cell lines reacted differently to radiation with or without ID. In MCF12A cells, a single X-ray dose of 3 Gy increased VEGF mRNA expression similarly to acute ID, and their effects on VEGF mRNA were additive. This VEGF up-regulation was accompanied by an increased oxidative stress, visualized by HNE staining, that followed the same pattern. In MCF7 cells, radiations did not affect VEGF mRNA. The combination of X-rays with ID up-regulated VEGF mRNA expression only to a similar extent as did acute ID alone. Nevertheless, OS was slightly increased by the three treatments, i.e. ID, 3 Gy of X-Rays, and the combination of ID and irradiation. Thus, radiation-induced OS did not affect VEGF mRNA expression at the studied time points and it is likely that the effects observed on VEGF expression in irradiated ID cells were only due to acute ID. Of note, another group observed that electromagnetic radiations induced VEGF up-regulation in MCF7 cells but at longer timing (44). It is thus possible that radiations could induce VEGF mRNA up-regulation later after exposure to IR. However, we do not observe any changes in VEGF mRNA expression 24 h after exposure (unpublished results).

Because MCF7 cells are cancerous and MCF12A are not, an interesting question to be raised is whether the differential VEGF regulation reflects the physiological state of those cells (normal vs cancerous) which could be addressed using primary cultures and/or in vivo experiments. It will be thus very interesting to expose primary culture from cancerous breast mastectomy/tumorectomy and breast reduction to IR in iodide-sufficient and iodide-deficient conditions.

Several studies have shown that doses over 1 Gy induce VEGF up-regulation in various cell types or tissues (1; 16; 21; 44). Here we showed that the low X-ray dose of 0,1 Gy also induced an increase in VEGF mRNA expression in iodide-sufficient conditions in MCF12A cells, but not in MCF7 cells. Moreover, though the effect of the low dose irradiation in iodide-deficient conditions on VEGF mRNA expression was not significantly higher than that of acute ID or irradiation separately in MCF12A cells, it is interesting to note that the statistical significance of it is increased in the presence of both factors.

Radiations, among which X-rays, were shown to affect alternative splicing in various cell and tissue types, including breast (27; 41). In our study, radiations were found to differentially influence the expression of VEGF alternative transcripts under both iodide conditions. Overall, the expression of VEGF165a mRNA followed the same trend as the total VEGF mRNA after exposure to 3 Gy X-rays in iodide-deficient and iodide-sufficient conditions, while that of VEGF165b mRNA did not change. Because VEGFxxxb splice variants are hypothesized to competitively inhibit the pro-angiogenic effects of VEGFxxxa splice variants and because VEGF165a is one of the principal pro-angiogenic variants of VEGF along with VEGF121 (4; 42), this result suggests that the up-regulation of VEGF mRNA is likely to induce a microvascular or angiogenic response. A matrigel test or in vivo experiments are thus necessary to confirm this hypothesis. Interestingly, acute ID also induced VEGF165a mRNA up-regulation while it had no effect on that of VEGF165b. To the best of our knowledge, this is the first study reporting that iodide status can influence alternative splicing and this result is in agreement with previous results showing a VEGF-dependent increased blood perfusion induced by ID in mice. Radiations affect alternative splicing both via the direct induction of alternative splicing and via specific alternative transcript preferential translation (41). It could be thus interesting to study VEGF splice variants expression at the protein level to verify whether their expression mirrors that of the transcripts variants or whether post-transcriptional mechanisms could modulate the observed response induced by radiation with and without acute ID.

Because difference in OS induced by the three treatments were visually observed in MCF12A cells exposed to 3 Gy X-rays and because OS plays an important role in VEGF induction, ROS production was further quantified at different time points by flow cytometry. Acute ID alone induced a modest increase in ROS after one and two hours. This modest increase is yet sufficient to induce VEGF as NAC treatment abrogates ID-induced VEGF. The radiation-induced ROS follow a different trend. In accord with the literature, radiation induced a strong rise in ROS content. It was not influenced by acute ID, and was not observed anymore 10 min after the end of the irradiation (3; 14). The sharp increase in ROS is probably mostly due to water radiolysis. However, the increase in ROS after irradiation was maintained longer in iodide deprived cells, reaching a point where ROS content was higher in irradiated ID cells than in irradiated cells and in ID cells, which probably accounts for the observed higher VEGF mRNA up-regulation since ROS and OS are known to be involved in VEGF regulation and ROS inhibition with NAC prevented VEGF mRNA up-regulation. It is possible that ROS induced by ID and/or radiations act either through the activation of the same pathway, or via

different mechanisms whose effects could be additional. To elucidate the molecular mechanisms involved in VEGF up-regulation in the three treatments, we investigated the source of ROS. To verify whether ROS other than ROS resulting from water radiolysis were involved in VEGF regulation, DPI was used to inhibit flavoenzymes, a major ROS cellular source. Flavoenzymes are mostly represented by NADPH oxidases but also include enzymes such as xanthine oxidase, NADPH cytochrome P450 oxidoreductase … DPI also partially inhibits mitochondrial ROS, another important ROS source (24). Thirdly, mitochondrial superoxide, which mainly comes from mitochondrial electron chain transport leaks but could also partly originate from enzymes such as NOX4 which was suggested to be expressed in breast mitochondria (13; 30), and mitochondrial alkyl radicals were inhibited by mitoTEMPO. In MCF12A cells, acute ID induced VEGF up-regulation was found to be dependent on ROS from cellular activity, but not on mitochondrial superoxide and alkyl radicals. VEGF overexpression induced by 3 Gy of X-rays in iodide-deficient and iodide-sufficient conditions however was suppressed by both DPI and mitoTEMPO. Those results do not exclude a possible participation of ROS from radiolysis of water, and maybe from other sources. Nevertheless, it is interesting to note that VEGF mRNA up-regulation induced by radiation is not only dependent on ROS induced by water radiolysis, but also depends, at least partially, on intrinsic cellular ROS production.

A preliminary experiment quantifying ROS production in MCF12A cells in the presence of the same ROS inhibitors, DPI and mitoTEMPO, supported those results. Indeed, the inhibition of mitochondrial superoxide and alkyl radicals did not decrease ID-induced ROS as it did not decrease ID-induced VEGF mRNA up-regulation. However, it did decrease radiation-induced ROS in iodide-sufficient and -deficient cells, as it did for VEGF mRNA. DPI decreases ROS production in all conditions, as it decreased VEGF mRNA induction also in all conditions. However, though both inhibitors decreased ROS production associated to IR exposure, ROS level were not decreased to control level, suggesting that other sources of ROS, possibly resulting from cascades induced by water radiolysis, are involved in ROS induction, and might also have a role in VEGF mRNA up-regulation.

Though the induction of VEGF mRNA was not higher in cells exposed to X-rays combined to acute ID as compared to ID cells alone in MCF7 cell line, ROS were inhibited with the same inhibitor to see whether the source of ROS was the same in both treatments. VEGF up-regulation was found to be inhibited by DPI but not by mitoTEMPO in both treatments, suggesting that it depends on ROS resulting from cellular activity but not on mitochondrial superoxide and alkyl radicals.

Thus, both the high and low dose of X-rays up-regulate VEGF mRNA expression in MCF12A but not in MCF7 cells. During radiotherapy, healthy cells in the direct vicinity of cancer cells can be exposed to doses such as 0.1 Gy and could thus secrete VEGF, thereby protecting the tumor vasculature, which is a mechanism often described to participate to cancer radioresistance (1; 38). Moreover, 0.1 Gy can also be reached via repeated medical exposures to IR such as CT-scan (36). Therefore, the effect of dose accumulation on VEGF mRNA should be studied to see whether the increase in VEGF mRNA expression is still observed. Such VEGF up-regulation could have deleterious consequences in cancer or pre-cancer patients as it influences the disease progression and is associated to a bad prognosis in breast cancer patients (2; 9; 20). Higher doses of radiation are relevant to radiotherapy (29; 33), and if high doses of radiations are proved to induce a higher up-regulation of VEGF expression in iodide-deficient tissues than in iodide-sufficient conditions in other breast models, iodide status of patients undergoing radiotherapy should be taken into account before exposure to IR due to the potential role of VEGF in radio-resistance.

List of abbreviations

Diphenyleneiodonium (DPI), iodine deficiency (ID), N-acetylcysteine (NAC), sodium/iodide symporter (NIS), oxidative stress (OS), reactive oxygen species (ROS), vascular endothelial growth factor (VEGF)

Acknowledgements

The authors thank Christine de Ville de Goyet (UCL) for expert technical support.

Funding

This study was supported by the *Fonds National de la Recherche Scientifique* (F.R.S.-FNRS) (grant J.0112.13).

Competing interests

The authors declare that they have no conflict of interest.

Supplemental Data

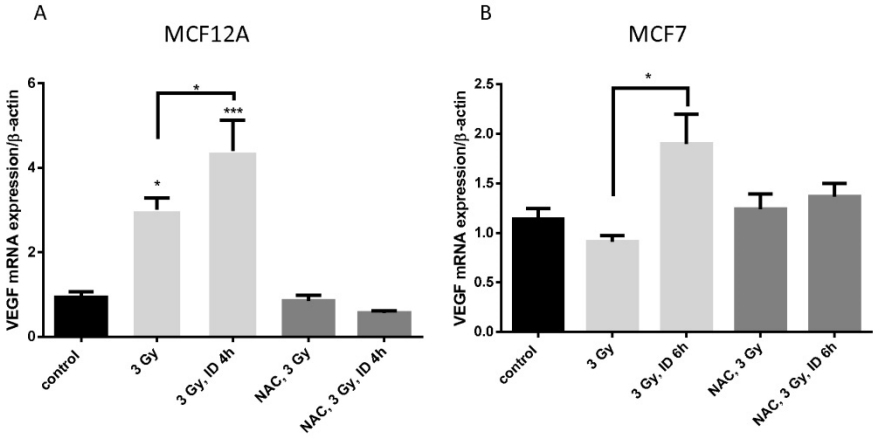

Figure 1. Acute ID and radiations-induced VEGF mRNA up-regulation depends on ROS production in both cell lines. *Cells were cultured in iodine-containing medium for 7 days. Medium was replaced by iodine-containing (control) or iodine deficient (ID) medium and cells were then irradiated with a dose of 3 Gy. Part of the cells was treated with the antioxidant NAC. Cells were harvested 4 or 6 hours (h) after medium change. VEGF mRNA expression in MCF12A (**A**) and MCF7 cells (**B**) was determined using RT-qPCR. Data are expressed as means ± SEM. N=1. P-values < 0,05 were considered as statistically significant.:*P < 0.05, **P < 0.01, ***P<0.001.*

Reference List

1. **Abdollahi A, Lipson KE, Han X, Krempien R, Trinh T, Weber KJ, Hahnfeldt P, Hlatky L, Debus J, Howlett AR and Huber PE**. SU5416 and SU6668 attenuate the angiogenic effects of radiation-induced tumor cell growth factor production and amplify the direct anti-endothelial action of radiation in vitro. *Cancer Res* 63: 3755-3763, 2003.
2. **Adams J, Carder PJ, Downey S, Forbes MA, MacLennan K, Allgar V, Kaufman S, Hallam S, Bicknell R, Walker JJ, Cairnduff F, Selby PJ, Perren TJ, Lansdown M and Banks RE**. Vascular endothelial growth factor (VEGF) in breast cancer: comparison of plasma, serum, and tissue VEGF and microvessel density and effects of tamoxifen. *Cancer Res* 60: 2898-2905, 2000.
3. **Azzam EI, Jay-Gerin JP and Pain D**. Ionizing radiation-induced metabolic oxidative stress and prolonged cell injury. *Cancer Lett* 327: 48-60, 2012.
4. **Bates DO, Cui TG, Doughty JM, Winkler M, Sugiono M, Shields JD, Peat D, Gillatt D and Harper SJ**. VEGF165b, an inhibitory splice variant of vascular endothelial growth factor, is down-regulated in renal cell carcinoma. *Cancer Res* 62: 4123-4131, 2002.
5. **Bedard K and Krause KH**. The NOX family of ROS-generating NADPH oxidases: physiology and pathophysiology. *Physiol Rev* 87: 245-313, 2007.

6. **Boltze C, Brabant G, Dralle H, Gerlach R, Roessner A and Hoang-Vu C**. Radiation-induced thyroid carcinogenesis as a function of time and dietary iodine supply: an in vivo model of tumorigenesis in the rat. *Endocrinology* 143: 2584-2592, 2002.
7. **Craps J, Wilvers C, Joris V, De JB, Vanderstraeten J, Lobysheva I, Balligand JL, Sonveaux P, Gilon P, Many MC, Gerard AC and Colin IM**. Involvement of nitric oxide in iodine deficiency-induced microvascular remodeling in the thyroid gland: role of nitric oxide synthase 3 and ryanodine receptors. *Endocrinology* 156: 707-720, 2015.
8. **Derry DM**. *Breast Cancer and Iodine*. Trafford Publishing, 2001,
9. **Dore-Savard L, Lee E, Kakkad S, Popel AS and Bhujwalla ZM**. The Angiogenic Secretome in VEGF overexpressing Breast Cancer Xenografts. *Sci Rep* 6: 39460, 2016.
10. **Eskin BA, Bartuska DG, Dunn MR, Jacob G and Dratman MB**. Mammary gland dysplasia in iodine deficiency. Studies in rats. *JAMA* 200: 691-695, 1967.
11. **Eskin BA, Shuman R, Krouse T and Merion JA**. Rat mammary gland atypia produced by iodine blockade with perchlorate. *Cancer Res* 35: 2332-2339, 1975.
12. **Gerard AC, Poncin S, Audinot JN, Denef JF and Colin IM**. Iodide deficiency-induced angiogenic stimulus in the thyroid occurs via HIF- and ROS-dependent VEGF-A secretion from thyrocytes. *Am J Physiol Endocrinol Metab* 296: E1414-E1422, 2009.
13. **Graham KA, Kulawiec M, Owens KM, Li X, Desouki MM, Chandra D and Singh KK**. NADPH oxidase 4 is an oncoprotein localized to mitochondria. *Cancer Biol Ther* 10: 223-231, 2010.
14. **Hall EJ and Giaccia E**. *Radiabiology for the Radiologist*. Philadelphia: 2006,
15. **Houck KA, Ferrara N, Winer J, Cachianes G, Li B and Leung DW**. The vascular endothelial growth factor family: identification of a fourth molecular species and characterization of alternative splicing of RNA. *Mol Endocrinol* 5: 1806-1814, 1991.
16. **Hovinga KE, Stalpers LJ, van BC, Donker M, Verhoeff JJ, Rodermond HM, Bosch DA and van Furth WR**. Radiation-enhanced vascular endothelial growth factor (VEGF) secretion in glioblastoma multiforme cell lines--a clue to radioresistance? *J Neurooncol* 74: 99-103, 2005.
17. **Inskip PD, Robison LL, Stovall M, Smith SA, Hammond S, Mertens AC, Whitton JA, Diller L, Kenney L, Donaldson SS, Meadows AT and Neglia JP**. Radiation dose and breast cancer risk in the childhood cancer survivor study. *J Clin Oncol* 27: 3901-3907, 2009.
18. **International Atomic Energy Agency**. *Radiation biology: a handbook for teachers and students*. Vienna: IAEA, 2010,
19. **Iodine Global Network**. Global Scorecard 2014: Number of iodine deficient countries more than halved in past decade. *IDD newsletter* 2015.
20. **Islam MS, Matsumoto M, Hidaka R, Miyoshi N and Yasuda N**. Expression of NOS and VEGF in feline mammary tumours and their correlation with angiogenesis. *Vet J* 192: 338-344, 2012.
21. **Kil WJ, Tofilon PJ and Camphausen K**. Post-radiation increase in VEGF enhances glioma cell motility in vitro. *Radiat Oncol* 7: 25, 2012.
22. **Krouse TB, Eskin BA and Mobini J**. Age-related changes resembling fibrocystic disease in iodine-blocked rat breasts. *Arch Pathol Lab Med* 103: 631-634, 1979.
23. **Krueger SA, Joiner MC, Weinfeld M, Piasentin E and Marples B**. Role of apoptosis in low-dose hyper-radiosensitivity. *Radiat Res* 167: 260-267, 2007.

24. **Lambert AJ, Buckingham JA, Boysen HM and Brand MD**. Diphenyleneiodonium acutely inhibits reactive oxygen species production by mitochondrial complex I during reverse, but not forward electron transport. *Biochim Biophys Acta* 1777: 397-403, 2008.
25. **Li Q, Fu GB, Zheng JT, He J, Niu XB, Chen QD, Yin Y, Qian X, Xu Q, Wang M, Sun AF, Shu Y, Rui H, Liu LZ and Jiang BH**. NADPH oxidase subunit p22(phox)-mediated reactive oxygen species contribute to angiogenesis and tumor growth through AKT and ERK1/2 signaling pathways in prostate cancer. *Biochim Biophys Acta* 1833: 3375-3385, 2013.
26. **Lund E and Bonaa KH**. Reduced breast cancer mortality among fishermen's wives in Norway. *Cancer Causes Control* 4: 283-287, 1993.
27. **Macaeva E, Saeys Y, Tabury K, Janssen A, Michaux A, Benotmane MA, De Vos WH, Baatout S and Quintens R**. Radiation-induced alternative transcription and splicing events and their applicability to practical biodosimetry. *Sci Rep* 6: 19251, 2016.
28. **Mansfield KD, Guzy RD, Pan Y, Young RM, Cash TP, Schumacker PT and Simon MC**. Mitochondrial dysfunction resulting from loss of cytochrome c impairs cellular oxygen sensing and hypoxic HIF-alpha activation. *Cell Metab* 1: 393-399, 2005.
29. **Montero A, Sanz X, Hernanz R, Cabrera D, Arenas M, Bayo E, Moreno F and Algara M**. Accelerated hypofractionated breast radiotherapy: FAQs (frequently asked questions) and facts. *Breast* 23: 299-309, 2014.
30. **Murphy MP**. How mitochondria produce reactive oxygen species. *Biochem J* 417: 1-13, 2009.
31. **Nowosielska EM, Wrembel-Wargocka J, Cheda A, Lisiak E and Janiak MK**. Enhanced cytotoxic activity of macrophages and suppressed tumor metastases in mice irradiated with low doses of X- rays. *J Radiat Res* 47: 229-236, 2006.
32. **Pisani P, Parkin DM, Bray F and Ferlay J**. Estimates of the worldwide mortality from 25 cancers in 1990. *Int J Cancer* 83: 18-29, 1999.
33. **Plataniotis G**. Hypofractionated radiotherapy in the treatment of early breast cancer. *World J Radiol* 2: 197-202, 2010.
34. **Preston DL, Kitahara CM, Freedman DM, Sigurdson AJ, Simon SL, Little MP, Cahoon EK, Rajaraman P, Miller JS, Alexander BH, Doody MM and Linet MS**. Breast cancer risk and protracted low-to-moderate dose occupational radiation exposure in the US Radiologic Technologists Cohort, 1983-2008. *Br J Cancer* 115: 1105-1112, 2016.
35. **Schafer G, Cramer T, Suske G, Kemmner W, Wiedenmann B and Hocker M**. Oxidative stress regulates vascular endothelial growth factor-A gene transcription through Sp1- and Sp3-dependent activation of two proximal GC-rich promoter elements. *J Biol Chem* 278: 8190-8198, 2003.
36. **Smith-Bindman R, Lipson J, Marcus R, Kim KP, Mahesh M, Gould R, Berrington de GA and Miglioretti DL**. Radiation dose associated with common computed tomography examinations and the associated lifetime attributable risk of cancer. *Arch Intern Med* 169: 2078-2086, 2009.
37. **Vaiserman AM**. Radiation hormesis: historical perspective and implications for low-dose cancer risk assessment. *Dose Response* 8: 172-191, 2010.
38. **Vala I, Martins LR, Imaizumi N, Nunes RJ, Rino J, Kuonen F, Carvalho LM, Ruegg C, Grillo IM, Barata JT, Mareel M and Santos SC**. Low doses of ionizing radiation

promote tumor growth and metastasis by enhancing angiogenesis. *PLoS One* 5: e11222, 2010.

39. **Vanderstraeten J, Derradji H, Craps J, Sonveaux P, Colin IM, Many MC and Gerard AC**. Iodine deficiency induces a VEGF-dependent microvascular response in salivary glands and in the stomach. *Histol Histopathol* 31: 897-909, 2016.
40. Vanderstraeten, J., Derradji, H., Sonveaux, P., Colin, I. M., Many, M. C., and Gerard, A. C. Acute iodine deficiency induces a transient VEGF dependent microvascular response in mammary glands involving HIF-1, ROS and mTOR. 2017.

Ref Type: Unpublished Work

41. Wahba, A., Ryan, M. C., Shankavaram, U., Camphausen, K., and Tofilon, P. J. Radiation-induced alternative splicing as detected in total and polysome-bound mRNA in glioblastoma stem-like cells. Cancer Res. 76(14). 2016.

Ref Type: Abstract

42. **Woolard J, Bevan HS, Harper SJ and Bates DO**. Molecular diversity of VEGF-A as a regulator of its biological activity. *Microcirculation* 16: 572-592, 2009.
43. **Woolard J, Wang WY, Bevan HS, Qiu Y, Morbidelli L, Pritchard-Jones RO, Cui TG, Sugiono M, Waine E, Perrin R, Foster R, Digby-Bell J, Shields JD, Whittles CE, Mushens RE, Gillatt DA, Ziche M, Harper SJ and Bates DO**. VEGF165b, an inhibitory vascular endothelial growth factor splice variant: mechanism of action, in vivo effect on angiogenesis and endogenous protein expression. *Cancer Res* 64: 7822-7835, 2004.
44. **Yu H, Mohan S and Natarajan M**. Radiation-Triggered NF-kappaB Activation is Responsible for the Angiogenic Signaling Pathway and Neovascularization for Breast Cancer Cell Proliferation and Growth. *Breast Cancer (Auckl)* 6: 125-135, 2012.

4 Discussion, perspectives and conclusions

4.1 Main scientific outcome

Iodine is a scarce element essential for thyroid hormone synthesis. Due to the crucial roles of TH, consequences of iodine scarcity linked to the subsequent low TH synthesis have long been investigated as well as the direct consequences of ID on thyrocytes and thyroid function. One of them is a VEGF-dependent increase in the surrounding blood perfusion. Indeed, thyrocytes were shown to up-regulate and secrete VEGF when facing iodine withdrawal (112; 113). More recently, the iodide/sodium symporter NIS was found to be expressed in several other organs, though iodide uptake was not shown in all of them (322). In addition, pathologies of some of those organs were linked to ID (435; 436). However, only few studies have so far addressed the molecular pathways potentially induced by ID in those organs.

In this work, we have investigated the microvascular effects of acute ID on 3 different NIS-expressing organs: stomach, salivary and mammary glands. We report that acute ID induces a VEGF up-regulation in the 3 cited organs, which further leads to increased blood perfusion in salivary and mammary glands. VEGF mRNA up-regulation was shown to be dependent on ROS and mTOR in two breast cell lines, which is similar to former observations made in the thyroid.

Thus, ID seems to induce a common microvascular reaction in NIS-expressing organs, probably in order to increase iodide supply, to benefit from its antioxidant properties or bactericidal capacity in the case of salivary glands and stomach. Another hypothesis is that increasing the iodide supply through vascularization might aim at increasing iodide recycling through the gastroenteric cycle.

In addition, in breast, ID effects on VEGF mRNA were shown to be cumulative to other stress factors as radiations, also leading to VEGF overexpression *in vitro*, raising interesting questions to be addressed on iodide status in the context of radiation side-effect prevention.

4.2 ID in NIS-expressing organs

4.2.1 Role of VEGF in ID-induced effects in stomach, salivary glands and breast

Interestingly, immunohistochemical analyses revealed VEGF overexpression in salivary gland duct cells, mucin-secreting cells from the stomach surface epithelium, and breast epithelial cells, which are all NIS-expressing cells in the three respective organs studied. VEGF staining was also observed in the surrounding stroma in the 3 organs, which we hypothesized to be secreted by NIS-expressing cells. Under certain conditions, fibroblasts can be activated by external stimuli or paracrine signaling from other surrounding cells, and secrete VEGF in extracellular matrices (75). However, *in vitro* studies showed that fibroblasts did not increase VEGF mRNA at the studied time points upon acute ID unlike thyrocytes and mammary cells, supporting the hypothesis that VEGF is secreted and accumulated in the stroma by NIS-expressing cells rather than overexpressed in fibroblasts. However, we do not exclude a fibroblast role in VEGF secretion through paracrine signaling-induced interactions between compartments, leading to fibroblasts indirect activation by NIS-expressing cells for instance.

Of note, VEGF increase was observed in gastric endocrine cells, even though such cells are not known to express NIS. Further research is needed to explain how these cells are activated and the physiological relevance of this activation. ID might induce redox changes in the close environment of blood vessels and one could consider the close relationship existing between endocrine and EC as possible explanation.

ID was shown to induce an increase in blood perfusion in salivary and mammary glands, but blood perfusion was not measured in stomach for practical reasons. VEGF involvement was then assessed with two different inhibitors: a direct VEGF inhibitor, bevacizumab, and a VEGF receptors inhibitor, SU5416.

Though bevacizumab is a humanized antibody, ID-induced blood perfusion increase was not detected in mice injected with a high dose of this antibody. Supporting this observation, Bock et al. (2007) showed bevacizumab affinity for murine VEGF by different methods, though much weaker than that for human VEGF (35). Moreover, several authors reported the inhibition of VEGF by bevacizumab in mice and other animal models such as rabbit (255; 310; 461). VEGF inhibition by bevacizumab might thus be incomplete, but it is conceivable that a partial inhibition is sufficient

to prevent the ID-induced increase in blood perfusion. Therefore, we also used the inhibitor SU5416 which also prevented ID-induced microvascular response. Though SU5416 is not perfectly specific as it weakly inhibits FGF and PDGF receptors, the confirmation of our results by inhibiting VEGF receptors with SU5416 consolidate our conclusions both in breast (426) and in salivary glands (annexes, fig. 1).

Thus, it appears that ID acts on studied NIS expressing organs (namely thyroid, mammary glands, salivary glands and stomach) via a common pathway: it induces a transient increase in VEGF expression, which leads to a transient increase in blood perfusion. As this controlled microvascular reaction seems to be a common mechanism to face ID in NIS-expressing organs, it could thus be interesting to verify whether this microvascular reaction is also observed in other NIS-expressing organs such as placenta, intestine, etc.

4.2.2 Molecular mechanisms induced by acute ID in breast

4.2.2.1 Models used

Due to the health burden that breast pathologies represent worldwide, the molecular mechanisms triggered by acute ID were further characterized in two breast cell lines known to express NIS. An *in vitro* approach was chosen to study the potential implication of several pathways and their regulation by using diverse inhibitors without sacrificing many animals, as nothing was known yet on ID microvascular effects in mammary glands. The use of cell lines imposes limitations in the results interpretation. Indeed, cell lines are modified cells and do not represent a physiological situation. Moreover, the use of cell lines implies the loss of interaction between different cell types within a same system or from different systems through hormones signaling for instance. In this regard, TH and estrogens might be modulated by ID *in vivo*. Concerning TH, their level drop only occurs after 10 days of ID, suggesting that the reaction observed in virgin mice and at least the initiation of the reaction in lactating glands are not dependent on TH (112). But, as we don't know the modulation of estrogen by ID in our model, they might thus also have a role in ID effects that will not be seen in cell lines. However, the advantage of this *in vitro* model is that it allows seeing the direct effects of ID solely in breast cells excluding potential indirect modulations induced by those hormones.

Acute ID induces an increase in VEGF mRNA in both cell lines, which is in line with our *in vivo* observations. This increase is ROS- and mTOR-dependent as both ROS

and mTOR were necessary to increase HIF-1α expression, which then led to VEGF mRNA overexpression.

4.2.2.2 Role of ROS

ROS are known to regulate several transcription factors linked to VEGF expression, such as HIF-1 and Sp1. For instance, NOXs were shown to up-regulate HIF-1α through PI3K/AKT activation (231), while mitochondrial electron chain transport system was shown to be involved in HIF-1α stabilization under hypoxic conditions (131). Due to their importance in microcirculation regulation, ROS implication was thus studied in this work, and first experiments were carried out to further study their nature and origin.

The origin of ROS involved in VEGF regulation under ID conditions was determined to be independent of mitochondrial superoxide and alkyl radicals. The determination of the pre-cited actors implication in VEGF up-regulation partially relied on the use of different pharmacological inhibitors. However, one might be concerned with their specificity and work concentrations must be thus carefully chosen.

ROS involvement was first assessed with a general ROS inhibitor: N-acetylcysteine (NAC). It can act directly as a ROS scavenger and indirectly by increasing reduced GSH levels. However, NAC can induce different cellular effects that may vary according to its concentration and that must be kept in mind. NAC is often used in the literature at concentration between 1 and 10 mM. However, high concentration such as 10 mM can decrease medium pH and thereby influence the expression of certain molecules such as HIF-1. Here, we have used a concentration of 0,75 mM and have verified that NAC does not induce changes in HIF-1α expression. Moreover, Mukherjee et al. (2007) have shown that low NAC concentration (3 mM) effectively decreased ROS content whereas high concentrations (30 mM) did not decrease it in EC, further emphasizing the importance of the chosen concentration (274). Besides, several groups have shown that NAC could sometimes trigger unspecific reactions, such as the direct interaction with cysteine or thiol group-containing proteins such as Raf-1, MEK or ERK (198; 472).

To approach the origin of ID-induced ROS, we used mitoTEMPO. Indeed, mitochondria are a major source of intracellular ROS, and mitoTEMPO was designed to pass through membranes bilayers thanks to its lipophilic triphenylphosphonium group and to rapidly accumulate in mitochondria via its positive charge. MitoTEMPO was indeed shown to accumulate a several hundred-fold in mitochondria where it exerted its scavenging activity on superoxide and alkyl radical. Though mitoTEMPO does not decrease cytoplasmic superoxide at low concentration, it is not perfectly selective to mitochondrial superoxide at concentration higher than 20 µM. MitoTEMPO is often presented as SOD mimic and one could thus be concerned by a possible increase in H_2O_2 by using mitoTEMPO. However, its mechanism of action is not yet perfectly understood and no increase in H_2O_2 following mitoTEMPO use was reported, suggesting that it does not act as SODs do (81; 278).

Because hydrogen peroxide and superoxide anion are prevalent cellular ROS, we are planning to study their potential implication. A preliminary experiment revealed that the addition of SOD did not prevent ID-induced VEGF mRNA up-regulation while catalase did in both breast cell lines, suggesting that hydrogen peroxide rather than superoxide anion might be involved in VEGF regulation. However, this experiment was only carried out once and must be repeated. Those results should thus be taken with caution (annexes, fig. 2).

Furthermore, immunostaining of 4-hydroxynonenal (4-HNE) in mice to reveal oxidative stress and mice treatment with a ROS inhibitor could be useful to verify whether ROS are involved in ID-induced microvascular reaction *in vivo*.

4.2.2.3 Role of mTOR

Because mTOR has a central role in the regulation of many cellular pathways, including pathways regulating microcirculation, its activity was assessed through the study of one of its main targets phosphorylation, P70S6K, and rapamycin, an mTOR inhibitor, was used to assess mTOR involvement in our model. P70S6K phosphorylation was increased by acute ID and rapamycin prevented VEGF mRNA up-regulation. Rapamycin is described as a specific inhibitor of mTORC1, known to regulate HIF-1α and thereby VEGF. However, longer exposure to rapamycin was shown to impede mTORC2 assembly (355). As exposure times here are much

shorter than those necessary to inhibit mTORC2, we can reasonably suppose that only mTORC1 was targeted.

We currently do not know how mTOR is activated by acute ID. Several models have shown that ROS could activate mTOR signaling (474). However, the inhibition of ROS by NAC did not prevent mTOR activation by ID, which was assessed by studying P70S6K phosphorylation. Different hypotheses could be put forward as possible explanations for mTOR activation, leading to different experimental perspectives. ID might activate the PI3K/AKT signaling pathway, which is known to regulate mTOR. Because iodide itself is an antioxidant, we could hypothesize that it decreases the oxidized form of PTEN, a negative inhibitor of the AKT/mTOR pathway, which then leads to PTEN activation, and that a sudden drop in iodide could reverse this inhibition (fig. 19) (474). Likewise, a role for the unfolded protein response (UPR) pathway could also be considered, as it is known to activate the mTOR pathway (474). ID was shown to induce intracellular Ca2+ leaks via the RYRs in the thyroid (70) and such a mechanism could be conceivable in breast cells, thereby activating the UPR. Moreover, it is possible that the presence of iodide influences disulfide bonds or affect membrane lipids in the ER and its sudden removal could therefore trigger the UPR (fig. 19) (16; 471). The activation of mTOR by ID and the mTOR downstream signaling leading to HIF-1/VEGF upregulation require further investigation. Moreover, to assess mTOR implication *in vivo*, pP70S6K/P70S6K immunohistochemical staining in mice could be carried out and mice treated with rapamycin could be exposed to ID.

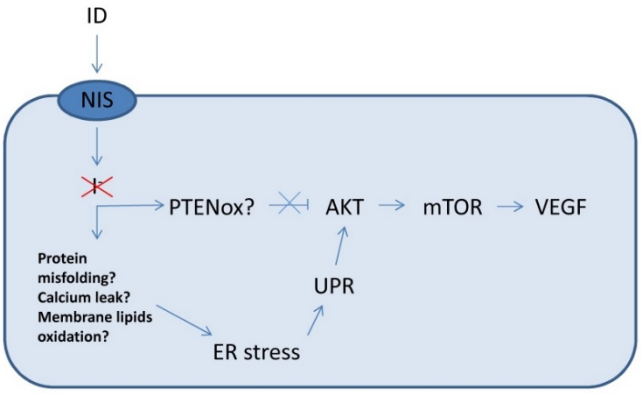

Fig. 19. Hypothetical molecular pathways involved in ID- -induced activation of mTOR and up-regulation of VEGF in breast cells.

4.2.2.4 Role of HIF

HIF-1 activity was inhibited by echinomycin, a DNA intercalator that prevents HIF-1 binding to its recognition sequence. However, other transcription factors have similar DNA binding sequences that could be recognized by echinomycin. For instance, Myc/Max transcription factors binding sequence partly encompasses the echinomycin recognition sequence. Echinomycin was shown to affect DNA binding of a matching oligonucleotide and could thus potentially play a role in VEGF regulation via Myc/Max activity inhibition (207). However, a 10 times higher concentration of echinomycin than the concentration used in this work, was used directly on nuclear extract to obtain this result. Echinomycin-induced inhibition of AP-1 activity was described by Vlaminck et al. (439) while Kong et al. observed no effect of echinomycin on AP-1 activity (207). Interestingly, Vlaminck et al. (2007) showed that echinomycin was able to induce HIF-1 expression and activity under normoxic conditions, but not under hypoxia, at low concentration (2 nM). They did not observe this effect at concentration higher than 10 nM. They attributed this effect to an increased activity of Sp1. However, the concentration used in our model (100 nM) was largely superior, excluding this potential off-target effect. To complete this analysis, HIF-1 could be targeted with specific siRNA and HIF-1 DNA binding could be assessed.

In our model, we have shown that ID-induced up-regulation of HIF-1α was dependent on ROS production and mTOR. However, it does not exclude other potential actors that could influence HIF-1α expression. In thyroid, it was shown that ID activates NOSIII and thereby increases nitric oxide (NO). NO was then proved to be involved in HIF-1α stabilization in thyroid cells (70). In addition, Nyska et al. (2001) showed that iodine reduces the expression of inducible nitric oxide synthase (iNOS) in a model of skin injury induced by free radicals (296). Given the relation between ID and NO synthases observed in other organs, and given that mammary glands strongly express iNOS (416), a role for NO in mammary glands vascular changes induced by ID could therefore also be considered. Moreover, NO is able to activate mTOR and could thus also indirectly influence HIF-1α expression (240).

4.2.2.5 VEGF isoforms

In both breast cell lines, PCR analyzes showed that the VEGF165a isoform is up-regulated by ID, but not the VEGF165b. VEGF165a isoform is an important mediator

of angiogenic response compared to certain other VEGF isoforms whereas VEGF165b is hypothesized to be a competitive inhibitor of VEGF-induced angiogenic response (454). The expression of the other main VEGF isoforms should be studied to confirm that acute ID influences alternative splicing in favor of some pro-angiogenic forms. Though we did not look at VEGF alternative splicing *in vivo*, VEGF165a is likely to have a role in ID-induced VEGF-dependent increase in mammary gland blood perfusion. Nevertheless, VEGF isoforms should be studied *in vivo*, to see whether ID influences VEGF alternative splicing in the same way. In addition, because we observed increased VEGF staining in the stroma around the glandular cells in the three organs studied, it could be interesting to see whether there is a difference between the expression of soluble isoforms such as VEGF121 and less soluble isoforms such as VEGF189 or VEGF206. Moreover, VEGFxxxb were reported to be down-regulated in lactating breast, favoring the action of pro-angiogenic isoforms in breast vascular expansion during lactation (327). This difference in VEGF isoforms expression during lactation might offer favorable conditions for the ID-induced microvascular response and might contribute to the longer lasting effects observed in lactating mammary glands compared to virgin glands.

4.2.3 Breast versus thyroid

ID induces a vascular response in breast which is strikingly similar to the response previously described in the thyroid, as it involves ROS, mTOR, HIF-1α and VEGF (fig. 20 A and B). However, ROS were shown not to be involved and HIF-1α was shown to have only a moderate role in cancerous thyrocytes compared to non-cancerous thyrocytes (fig. 20 C). Moreover, while VEGF overexpression was demonstrated to be tightly controlled in non-cancerous thyroid cell line, this overexpression was less controlled in cancerous thyrocytes, suggesting that regulation mechanisms in thyroid are influenced by the physiological state of the gland (111). Though the study of the molecular mechanisms involved in breast during ID were not as thoroughly studied as in the thyroid yet, such differences were not observed between the cancerous and non-cancerous breast cell line.

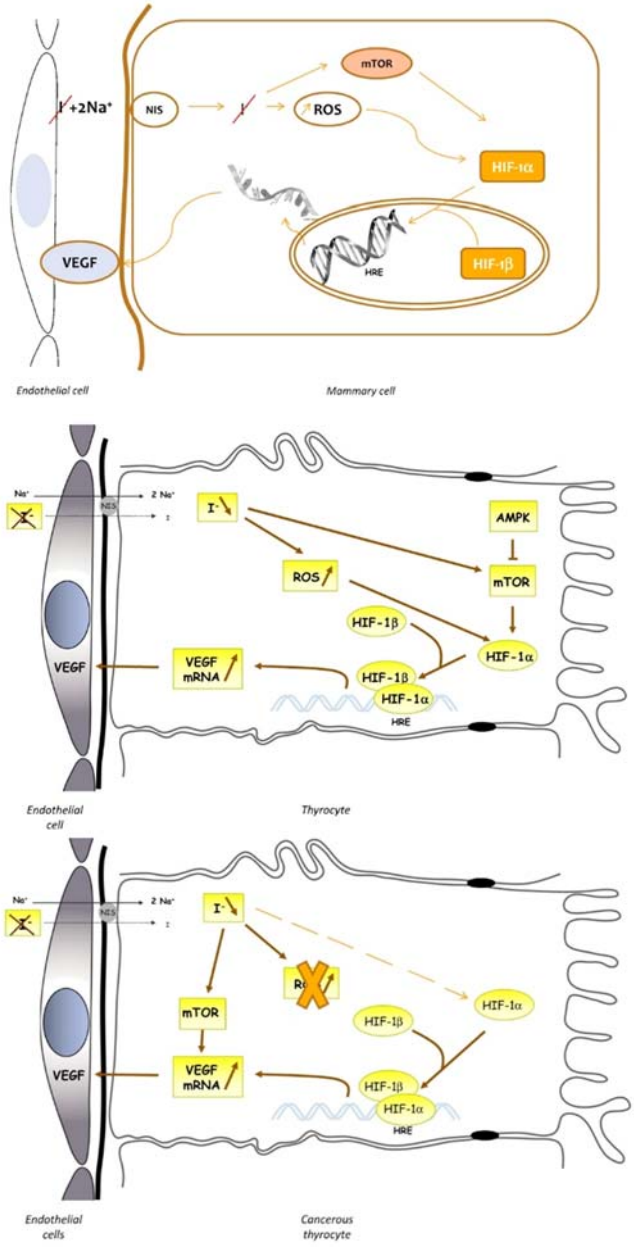

Fig. 20. Molecular pathways activated by ID in breast cells (A), thyrocytes (B) and cancerous thyrocytes (C) (adapted from Gérard et al., 2008).

However, this observation should be verified in other breast cell lines. Nevertheless, it would not be astonishing to see differences in the regulation of these effects between mammary cells and thyrocytes given the different role that iodide and ROS play in both organs. Studying ID effects *in vivo* on microvascularization in a breast cancer model could also be interesting. Of note, NIS expression is increased in most breast cancer tissues while it is strongly decreased in cancer thyrocytes. Such a difference in NIS expression could thus influence the ID-induced vascular response, and might even highlight some regulation mechanisms in breast.

4.2.4 Factors that influence ID response

4.2.4.1 Regulation of the microvascular reaction according to the physiological state

In this work, as in that of Gerard et al. (2008 and 2009) on thyroid, the microvascular activation induced by ID is transient. A question to be raised is whether there is a regulatory mechanism that controls VEGF up-regulation and the associated increase in blood perfusion. In healthy thyroid, in a second step, ID activates AMPK (fig. 20 B) (69). The latter negatively regulates mTOR during ID, blocking the signal cascade that leads to VEGF up-regulation. It is thus possible that a similar mechanism is involved in the 3 organs studied in this work, particularly in mammary glands where a role for mTOR was shown in ID signaling. However, thyroid is an endocrine organ that needs iodide to produce TH and the pathways activated in this organ might thus be quite different from those activated in other NIS-expressing organs where iodide has a less primordial function. Besides, it was shown in thyroid and in breast that ROS are one of the triggers leading to VEGF up-regulation. But ROS are constantly produced in thyroid to produce TH, and thyroid must face regular physiological variation of ROS or OS. Moreover, it was shown by Poncin et al. that the expression of proteins involved in TH synthesis was decreased by NAC, leading the authors to suggest that a minimal level of ROS is required for proper thyroid functioning (319). Thyroid is thus likely to initiate different mechanisms when facing ID-induced increase in ROS compared to breast and other NIS-expressing organs. It is thus also possible that a simpler mechanism is activated in breast, stomach and salivary glands where, for instance, the activation of antioxidant enzymes ends ROS signaling, provided that VEGF up-regulation in stomach and salivary glands also depends on ROS signaling. In this regard, we have

started to study the regulation of 3 antioxidant enzymes in both cell lines: catalase, SOD1 and SOD2. A first step was to look at their mRNA expression. However, none of the enzyme mRNA expression was changed by the treatment at the studied time-point (annexes, fig. 3). It is of course possible that an effect on their mRNA was missed because the studied time-point was not adequate, or that these enzymes are regulated at a post-transcriptional/translational level. Further investigation is thus needed to unravel a possible role of those enzymes in ID effects. Moreover, it is also likely that the type of ROS and their origin are different in each organ, leading to differences in ID-induced microvascular response regulation.

Moreover, this regulation seems to depend on the physiological state of the organ in thyroid and breast. Indeed, mammary gland blood perfusion increased from the first to the 10th day of ID in lactating mice while the increase was only significant at the first day of the treatment in virgin mice. This difference in regulation might arise from a possible conjunctive effect of ID and elevated level of estrogens or prolactin, which are known to be involved in the vascular expansion during lactation through mechanisms including VEGF up-regulation (429). Moreover, ID was linked to increased gonadotropin stimulation which can lead to hyperoestrogenic state in mice (390). Besides, Eskin et al. showed that perchlorate-induced histological atypia in rat mammary glands were worsened when animals were injected with estrogen (97).

Of note, VEGF increase was also observed in the milk secretion in lactating glands. VEGF secretion into the milk was already reported in various studies, but its effect on the progeny is still unclear. It was suggested that VEGF ingested during lactation could influence the growth and development of gastric cells (203; 303). The possibility of a greater impact on gastric cells growth due to an increased VEGF intake should then be considered and obviously needs further investigation.

Another physiological difference that is likely to influence the microvascular response is the cancerous versus non-cancerous state of the organ. Indeed, cancerous thyrocytes were shown to induce a persistent increase in VEGF upon ID, unlike non-cancerous ones (111). In stomach, iodide content and NIS expression is lower in cancer tissues than in surrounding tissues. On the contrary, NIS is overexpressed in the majority of breast cancers, though often mis-localized. It would thus be interesting to investigate the effects of acute ID in cancerous models of NIS-expressing organs to see whether it affects the response as it does in thyroid. Moreover, primary culture from human breast tissues from pathology units could

be considered and, as suggested before, breast cancer models *in vivo* could complete this research.

4.2.4.2 Acute versus repeated ID

This work focused on the effects of acute iodine withdrawal. However, human populations are usually exposed to varying intake of iodine according to their dietary habits. In mild or moderate iodine-deficient regions, individuals can face chronic insufficient iodine intake, interspaced by meals with higher iodine content. It would thus be interesting to investigate the microvascular effects of repeated acute ID on NIS-expressing organs, which would reflect a more physiological situation, to determine whether the organism finds a way to adapt the response or, on the contrary, whether the response is worsened. In order to answer that question, an experiment was carried out where virgin NMRI females were exposed to repeated acute ID that lasted two days, separated by intervals of either two or three days where mice received an iodide-containing diet. Mice exposed to repeated ID with two days of iodide-containing diet between each acute ID treatment had their blood perfusion increased only at the first acute ID in mammary gland and salivary gland, whereas the increase was persistent in thyroid blood perfusion, with an increasing trend in the response after the fourth exposure (annexes, fig. 4 A, C, E). Interestingly, if the recovering period between each acute ID treatment was prolonged to 3 days, the first and the second exposure to acute ID, but not the third, lead to increased blood perfusion in mammary and salivary glands. Again, thyroid blood perfusion was always increased with a trend to a more pronounced response after each exposure (annexes, fig. 4 B, D, F). The persistent increased thyroid blood perfusion might depend on a possible TSH increase due to a decrease in TH. However, it is interesting to note that if mammary gland and salivary gland are given more time to “recover” from acute ID, then the likelihood of a second microvascular response to acute ID is increased. This suggests that a regulatory mechanism could exist preventing the next ID-induced response as long as it is triggered. Such a mechanism would explain the transient nature of the ID-induced microvascular response observed in NIS-expressing organs. In this regard, a first step would be to study AMPK implication, as it was shown to down-regulate VEGF overexpression through mTOR inhibition in thyroid.

4.2.5 NIS regulation

In parallel to the microvascular activation described in this work, which we hypothesized to be a way to increase iodide local availability, ID also influenced iodide transport via NIS regulation. While iodide intake was described to affect NIS expression in thyroid, iodide was not known to regulate it in other organs to our knowledge. NIS regulation is strongly different according to the organ: thyroid NIS is TSH-sensitive, mammary gland NIS is regulated by prolactin, estrogen and oxytocin, and stomach and salivary gland NIS are described as constitutively expressed (322). Here, we observed a transient increase in NIS expression in the three studied organs as what had been observed in thyroid, though to different extents, and the duration of this increase was organ-dependent. However, while NIS expression returned to control values in breast, thyroid and salivary glands at the studied time points, NIS-expression increase was then followed by a decrease in stomach that lasted as long as the treatment, suggesting different organ-dependent regulation mechanisms. Moreover, NIS was not up-regulated in MCF12A non-cancerous cell line while it was in cancerous MCF7 cell line, suggesting that the physiological state could affect iodide influence on NIS expression. This hypothesis should be tested on other cell lines and/or animal models to be confirmed. NIS upregulation might represent another strategy to attempt iodide supply improvement in parallel, but independently of VEGF overexpression. In line with this hypothesis, it would be interesting to verify whether other transporters such as pendrin could also be influenced by iodide availability.

4.3 ID and radiation

ID and radiations being both known for their influence on breast diseases progression and because they can both up-regulate VEGF expression, we have hypothesized that the conjunction of the two factors could have additive effects on VEGF expression in the breast. We have used the two same breast cell lines as in the first part of this work as they were shown to be ID-sensitive. The simultaneous exposure to acute ID and a high dose of X-rays led to additive effects on VEGF mRNA overexpression in MCF12A cells, but not in MCF7 cells where acute ID in irradiated and non-irradiated cells induced VEGF mRNA overexpression to the same extent while radiations alone had no effect. Since VEGF expression is regulated at different levels, another control that needs to be carried out for this research is to study

VEGF protein expression after exposure to radiations with or without acute ID and thereby verify that the effects seen on its mRNA are also observed at the protein level. Because VEGF is alternatively spliced and that VEGF isoforms may elicit different responses (454), we have investigated the expression of two specific isoforms: VEGF 165a and VEGF165b. VEGF165a mRNA expression followed the same trend as total VEGF mRNA in our model while the potential inhibitor VEGF165b mRNA remained unchanged, suggesting that proangiogenic effects are likely. Nevertheless, before submitting this research to a journal, we are planning to analyze the transcription of other important splice variants such as VEGF121, an inducer of angiogenesis, and a blood vessel permeabilizing agent. It is possible that ID and/or radiation will regulate VEGF alternate splicing differently, eventually leading to different vascular responses *in vivo*.

In this regard, and because of the cell line models limitations mentioned earlier, our results should be verified *in vivo* and, at the same time, the potential pro-angiogenic effects of VEGF overexpression should be assessed. Indeed, though VEGF overexpression was shown to increase blood perfusion *in vivo*, the mechanisms induced by radiation under iodide-sufficient and iodide-deficient conditions are probably not the same. It is thus possible that different regulatory mechanisms or post-translational mechanisms are triggered when ID is induced in irradiated and in non-irradiated cells, which could then influence the response, either increasing it or decreasing it. The VEGF alternative splicing study is also of interest *in vivo*, since the different isoforms may trigger different angiogenic response, according to their diffusibility for instance. Moreover, as mentioned before, the interplay between the different tissue systems could also influence the response, through hormone secretion or metabolism, such as estrogens for instance. Indeed, ID was associated with a hyperoestrogenic state and radiations were shown to increase serum estrogens, particularly the 16αOHE1 metabolite, and nuclear estrogen receptor in mammary tissues (390; 398). Since estrogen can regulate VEGF (394), interaction between different pathways can occur *in vivo* and thereby influence the global vascular response.

An *in vivo* experiment would also give us the opportunity to look at the behavior of other NIS-expressing organs and compare them, especially thyroid. Indeed, Boltze et al. have shown increased tissue damage and carcinogenesis following a single exposure to 4 Gy of X-rays in iodide-deficient rats compared to iodide-sufficient rats, suggesting that ID increases thyroid sensitivity towards radiations (38).

Of note, NIS mRNA expression was assessed under the same conditions as for VEGF mRNA assessment. Interestingly, the answer was the opposite to that of VEGF mRNA: the increase in mRNA expression induced by the combination of ID and 3 Gy of X-rays was stronger compared to the one induced by both factors separately only in MCF7 cells (supplemental data, fig. 5 A). On the contrary, exposure to 3 Gy of X-rays in MCF12A cells tended to lead to a decrease in NIS mRNA expression, while the combination of ID and radiation induced a variable response (either a decrease or no effect) from experiment to experiment (annexes, fig. 5 B). This analysis should thus be repeated to clarify those results.

4.3.1 Role of ROS

ROS involvement in our model was assessed. A strong ROS increase was observed just after the irradiation, which rapidly decreased to control level in iodide-sufficient conditions. In iodide deficient conditions, the ROS increase persisted longer before reaching control level. However, a limitation of the analysis resides in the possibility that radiation might affect the dye at the first time point studied, as the dye was added before radiation exposure. The intracellular de-esterified DFC-DA dye (the chemical form that is reactive to ROS) could be damaged by radiations and either become fluorescent, or become nonfunctional, reducing its concentration compared to non-irradiated controls. Rappole et al. (2012) exposed de-esterified DFC-DA dye in a 100 µM water solution without cells to 1 Gy of X-rays and observed that almost 3 % of the dye became fluorescent. To determine whether the fluorescence was due to ROS exposure from water radiolysis, they conducted the same experiment in presence and absence of strong antioxidant, ascorbic acid. The radiation-induced fluorescence was strongly decreased in presence of ascorbic acid and reached only 20 % of the fluorescence observed in absence of the antioxidant, suggesting that less than 0.6 % of the dye will fluoresce due to other causes than ROS increase in their model after exposure to an X-ray dose of 1 Gy (330). We carried out a similar experiment in our laboratory to assess DCFDA dye sensitivity towards X-rays in our model. A strong increase in fluorescence was induced by the exposure of the de-esterified dye to 3 Gy of X-rays, but this increase was not observed in presence of NAC, suggesting that it was only due to ROS production following water radiolysis and not the sensitivity of the dye towards radiation exposure.

A preliminary experiment using NAC suggests that ROS were responsible for VEGF mRNA overexpression in iodide-deficient and iodide-sufficient irradiated cells. NAC

is a broad-scaled ROS inhibitor that does not differentiate ROS from water radiolysis and ROS from cellular sources. Therefore, DPI and mitoTEMPO were used as a first step in the determination of the origin of the ROS involved in VEGF up-regulation in our cell lines. DPI is generally used as a NOXs inhibitor; however, though its main target are indeed NOXs enzymes, DPI was also shown to inhibit other flavoenzymes such as xanthine oxidase or NADPH cytochrome P450 oxidoreductase. Moreover, it was shown to reduce mitochondrial ROS not only by inhibiting flavoenzymes but also by interacting with the components of the electron mitochondrial chain from complex 1 (219). The use of DPI allows us to prove that ROS from different cellular compartments (enzymatic and partly from mitochondrial respiration) are involved in VEGF mRNA up-regulation, and not only ROS from physico-chemical origin such as water radiolysis. The use of mitoTEMPO then allowed us to say that superoxide and alkyl radicals from mitochondria were at least partly involved in the effects of radiations in iodide-deprived and iodide-sufficient MCF12A cells, but not in the effects of ID alone in both cell lines, nor in the effects of radiations in iodide-deficient MFC7 cells. Other more specific inhibitors and dyes are thus necessary to carry on this project. NOXs are widely admitted as a main enzymatic source of ROS in cells and are thus likely to be involved in our model, especially to study the effects of ID alone in both cell lines and those of ID associated with radiation in MCF7 cells, where mitochondrial superoxide was shown not to be involved. For instance siRNA targeting NOXs known to be expressed in the human breast such as NOX1, 4 and 5 (15; 124; 412) should be used to confirm their implication. Also, inhibitors of specific types of ROS such as catalase or SOD along with the use of specific dyes that recognize different types of ROS in immunofluorescence could help us determining the type of ROS involved and the compartment from where they originate. Because OS was increased by ID and radiation in both cell lines, a subsequent regulation of antioxidant enzymes is likely. We were thus interested in assessing the expression of some of the major antioxidant enzymes: catalase, SOD1 and SOD2. Moreover, if their expression is proved to be modulated by our treatments, it could be interesting to study whether they have an impact on VEGF regulation. To start this study, the antioxidant enzymes mRNA expression was measured at the same timing as for VEGF mRNA expression. None of the treatment led to significant changes in their expression compared to the control cells (annexes, fig. 6). However, as suggested before (cfr 4.5.1), the time points might not be appropriate and these enzymes might also be regulated at post-transcriptional levels. Further research is therefore needed. Nevertheless, SOD2 mRNA expression was significantly higher in MCF12A cells exposed to ID and radiations than in cells only exposed to ID. As this isoform is expressed in the

mitochondria, and VEGF induction was inhibited by mitoTEMPO in MCF12A cells exposed to ID and radiations but not in cells exposed to ID, the relevance of this result should be further investigated.

4.3.2 Medical relevance of the doses used

To begin the research on the effects of radiations in iodide-deficient conditions, a low dose and a high dose of X-rays were chosen. However, a dose-response curve could be valuable. As a first step, VEGF mRNA expression was studied after exposure to an intermediate dose (1 Gy) in presence and absence of iodide. However, the response to radiation was variable in both cell lines as it either increased VEGF mRNA expression or did not affect it according to the experiment, (annexes, fig. 7). This experiment should thus be repeated to clarify the effects of this dose. Besides, VEGF mRNA overexpression in MCF12A cells after exposure to the low dose of 0.1 Gy is somewhat worrisome, and it could be interesting to determine the minimal dose necessary to trigger such a response.

Nevertheless, though this work was designed for fundamental purposes, the doses used are relevant to medical situations. Fractionated radiotherapy for breast cancer can be carried out with different dose fractions. For instance, 40.05 Gy in 15 fractions over three weeks, which implies 2.67 Gy/fraction, 50 Gy in 25 fractions over five weeks, so 2 Gy/fraction, which is one of the most common design, or alternatively, 41.6 Gy dose in 13 fractions over 5 weeks implying 3.2 Gy/fraction (267; 317).

Regarding the exposure to low doses of radiations, we chose to work with a dose of 0.1 Gy to start this study because biological responses to radiation under this dose are still not clear, especially concerning cancers, and raise many debates amongst scientists. A simple radiography will deliver doses of radiation lower than 1 mGy, for instance, a chest radiography delivers 0.1 mGy. But some procedure such as CT-scans can reach higher doses. Most CT-scans will deliver doses to the targeted organ between 1 and 30 mGy. For instance, a head and neck scan median dose varies between 2 and 14 mGy and a chest scan from 8 to 22 mGy. However, pelvis scan delivers from 21 to 43 mGy, and a CT coronary angiogram can deliver 51 mGy to the breast and 64 mGy to the lung (379). So, some procedures can deliver doses not far from the 0.1 Gy dose used in this work, hence our interest in performing a dose-response curve, to see whether doses between 0.01 and 0.1 Gy could also trigger VEGF mRNA overexpression, or in studying the effects of dose

accumulation, as suggested before (see discussion of the third research manuscript). In this regard, previous studies detected an increased breast cancer risk after repeated chest fluoroscopic exposure while cohort studies found an increased mortality from other solid cancers in nuclear workers which was proportional to the cumulative dose (37; 85; 261; 336; 342).

4.4 Conclusions

To summarize, ID up-regulates VEGF expression in four NIS-expressing organs: the stomach, salivary glands, mammary glands, and thyroid (112). This VEGF overexpression was shown to increase blood perfusion in 3 of them but could not be demonstrated in stomach. VEGF overexpression was shown to be dependent on ROS- and mTOR-dependent increase in HIF-1α expression in breast *in vitro*. Interestingly, the pathways activated by ID in breast cells were similar to those activated in thyroid. Though differences in HIF-1 and ROS involvement were observed between cancerous and non-cancerous thyrocytes, such was not the case in breast. Moreover, *VEGF* mRNA was also shown to be significantly increased when ID was associated with a single exposure to a 3 Gy dose of X-rays in one of the cell lines: MCF12A.

As ID-induced ROS are not associated to mitochondrial activity, they could originate from another important ROS source such as the ER, which expresses several enzymatic ROS-producing systems such as NOX4 or NADPH cytochrome P450 oxidoreductase (471). It is thus possible that an acute drop in iodide content induces a “redox imbalance”, disturbs disulfide bonds, and thereby protein folding or affects ER membrane lipids. ER stress could lead to ROS production and UPR could be activated leading to mTOR activation (fig.21). This mechanism could be amplified by IR exposure in certain cells, since IR were shown to induce ER stress (197). Moreover, additional sources of ROS, such as mitochondria, induced by IR exposure could also amplify the response (fig. 21).

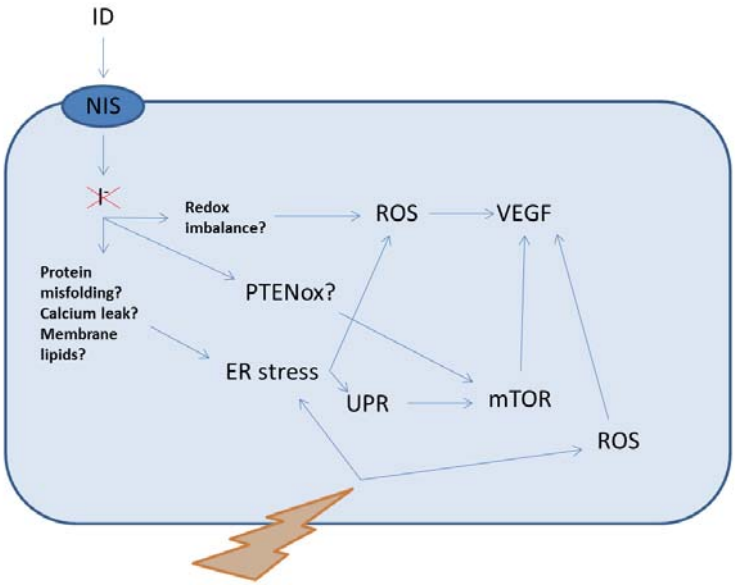

Fig. 21. Hypothetical molecular pathways involved in ID- and radiation-induced up-regulation of VEGF in breast cells.

VEGF, ROS, HIF-1 and mTOR have been associated with cancer initiation and/or progression as they are all involved in cellular surviving pathways (75; 150; 220; 440). ROS is the trigger of several stress responses. mTOR has a central role in cell survival growth, proliferation and motility. It has a pivotal position in many pathways. Likewise, HIF-1 regulates genes involved in metabolism, angiogenesis, cell proliferation and apoptosis. Therefore, though the study focused on their effects in ID-induced VEGF mRNA up-regulation, it is also possible that those factors will induce other pathways that could be deleterious, especially in a cancerous environment. Supporting this hypothesis, Stoddard et al. (2008) showed that iodine supplementation alters gene expression in MCF7 breast cancer cells, including genes involved in hormone metabolism and in cell cycle regulation (393). It could thus be interesting to investigate ID effects on other pathways involved in cell metabolism and survival, metastasis along with processes related more specifically to this research as angiogenic activation and EC protection, in cancerous and non-cancerous mice models and, on the same occasion, examine whether longer exposure to ID or fluctuating ID episodes could lead to pathological consequences.

Moreover, VEGF overexpression was associated to worse outcome in breast cancer. Again, a long-term animal study could determine whether ID-induced VEGF overexpression could influence the disease progression, especially if ID is associated with radiation exposure, since radiotherapy is often used for breast cancer. In this regard, interesting data could also be obtained from epidemiological studies comparing breast cancer patient outcome according to their UIC and to the type of therapy they undergo: whether it includes radiotherapy and the dose and dose rate received. The type of breast cancer could also bring interesting information as NIS and other iodine transporters expression may differ. Biopsies from patients could provide this kind of information which could then be related to the UIC and the cancer severity. Since stomach, thyroid and salivary glands also increase VEGF expression in response to ID, such research could be extended to those organs, particularly to thyroid for which long-term ID-induced TSH increase may further influence cancer progression. If cancer prognosis is proven to be worse after epidemiological studies and *in vivo* studies using animal fed with LID and exposed or not to radiation doses relevant to radiotherapy, a regular and sufficient iodide intake could be considered as a general prevention mean. More specifically, iodide status should be taken into account before exposure to radiation for therapy purposes. Furthermore, such results could be added to the numerous results highlighting ID-induced molecular changes in NIS-expressing organs or linking ID to diverse conditions in those organs, to be exposed to healthcare deciders in the objective of increasing the citizens' awareness of iodide nutritive importance, but also of convincing those deciders to implement strategies aiming at improving iodide supply worldwide, in iodine-deficient countries as in countries considered iodine-sufficient since individual iodide intake can vary significantly and diverse population subgroups are still often iodine-deficient in those countries.

4.5 Annexes

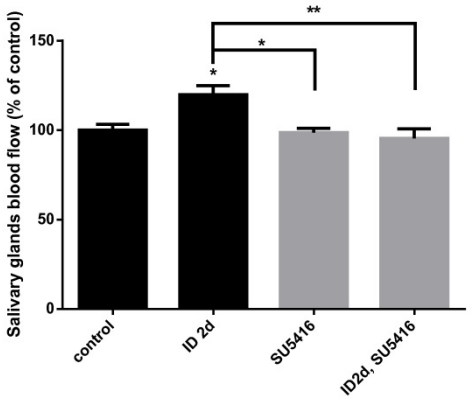

*Fig. 1. ID-induced increase in salivary glands blood perfusion is prevented in presence of VEGFR inhibitor, SU5416. Female NMRI mice were fed with an iodine-deficient diet and NaClO4 in their drinking water (ID) or normal diet (control) during 2 days (d), with or without SU5416 injection. Salivary glands blood flow was measured with a Laser Doppler. N=5. Values are expressed as means ± SEM. Statistical test: One-way ANOVA followed by a Tukey post-hoc test. *p value < 0,05, **p <0,01.*

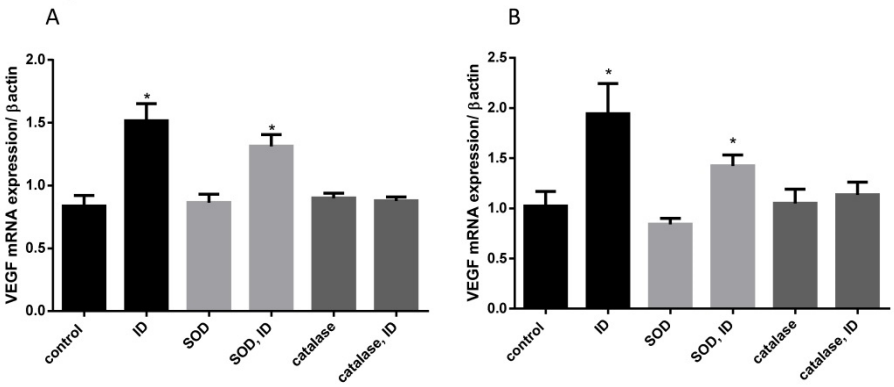

*Fig. 2. ID-induced increase in VEGF mRNA expression in breast cells is prevented by the addition of catalase but not that of SOD. MCF7 (A) and MCF12A (B) cells were cultured in iodine-containing medium for 7 days. Medium was replaced by iodine-containing (control) or iodine deficient (ID) medium for 6 or 3 hours respectively. VEGF mRNA expression was determined using RT-qPCR. N=1. Data are expressed as means ± SEM. Statistical test: one-way ANOVA with Tukey post-hoc test. *P < 0.05.*

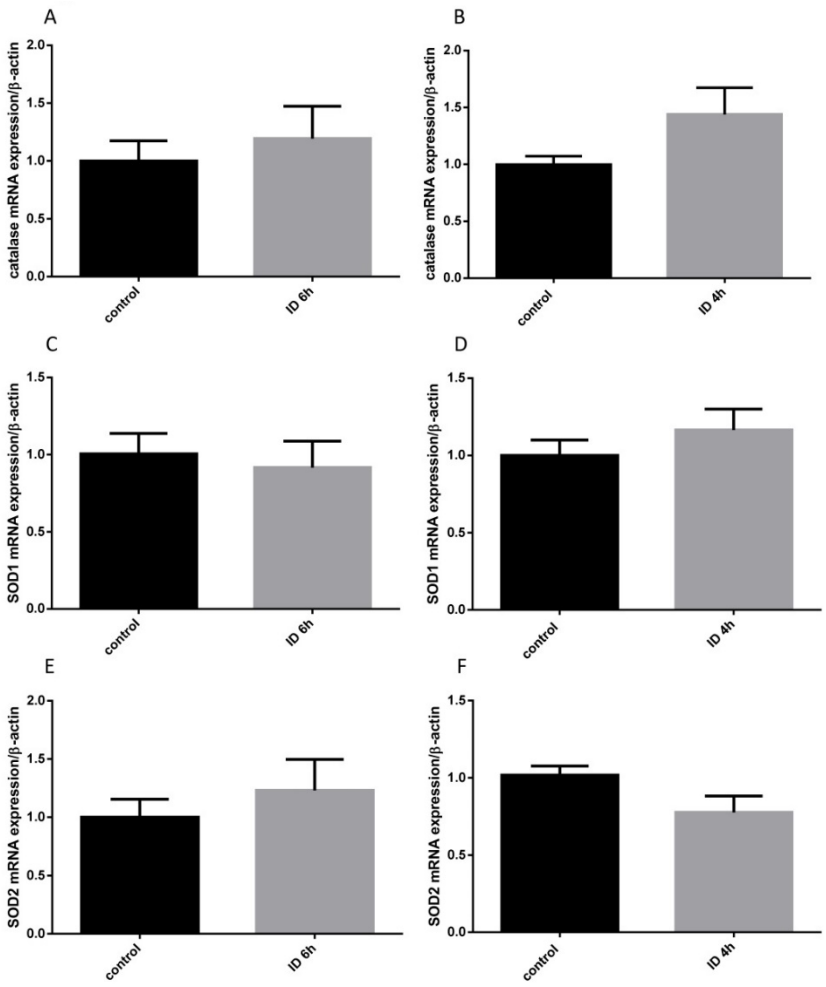

*Fig. 3. ID does not modulate catalase, SOD1 and SOD2 mRNA expression after 6 or 4 hours in MCF7 and MCF12A cells respectively. MCF7 (A, C, E) and MCF12A (B, D, F) cells were cultured in iodine-containing medium for 7 days. Medium was replaced by iodine-containing (control) or iodine deficient (ID) medium for 6 or 4 hours respectively. mRNA expression was determined using RT-qPCR. (A:N=7, B, F: N=5, C, D: N=2, E: N=4). Data are expressed as means ± SEM. Statistical test: Unpaired Student's t test.. *P < 0.05.*

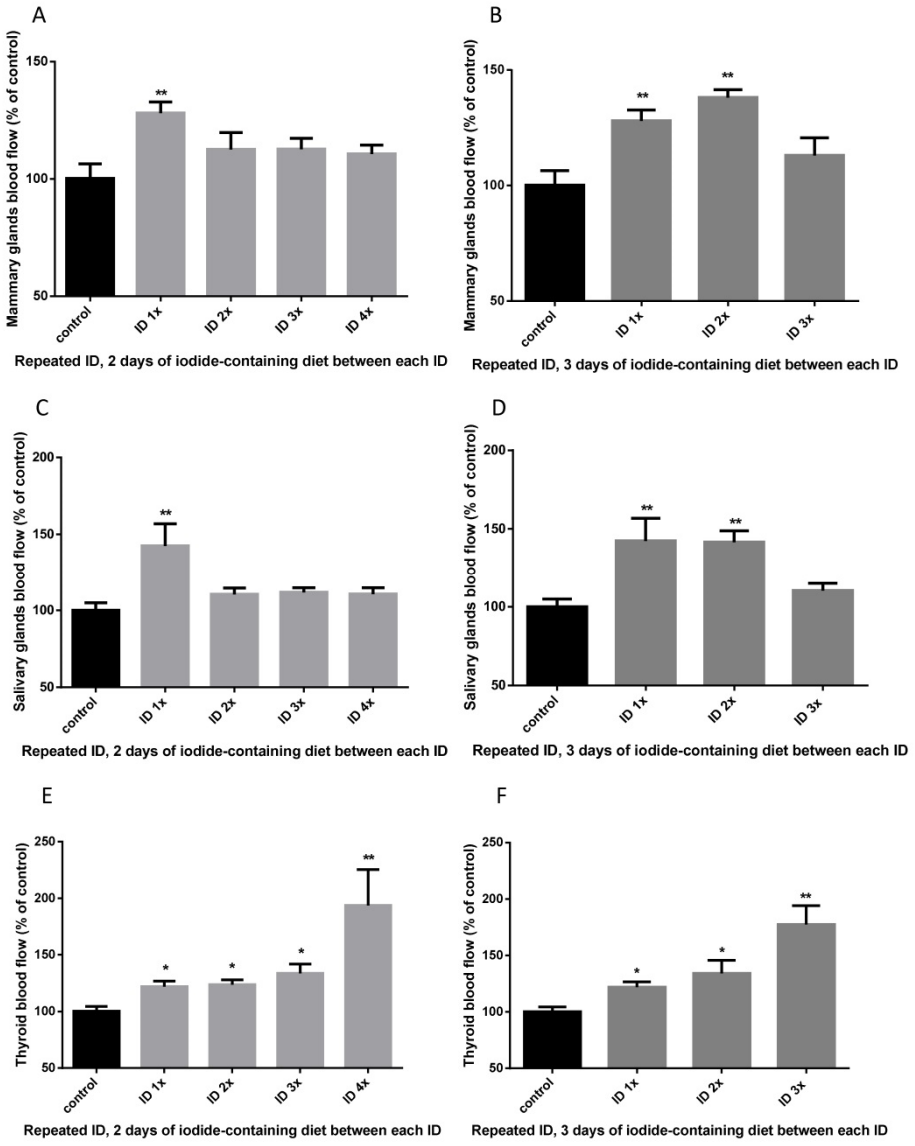

*Fig. 4**. Mammary gland, salivary gland and thyroid blood perfusion after repeated exposure to ID treatment.** Virgin female mice were exposed to iodine-deficient diet with perchlorate in the drinking water once, twice, 3 or 4 times for 2 days. Each ID exposure was separated by 2 (A, C, E) or 3 (B, D, F) days of normal diet with tap water. Mammary gland (A, B), salivary gland (C, D) and thyroid (E, F) blood perfusion was measured with laser Doppler. N=4 to 5. Values are expressed as means ± SEM. Statistical test: One-way ANOVA followed by a Dunnett post-hoc test. *p value < 0.05, **p<0.01.*

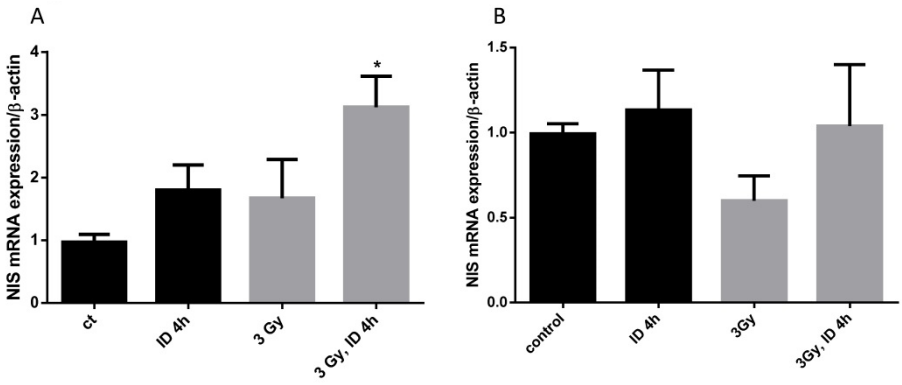

Fig. 5. ***ID combined to an exposure to 3 Gy of X-rays induces an increase in NIS mRNA expression in breast cancer cells but not in non-cancerous cells.*** *MCF7 (A) and MCF12A (B) cells were cultured in iodine-containing medium for 7 days. Medium was replaced by iodine-containing (control) or iodine deficient (ID) medium for 4 hours respectively, and were then x-irradiated with a dose of 3 Gy. NIS mRNA expression was determined using RT-qPCR. N=3. Data are expressed as means ± SEM. Statistical test: one-way ANOVA with Tukey post-hoc test. *P < 0.05.*

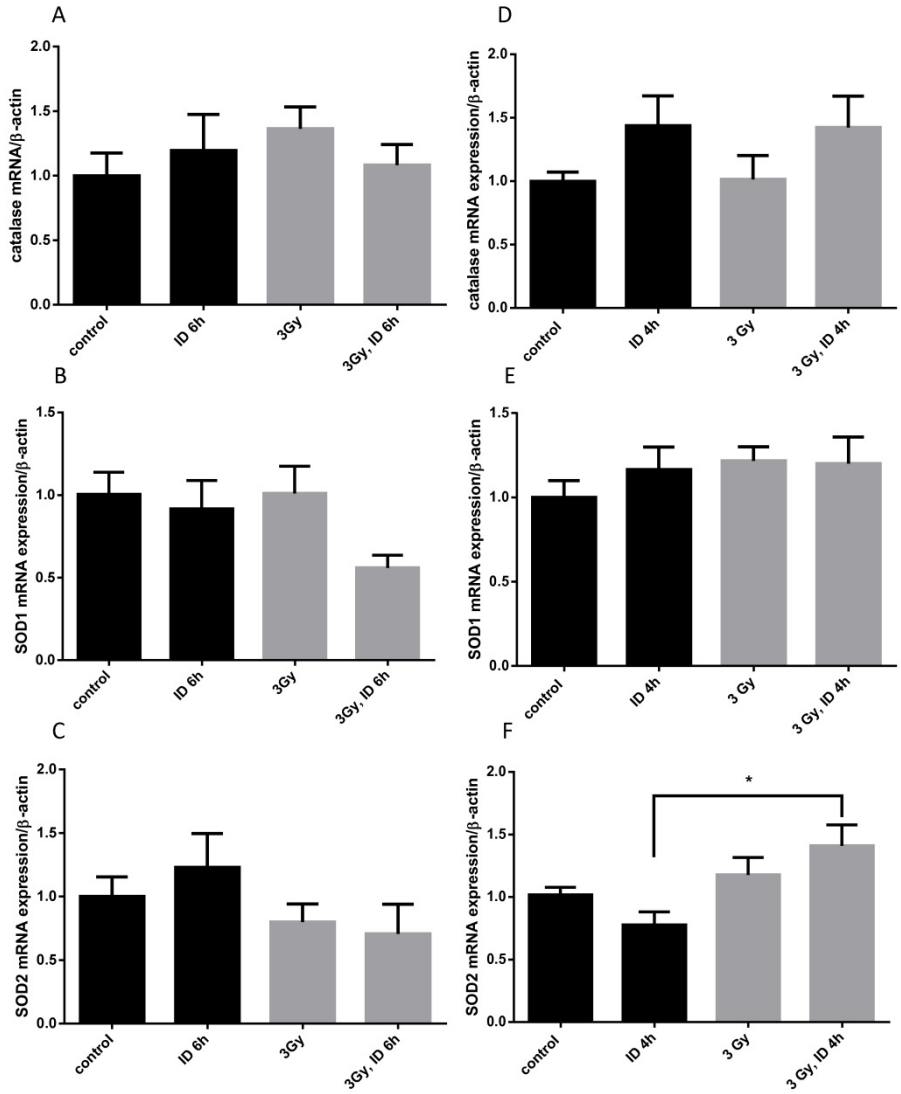

Fig. 6. ***ID and X-irradiation (3Gy) do not modulate catalase, SOD1 and SOD2 mRNA expression after 6 or 4 hours in MCF7 and MCF12A cells respectively compared to controls. SOD2 mRNA expression is higher in MCF12A cells exposed to X-rays and ID than in cells only exposed to ID.*** *MCF7 (A, C, E) and MCF12A (B, D, F) cells were cultured in iodine-containing medium for 7 days. Medium was replaced by iodine-containing (control) or iodine deficient (ID) medium for 6 or 4 hours respectively. mRNA expression was determined using RT-qPCR. (A:N=7, B, F: N=5, C, D: N=2, E: N=4). Data are expressed as means ± SEM. Statistical test: one-way ANOVA with Tukey post-hoc test. *P < 0.05.*

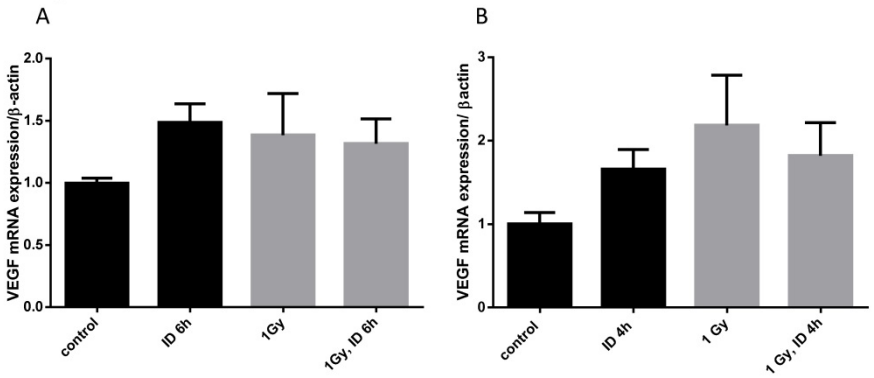

Fig. 7. ***Exposure to 1 Gy of X-rays does not induce a significant increase in VEGF mRNA expression in breast cells.*** *MCF7 (A) and MCF12A (B) cells were cultured in iodine-containing medium for 7 days. Medium was replaced by iodine-containing (control) or iodine deficient (ID) medium for 6 or 4 hours respectively, and were then x-irradiated with a dose of 1 Gy. VEGF mRNA expression was determined using RT-qPCR. N=3. Data are expressed as means ± SEM. Statistical test: one-way ANOVA.*

References

1. **Abdollahi A, Griggs DW, Zieher H, Roth A, Lipson KE, Saffrich R, Grone HJ, Hallahan DE, Reisfeld RA, Debus J, Niethammer AG and Huber PE**. Inhibition of alpha(v)beta3 integrin survival signaling enhances antiangiogenic and antitumor effects of radiotherapy. *Clin Cancer Res* 11: 6270-6279, 2005.
2. **Abdollahi A, Lipson KE, Han X, Krempien R, Trinh T, Weber KJ, Hahnfeldt P, Hlatky L, Debus J, Howlett AR and Huber PE**. SU5416 and SU6668 attenuate the angiogenic effects of radiation-induced tumor cell growth factor production and amplify the direct anti-endothelial action of radiation in vitro. *Cancer Res* 63: 3755-3763, 2003.
3. **Abnet CC, Fan JH, Kamangar F, Sun XD, Taylor PR, Ren JS, Mark SD, Zhao P, Fraumeni JF, Jr., Qiao YL and Dawsey SM**. Self-reported goiter is associated with a significantly increased risk of gastric noncardia adenocarcinoma in a large population-based Chinese cohort. *Int J Cancer* 119: 1508-1510, 2006.
4. **Aceves C, Anguiano B and Delgado G**. The extrathyronine actions of iodine as antioxidant, apoptotic, and differentiation factor in various tissues. *Thyroid* 23: 938-946, 2013.
5. **Acuna UM, Wittwer J, Ayers S, Pearce CJ, Oberlies NH and DE Blanco EJ**. Effects of (5Z)-7-oxozeaenol on the oxidative pathway of cancer cells. *Anticancer Res* 32: 2665-2671, 2012.
6. **Adams J, Carder PJ, Downey S, Forbes MA, MacLennan K, Allgar V, Kaufman S, Hallam S, Bicknell R, Walker JJ, Cairnduff F, Selby PJ, Perren TJ, Lansdown M and Banks RE**. Vascular endothelial growth factor (VEGF) in breast cancer: comparison of plasma, serum, and tissue VEGF and microvessel density and effects of tamoxifen. *Cancer Res* 60: 2898-2905, 2000.
7. **Adams MJ, Dozier A, Shore RE, Lipshultz SE, Schwartz RG, Constine LS, Pearson TA, Stovall M, Winters P and Fisher SG**. Breast cancer risk 55+ years after irradiation for an enlarged thymus and its implications for early childhood medical irradiation today. *Cancer Epidemiol Biomarkers Prev* 19: 48-58, 2010.
8. **Al-Dakheel MH, Haridi HK, Al-Bashir BM, Al-Shingiti A, Al-Shehri S, Gassem MA and Hussein I**. Prevalence of iodine deficiency disorders among school children in Saudi Arabia: results of a national iodine nutrition study. *East Mediterr Health J* 22: 301-308, 2016.
9. **Alotaibi H, Tuzlakoglu-Ozturk M and Tazebay UH**. The Thyroid Na+/I- Symporter: Molecular Characterization and Genomic Regulation. *Mol Imaging Radionucl Ther* 26: 92-101, 2017.
10. **Alphonse G, Maalouf M, Battiston-Montagne P, Ardail D, Beuve M, Rousson R, Taucher-Scholz G, Fournier C and Rodriguez-Lafrasse C**. p53-independent early and late apoptosis is mediated by ceramide after exposure of tumor cells to photon or carbon ion irradiation. *BMC Cancer* 13: 151, 2013.

11. **Als C, Haldimann M, Burgi E, Donati F, Gerber H and Zimmerli B**. Swiss pilot study of individual seasonal fluctuations of urinary iodine concentration over two years: is age-dependency linked to the major source of dietary iodine? *Eur J Clin Nutr* 57: 636-646, 2003.
12. **Altorjay A, Dohan O, Szilagyi A, Paroder M, Wapnir IL and Carrasco N**. Expression of the Na+/I- symporter (NIS) is markedly decreased or absent in gastric cancer and intestinal metaplastic mucosa of Barrett esophagus. *BMC Cancer* 7: 5, 2007.
13. **Ameziane-El-Hassani R, Talbot M, de Souza Dos Santos MC, Al GA, Hartl D, Bidart JM, De Deken, X, Miot F, Diallo I, de VF, Schlumberger M and Dupuy C**. NADPH oxidase DUOX1 promotes long-term persistence of oxidative stress after an exposure to irradiation. *Proc Natl Acad Sci U S A* 112: 5051-5056, 2015.
14. **Andersson, M. and Zimmermann, M**. Global iodine nutrition: a remarkable leap forward in the past decade. IDD newsletter 40. 2012.

Ref Type: Generic

15. **Antony S, Wu Y, Hewitt SM, Anver MR, Butcher D, Jiang G, Meitzler JL, Liu H, Juhasz A, Lu J, Roy KK and Doroshow JH**. Characterization of NADPH oxidase 5 expression in human tumors and tumor cell lines with a novel mouse monoclonal antibody. *Free Radic Biol Med* 65: 497-508, 2013.
16. **Appenzeller-Herzog C and Hall MN**. Bidirectional crosstalk between endoplasmic reticulum stress and mTOR signaling. *Trends Cell Biol* 22: 274-282, 2012.
17. **Arany Z, Huang LE, Eckner R, Bhattacharya S, Jiang C, Goldberg MA, Bunn HF and Livingston DM**. An essential role for p300/CBP in the cellular response to hypoxia. *Proc Natl Acad Sci U S A* 93: 12969-12973, 1996.
18. **Arbiser JL, Petros J, Klafter R, Govindajaran B, McLaughlin ER, Brown LF, Cohen C, Moses M, Kilroy S, Arnold RS and Lambeth JD**. Reactive oxygen generated by Nox1 triggers the angiogenic switch. *Proc Natl Acad Sci U S A* 99: 715-720, 2002.
19. **Arroyo-Helguera O, Anguiano B, Delgado G and Aceves C**. Uptake and antiproliferative effect of molecular iodine in the MCF-7 breast cancer cell line. *Endocr Relat Cancer* 13: 1147-1158, 2006.
20. Austin Community College. Reproductive system. 2008.

Ref Type: Audiovisual Material

21. **Ayala A, Munoz MF and Arguelles S**. Lipid peroxidation: production, metabolism, and signaling mechanisms of malondialdehyde and 4-hydroxy-2-nonenal. *Oxid Med Cell Longev* 2014: 360438, 2014.
22. **Azzam EI, Jay-Gerin JP and Pain D**. Ionizing radiation-induced metabolic oxidative stress and prolonged cell injury. *Cancer Lett* 327: 48-60, 2012.
23. **Bahar G, Feinmesser R, Shpitzer T, Popovtzer A and Nagler RM**. Salivary analysis in oral cancer patients: DNA and protein oxidation, reactive nitrogen species, and antioxidant profile. *Cancer* 109: 54-59, 2007.
24. **Balamurugan M, Sivakumar K, Mariadoss AV and Suresh K**. Modulating Effect of Hypnea musciformis (Red Seaweed) on Lipid Peroxidation, Antioxidants and Biotransforming Enzymes in 7,12-Dimethylbenz (a) Anthracene Induced Mammary Carcinogenesis in Experimental Animals. *Pharmacognosy Res* 9: 108-115, 2017.

25. **Barleon B, Sozzani S, Zhou D, Weich HA, Mantovani A and Marme D**. Migration of human monocytes in response to vascular endothelial growth factor (VEGF) is mediated via the VEGF receptor flt-1. *Blood* 87: 3336-3343, 1996.
26. **Bates DO, Cui TG, Doughty JM, Winkler M, Sugiono M, Shields JD, Peat D, Gillatt D and Harper SJ**. VEGF165b, an inhibitory splice variant of vascular endothelial growth factor, is down-regulated in renal cell carcinoma. *Cancer Res* 62: 4123-4131, 2002.
27. **Bates DO, MacMillan PP, Manjaly JG, Qiu Y, Hudson SJ, Bevan HS, Hunter AJ, Soothill PW, Read M, Donaldson LF and Harper SJ**. The endogenous anti-angiogenic family of splice variants of VEGF, VEGFxxxb, are down-regulated in pre-eclamptic placentae at term. *Clin Sci (Lond)* 110: 575-585, 2006.
28. **Bedard K and Krause KH**. The NOX family of ROS-generating NADPH oxidases: physiology and pathophysiology. *Physiol Rev* 87: 245-313, 2007.
29. **Beebe DC, Holekamp NM and Shui YB**. Oxidative damage and the prevention of age-related cataracts. *Ophthalmic Res* 44: 155-165, 2010.
30. **Behrouzian R and Aghdami N**. Urinary iodine/creatinine ratio in patients with stomach cancer in Urmia, Islamic Republic of Iran. *East Mediterr Health J* 10: 921-924, 2004.
31. **Berking S, Czech N, Gerharz M, Herrmann K, Hoffmann U, Raifer H, Sekul G, Siefker B, Sommerei A and Vedder F**. A newly discovered oxidant defence system and its involvement in the development of Aurelia aurita (Scyphozoa, Cnidaria): reactive oxygen species and elemental iodine control medusa formation. *Int J Dev Biol* 49: 969-976, 2005.
32. **Bernroitner M, Zamocky M, Furtmuller PG, Peschek GA and Obinger C**. Occurrence, phylogeny, structure, and function of catalases and peroxidases in cyanobacteria. *J Exp Bot* 60: 423-440, 2009.
33. **Beyer SJ, Jimenez RE, Shapiro CL, Cho JY and Jhiang SM**. Do cell surface trafficking impairments account for variable cell surface sodium iodide symporter levels in breast cancer? *Breast Cancer Res Treat* 115: 205-212, 2009.
34. **Bizhanova A and Kopp P**. Minireview: The sodium-iodide symporter NIS and pendrin in iodide homeostasis of the thyroid. *Endocrinology* 150: 1084-1090, 2009.
35. **Bock F, Onderka J, Dietrich T, Bachmann B, Kruse FE, Paschke M, Zahn G and Cursiefen C**. Bevacizumab as a potent inhibitor of inflammatory corneal angiogenesis and lymphangiogenesis. *Invest Ophthalmol Vis Sci* 48: 2545-2552, 2007.
36. **Bogdandi EN, Balogh A, Felgyinszki N, Szatmari T, Persa E, Hildebrandt G, Safrany G and Lumniczky K**. Effects of low-dose radiation on the immune system of mice after total-body irradiation. *Radiat Res* 174: 480-489, 2010.
37. **Boice JD, Jr., Preston D, Davis FG and Monson RR**. Frequent chest X-ray fluoroscopy and breast cancer incidence among tuberculosis patients in Massachusetts. *Radiat Res* 125: 214-222, 1991.
38. **Boltze C, Brabant G, Dralle H, Gerlach R, Roessner A and Hoang-Vu C**. Radiation-induced thyroid carcinogenesis as a function of time and dietary iodine supply: an in vivo model of tumorigenesis in the rat. *Endocrinology* 143: 2584-2592, 2002.

39. **Bos R, van Diest PJ, van der Groep P, Shvarts A, Greijer AE and van der Wall E**. Expression of hypoxia-inducible factor-1alpha and cell cycle proteins in invasive breast cancer are estrogen receptor related. *Breast Cancer Res* 6: R450-R459, 2004.
40. **Boveris A, Cadenas E and Stoppani AO**. Role of ubiquinone in the mitochondrial generation of hydrogen peroxide. *Biochem J* 156: 435-444, 1976.
41. **Boveris A and Chance B**. The mitochondrial generation of hydrogen peroxide. General properties and effect of hyperbaric oxygen. *Biochem J* 134: 707-716, 1973.
42. **Boyd SR, Gittos A, Richter M, Hungerford JL, Errington RD and Cree IA**. Proton beam therapy and iris neovascularisation in uveal melanoma. *Eye (Lond)* 20: 832-836, 2006.
43. **Brunelle JK, Bell EL, Quesada NM, Vercauteren K, Tiranti V, Zeviani M, Scarpulla RC and Chandel NS**. Oxygen sensing requires mitochondrial ROS but not oxidative phosphorylation. *Cell Metab* 1: 409-414, 2005.
44. **Burns R, O'Herlihy C and Smyth PP**. Regulation of iodide uptake in placental primary cultures. *Eur Thyroid J* 2: 243-251, 2013.
45. **Burrows N, Babur M, Resch J, Williams KJ and Brabant G**. Hypoxia-inducible factor in thyroid carcinoma. *J Thyroid Res* 2011: 762905, 2011.
46. **Buteau-Lozano H, Ancelin M, Lardeux B, Milanini J and Perrot-Applanat M**. Transcriptional regulation of vascular endothelial growth factor by estradiol and tamoxifen in breast cancer cells: a complex interplay between estrogen receptors alpha and beta. *Cancer Res* 62: 4977-4984, 2002.
47. **Cahoon EK, Nadyrov EA, Polyanskaya ON, Yauseyenka VV, Veyalkin IV, Yeudachkova TI, Maskvicheva TI, Minenko VF, Liu W, Drozdovitch V, Mabuchi K, Little MP, Zablotska LB, McConnell RJ, Hatch M, Peters KO, Rozhko AV and Brenner AV**. Risk of Thyroid Nodules in Residents of Belarus Exposed to Chernobyl Fallout as Children and Adolescents. *J Clin Endocrinol Metab* 102: 2207-2217, 2017.
48. **Caldwell KL, Pan Y, Mortensen ME, Makhmudov A, Merrill L and Moye J**. Iodine status in pregnant women in the National Children's Study and in U.S. women (15-44 years), National Health and Nutrition Examination Survey 2005-2010. *Thyroid* 23: 927-937, 2013.
49. **Cardis E, Kesminiene A, Ivanov V, Malakhova I, Shibata Y, Khrouch V, Drozdovitch V, Maceika E, Zvonova I, Vlassov O, Bouville A, Goulko G, Hoshi M, Abrosimov A, Anoshko J, Astakhova L, Chekin S, Demidchik E, Galanti R, Ito M, Korobova E, Lushnikov E, Maksioutov M, Masyakin V, Nerovnia A, Parshin V, Parshkov E, Piliptsevich N, Pinchera A, Polyakov S, Shabeka N, Suonio E, Tenet V, Tsyb A, Yamashita S and Williams D**. Risk of thyroid cancer after exposure to 131I in childhood. *J Natl Cancer Inst* 97: 724-732, 2005.
50. **Cebe SS, Pieren M, Cariolato L, Arn S, Hoffmann U, Bogucki A, Manlius C, Wood J and Ballmer-Hofer K**. A VEGF-A splice variant defective for heparan sulfate and neuropilin-1 binding shows attenuated signaling through VEGFR-2. *Cell Mol Life Sci* 63: 2067-2077, 2006.
51. **Cebe-Suarez S, Grunewald FS, Jaussi R, Li X, Claesson-Welsh L, Spillmann D, Mercer AA, Prota AE and Ballmer-Hofer K**. Orf virus VEGF-E NZ2 promotes

paracellular NRP-1/VEGFR-2 coreceptor assembly via the peptide RPPR. *FASEB J* 22: 3078-3086, 2008.

52. **Centanni M, Marignani M, Gargano L, Corleto VD, Casini A, Delle FG, Andreoli M and Annibale B**. Atrophic body gastritis in patients with autoimmune thyroid disease: an underdiagnosed association. *Arch Intern Med* 159: 1726-1730, 1999.
53. **Chan JY, Gooi Z, Mydlarz WK and Agrawal N**. Risk of thyroid malignancy following an index head and neck squamous cell carcinoma: A population-based study. *Ear Nose Throat J* 95: E7-E11, 2016.
54. **Cheda A, Nowosielska EM, Wrembel-Wargocka J and Janiak MK**. Production of cytokines by peritoneal macrophages and splenocytes after exposures of mice to low doses of X-rays. *Radiat Environ Biophys* 47: 275-283, 2008.
55. **Cheda A, Wrembel-Wargocka J, Lisiak E, Nowosielska EM, Marciniak M and Janiak MK**. Single low doses of X rays inhibit the development of experimental tumor metastases and trigger the activities of NK cells in mice. *Radiat Res* 161: 335-340, 2004.
56. **Chen AY, Levy L, Goepfert H, Brown BW, Spitz MR and Vassilopoulou-Sellin R**. The development of breast carcinoma in women with thyroid carcinoma. *Cancer* 92: 225-231, 2001.
57. **Chen TT, Luque A, Lee S, Anderson SM, Segura T and Iruela-Arispe ML**. Anchorage of VEGF to the extracellular matrix conveys differential signaling responses to endothelial cells. *J Cell Biol* 188: 595-609, 2010.
58. **Cheong SJ, Jang D, Jeong HJ, Lim ST, Sohn MH, Katzenellenbogen JA and Kim DW**. Reduction of stimulated sodium iodide symporter expression by estrogen receptor ligands in breast cancer cells. *Nucl Med Biol* 38: 287-294, 2011.
59. **Cho JY, Leveille R, Kao R, Rousset B, Parlow AF, Burak WE, Jr., Mazzaferri EL and Jhiang SM**. Hormonal regulation of radioiodide uptake activity and Na+/I- symporter expression in mammary glands. *J Clin Endocrinol Metab* 85: 2936-2943, 2000.
60. **Choi SH, Kim M, Lee HJ, Kim EH, Kim CH and Lee YJ**. Effects of NOX1 on fibroblastic changes of endothelial cells in radiationinduced pulmonary fibrosis. *Mol Med Rep* 13: 4135-4142, 2016.
61. **Choo AY, Yoon SO, Kim SG, Roux PP and Blenis J**. Rapamycin differentially inhibits S6Ks and 4E-BP1 to mediate cell-type-specific repression of mRNA translation. *Proc Natl Acad Sci U S A* 105: 17414-17419, 2008.
62. **Chung AS and Ferrara N**. Developmental and pathological angiogenesis. *Annu Rev Cell Dev Biol* 27: 563-584, 2011.
63. **Clero E, Doyon F, Chungue V, Rachedi F, Boissin JL, Sebbag J, Shan L, Bost-Bezeaud F, Petitdidier P, Dewailly E, Rubino C and de VF**. Dietary iodine and thyroid cancer risk in French Polynesia: a case-control study. *Thyroid* 22: 422-429, 2012.
64. Cocchi M and Venturi S. Iodide, antioxidant function and omega-6 and omega-3 fatty acids: a new hypothesis of biochemical cooperation? Prog Nutr 2, 15-19. 2000.
65. **Cohen BL**. Dose-response relationship for radiation carcinogenesis in the low-dose region. *Int Arch Occup Environ Health* 66: 71-75, 1994.

66. **Colin C, Leblanc C, Wagner E, Delage L, Leize-Wagner E, Van DA, Kloareg B and Potin P**. The brown algal kelp Laminaria digitata features distinct bromoperoxidase and iodoperoxidase activities. *J Biol Chem* 278: 23545-23552, 2003.
67. **Colin IM, Denef JF, Lengele B, Many MC and Gerard AC**. Recent insights into the cell biology of thyroid angiofollicular units. *Endocr Rev* 34: 209-238, 2013.
68. **Cooke R, Jones ME, Cunningham D, Falk SJ, Gilson D, Hancock BW, Harris SJ, Horwich A, Hoskin PJ, Illidge T, Linch DC, Lister TA, Lucraft HH, Radford JA, Stevens AM, Syndikus I, Williams MV and Swerdlow AJ**. Breast cancer risk following Hodgkin lymphoma radiotherapy in relation to menstrual and reproductive factors. *Br J Cancer* 108: 2399-2406, 2013.
69. **Craps J, Joris V, De JB, Sonveaux P, Horman S, Lengele B, Bertrand L, Many MC, Colin IM and Gerard AC**. Involvement of mTOR and Regulation by AMPK in Early Iodine Deficiency-Induced Thyroid Microvascular Activation. *Endocrinology* 157: 2545-2559, 2016.
70. **Craps J, Wilvers C, Joris V, De JB, Vanderstraeten J, Lobysheva I, Balligand JL, Sonveaux P, Gilon P, Many MC, Gerard AC and Colin IM**. Involvement of nitric oxide in iodine deficiency-induced microvascular remodeling in the thyroid gland: role of nitric oxide synthase 3 and ryanodine receptors. *Endocrinology* 156: 707-720, 2015.
71. **Cunningham JT, Rodgers JT, Arlow DH, Vazquez F, Mootha VK and Puigserver P**. mTOR controls mitochondrial oxidative function through a YY1-PGC-1alpha transcriptional complex. *Nature* 450: 736-740, 2007.
72. **Czapski G and Goldstein S**. The role of the reactions of .NO with superoxide and oxygen in biological systems: a kinetic approach. *Free Radic Biol Med* 19: 785-794, 1995.
73. **Dai G, Levy O and Carrasco N**. Cloning and characterization of the thyroid iodide transporter. *Nature* 379: 458-460, 1996.
74. **De Bruin ML, Sparidans J, van't Veer MB, Noordijk EM, Louwman MW, Zijlstra JM, van den Berg H, Russell NS, Broeks A, Baaijens MH, Aleman BM and van Leeuwen FE**. Breast cancer risk in female survivors of Hodgkin's lymphoma: lower risk after smaller radiation volumes. *J Clin Oncol* 27: 4239-4246, 2009.
75. **De Francesco EM, Lappano R, Santolla MF, Marsico S, Caruso A and Maggiolini M**. HIF-1alpha/GPER signaling mediates the expression of VEGF induced by hypoxia in breast cancer associated fibroblasts (CAFs). *Breast Cancer Res* 15: R64, 2013.
76. **DeFatta RJ, Turbat-Herrera EA, Li BD, Anderson W and De BA**. Elevated expression of eIF4E in confined early breast cancer lesions: possible role of hypoxia. *Int J Cancer* 80: 516-522, 1999.
77. **Delgado G, Munoz-Torres C, Orozco-Esquivel T, Anguiano B and Aceves C**. Total iodine quantification in fluids and tissues from iodine- or iodide-supplemented rats by ion chromatography following microwave-assisted digestion. *Thyroid* 25: 352-360, 2015.
78. **Derry DM**. *Breast Cancer and Iodine*. Trafford Publishing, 2001,
79. **DeYoung MP, Horak P, Sofer A, Sgroi D and Ellisen LW**. Hypoxia regulates TSC1/2-mTOR signaling and tumor suppression through REDD1-mediated 14-3-3 shuttling. *Genes Dev* 22: 239-251, 2008.

80. **Dhawan V**. Reactive Oxygen and Nitrogen Species: General Considerations. *applied Basic Research and Clinical Practice* 12: 26-47, 2014.
81. **Dikalova AE, Bikineyeva AT, Budzyn K, Nazarewicz RR, McCann L, Lewis W, Harrison DG and Dikalov SI**. Therapeutic targeting of mitochondrial superoxide in hypertension. *Circ Res* 107: 106-116, 2010.
82. **Discher DJ, Bishopric NH, Wu X, Peterson CA and Webster KA**. Hypoxia regulates beta-enolase and pyruvate kinase-M promoters by modulating Sp1/Sp3 binding to a conserved GC element. *J Biol Chem* 273: 26087-26093, 1998.
83. **Dohan O, De l, V, Paroder V, Riedel C, Artani M, Reed M, Ginter CS and Carrasco N**. The sodium/iodide Symporter (NIS): characterization, regulation, and medical significance. *Endocr Rev* 24: 48-77, 2003.
84. **Dohan O, Portulano C, Basquin C, Reyna-Neyra A, Amzel LM and Carrasco N**. The Na+/I symporter (NIS) mediates electroneutral active transport of the environmental pollutant perchlorate. *Proc Natl Acad Sci U S A* 104: 20250-20255, 2007.
85. **Doody MM, Lonstein JE, Stovall M, Hacker DG, Luckyanov N and Land CE**. Breast cancer mortality after diagnostic radiography: findings from the U.S. Scoliosis Cohort Study. *Spine (Phila Pa 1976)* 25: 2052-2063, 2000.
86. **Dore-Savard L, Lee E, Kakkad S, Popel AS and Bhujwalla ZM**. The Angiogenic Secretome in VEGF overexpressing Breast Cancer Xenografts. *Sci Rep* 6: 39460, 2016.
87. **Dores GM, Anderson WF, Beane Freeman LE, Fraumeni JF, Jr. and Curtis RE**. Risk of breast cancer according to clinicopathologic features among long-term survivors of Hodgkin's lymphoma treated with radiotherapy. *Br J Cancer* 103: 1081-1084, 2010.
88. **Dunn JT and Delange F**. Damaged reproduction: the most important consequence of iodine deficiency. *J Clin Endocrinol Metab* 86: 2360-2363, 2001.
89. **Duvel K, Yecies JL, Menon S, Raman P, Lipovsky AI, Souza AL, Triantafellow E, Ma Q, Gorski R, Cleaver S, Vander Heiden MG, MacKeigan JP, Finan PM, Clish CB, Murphy LO and Manning BD**. Activation of a metabolic gene regulatory network downstream of mTOR complex 1. *Mol Cell* 39: 171-183, 2010.
90. **Dykhuizen RS, Fraser A, McKenzie H, Golden M, Leifert C and Benjamin N**. Helicobacter pylori is killed by nitrite under acidic conditions. *Gut* 42: 334-337, 1998.
91. **Endo T, Kaneshige M, Nakazato M, Ohmori M, Harii N and Onaya T**. Thyroid transcription factor-1 activates the promoter activity of rat thyroid Na+/I-symporter gene. *Mol Endocrinol* 11: 1747-1755, 1997.
92. **Eng PH, Cardona GR, Fang SL, Previti M, Alex S, Carrasco N, Chin WW and Braverman LE**. Escape from the acute Wolff-Chaikoff effect is associated with a decrease in thyroid sodium/iodide symporter messenger ribonucleic acid and protein. *Endocrinology* 140: 3404-3410, 1999.
93. **Enns L, Bogen KT, Wizniak J, Murtha AD and Weinfeld M**. Low-dose radiation hypersensitivity is associated with p53-dependent apoptosis. *Mol Cancer Res* 2: 557-566, 2004.

94. **Eskandari S, Loo DD, Dai G, Levy O, Wright EM and Carrasco N**. Thyroid Na+/I- symporter. Mechanism, stoichiometry, and specificity. *J Biol Chem* 272: 27230-27238, 1997.
95. **Eskin BA, Bartuska DG, Dunn MR, Jacob G and Dratman MB**. Mammary gland dysplasia in iodine deficiency. Studies in rats. *JAMA* 200: 691-695, 1967.
96. **Eskin BA, Grotkowski CE, Connolly CP and Ghent WR**. Different tissue responses for iodine and iodide in rat thyroid and mammary glands. *Biol Trace Elem Res* 49: 9-19, 1995.
97. **Eskin BA, Shuman R, Krouse T and Merion JA**. Rat mammary gland atypia produced by iodine blockade with perchlorate. *Cancer Res* 35: 2332-2339, 1975.
98. **Everett LA, Belyantseva IA, Noben-Trauth K, Cantos R, Chen A, Thakkar SI, Hoogstraten-Miller SL, Kachar B, Wu DK and Green ED**. Targeted disruption of mouse Pds provides insight about the inner-ear defects encountered in Pendred syndrome. *Hum Mol Genet* 10: 153-161, 2001.
99. **Fan XC and Steitz JA**. Overexpression of HuR, a nuclear-cytoplasmic shuttling protein, increases the in vivo stability of ARE-containing mRNAs. *EMBO J* 17: 3448-3460, 1998.
100. **Farnedi A, Eusebi LH, Poli F and Foschini M**. Immunohistochemical Expression of the Human Sodium/Iodide Symporter Distinguishes Malignant From Benign Gastric Lesions. *International Journal of Surgical Pathology* 17: 327-334, 2009.
101. **Fite A, Dykhuizen R, Litterick A, Golden M and Leifert C**. Effects of ascorbic acid, glutathione, thiocyanate, and iodide on antimicrobial activity of acidified nitrite. *Antimicrob Agents Chemother* 48: 655-658, 2004.
102. **Fong GH, Rossant J, Gertsenstein M and Breitman ML**. Role of the Flt-1 receptor tyrosine kinase in regulating the assembly of vascular endothelium. *Nature* 376: 66-70, 1995.
103. **Forsythe JA, Jiang BH, Iyer NV, Agani F, Leung SW, Koos RD and Semenza GL**. Activation of vascular endothelial growth factor gene transcription by hypoxia-inducible factor 1. *Mol Cell Biol* 16: 4604-4613, 1996.
104. **Funahashi H, Imai T, Tanaka Y, Tsukamura K, Hayakawa Y, Kikumori T, Mase T, Itoh T, Nishikawa M, Hayashi H, Shibata A, Hibi Y, Takahashi M and Narita T**. Wakame seaweed suppresses the proliferation of 7,12-dimethylbenz(a)-anthracene-induced mammary tumors in rats. *Jpn J Cancer Res* 90: 922-927, 1999.
105. **Furukawa K, Preston D, Funamoto S, Yonehara S, Ito M, Tokuoka S, Sugiyama H, Soda M, Ozasa K and Mabuchi K**. Long-term trend of thyroid cancer risk among Japanese atomic-bomb survivors: 60 years after exposure. *Int J Cancer* 132: 1222-1226, 2013.
106. **Garcia-Barros M, Paris F, Cordon-Cardo C, Lyden D, Rafii S, Haimovitz-Friedman A, Fuks Z and Kolesnick R**. Tumor response to radiotherapy regulated by endothelial cell apoptosis. *Science* 300: 1155-1159, 2003.
107. **Garcia-Martinez JM and Alessi DR**. mTOR complex 2 (mTORC2) controls hydrophobic motif phosphorylation and activation of serum- and glucocorticoid-induced protein kinase 1 (SGK1). *Biochem J* 416: 375-385, 2008.
108. **Garcia-Solis P, Alfaro Y, Anguiano B, Delgado G, Guzman RC, Nandi S, Diaz-Munoz M, Vazquez-Martinez O and Aceves C**. Inhibition of N-methyl-N-nitrosourea-

induced mammary carcinogenesis by molecular iodine (I2) but not by iodide (I-) treatment Evidence that I2 prevents cancer promotion. *Mol Cell Endocrinol* 236: 49-57, 2005.

109. **Geiszt M, Witta J, Baffi J, Lekstrom K and Leto TL**. Dual oxidases represent novel hydrogen peroxide sources supporting mucosal surface host defense. *FASEB J* 17: 1502-1504, 2003.
110. **Geng L, Donnelly E, McMahon G, Lin PC, Sierra-Rivera E, Oshinka H and Hallahan DE**. Inhibition of vascular endothelial growth factor receptor signaling leads to reversal of tumor resistance to radiotherapy. *Cancer Res* 61: 2413-2419, 2001.
111. **Gerard AC, Humblet K, Wilvers C, Poncin S, Derradji H, de Ville de GC, Abou-el-Ardat K, Baatout S, Sonveaux P, Denef JF and Colin IM**. Iodine-deficiency-induced long lasting angiogenic reaction in thyroid cancers occurs via a vascular endothelial growth factor-hypoxia inducible factor-1-dependent, but not a reactive oxygen species-dependent, pathway. *Thyroid* 22: 699-708, 2012.
112. **Gerard AC, Poncin S, Audinot JN, Denef JF and Colin IM**. Iodide deficiency-induced angiogenic stimulus in the thyroid occurs via HIF- and ROS-dependent VEGF-A secretion from thyrocytes. *Am J Physiol Endocrinol Metab* 296: E1414-E1422, 2009.
113. **Gerard AC, Poncin S, Caetano B, Sonveaux P, Audinot JN, Feron O, Colin IM and Soncin F**. Iodine deficiency induces a thyroid stimulating hormone-independent early phase of microvascular reshaping in the thyroid. *Am J Pathol* 172: 748-760, 2008.
114. **Ghent WR, Eskin BA, Low DA and Hill LP**. Iodine replacement in fibrocystic disease of the breast. *Can J Surg* 36: 453-460, 1993.
115. **Gille J, Swerlick RA and Caughman SW**. Transforming growth factor-alpha-induced transcriptional activation of the vascular permeability factor (VPF/VEGF) gene requires AP-2-dependent DNA binding and transactivation. *EMBO J* 16: 750-759, 1997.
116. **Girdhani S, Lamont C, Hahnfeldt P, Abdollahi A and Hlatky L**. Proton irradiation suppresses angiogenic genes and impairs cell invasion and tumor growth. *Radiat Res* 178: 33-45, 2012.
117. **Go YM, Ziegler TR, Johnson JM, Gu L, Hansen JM and Jones DP**. Selective protection of nuclear thioredoxin-1 and glutathione redox systems against oxidation during glucose and glutamine deficiency in human colonic epithelial cells. *Free Radic Biol Med* 42: 363-370, 2007.
118. **Goldberg-Cohen I, Furneauxb H and Levy AP**. A 40-bp RNA element that mediates stabilization of vascular endothelial growth factor mRNA by HuR. *J Biol Chem* 277: 13635-13640, 2002.
119. **Goldhar AS, Vonderhaar BK, Trott JF and Hovey RC**. Prolactin-induced expression of vascular endothelial growth factor via Egr-1. *Mol Cell Endocrinol* 232: 9-19, 2005.
120. **Golkowski F, Szybinski Z, Rachtan J, Sokolowski A, Buziak-Bereza M, Trofimiuk M, Hubalewska-Dydejczyk A, Przybylik-Mazurek E and Huszno B**. Iodine prophylaxis--the protective factor against stomach cancer in iodine deficient areas. *Eur J Nutr* 46: 251-256, 2007.
121. **Gorski DH, Beckett MA, Jaskowiak NT, Calvin DP, Mauceri HJ, Salloum RM, Seetharam S, Koons A, Hari DM, Kufe DW and Weichselbaum RR**. Blockage of the

vascular endothelial growth factor stress response increases the antitumor effects of ionizing radiation. *Cancer Res* 59: 3374-3378, 1999.

122. **Grabham P and Sharma P**. The effects of radiation on angiogenesis. *Vasc Cell* 5: 19, 2013.
123. **Grabham P, Sharma P, Bigelow A and Geard C**. Two distinct types of the inhibition of vasculogenesis by different species of charged particles. *Vasc Cell* 5: 16, 2013.
124. **Graham KA, Kulawiec M, Owens KM, Li X, Desouki MM, Chandra D and Singh KK**. NADPH oxidase 4 is an oncoprotein localized to mitochondria. *Cancer Biol Ther* 10: 223-231, 2010.
125. **Grudzenski S, Raths A, Conrad S, Rube CE and Lobrich M**. Inducible response required for repair of low-dose radiation damage in human fibroblasts. *Proc Natl Acad Sci U S A* 107: 14205-14210, 2010.
126. **Guertin DA, Stevens DM, Thoreen CC, Burds AA, Kalaany NY, Moffat J, Brown M, Fitzgerald KJ and Sabatini DM**. Ablation in mice of the mTORC components raptor, rictor, or mLST8 reveals that mTORC2 is required for signaling to Akt-FOXO and PKCalpha, but not S6K1. *Dev Cell* 11: 859-871, 2006.
127. **Guida M, Maraldi T, Beretti F, Follo MY, Manzoli L and De PA**. Nuclear Nox4-derived reactive oxygen species in myelodysplastic syndromes. *Biomed Res Int* 2014: 456937, 2014.
128. **Gulaboglu M, Yildiz L, Celebi F, Gul M and Peker K**. Comparison of iodine contents in gastric cancer and surrounding normal tissues. *Clin Chem Lab Med* 43: 581-584, 2005.
129. **Gupta VK, Jaskowiak NT, Beckett MA, Mauceri HJ, Grunstein J, Johnson RS, Calvin DA, Nodzenski E, Pejovic M, Kufe DW, Posner MC and Weichselbaum RR**. Vascular endothelial growth factor enhances endothelial cell survival and tumor radioresistance. *Cancer J* 8: 47-54, 2002.
130. **Gutierrez-Repiso C, Velasco I, Garcia-Escobar E, Garcia-Serrano S, Rodriguez-Pacheco F, Linares F, Ruiz de Adana MS, Rubio-Martin E, Garrido-Sanchez L, Cobos-Bravo JF, Priego-Puga T, Rojo-Martinez G, Soriguer F and Garcia-Fuentes E**. Does dietary iodine regulate oxidative stress and adiponectin levels in human breast milk? *Antioxid Redox Signal* 20: 847-853, 2014.
131. **Guzy RD, Hoyos B, Robin E, Chen H, Liu L, Mansfield KD, Simon MC, Hammerling U and Schumacker PT**. Mitochondrial complex III is required for hypoxia-induced ROS production and cellular oxygen sensing. *Cell Metab* 1: 401-408, 2005.
132. **Gwinn DM, Shackelford DB, Egan DF, Mihaylova MM, Mery A, Vasquez DS, Turk BE and Shaw RJ**. AMPK phosphorylation of raptor mediates a metabolic checkpoint. *Mol Cell* 30: 214-226, 2008.
133. **Haimovitz-Friedman A, Kan CC, Ehleiter D, Persaud RS, McLoughlin M, Fuks Z and Kolesnick RN**. Ionizing radiation acts on cellular membranes to generate ceramide and initiate apoptosis. *J Exp Med* 180: 525-535, 1994.
134. **Hall EJ and Giaccia E**. *Radiabiology for the Radiologist*. Philadelphia: 2006,
135. **Halliwell B, Clement MV and Long LH**. Hydrogen peroxide in the human body. *FEBS Lett* 486: 10-13, 2000.
136. **Hammami MM and Bakheet S**. Radioiodine breast uptake in nonbreastfeeding women: clinical and scintigraphic characteristics. *J Nucl Med* 37: 26-31, 1996.

137. **Hanukoglu I, Rapoport R, Weiner L and Sklan D**. Electron leakage from the mitochondrial NADPH-adrenodoxin reductase-adrenodoxin-P450scc (cholesterol side chain cleavage) system. *Arch Biochem Biophys* 305: 489-498, 1993.
138. **Hara K, Maruki Y, Long X, Yoshino K, Oshiro N, Hidayat S, Tokunaga C, Avruch J and Yonezawa K**. Raptor, a binding partner of target of rapamycin (TOR), mediates TOR action. *Cell* 110: 177-189, 2002.
139. **Harada H, Itasaka S, Kizaka-Kondoh S, Shibuya K, Morinibu A, Shinomiya K and Hiraoka M**. The Akt/mTOR pathway assures the synthesis of HIF-1alpha protein in a glucose- and reoxygenation-dependent manner in irradiated tumors. *J Biol Chem* 284: 5332-5342, 2009.
140. **Harada H, Itasaka S, Zhu Y, Zeng L, Xie X, Morinibu A, Shinomiya K and Hiraoka M**. Treatment regimen determines whether an HIF-1 inhibitor enhances or inhibits the effect of radiation therapy. *Br J Cancer* 100: 747-757, 2009.
141. **Harrington LS, Findlay GM and Lamb RF**. Restraining PI3K: mTOR signalling goes back to the membrane. *Trends Biochem Sci* 30: 35-42, 2005.
142. **Harvey CB and Williams GR**. Mechanism of thyroid hormone action. *Thyroid* 12: 441-446, 2002.
143. **Hattori K, Heissig B, Wu Y, Dias S, Tejada R, Ferris B, Hicklin DJ, Zhu Z, Bohlen P, Witte L, Hendrikx J, Hackett NR, Crystal RG, Moore MA, Werb Z, Lyden D and Rafii S**. Placental growth factor reconstitutes hematopoiesis by recruiting VEGFR1(+) stem cells from bone-marrow microenvironment. *Nat Med* 8: 841-849, 2002.
144. **Hayashi Y, Lagarde F, Tsuda N, Funamoto S, Preston DL, Koyama K, Mabuchi K, Ron E, Kodama K and Tokuoka S**. Papillary microcarcinoma of the thyroid among atomic bomb survivors: tumor characteristics and radiation risk. *Cancer* 116: 1646-1655, 2010.
145. **He Z, Opland DM, Way KJ, Ueki K, Bodyak N, Kang PM, Izumo S, Kulkarni RN, Wang B, Liao R, Kahn CR and King GL**. Regulation of vascular endothelial growth factor expression and vascularization in the myocardium by insulin receptor and PI3K/Akt pathways in insulin resistance and ischemia. *Arterioscler Thromb Vasc Biol* 26: 787-793, 2006.
146. **Heath JW, Lowe J, Stevens A and Young B**. *Atlas d'histologie fonctionelle de Weather*. 2008,
147. **Hingorani M, Spitzweg C, Vassaux G, Newbold K, Melcher A, Pandha H, Vile R and Harrington K**. The biology of the sodium iodide symporter and its potential for targeted gene delivery. *Curr Cancer Drug Targets* 10: 242-267, 2010.
148. **Hiroi Y, Kim HH, Ying H, Furuya F, Huang Z, Simoncini T, Noma K, Ueki K, Nguyen NH, Scanlan TS, Moskowitz MA, Cheng SY and Liao JK**. Rapid nongenomic actions of thyroid hormone. *Proc Natl Acad Sci U S A* 103: 14104-14109, 2006.
149. **Hofer T, Badouard C, Bajak E, Ravanat JL, Mattsson A and Cotgreave IA**. Hydrogen peroxide causes greater oxidation in cellular RNA than in DNA. *Biol Chem* 386: 333-337, 2005.
150. **Holmstrom KM and Finkel T**. Cellular mechanisms and physiological consequences of redox-dependent signalling. *Nat Rev Mol Cell Biol* 15: 411-421, 2014.
151. **Hosokawa N, Hara T, Kaizuka T, Kishi C, Takamura A, Miura Y, Iemura S, Natsume T, Takehana K, Yamada N, Guan JL, Oshiro N and Mizushima N**. Nutrient-

dependent mTORC1 association with the ULK1-Atg13-FIP200 complex required for autophagy. *Mol Biol Cell* 20: 1981-1991, 2009.

152. **Houck KA, Ferrara N, Winer J, Cachianes G, Li B and Leung DW**. The vascular endothelial growth factor family: identification of a fourth molecular species and characterization of alternative splicing of RNA. *Mol Endocrinol* 5: 1806-1814, 1991.
153. **Hovinga KE, Stalpers LJ, van BC, Donker M, Verhoeff JJ, Rodermond HM, Bosch DA and van Furth WR**. Radiation-enhanced vascular endothelial growth factor (VEGF) secretion in glioblastoma multiforme cell lines--a clue to radioresistance? *J Neurooncol* 74: 99-103, 2005.
154. **Huang LE, Arany Z, Livingston DM and Bunn HF**. Activation of hypoxia-inducible transcription factor depends primarily upon redox-sensitive stabilization of its alpha subunit. *J Biol Chem* 271: 32253-32259, 1996.
155. **Huang LE, Gu J, Schau M and Bunn HF**. Regulation of hypoxia-inducible factor 1alpha is mediated by an O2-dependent degradation domain via the ubiquitin-proteasome pathway. *Proc Natl Acad Sci U S A* 95: 7987-7992, 1998.
156. **Huez I, Creancier L, Audigier S, Gensac MC, Prats AC and Prats H**. Two independent internal ribosome entry sites are involved in translation initiation of vascular endothelial growth factor mRNA. *Mol Cell Biol* 18: 6178-6190, 1998.
157. **Ignarro LJ, Buga GM, Wood KS, Byrns RE and Chaudhuri G**. Endothelium-derived relaxing factor produced and released from artery and vein is nitric oxide. *Proc Natl Acad Sci U S A* 84: 9265-9269, 1987.
158. **Ikeda E, Achen MG, Breier G and Risau W**. Hypoxia-induced transcriptional activation and increased mRNA stability of vascular endothelial growth factor in C6 glioma cells. *J Biol Chem* 270: 19761-19766, 1995.
159. **Imaizumi M, Ohishi W, Nakashima E, Sera N, Neriishi K, Yamada M, Tatsukawa Y, Takahashi I, Fujiwara S, Sugino K, Ando T, Usa T, Kawakami A, Akahoshi M and Hida A**. Association of radiation dose with prevalence of thyroid nodules among atomic bomb survivors exposed in childhood (2007-2011). *JAMA Intern Med* 175: 228-236, 2015.
160. **Incerpi S, Luly P, De VP and Farias RN**. Short-term effects of thyroid hormones on the Na/H antiport in L-6 myoblasts: high molecular specificity for 3,3',5-triiodo-L-thyronine. *Endocrinology* 140: 683-689, 1999.
161. **Inoki K, Ouyang H, Zhu T, Lindvall C, Wang Y, Zhang X, Yang Q, Bennett C, Harada Y, Stankunas K, Wang CY, He X, MacDougald OA, You M, Williams BO and Guan KL**. TSC2 integrates Wnt and energy signals via a coordinated phosphorylation by AMPK and GSK3 to regulate cell growth. *Cell* 126: 955-968, 2006.
162. **Inskip PD, Robison LL, Stovall M, Smith SA, Hammond S, Mertens AC, Whitton JA, Diller L, Kenney L, Donaldson SS, Meadows AT and Neglia JP**. Radiation dose and breast cancer risk in the childhood cancer survivor study. *J Clin Oncol* 27: 3901-3907, 2009.
163. **International Atomic Energy Agency**. *Radiation biology: a handbook for teachers and students*. Vienna: IAEA, 2010,
164. **International Council For Control of Iodine Deficiency Disorders**. Progress against widespread iodine deficiency in Europe. *IDD newsletter* 29: 2008.

165. **Iodine Global Network**. Global Scorecard 2014: Number of iodine deficient countries more than halved in past decade. *IDD newsletter* 2015.
166. **Iosco C, Cosentino C, Sirna L, Romano R, Cursano S, Mongia A, Pompeo G, di BJ, Ceccarelli C, Tallini G and Rhoden KJ**. Anoctamin 1 is apically expressed on thyroid follicular cells and contributes to ATP- and calcium-activated iodide efflux. *Cell Physiol Biochem* 34: 966-980, 2014.
167. **Isaacs JS, Jung YJ, Mimnaugh EG, Martinez A, Cuttitta F and Neckers LM**. Hsp90 regulates a von Hippel Lindau-independent hypoxia-inducible factor-1 alpha-degradative pathway. *J Biol Chem* 277: 29936-29944, 2002.
168. **Ischiropoulos H and al-Mehdi AB**. Peroxynitrite-mediated oxidative protein modifications. *FEBS Lett* 364: 279-282, 1995.
169. **Islam MS, Matsumoto M, Hidaka R, Miyoshi N and Yasuda N**. Expression of NOS and VEGF in feline mammary tumours and their correlation with angiogenesis. *Vet J* 192: 338-344, 2012.
170. **Jaakkola P, Mole DR, Tian YM, Wilson MI, Gielbert J, Gaskell SJ, von KA, Hebestreit HF, Mukherji M, Schofield CJ, Maxwell PH, Pugh CW and Ratcliffe PJ**. Targeting of HIF-alpha to the von Hippel-Lindau ubiquitylation complex by O2-regulated prolyl hydroxylation. *Science* 292: 468-472, 2001.
171. **Jacinto E, Facchinetti V, Liu D, Soto N, Wei S, Jung SY, Huang Q, Qin J and Su B**. SIN1/MIP1 maintains rictor-mTOR complex integrity and regulates Akt phosphorylation and substrate specificity. *Cell* 127: 125-137, 2006.
172. **Jane EP, Premkumar DR and Pollack IF**. Coadministration of sorafenib with rottlerin potently inhibits cell proliferation and migration in human malignant glioma cells. *J Pharmacol Exp Ther* 319: 1070-1080, 2006.
173. **Jang GH, Ha JH, Huh TL and Lee YM**. Effect of proton beam on blood vessel formation in early developing zebrafish (Danio rerio) embryos. *Arch Pharm Res* 31: 779-785, 2008.
174. **Jeong YJ, Cho HJ, Magae J, Lee IK, Park KG and Chang YC**. Ascofuranone suppresses EGF-induced HIF-1alpha protein synthesis by inhibition of the Akt/mTOR/p70S6K pathway in MDA-MB-231 breast cancer cells. *Toxicol Appl Pharmacol* 273: 542-550, 2013.
175. **Jhiang SM, Cho JY, Ryu KY, DeYoung BR, Smanik PA, McGaughy VR, Fischer AH and Mazzaferri EL**. An immunohistochemical study of Na+/I- symporter in human thyroid tissues and salivary gland tissues. *Endocrinology* 139: 4416-4419, 1998.
176. **Jiang H, Tian Y, Yan W, Kong Y, Wang H, Wang A, Dou J, Liang P and Mu Y**. The Prevalence of Thyroid Nodules and an Analysis of Related Lifestyle Factors in Beijing Communities. *Int J Environ Res Public Health* 13: 442, 2016.
177. **Jiang ZY, He Z, King BL, Kuroki T, Opland DM, Suzuma K, Suzuma I, Ueki K, Kulkarni RN, Kahn CR and King GL**. Characterization of multiple signaling pathways of insulin in the regulation of vascular endothelial growth factor expression in vascular cells and angiogenesis. *J Biol Chem* 278: 31964-31971, 2003.
178. Johnston, A. E. Trace elements in soil: status and management. Essential trace elements for plants, animals and humans, NJF Seminars. 2005.

Ref Type: Conference Proceeding

179. **Jones KR, Elmore LW, Jackson-Cook C, Demasters G, Povirk LF, Holt SE and Gewirtz DA**. p53-Dependent accelerated senescence induced by ionizing radiation in breast tumour cells. *Int J Radiat Biol* 81: 445-458, 2005.
180. **Josefsson M, Evilevitch L, Westrom B, Grunditz T and Ekblad E**. Sodium-iodide symporter mediates iodide secretion in rat gastric mucosa in vitro. *Exp Biol Med (Maywood)* 231: 277-281, 2006.
181. **Josefsson M, Grunditz T, Ohlsson T and Ekblad E**. Sodium/iodide-symporter: distribution in different mammals and role in entero-thyroid circulation of iodide. *Acta Physiol Scand* 175: 129-137, 2002.
182. **Kaizuka T, Hara T, Oshiro N, Kikkawa U, Yonezawa K, Takehana K, Iemura S, Natsume T and Mizushima N**. Tti1 and Tel2 are critical factors in mammalian target of rapamycin complex assembly. *J Biol Chem* 285: 20109-20116, 2010.
183. **Kaminsky SM, Levy O, Salvador C, Dai G and Carrasco N**. Na(+)-I- symport activity is present in membrane vesicles from thyrotropin-deprived non-I(-)-transporting cultured thyroid cells. *Proc Natl Acad Sci U S A* 91: 3789-3793, 1994.
184. **KandemIr EG, Yonem A and NarIn Y**. Gastric carcinoma and thyroid status. *J Int Med Res* 33: 222-227, 2005.
185. **Kanofsky JR**. Singlet oxygen production by lactoperoxidase. *J Biol Chem* 258: 5991-5993, 1983.
186. **Kanofsky JR and Axelrod B**. Singlet oxygen production by soybean lipoxygenase isozymes. *J Biol Chem* 261: 1099-1104, 1986.
187. **Kaplan RN, Riba RD, Zacharoulis S, Bramley AH, Vincent L, Costa C, MacDonald DD, Jin DK, Shido K, Kerns SA, Zhu Z, Hicklin D, Wu Y, Port JL, Altorki N, Port ER, Ruggero D, Shmelkov SV, Jensen KK, Rafii S and Lyden D**. VEGFR1-positive haematopoietic bone marrow progenitors initiate the pre-metastatic niche. *Nature* 438: 820-827, 2005.
188. **Kawamura H, Li X, Goishi K, van Meeteren LA, Jakobsson L, Cebe-Suarez S, Shimizu A, Edholm D, Ballmer-Hofer K, Kjellen L, Klagsbrun M and Claesson-Welsh L**. Neuropilin-1 in regulation of VEGF-induced activation of p38MAPK and endothelial cell organization. *Blood* 112: 3638-3649, 2008.
189. **Kawamura H, Li X, Harper SJ, Bates DO and Claesson-Welsh L**. Vascular endothelial growth factor (VEGF)-A165b is a weak in vitro agonist for VEGF receptor-2 due to lack of coreceptor binding and deficient regulation of kinase activity. *Cancer Res* 68: 4683-4692, 2008.
190. **Ke Q and Costa M**. Hypoxia-inducible factor-1 (HIF-1). *Mol Pharmacol* 70: 1469-1480, 2006.
191. **Kessler JH**. The effect of supraphysiologic levels of iodine on patients with cyclic mastalgia. *Breast J* 10: 328-336, 2004.
192. **Khatri DK and Juvekar AR**. Kinetics of Inhibition of Monoamine Oxidase Using Curcumin and Ellagic Acid. *Pharmacogn Mag* 12: S116-S120, 2016.
193. **Kikuchi A, Takeda A, Onodera H, Kimpara T, Hisanaga K, Sato N, Nunomura A, Castellani RJ, Perry G, Smith MA and Itoyama Y**. Systemic increase of oxidative nucleic acid damage in Parkinson's disease and multiple system atrophy. *Neurobiol Dis* 9: 244-248, 2002.

194. **Kil WJ, Tofilon PJ and Camphausen K**. Post-radiation increase in VEGF enhances glioma cell motility in vitro. *Radiat Oncol* 7: 25, 2012.
195. **Kilbane MT, Ajjan RA, Weetman AP, Dwyer R, McDermott EW, O'Higgins NJ and Smyth PP**. Tissue iodine content and serum-mediated 125I uptake-blocking activity in breast cancer. *J Clin Endocrinol Metab* 85: 1245-1250, 2000.
196. **Kim JE and Chen J**. regulation of peroxisome proliferator-activated receptor-gamma activity by mammalian target of rapamycin and amino acids in adipogenesis. *Diabetes* 53: 2748-2756, 2004.
197. **Kim KW, Moretti L, Mitchell LR, Jung DK and Lu B**. Endoplasmic reticulum stress mediates radiation-induced autophagy by perk-eIF2alpha in caspase-3/7-deficient cells. *Oncogene* 29: 3241-3251, 2010.
198. **Kim KY, Rhim T, Choi I and Kim SS**. N-acetylcysteine induces cell cycle arrest in hepatic stellate cells through its reducing activity. *J Biol Chem* 276: 40591-40598, 2001.
199. **Kim RK, Suh Y, Cui YH, Hwang E, Lim EJ, Yoo KC, Lee GH, Yi JM, Kang SG and Lee SJ**. Fractionated radiation-induced nitric oxide promotes expansion of glioma stem-like cells. *Cancer Sci* 104: 1172-1177, 2013.
200. **Kimura H and Esumi H**. Reciprocal regulation between nitric oxide and vascular endothelial growth factor in angiogenesis. *Acta Biochim Pol* 50: 49-59, 2003.
201. **Kitsukawa T, Shimono A, Kawakami A, Kondoh H and Fujisawa H**. Overexpression of a membrane protein, neuropilin, in chimeric mice causes anomalies in the cardiovascular system, nervous system and limbs. *Development* 121: 4309-4318, 1995.
202. **Klebanoff SJ**. Myeloperoxidase: contribution to the microbicidal activity of intact leukocytes. *Science* 169: 1095-1097, 1970.
203. **Kobata R, Tsukahara H, Ohshima Y, Ohta N, Tokuriki S, Tamura S and Mayumi M**. High levels of growth factors in human breast milk. *Early Hum Dev* 84: 67-69, 2008.
204. **Kogai T and Brent GA**. The sodium iodide symporter (NIS): regulation and approaches to targeting for cancer therapeutics. *Pharmacol Ther* 135: 355-370, 2012.
205. **Kogai T, Sajid-Crockett S, Newmarch LS, Liu YY and Brent GA**. Phosphoinositide-3-kinase inhibition induces sodium/iodide symporter expression in rat thyroid cells and human papillary thyroid cancer cells. *J Endocrinol* 199: 243-252, 2008.
206. **Komatsu D, Kato M, Nakayama J, Miyagawa S and Kamata T**. NADPH oxidase 1 plays a critical mediating role in oncogenic Ras-induced vascular endothelial growth factor expression. *Oncogene* 27: 4724-4732, 2008.
207. **Kong D, Park EJ, Stephen AG, Calvani M, Cardellina JH, Monks A, Fisher RJ, Shoemaker RH and Melillo G**. Echinomycin, a small-molecule inhibitor of hypoxia-inducible factor-1 DNA-binding activity. *Cancer Res* 65: 9047-9055, 2005.
208. **Kontos HA, Wei EP, Ellis EF, Jenkins LW, Povlishock JT, Rowe GT and Hess ML**. Appearance of superoxide anion radical in cerebral extracellular space during increased prostaglandin synthesis in cats. *Circ Res* 57: 142-151, 1985.
209. **Krouse TB, Eskin BA and Mobini J**. Age-related changes resembling fibrocystic disease in iodine-blocked rat breasts. *Arch Pathol Lab Med* 103: 631-634, 1979.

210. **Krueger SA, Joiner MC, Weinfeld M, Piasentin E and Marples B**. Role of apoptosis in low-dose hyper-radiosensitivity. *Radiat Res* 167: 260-267, 2007.
211. **Kuo JH, Chabot JA and Lee JA**. Breast cancer in thyroid cancer survivors: An analysis of the Surveillance, Epidemiology, and End Results-9 database. *Surgery* 159: 23-29, 2016.
212. **Kupper FC, Carpenter LJ, Leblanc C, Toyama C, Uchida Y, Maskrey BH, Robinson J, Verhaeghe EF, Malin G, Luther GW, III, Kroneck PM, Kloareg B, Meyer-Klaucke W, Muramatsu Y, Megson IL, Potin P and Feiters MC**. In vivo speciation studies and antioxidant properties of bromine in Laminaria digitata reinforce the significance of iodine accumulation for kelps. *J Exp Bot* 64: 2653-2664, 2013.
213. **Kupper FC, Carpenter LJ, McFiggans GB, Palmer CJ, Waite TJ, Boneberg EM, Woitsch S, Weiller M, Abela R, Grolimund D, Potin P, Butler A, Luther GW, III, Kroneck PM, Meyer-Klaucke W and Feiters MC**. Iodide accumulation provides kelp with an inorganic antioxidant impacting atmospheric chemistry. *Proc Natl Acad Sci U S A* 105: 6954-6958, 2008.
214. **Kuppusamy P and Zweier JL**. Characterization of free radical generation by xanthine oxidase. Evidence for hydroxyl radical generation. *J Biol Chem* 264: 9880-9884, 1989.
215. **Kuroda J, Nakagawa K, Yamasaki T, Nakamura K, Takeya R, Kuribayashi F, Imajoh-Ohmi S, Igarashi K, Shibata Y, Sueishi K and Sumimoto H**. The superoxide-producing NAD(P)H oxidase Nox4 in the nucleus of human vascular endothelial cells. *Genes Cells* 10: 1139-1151, 2005.
216. **La Perle KM, Kim DC, Hall NC, Bobbey A, Shen DH, Nagy RS, Wakely PE, Jr., Lehman A, Jarjoura D and Jhiang SM**. Modulation of sodium/iodide symporter expression in the salivary gland. *Thyroid* 23: 1029-1036, 2013.
217. **Lacza Z, Pankotai E and Busija DW**. Mitochondrial nitric oxide synthase: current concepts and controversies. *Front Biosci (Landmark Ed)* 14: 4436-4443, 2009.
218. **Lall R, Ganapathy S, Yang M, Xiao S, Xu T, Su H, Shadfan M, Asara JM, Ha CS, Ben-Sahra I, Manning BD, Little JB and Yuan ZM**. Low-dose radiation exposure induces a HIF-1-mediated adaptive and protective metabolic response. *Cell Death Differ* 21: 836-844, 2014.
219. **Lambert AJ, Buckingham JA, Boysen HM and Brand MD**. Diphenyleneiodonium acutely inhibits reactive oxygen species production by mitochondrial complex I during reverse, but not forward electron transport. *Biochim Biophys Acta* 1777: 397-403, 2008.
220. **Laplante M and Sabatini DM**. mTOR signaling in growth control and disease. *Cell* 149: 274-293, 2012.
221. **Laughner E, Taghavi P, Chiles K, Mahon PC and Semenza GL**. HER2 (neu) signaling increases the rate of hypoxia-inducible factor 1alpha (HIF-1alpha) synthesis: novel mechanism for HIF-1-mediated vascular endothelial growth factor expression. *Mol Cell Biol* 21: 3995-4004, 2001.
222. **Leach JK, Black SM, Schmidt-Ullrich RK and Mikkelsen RB**. Activation of constitutive nitric-oxide synthase activity is an early signaling event induced by ionizing radiation. *J Biol Chem* 277: 15400-15406, 2002.

223. **Lee SR, Kwon KS, Kim SR and Rhee SG**. Reversible inactivation of protein-tyrosine phosphatase 1B in A431 cells stimulated with epidermal growth factor. *J Biol Chem* 273: 15366-15372, 1998.
224. **Lei J, Mariash CN, Bhargava M, Wattenberg EV and Ingbar DH**. T3 increases Na-K-ATPase activity via a MAPK/ERK1/2-dependent pathway in rat adult alveolar epithelial cells. *Am J Physiol Lung Cell Mol Physiol* 294: L749-L754, 2008.
225. **Lemmon MA and Schlessinger J**. Cell signaling by receptor tyrosine kinases. *Cell* 141: 1117-1134, 2010.
226. **Leonard BE and Lucas AC**. LDR brachytherapy: can low dose rate hypersensitivity from the "inverse" dose rate effect cause excessive cell killing to peripherial connective tissues and organs? *Br J Radiol* 82: 131-139, 2009.
227. **Leoni SG, Kimura ET, Santisteban P and De l, V**. Regulation of thyroid oxidative state by thioredoxin reductase has a crucial role in thyroid responses to iodide excess. *Mol Endocrinol* 25: 1924-1935, 2011.
228. **Lesslie DP, Summy JM, Parikh NU, Fan F, Trevino JG, Sawyer TK, Metcalf CA, Shakespeare WC, Hicklin DJ, Ellis LM and Gallick GE**. Vascular endothelial growth factor receptor-1 mediates migration of human colorectal carcinoma cells by activation of Src family kinases. *Br J Cancer* 94: 1710-1717, 2006.
229. **Leung AM, Braverman LE and Pearce EN**. History of U.S. iodine fortification and supplementation. *Nutrients* 4: 1740-1746, 2012.
230. **Li H, Ganta S and Fong P**. Altered ion transport by thyroid epithelia from CFTR(-/-) pigs suggests mechanisms for hypothyroidism in cystic fibrosis. *Exp Physiol* 95: 1132-1144, 2010.
231. **Li Q, Fu GB, Zheng JT, He J, Niu XB, Chen QD, Yin Y, Qian X, Xu Q, Wang M, Sun AF, Shu Y, Rui H, Liu LZ and Jiang BH**. NADPH oxidase subunit p22(phox)-mediated reactive oxygen species contribute to angiogenesis and tumor growth through AKT and ERK1/2 signaling pathways in prostate cancer. *Biochim Biophys Acta* 1833: 3375-3385, 2013.
232. **Liang Y and Hyder SM**. Proliferation of endothelial and tumor epithelial cells by progestin-induced vascular endothelial growth factor from human breast cancer cells: paracrine and autocrine effects. *Endocrinology* 146: 3632-3641, 2005.
233. **Limon JJ and Fruman DA**. Akt and mTOR in B Cell Activation and Differentiation. *Front Immunol* 3: 228, 2012.
234. **Lin HY, Sun M, Tang HY, Lin C, Luidens MK, Mousa SA, Incerpi S, Drusano GL, Davis FB and Davis PJ**. L-Thyroxine vs. 3,5,3'-triiodo-L-thyronine and cell proliferation: activation of mitogen-activated protein kinase and phosphatidylinositol 3-kinase. *Am J Physiol Cell Physiol* 296: C980-C991, 2009.
235. **Lin HY, Zhang S, West BL, Tang HY, Passaretti T, Davis FB and Davis PJ**. Identification of the putative MAP kinase docking site in the thyroid hormone receptor-beta1 DNA-binding domain: functional consequences of mutations at the docking site. *Biochemistry* 42: 7571-7579, 2003.
236. **Little MP, Wakeford R and Kendall GM**. Updated estimates of the proportion of childhood leukaemia incidence in Great Britain that may be caused by natural background ionising radiation. *J Radiol Prot* 29: 467-482, 2009.

237. **Liu L, Cash TP, Jones RG, Keith B, Thompson CB and Simon MC**. Hypoxia-induced energy stress regulates mRNA translation and cell growth. *Mol Cell* 21: 521-531, 2006.
238. **Liu LZ, Hu XW, Xia C, He J, Zhou Q, Shi X, Fang J and Jiang BH**. Reactive oxygen species regulate epidermal growth factor-induced vascular endothelial growth factor and hypoxia-inducible factor-1alpha expression through activation of AKT and P70S6K1 in human ovarian cancer cells. *Free Radic Biol Med* 41: 1521-1533, 2006.
239. **Lope V, Pollan M, Perez-Gomez B, Aragones N, Ramis R, Gomez-Barroso D and Lopez-Abente G**. Municipal mortality due to thyroid cancer in Spain. *BMC Public Health* 6: 302, 2006.
240. **Lopez-Rivera E, Jayaraman P, Parikh F, Davies MA, Ekmekcioglu S, Izadmehr S, Milton DR, Chipuk JE, Grimm EA, Estrada Y, Aguirre-Ghiso J and Sikora AG**. Inducible nitric oxide synthase drives mTOR pathway activation and proliferation of human melanoma by reversible nitrosylation of TSC2. *Cancer Res* 74: 1067-1078, 2014.
241. **Lund E and Bonaa KH**. Reduced breast cancer mortality among fishermen's wives in Norway. *Cancer Causes Control* 4: 283-287, 1993.
242. **Lundell M, Mattsson A, Karlsson P, Holmberg E, Gustafsson A and Holm LE**. Breast cancer risk after radiotherapy in infancy: a pooled analysis of two Swedish cohorts of 17,202 infants. *Radiat Res* 151: 626-632, 1999.
243. **Ma L, Chen Z, Erdjument-Bromage H, Tempst P and Pandolfi PP**. Phosphorylation and functional inactivation of TSC2 by Erk implications for tuberous sclerosis and cancer pathogenesis. *Cell* 121: 179-193, 2005.
244. **Ma Y, Freitag P, Zhou J, Brune B, Frede S and Fandrey J**. Thyroid hormone induces erythropoietin gene expression through augmented accumulation of hypoxia-inducible factor-1. *Am J Physiol Regul Integr Comp Physiol* 287: R600-R607, 2004.
245. **Maenhaut C, Detours V, Dom G, Handkiewicz-Junak D, Oczko-Wojciechowska M and Jarzab B**. Gene expression profiles for radiation-induced thyroid cancer. *Clin Oncol (R Coll Radiol)* 23: 282-288, 2011.
246. **Mahon PC, Hirota K and Semenza GL**. FIH-1: a novel protein that interacts with HIF-1alpha and VHL to mediate repression of HIF-1 transcriptional activity. *Genes Dev* 15: 2675-2686, 2001.
247. **Malpani BL, Samuel AM and Ray S**. Differential kinetics of parotid and submandibular gland function as demonstrated by scintigraphic means and its possible implications. *Nucl Med Commun* 16: 706-709, 1995.
248. **Mamane Y, Petroulakis E, Rong L, Yoshida K, Ler LW and Sonenberg N**. eIF4E--from translation to transformation. *Oncogene* 23: 3172-3179, 2004.
249. **Mandel SJ and Mandel L**. Radioactive iodine and the salivary glands. *Thyroid* 13: 265-271, 2003.
250. **Mansfield KD, Guzy RD, Pan Y, Young RM, Cash TP, Schumacker PT and Simon MC**. Mitochondrial dysfunction resulting from loss of cytochrome c impairs cellular oxygen sensing and hypoxic HIF-alpha activation. *Cell Metab* 1: 393-399, 2005.

251. **Many MC, Denef JF and Haumont S**. Precocity of the endothelial proliferation during a course of rapid goitrogenesis. *Acta Endocrinol (Copenh)* 105: 487-491, 1984.
252. **Masoud GN and Li W**. HIF-1alpha pathway: role, regulation and intervention for cancer therapy. *Acta Pharm Sin B* 5: 378-389, 2015.
253. **Masui K, Tanaka K, Akhavan D, Babic I, Gini B, Matsutani T, Iwanami A, Liu F, Villa GR, Gu Y, Campos C, Zhu S, Yang H, Yong WH, Cloughesy TF, Mellinghoff IK, Cavenee WK, Shaw RJ and Mischel PS**. mTOR complex 2 controls glycolytic metabolism in glioblastoma through FoxO acetylation and upregulation of c-Myc. *Cell Metab* 18: 726-739, 2013.
254. **Matei D, Kelich S, Cao L, Menning N, Emerson RE, Rao J, Jeng MH and Sledge GW**. PDGF BB induces VEGF secretion in ovarian cancer. *Cancer Biol Ther* 6: 1951-1959, 2007.
255. **Mathis U, Ziemssen F and Schaeffel F**. Effects of a human VEGF antibody (Bevacizumab) on deprivation myopia and choroidal thickness in the chicken. *Exp Eye Res* 127: 161-169, 2014.
256. **Mayer C, Zhao J, Yuan X and Grummt I**. mTOR-dependent activation of the transcription factor TIF-IA links rRNA synthesis to nutrient availability. *Genes Dev* 18: 423-434, 2004.
257. **Mencalha A, Victorino VJ, Cecchini R and Panis C**. Mapping oxidative changes in breast cancer: understanding the basic to reach the clinics. *Anticancer Res* 34: 1127-1140, 2014.
258. **Metzen E, Zhou J, Jelkmann W, Fandrey J and Brune B**. Nitric oxide impairs normoxic degradation of HIF-1alpha by inhibition of prolyl hydroxylases. *Mol Biol Cell* 14: 3470-3481, 2003.
259. **Milanini-Mongiat J, Pouyssegur J and Pages G**. Identification of two Sp1 phosphorylation sites for p42/p44 mitogen-activated protein kinases: their implication in vascular endothelial growth factor gene transcription. *J Biol Chem* 277: 20631-20639, 2002.
260. **Millauer B, Wizigmann-Voos S, Schnurch H, Martinez R, Moller NP, Risau W and Ullrich A**. High affinity VEGF binding and developmental expression suggest Flk-1 as a major regulator of vasculogenesis and angiogenesis. *Cell* 72: 835-846, 1993.
261. **Miller AB, Howe GR, Sherman GJ, Lindsay JP, Yaffe MJ, Dinner PJ, Risch HA and Preston DL**. Mortality from breast cancer after irradiation during fluoroscopic examinations in patients being treated for tuberculosis. *N Engl J Med* 321: 1285-1289, 1989.
262. **Miller JK, Swanson EW and Spalding GE**. Iodine absorption, excretion, recycling, and tissue distribution in the dairy cow. *J Dairy Sci* 58: 1578-1593, 1975.
263. **Mitchell G, Pratt BE, Vini L, McCready VR and Harmer CL**. False positive 131I whole body scans in thyroid cancer. *Br J Radiol* 73: 627-635, 2000.
264. **Moeller BJ, Cao Y, Li CY and Dewhirst MW**. Radiation activates HIF-1 to regulate vascular radiosensitivity in tumors: role of reoxygenation, free radicals, and stress granules. *Cancer Cell* 5: 429-441, 2004.
265. **Moeller LC, Cao X, Dumitrescu AM, Seo H and Refetoff S**. Thyroid hormone mediated changes in gene expression can be initiated by cytosolic action of the

thyroid hormone receptor beta through the phosphatidylinositol 3-kinase pathway. *Nucl Recept Signal* 4: e020, 2006.

266. **Molitoris KH, Kazi AA and Koos RD**. Inhibition of oxygen-induced hypoxia-inducible factor-1alpha degradation unmasks estradiol induction of vascular endothelial growth factor expression in ECC-1 cancer cells in vitro. *Endocrinology* 150: 5405-5414, 2009.
267. **Montero A, Sanz X, Hernanz R, Cabrera D, Arenas M, Bayo E, Moreno F and Algara M**. Accelerated hypofractionated breast radiotherapy: FAQs (frequently asked questions) and facts. *Breast* 23: 299-309, 2014.
268. **Moon DH, Lee SJ, Park KY, Park KK, Ahn SH, Pai MS, Chang H, Lee HK and Ahn IM**. Correlation between 99mTc-pertechnetate uptakes and expressions of human sodium iodide symporter gene in breast tumor tissues. *Nucl Med Biol* 28: 829-834, 2001.
269. **Moreno-Reyes R**. Bread with iodized salt boosts iodine nutrition in Belgian children, but nonpregnant and pregnant women remain mildly deficient. *IDD newsletter* 2012.
270. **Moreno-Reyes R, Carpentier YA, Macours P, Gulbis B, Corvilain B, Glinoer D and Goldman S**. Seasons but not ethnicity influence urinary iodine concentrations in Belgian adults. *Eur J Nutr* 50: 285-290, 2011.
271. **Moreno-Reyes R, Glinoer D, Van OH and Vandevijvere S**. High prevalence of thyroid disorders in pregnant women in a mildly iodine-deficient country: a population-based study. *J Clin Endocrinol Metab* 98: 3694-3701, 2013.
272. **Moreno-Reyes R, Van OH and Vandevijvere S**. Optimization of iodine intake in Belgium. *Ann Endocrinol (Paris)* 72: 158-161, 2011.
273. **Mueller MD, Vigne JL, Pritts EA, Chao V, Dreher E and Taylor RN**. Progestins activate vascular endothelial growth factor gene transcription in endometrial adenocarcinoma cells. *Fertil Steril* 79: 386-392, 2003.
274. **Mukherjee TK, Mishra AK, Mukhopadhyay S and Hoidal JR**. High concentration of antioxidants N-acetylcysteine and mitoquinone-Q induces intercellular adhesion molecule 1 and oxidative stress by increasing intracellular glutathione. *J Immunol* 178: 1835-1844, 2007.
275. **Mukhopadhyay D, Knebelmann B, Cohen HT, Ananth S and Sukhatme VP**. The von Hippel-Lindau tumor suppressor gene product interacts with Sp1 to repress vascular endothelial growth factor promoter activity. *Mol Cell Biol* 17: 5629-5639, 1997.
276. **Munshi N, Groopman JE, Gill PS and Ganju RK**. c-Src mediates mitogenic signals and associates with cytoskeletal proteins upon vascular endothelial growth factor stimulation in Kaposi's sarcoma cells. *J Immunol* 164: 1169-1174, 2000.
277. **Murphy MP**. How mitochondria produce reactive oxygen species. *Biochem J* 417: 1-13, 2009.
278. **Murphy MP and Smith RA**. Targeting antioxidants to mitochondria by conjugation to lipophilic cations. *Annu Rev Pharmacol Toxicol* 47: 629-656, 2007.
279. **Myrden JA and Hiltz JE**. Breast cancer following multiple fluoroscopies during artificial pneumothorax treatment of pulmonary tuberculosis. *Can Med Assoc J* 100: 1032-1034, 1969.

280. **Nagataki S**. Thyroid consequences of the fukushima nuclear reactor accident. *Eur Thyroid J* 1: 148-158, 2012.
281. **Nagataki S, Shibata Y, Inoue S, Yokoyama N, Izumi M and Shimaoka K**. Thyroid diseases among atomic bomb survivors in Nagasaki. *JAMA* 272: 364-370, 1994.
282. **Nakopoulou L, Stefanaki K, Panayotopoulou E, Giannopoulou I, Athanassiadou P, Gakiopoulou-Givalou H and Louvrou A**. Expression of the vascular endothelial growth factor receptor-2/Flk-1 in breast carcinomas: correlation with proliferation. *Hum Pathol* 33: 863-870, 2002.
283. **Nasonova EA, Shmakova NL, Komova OV, Mel'nikova LA, Fadeeva TA and Krasavin EA**. [Cytogenetic effects of low dose radiation with different LET in human peripheral blood lymphocytes and possible mechanisms of their realization]. *Radiats Biol Radioecol* 46: 457-460, 2006.
284. **Neumaier T, Swenson J, Pham C, Polyzos A, Lo AT, Yang P, Dyball J, Asaithamby A, Chen DJ, Bissell MJ, Thalhammer S and Costes SV**. Evidence for formation of DNA repair centers and dose-response nonlinearity in human cells. *Proc Natl Acad Sci U S A* 109: 443-448, 2012.
285. **Newhauser WD and Zhang R**. The physics of proton therapy. *Phys Med Biol* 60: 155-209, 2015.
286. **Nicklin P, Bergman P, Zhang B, Triantafellow E, Wang H, Nyfeler B, Yang H, Hild M, Kung C, Wilson C, Myer VE, MacKeigan JP, Porter JA, Wang YK, Cantley LC, Finan PM and Murphy LO**. Bidirectional transport of amino acids regulates mTOR and autophagy. *Cell* 136: 521-534, 2009.
287. **Nicola JP, Basquin C, Portulano C, Reyna-Neyra A, Paroder M and Carrasco N**. The Na+/I- symporter mediates active iodide uptake in the intestine. *Am J Physiol Cell Physiol* 296: C654-C662, 2009.
288. **Nicola JP, Nazar M, Mascanfroni ID, Pellizas CG and Masini-Repiso AM**. NF-kappaB p65 subunit mediates lipopolysaccharide-induced Na(+)/I(-) symporter gene expression by involving functional interaction with the paired domain transcription factor Pax8. *Mol Endocrinol* 24: 1846-1862, 2010.
289. **Nilsson M, Bjorkman U, Ekholm R and Ericson LE**. Iodide transport in primary cultured thyroid follicle cells: evidence of a TSH-regulated channel mediating iodide efflux selectively across the apical domain of the plasma membrane. *Eur J Cell Biol* 52: 270-281, 1990.
290. **Nisimoto Y, Diebold BA, Cosentino-Gomes D and Lambeth JD**. Nox4: a hydrogen peroxide-generating oxygen sensor. *Biochemistry* 53: 5111-5120, 2014.
291. **Niu G, Wright KL, Huang M, Song L, Haura E, Turkson J, Zhang S, Wang T, Sinibaldi D, Coppola D, Heller R, Ellis LM, Karras J, Bromberg J, Pardoll D, Jove R and Yu H**. Constitutive Stat3 activity up-regulates VEGF expression and tumor angiogenesis. *Oncogene* 21: 2000-2008, 2002.
292. **Nowosielska EM, Wrembel-Wargocka J, Cheda A, Lisiak E and Janiak MK**. Enhanced cytotoxic activity of macrophages and suppressed tumor metastases in mice irradiated with low doses of X- rays. *J Radiat Res* 47: 229-236, 2006.
293. **Nozaki M, Sakurai E, Raisler BJ, Baffi JZ, Witta J, Ogura Y, Brekken RA, Sage EH, Ambati BK and Ambati J**. Loss of SPARC-mediated VEGFR-1 suppression after

injury reveals a novel antiangiogenic activity of VEGF-A. *J Clin Invest* 116: 422-429, 2006.

294. **Nozue M, Isaka N and Fukao K**. Over-expression of vascular endothelial growth factor after preoperative radiation therapy for rectal cancer. *Oncol Rep* 8: 1247-1249, 2001.
295. **Nunez-Anita RE, Arroyo-Helguera O, Cajero-Juarez M, Lopez-Bojorquez L and Aceves C**. A complex between 6-iodolactone and the peroxisome proliferator-activated receptor type gamma may mediate the antineoplastic effect of iodine in mammary cancer. *Prostaglandins Other Lipid Mediat* 89: 34-42, 2009.
296. **Nyska A, Lomnitski L, Maronpot R, Moomaw C, Brodsky B, Sintov A and Wormser U**. Effects of iodine on inducible nitric oxide synthase and cyclooxygenase-2 expression in sulfur mustard-induced skin. *Arch Toxicol* 74: 768-774, 2001.
297. **Ohmori M, Endo T, Harii N and Onaya T**. A novel thyroid transcription factor is essential for thyrotropin-induced up-regulation of Na+/I- symporter gene expression. *Mol Endocrinol* 12: 727-736, 1998.
298. **Ohno M, Zannini M, Levy O, Carrasco N and di LR**. The paired-domain transcription factor Pax8 binds to the upstream enhancer of the rat sodium/iodide symporter gene and participates in both thyroid-specific and cyclic-AMP-dependent transcription. *Mol Cell Biol* 19: 2051-2060, 1999.
299. **Okere PC, Olusina DB, Shamim SA, Shandra V, Tushar M, Sellam K and Bal C**. Pattern of second primary malignancies in thyroid cancer patients. *Niger J Clin Pract* 16: 96-99, 2013.
300. **Okuno Y, Nakamura-Ishizu A, Otsu K, Suda T and Kubota Y**. Pathological neoangiogenesis depends on oxidative stress regulation by ATM. *Nat Med* 18: 1208-1216, 2012.
301. **Onyango AN**. Endogenous Generation of Singlet Oxygen and Ozone in Human and Animal Tissues: Mechanisms, Biological Significance, and Influence of Dietary Components. *Oxid Med Cell Longev* 2016: 2398573, 2016.
302. **Otulakowski G and O'Brodovich H**. Thyroid hormone and Na+-K+-ATPase: more than simple transcription. *Am J Physiol Lung Cell Mol Physiol* 292: L4-L5, 2007.
303. **Ozgurtas T, Aydin I, Turan O, Koc E, Hirfanoglu IM, Acikel CH, Akyol M and Erbil MK**. Vascular endothelial growth factor, basic fibroblast growth factor, insulin-like growth factor-I and platelet-derived growth factor levels in human milk of mothers with term and preterm neonates. *Cytokine* 50: 192-194, 2010.
304. **Pages G and Pouyssegur J**. Transcriptional regulation of the Vascular Endothelial Growth Factor gene--a concert of activating factors. *Cardiovasc Res* 65: 564-573, 2005.
305. **Paris F, Fuks Z, Kang A, Capodieci P, Juan G, Ehleiter D, Haimovitz-Friedman A, Cordon-Cardo C and Kolesnick R**. Endothelial apoptosis as the primary lesion initiating intestinal radiation damage in mice. *Science* 293: 293-297, 2001.
306. **Park CM, Park MJ, Kwak HJ, Lee HC, Kim MS, Lee SH, Park IC, Rhee CH and Hong SI**. Ionizing radiation enhances matrix metalloproteinase-2 secretion and invasion of glioma cells through Src/epidermal growth factor receptor-mediated p38/Akt and phosphatidylinositol 3-kinase/Akt signaling pathways. *Cancer Res* 66: 8511-8519, 2006.

307. **Patrick L**. Iodine: deficiency and therapeutic considerations. *Altern Med Rev* 13: 116-127, 2008.
308. **Pearce EN, Andersson M and Zimmermann MB**. Global iodine nutrition: Where do we stand in 2013? *Thyroid* 23: 523-528, 2013.
309. **Pedersén M , Collén J, brahamson J and kdahl A**. Production of halocarbons from seaweeds: an oxidative stress reaction? *Sci Mar* 60: 257-263, 1996.
310. **Perez-Santonja JJ, Campos-Mollo E, Lledo-Riquelme M, Javaloy J and Alio JL**. Inhibition of corneal neovascularization by topical bevacizumab (Anti-VEGF) and Sunitinib (Anti-VEGF and Anti-PDGF) in an animal model. *Am J Ophthalmol* 150: 519-528, 2010.
311. **Perron B, Rodriguez AM, Leblanc G and Pourcher T**. Cloning of the mouse sodium iodide symporter and its expression in the mammary gland and other tissues. *J Endocrinol* 170: 185-196, 2001.
312. **Pesce L, Bizhanova A, Caraballo JC, Westphal W, Butti ML, Comellas A and Kopp P**. TSH regulates pendrin membrane abundance and enhances iodide efflux in thyroid cells. *Endocrinology* 153: 512-521, 2012.
313. **Peterson TR, Laplante M, Thoreen CC, Sancak Y, Kang SA, Kuehl WM, Gray NS and Sabatini DM**. DEPTOR is an mTOR inhibitor frequently overexpressed in multiple myeloma cells and required for their survival. *Cell* 137: 873-886, 2009.
314. **Peterson TR, Sengupta SS, Harris TE, Carmack AE, Kang SA, Balderas E, Guertin DA, Madden KL, Carpenter AE, Finck BN and Sabatini DM**. mTOR complex 1 regulates lipin 1 localization to control the SREBP pathway. *Cell* 146: 408-420, 2011.
315. **Phaniendra A, Jestadi DB and Periyasamy L**. Free radicals: properties, sources, targets, and their implication in various diseases. *Indian J Clin Biochem* 30: 11-26, 2015.
316. **Pisani P, Parkin DM, Bray F and Ferlay J**. Estimates of the worldwide mortality from 25 cancers in 1990. *Int J Cancer* 83: 18-29, 1999.
317. **Plataniotis G**. Hypofractionated radiotherapy in the treatment of early breast cancer. *World J Radiol* 2: 197-202, 2010.
318. Pocket Dentistery. Head and Neck Structures. 2015.

Ref Type: Audiovisual Material

319. **Poncin S, Colin IM and Gerard AC**. Minimal oxidative load: a prerequisite for thyroid cell function. *J Endocrinol* 201: 161-167, 2009.
320. **Poncin S, Gerard AC, Boucquey M, Senou M, Calderon PB, Knoops B, Lengele B, Many MC and Colin IM**. Oxidative stress in the thyroid gland: from harmlessness to hazard depending on the iodine content. *Endocrinology* 149: 424-433, 2008.
321. **Poncin S, Van ES, Humblet K, Colin IM and Gerard AC**. Oxidative stress: a required condition for thyroid cell proliferation. *Am J Pathol* 176: 1355-1363, 2010.
322. **Portulano C, Paroder-Belenitsky M and Carrasco N**. The Na+/I- symporter (NIS): mechanism and medical impact. *Endocr Rev* 35: 106-149, 2014.
323. **Prasad S, Gupta SC and Tyagi AK**. Reactive oxygen species (ROS) and cancer: Role of antioxidative nutraceuticals. *Cancer Lett* 2016.
324. **Preston DL, Kitahara CM, Freedman DM, Sigurdson AJ, Simon SL, Little MP, Cahoon EK, Rajaraman P, Miller JS, Alexander BH, Doody MM and Linet MS**. Breast cancer risk and protracted low-to-moderate dose occupational radiation

exposure in the US Radiologic Technologists Cohort, 1983-2008. *Br J Cancer* 115: 1105-1112, 2016.

325. **Price DJ, Miralem T, Jiang S, Steinberg R and Avraham H**. Role of vascular endothelial growth factor in the stimulation of cellular invasion and signaling of breast cancer cells. *Cell Growth Differ* 12: 129-135, 2001.
326. **Prysyazhnyuk AY, Bazyka DA, Romanenko AY, Gudzenko NA, Fuzik MM, Trotsyuk NK, Fedorenko ZP, Gulak LO, Slipenyuk KM, Babkina NG, Khukhrianska OM, Goroh YL and Berestyana Z**. Quarter of century since the Chornobyl accident: small es, Cyrillicancer risks in affected groups of population. *Probl Radiac Med Radiobiol* 19: 147-169, 2014.
327. **Qiu Y, Bevan H, Weeraperuma S, Wratting D, Murphy D, Neal CR, Bates DO and Harper SJ**. Mammary alveolar development during lactation is inhibited by the endogenous antiangiogenic growth factor isoform, VEGF165b. *FASEB J* 22: 1104-1112, 2008.
328. **Ramachandran BR, Gentles AB, Cox SB and Smith EE**. Age-dependent characterization of pendrin gene expression in various tissues of deer mice. *Comp Biochem Physiol B Biochem Mol Biol* 145: 338-345, 2006.
329. **Rankin EB and Giaccia AJ**. The role of hypoxia-inducible factors in tumorigenesis. *Cell Death Differ* 15: 678-685, 2008.
330. **Rappole CA, Mitra K and Wen H**. Dynamic fluorescence imaging of the free radical products of X-ray absorption in live cells. *Optical Nanoscopy* 1: 1-9, 2012.
331. **Ravanat JL, Di MP, Martinez GR and Medeiros MH**. Singlet oxygen induces oxidation of cellular DNA. *J Biol Chem* 276: 40601-40604, 2001.
332. **Ravi R, Mookerjee B, Bhujwalla ZM, Sutter CH, Artemov D, Zeng Q, Dillehay LE, Madan A, Semenza GL and Bedi A**. Regulation of tumor angiogenesis by p53-induced degradation of hypoxia-inducible factor 1alpha. *Genes Dev* 14: 34-44, 2000.
333. **Reeves EP, Nagl M, Godovac-Zimmermann J and Segal AW**. Reassessment of the microbicidal activity of reactive oxygen species and hypochlorous acid with reference to the phagocytic vacuole of the neutrophil granulocyte. *J Med Microbiol* 52: 643-651, 2003.
334. **Rhoden KJ, Cianchetta S, Duchi S and Romeo G**. Fluorescence quantitation of thyrocyte iodide accumulation with the yellow fluorescent protein variant YFP-H148Q/I152L. *Anal Biochem* 373: 239-246, 2008.
335. **Richardson DB**. Exposure to ionizing radiation in adulthood and thyroid cancer incidence. *Epidemiology* 20: 181-187, 2009.
336. **Richardson DB, Cardis E, Daniels RD, Gillies M, O'Hagan JA, Hamra GB, Haylock R, Laurier D, Leuraud K, Moissonnier M, Schubauer-Berigan MK, Thierry-Chef I and Kesminiene A**. Risk of cancer from occupational exposure to ionising radiation: retrospective cohort study of workers in France, the United Kingdom, and the United States (INWORKS). *BMJ* 351: h5359, 2015.
337. **Riedel C, Levy O and Carrasco N**. Post-transcriptional regulation of the sodium/iodide symporter by thyrotropin. *J Biol Chem* 276: 21458-21463, 2001.
338. **Rillema JA and Hill MA**. Pendrin transporter carries out iodide uptake into MCF-7 human mammary cancer cells. *Exp Biol Med (Maywood)* 228: 1078-1082, 2003.

339. **Rillema JA and Hill MA**. Prolactin regulation of the pendrin-iodide transporter in the mammary gland. *Am J Physiol Endocrinol Metab* 284: E25-E28, 2003.
340. **Rillema JA, Yu TX and Jhiang SM**. Effect of prolactin on sodium iodide symporter expression in mouse mammary gland explants. *Am J Physiol Endocrinol Metab* 279: E769-E772, 2000.
341. **Roepke TK, King EC, Reyna-Neyra A, Paroder M, Purtell K, Koba W, Fine E, Lerner DJ, Carrasco N and Abbott GW**. Kcne2 deletion uncovers its crucial role in thyroid hormone biosynthesis. *Nat Med* 15: 1186-1194, 2009.
342. **Ron E**. Cancer risks from medical radiation. *Health Phys* 85: 47-59, 2003.
343. **Ronckers CM, Doody MM, Lonstein JE, Stovall M and Land CE**. Multiple diagnostic X-rays for spine deformities and risk of breast cancer. *Cancer Epidemiol Biomarkers Prev* 17: 605-613, 2008.
344. **Ronckers CM, Land CE, Miller JS, Stovall M, Lonstein JE and Doody MM**. Cancer mortality among women frequently exposed to radiographic examinations for spinal disorders. *Radiat Res* 174: 83-90, 2010.
345. **Rosner H, Moller W, Groebner S and Torremante P**. Antiproliferative/cytotoxic effects of molecular iodine, povidone-iodine and Lugol's solution in different human carcinoma cell lines. *Oncol Lett* 12: 2159-2162, 2016.
346. **Rothkamm K and Lobrich M**. Evidence for a lack of DNA double-strand break repair in human cells exposed to very low x-ray doses. *Proc Natl Acad Sci U S A* 100: 5057-5062, 2003.
347. **Roux PP, Ballif BA, Anjum R, Gygi SP and Blenis J**. Tumor-promoting phorbol esters and activated Ras inactivate the tuberous sclerosis tumor suppressor complex via p90 ribosomal S6 kinase. *Proc Natl Acad Sci U S A* 101: 13489-13494, 2004.
348. **Ruiz M, Pettaway C, Song R, Stoeltzing O, Ellis L and Bar-Eli M**. Activator protein 2alpha inhibits tumorigenicity and represses vascular endothelial growth factor transcription in prostate cancer cells. *Cancer Res* 64: 631-638, 2004.
349. **Ruohola JK, Valve EM, Karkkainen MJ, Joukov V, Alitalo K and Harkonen PL**. Vascular endothelial growth factors are differentially regulated by steroid hormones and antiestrogens in breast cancer cells. *Mol Cell Endocrinol* 149: 29-40, 1999.
350. **Ryden L, Linderholm B, Nielsen NH, Emdin S, Jonsson PE and Landberg G**. Tumor specific VEGF-A and VEGFR2/KDR protein are co-expressed in breast cancer. *Breast Cancer Res Treat* 82: 147-154, 2003.
351. **Salomon RG, Hong L and Hollyfield JG**. Discovery of carboxyethylpyrroles (CEPs): critical insights into AMD, autism, cancer, and wound healing from basic research on the chemistry of oxidized phospholipids. *Chem Res Toxicol* 24: 1803-1816, 2011.
352. **Sancak Y, Peterson TR, Shaul YD, Lindquist RA, Thoreen CC, Bar-Peled L and Sabatini DM**. The Rag GTPases bind raptor and mediate amino acid signaling to mTORC1. *Science* 320: 1496-1501, 2008.
353. **Sang N, Stiehl DP, Bohensky J, Leshchinsky I, Srinivas V and Caro J**. MAPK signaling up-regulates the activity of hypoxia-inducible factors by its effects on p300. *J Biol Chem* 278: 14013-14019, 2003.
354. **Sarbassov DD, Ali SM, Kim DH, Guertin DA, Latek RR, Erdjument-Bromage H, Tempst P and Sabatini DM**. Rictor, a novel binding partner of mTOR, defines a

rapamycin-insensitive and raptor-independent pathway that regulates the cytoskeleton. *Curr Biol* 14: 1296-1302, 2004.

355. **Sarbassov DD, Ali SM, Sengupta S, Sheen JH, Hsu PP, Bagley AF, Markhard AL and Sabatini DM**. Prolonged rapamycin treatment inhibits mTORC2 assembly and Akt/PKB. *Mol Cell* 22: 159-168, 2006.
356. **Sarbassov DD, Guertin DA, Ali SM and Sabatini DM**. Phosphorylation and regulation of Akt/PKB by the rictor-mTOR complex. *Science* 307: 1098-1101, 2005.
357. **Savina A, Jancic C, Hugues S, Guermonprez P, Vargas P, Moura IC, Lennon-Dumenil AM, Seabra MC, Raposo G and Amigorena S**. NOX2 controls phagosomal pH to regulate antigen processing during crosspresentation by dendritic cells. *Cell* 126: 205-218, 2006.
358. **Schaafhausen MK, Yang WJ, Centanin L, Wittbrodt J, Bosserhoff A, Fischer A, Schartl M and Meierjohann S**. Tumor angiogenesis is caused by single melanoma cells in a manner dependent on reactive oxygen species and NF-kappaB. *J Cell Sci* 126: 3862-3872, 2013.
359. **Schafer G, Cramer T, Suske G, Kemmner W, Wiedenmann B and Hocker M**. Oxidative stress regulates vascular endothelial growth factor-A gene transcription through Sp1- and Sp3-dependent activation of two proximal GC-rich promoter elements. *J Biol Chem* 278: 8190-8198, 2003.
360. **Schieke SM, Phillips D, McCoy JP, Jr., Aponte AM, Shen RF, Balaban RS and Finkel T**. The mammalian target of rapamycin (mTOR) pathway regulates mitochondrial oxygen consumption and oxidative capacity. *J Biol Chem* 281: 27643-27652, 2006.
361. **Schrader M and Fahimi HD**. Peroxisomes and oxidative stress. *Biochim Biophys Acta* 1763: 1755-1766, 2006.
362. **Schreml S, Szeimies RM, Prantl L, Karrer S, Landthaler M and Babilas P**. Oxygen in acute and chronic wound healing. *Br J Dermatol* 163: 257-268, 2010.
363. **Scott BR, Belinsky SA, Leng S, Lin Y, Wilder JA and Damiani LA**. Radiation-stimulated epigenetic reprogramming of adaptive-response genes in the lung: an evolutionary gift for mounting adaptive protection against lung cancer. *Dose Response* 7: 104-131, 2009.
364. **Sebastiano Venturi**. **Evolutionary Significance of Iodine**. *Current Chemical Biology* 5: 2011.
365. **Senou M, Khalifa C, Thimmesch M, Jouret F, Devuyst O, Col V, Audinot JN, Lipnik P, Moreno JC, Van SJ, Dumont JE, Many MC, Colin IM and Gerard AC**. A coherent organization of differentiation proteins is required to maintain an appropriate thyroid function in the Pendred thyroid. *J Clin Endocrinol Metab* 95: 4021-4030, 2010.
366. **Serrano-Nascimento C, Calil-Silveira J and Nunes MT**. Posttranscriptional regulation of sodium-iodide symporter mRNA expression in the rat thyroid gland by acute iodide administration. *Am J Physiol Cell Physiol* 298: C893-C899, 2010.
367. **Seth I, Joiner MC and Tucker JD**. Cytogenetic low-dose hyperradiosensitivity is observed in human peripheral blood lymphocytes. *Int J Radiat Oncol Biol Phys* 91: 82-90, 2015.
368. **Settembre C, Zoncu R, Medina DL, Vetrini F, Erdin S, Erdin S, Huynh T, Ferron M, Karsenty G, Vellard MC, Facchinetti V, Sabatini DM and Ballabio A**. A lysosome-

to-nucleus signalling mechanism senses and regulates the lysosome via mTOR and TFEB. *EMBO J* 31: 1095-1108, 2012.

369. **Shah NM, Eskin BA, Krouse TB and Sparks CE**. Iodoprotein formation by rat mammary glands during pregnancy and early postpartum period. *Proc Soc Exp Biol Med* 181: 443-449, 1986.
370. **Shcheynikov N, Yang D, Wang Y, Zeng W, Karniski LP, So I, Wall SM and Muallem S**. The Slc26a4 transporter functions as an electroneutral Cl-/I-/. *J Physiol* 586: 3813-3824, 2008.
371. **Shi Q, Le X, Abbruzzese JL, Peng Z, Qian CN, Tang H, Xiong Q, Wang B, Li XC and Xie K**. Constitutive Sp1 activity is essential for differential constitutive expression of vascular endothelial growth factor in human pancreatic adenocarcinoma. *Cancer Res* 61: 4143-4154, 2001.
372. **Shima DT, Deutsch U and D'Amore PA**. Hypoxic induction of vascular endothelial growth factor (VEGF) in human epithelial cells is mediated by increases in mRNA stability. *FEBS Lett* 370: 203-208, 1995.
373. **Shor B, Wu J, Shakey Q, Toral-Barza L, Shi C, Follettie M and Yu K**. Requirement of the mTOR kinase for the regulation of Maf1 phosphorylation and control of RNA polymerase III-dependent transcription in cancer cells. *J Biol Chem* 285: 15380-15392, 2010.
374. **Shrivastava A, Tiwari M, Sinha RA, Kumar A, Balapure AK, Bajpai VK, Sharma R, Mitra K, Tandon A and Godbole MM**. Molecular iodine induces caspase-independent apoptosis in human breast carcinoma cells involving the mitochondria-mediated pathway. *J Biol Chem* 281: 19762-19771, 2006.
375. **Simic DV, Mimic-Oka J, Pljesa-Ercegovac M, Savic-Radojevic A, Opacic M, Matic D, Ivanovic B and Simic T**. Byproducts of oxidative protein damage and antioxidant enzyme activities in plasma of patients with different degrees of essential hypertension. *J Hum Hypertens* 20: 149-155, 2006.
376. **Simons M, Gordon E and Claesson-Welsh L**. Mechanisms and regulation of endothelial VEGF receptor signalling. *Nat Rev Mol Cell Biol* 17: 611-625, 2016.
377. **Sipkens JA, Hahn N, van den Brand CS, Meischl C, Cillessen SA, Smith DE, Juffermans LJ, Musters RJ, Roos D, Jakobs C, Blom HJ, Smulders YM, Krijnen PA, Stehouwer CD, Rauwerda JA, van Hinsbergh VW and Niessen HW**. Homocysteine-induced apoptosis in endothelial cells coincides with nuclear NOX2 and peri-nuclear NOX4 activity. *Cell Biochem Biophys* 67: 341-352, 2013.
378. **Smanik PA, Liu Q, Furminger TL, Ryu K, Xing S, Mazzaferri EL and Jhiang SM**. Cloning of the human sodium lodide symporter. *Biochem Biophys Res Commun* 226: 339-345, 1996.
379. **Smith-Bindman R, Lipson J, Marcus R, Kim KP, Mahesh M, Gould R, Berrington de GA and Miglioretti DL**. Radiation dose associated with common computed tomography examinations and the associated lifetime attributable risk of cancer. *Arch Intern Med* 169: 2078-2086, 2009.
380. **Smyth PP**. The thyroid, iodine and breast cancer. *Breast Cancer Res* 5: 235-238, 2003.

381. **Smyth PP, Smith DF, McDermott EW, Murray MJ, Geraghty JG and O'Higgins NJ**. A direct relationship between thyroid enlargement and breast cancer. *J Clin Endocrinol Metab* 81: 937-941, 1996.
382. **Soker S, Takashima S, Miao HQ, Neufeld G and Klagsbrun M**. Neuropilin-1 is expressed by endothelial and tumor cells as an isoform-specific receptor for vascular endothelial growth factor. *Cell* 92: 735-745, 1998.
383. **Soleimani M, Greeley T, Petrovic S, Wang Z, Amlal H, Kopp P and Burnham CE**. Pendrin: an apical Cl-/OH-/. *Am J Physiol Renal Physiol* 280: F356-F364, 2001.
384. **Sondell M, Lundborg G and Kanje M**. Vascular endothelial growth factor stimulates Schwann cell invasion and neovascularization of acellular nerve grafts. *Brain Res* 846: 219-228, 1999.
385. **Sonveaux P, Brouet A, Havaux X, Gregoire V, Dessy C, Balligand JL and Feron O**. Irradiation-induced angiogenesis through the up-regulation of the nitric oxide pathway: implications for tumor radiotherapy. *Cancer Res* 63: 1012-1019, 2003.
386. **Soriano O, Delgado G, Anguiano B, Petrosyan P, Molina-Servin ED, Gonsebatt ME and Aceves C**. Antineoplastic effect of iodine and iodide in dimethylbenz[a]anthracene-induced mammary tumors: association between lactoperoxidase and estrogen-adduct production. *Endocr Relat Cancer* 18: 529-539, 2011.
387. **Sorolla MA, Rodriguez-Colman MJ, Tamarit J, Ortega Z, Lucas JJ, Ferrer I, Ros J and Cabiscol E**. Protein oxidation in Huntington disease affects energy production and vitamin B6 metabolism. *Free Radic Biol Med* 49: 612-621, 2010.
388. **Spirig R, Djafarzadeh S, Regueira T, Shaw SG, von GC, Takala J, Jakob SM, Rieben R and Lepper PM**. Effects of TLR agonists on the hypoxia-regulated transcription factor HIF-1alpha and dendritic cell maturation under normoxic conditions. *PLoS One* 5: e0010983, 2010.
389. **Spitzweg C, Joba W, Schriever K, Goellner JR, Morris JC and Heufelder AE**. Analysis of human sodium iodide symporter immunoreactivity in human exocrine glands. *J Clin Endocrinol Metab* 84: 4178-4184, 1999.
390. **Stadel BV**. Dietary iodine and risk of breast, endometrial, and ovarian cancer. *Lancet* 1: 890-891, 1976.
391. **Starkov AA, Fiskum G, Chinopoulos C, Lorenzo BJ, Browne SE, Patel MS and Beal MF**. Mitochondrial alpha-ketoglutarate dehydrogenase complex generates reactive oxygen species. *J Neurosci* 24: 7779-7788, 2004.
392. Steinnes, E. Biogeochemical cycling of iodine and selenium and potential geomedical relevance. Food and Agriculture Organization of the United Nations . 2002.

Ref Type: Internet Communication

393. **Stoddard FR, Brooks AD, Eskin BA and Johannes GJ**. Iodine alters gene expression in the MCF7 breast cancer cell line: evidence for an anti-estrogen effect of iodine. *Int J Med Sci* 5: 189-196, 2008.
394. **Stoner M, Wormke M, Saville B, Samudio I, Qin C, Abdelrahim M and Safe S**. Estrogen regulation of vascular endothelial growth factor gene expression in ZR-75 breast cancer cells through interaction of estrogen receptor alpha and SP proteins. *Oncogene* 23: 1052-1063, 2004.

395. **Strodtbeck K, Sloan A, Rogers L, Fisher PG, Stearns D, Campbell L and Barnholtz-Sloan J**. Risk of subsequent cancer following a primary CNS tumor. *J Neurooncol* 112: 285-295, 2013.
396. **Strum JM**. Effect of iodide-deficiency on rat mammary gland. *Virchows Arch B Cell Pathol Incl Mol Pathol* 30: 209-220, 1979.
397. **Sullivan LA and Brekken RA**. The VEGF family in cancer and antibody-based strategies for their inhibition. *MAbs* 2: 165-175, 2010.
398. **Suman S, Johnson MD, Fornace AJ, Jr. and Datta K**. Exposure to ionizing radiation causes long-term increase in serum estradiol and activation of PI3K-Akt signaling pathway in mouse mammary gland. *Int J Radiat Oncol Biol Phys* 84: 500-507, 2012.
399. **Sutter CW, Masilungan BG and Stadalnik RC**. False-positive results of I-131 whole-body scans in patients with thyroid cancer. *Semin Nucl Med* 25: 279-282, 1995.
400. **Syrigos KN, Konstantoulakis MM, Constantoulakis M, Marafelia P, Koutras D and Golematis BC**. Thyroid autoantibodies and thyroid function in patients with gastric cancer. *Acta Oncol* 33: 905-907, 1994.
401. **Szatrowski TP and Nathan CF**. Production of large amounts of hydrogen peroxide by human tumor cells. *Cancer Res* 51: 794-798, 1991.
402. **Taghian A, Ramsay J, Allalunis-Turner J, Budach W, Gioioso D, Pardo F, Okunieff P, Bleehen N, Urtasun R and Suit H**. Intrinsic radiation sensitivity may not be the major determinant of the poor clinical outcome of glioblastoma multiforme. *Int J Radiat Oncol Biol Phys* 25: 243-249, 1993.
403. **Takahashi A, Kureishi Y, Yang J, Luo Z, Guo K, Mukhopadhyay D, Ivashchenko Y, Branellec D and Walsh K**. Myogenic Akt signaling regulates blood vessel recruitment during myofiber growth. *Mol Cell Biol* 22: 4803-4814, 2002.
404. **Takahashi Y, Teshima T, Kawaguchi N, Hamada Y, Mori S, Madachi A, Ikeda S, Mizuno H, Ogata T, Nojima K, Furusawa Y and Matsuura N**. Heavy ion irradiation inhibits in vitro angiogenesis even at sublethal dose. *Cancer Res* 63: 4253-4257, 2003.
405. **Taki K, Kogai T, Kanamoto Y, Hershman JM and Brent GA**. A thyroid-specific far-upstream enhancer in the human sodium/iodide symporter gene requires Pax-8 binding and cyclic adenosine 3',5'-monophosphate response element-like sequence binding proteins for full activity and is differentially regulated in normal and thyroid cancer cells. *Mol Endocrinol* 16: 2266-2282, 2002.
406. **Tazebay UH, Wapnir IL, Levy O, Dohan O, Zuckier LS, Zhao QH, Deng HF, Amenta PS, Fineberg S, Pestell RG and Carrasco N**. The mammary gland iodide transporter is expressed during lactation and in breast cancer. *Nat Med* 6: 871-878, 2000.
407. **Teas J, Harbison ML and Gelman RS**. Dietary seaweed (Laminaria) and mammary carcinogenesis in rats. *Cancer Res* 44: 2758-2761, 1984.
408. **Tee AR, Manning BD, Roux PP, Cantley LC and Blenis J**. Tuberous sclerosis complex gene products, Tuberin and Hamartin, control mTOR signaling by acting as a GTPase-activating protein complex toward Rheb. *Curr Biol* 13: 1259-1268, 2003.
409. **Thomas DD, Ridnour LA, Isenberg JS, Flores-Santana W, Switzer CH, Donzelli S, Hussain P, Vecoli C, Paolocci N, Ambs S, Colton CA, Harris CC, Roberts DD and Wink DA**. The chemical biology of nitric oxide: implications in cellular signaling. *Free Radic Biol Med* 45: 18-31, 2008.

410. **Thoreen CC, Kang SA, Chang JW, Liu Q, Zhang J, Gao Y, Reichling LJ, Sim T, Sabatini DM and Gray NS**. An ATP-competitive mammalian target of rapamycin inhibitor reveals rapamycin-resistant functions of mTORC1. *J Biol Chem* 284: 8023-8032, 2009.
411. **Timoshenko AV, Rastogi S and Lala PK**. Migration-promoting role of VEGF-C and VEGF-C binding receptors in human breast cancer cells. *Br J Cancer* 97: 1090-1098, 2007.
412. **Tobar N, Guerrero J, Smith PC and Martinez J**. NOX4-dependent ROS production by stromal mammary cells modulates epithelial MCF-7 cell migration. *Br J Cancer* 103: 1040-1047, 2010.
413. **Tojo T, Ushio-Fukai M, Yamaoka-Tojo M, Ikeda S, Patrushev N and Alexander RW**. Role of gp91phox (Nox2)-containing NAD(P)H oxidase in angiogenesis in response to hindlimb ischemia. *Circulation* 111: 2347-2355, 2005.
414. **Tonorezos ES, Barnea D, Moskowitz CS, Chou JF, Sklar CA, Elkin EB, Wong RJ, Li D, Tuttle RM, Korenstein D, Wolden SL and Oeffinger KC**. Screening for thyroid cancer in survivors of childhood and young adult cancer treated with neck radiation. *J Cancer Surviv* 11: 302-308, 2017.
415. **Treins C, Giorgetti-Peraldi S, Murdaca J, Semenza GL and Van OE**. Insulin stimulates hypoxia-inducible factor 1 through a phosphatidylinositol 3-kinase/target of rapamycin-dependent signaling pathway. *J Biol Chem* 277: 27975-27981, 2002.
416. **Tschugguel W, Schneeberger C, Unfried G, Czerwenka K, Weninger W, Mildner M, Gruber DM, Sator MO, Waldhor T and Huber JC**. Expression of inducible nitric oxide synthase in human breast cancer depends on tumor grade. *Breast Cancer Res Treat* 56: 145-151, 1999.
417. **Turken O, Narln Y, Demlrbas S, Onde ME, Sayan O, Kandemlr EG, Yaylacl M and Ozturk A**. Breast cancer in association with thyroid disorders. *Breast Cancer Res* 5: R110-R113, 2003.
418. University of California. Chemistry, LibreTexts Libraries, Halide ions as reducing agents. 2018.

Ref Type: Online Source

419. University of Michigan. Michigan Histology and Virtual Microscopy Learning Resources. 2017.

Ref Type: Audiovisual Material

420. **Uyttersprot N, Pelgrims N, Carrasco N, Gervy C, Maenhaut C, Dumont JE and Miot F**. Moderate doses of iodide in vivo inhibit cell proliferation and the expression of thyroperoxidase and Na+/I- symporter mRNAs in dog thyroid. *Mol Cell Endocrinol* 131: 195-203, 1997.
421. **Vadysirisack DD, Chen ES, Zhang Z, Tsai MD, Chang GD and Jhiang SM**. Identification of in vivo phosphorylation sites and their functional significance in the sodium iodide symporter. *J Biol Chem* 282: 36820-36828, 2007.
422. **Vaiserman AM**. Radiation hormesis: historical perspective and implications for low-dose cancer risk assessment. *Dose Response* 8: 172-191, 2010.
423. **Vala I, Martins LR, Imaizumi N, Nunes RJ, Rino J, Kuonen F, Carvalho LM, Ruegg C, Grillo IM, Barata JT, Mareel M and Santos SC**. Low doses of ionizing radiation

promote tumor growth and metastasis by enhancing angiogenesis. *PLoS One* 5: e11222, 2010.

424. **van den Hove MF, Croizet-Berger K, Jouret F, Guggino SE, Guggino WB, Devuyst O and Courtoy PJ**. The loss of the chloride channel, ClC-5, delays apical iodide efflux and induces a euthyroid goiter in the mouse thyroid gland. *Endocrinology* 147: 1287-1296, 2006.
425. **van der Kogel A**. *Basic Clinical Radiobiology*. London: Hodder Arnold, Hachette, 2009,
426. Vanderstraeten, J., Derradji, H., Sonveaux, P., Colin, I. M., Many, M. C., and Gerard, A. C. Acute iodine deficiency induces a transient VEGF dependent microvascular response in mammary glands involving HIF-1, ROS and mTOR. 2017.

Ref Type: Unpublished Work

427. **Vandevijvere S, Amsalkhir S, Mourri AB, Van OH and Moreno-Reyes R**. Iodine deficiency among Belgian pregnant women not fully corrected by iodine-containing multivitamins: a national cross-sectional survey. *Br J Nutr* 109: 2276-2284, 2013.
428. **Vandevijvere S, Mourri AB, Amsalkhir S, Avni F, Van OH and Moreno-Reyes R**. Fortification of bread with iodized salt corrected iodine deficiency in school-aged children, but not in their mothers: a national cross-sectional survey in Belgium. *Thyroid* 22: 1046-1053, 2012.
429. **VanKlompenberg MK, Manjarin R, Donovan CE, Trott JF and Hovey RC**. Regulation and localization of vascular endothelial growth factor within the mammary glands during the transition from late gestation to lactation. *Domest Anim Endocrinol* 54: 37-47, 2016.
430. **Vayre L, Sabourin JC, Caillou B, Ducreux M, Schlumberger M and Bidart JM**. Immunohistochemical analysis of Na+/I- symporter distribution in human extra-thyroidal tissues. *Eur J Endocrinol* 141: 382-386, 1999.
431. **Velu CS, Niture SK, Doneanu CE, Pattabiraman N and Srivenugopal KS**. Human p53 is inhibited by glutathionylation of cysteines present in the proximal DNA-binding domain during oxidative stress. *Biochemistry* 46: 7765-7780, 2007.
432. **Venturi S**. Is there a role for iodine in breast diseases? *Breast* 10: 379-382, 2001.
433. **Venturi S, Donati FM, Venturi A, Venturi M, Grossi L and Guidi A**. Role of iodine in evolution and carcinogenesis of thyroid, breast and stomach. *Adv Clin Path* 4: 11-17, 2000.
434. **Venturi S and Venturi M**. Evolution of Dietary Antioxidant Defences. *European Epi-Marker* 11: 1-12, 2007.
435. **Venturi S and Venturi M**. Iodide, thyroid and stomach carcinogenesis: evolutionary story of a primitive antioxidant? *Eur J Endocrinol* 140: 371-372, 1999.
436. **Venturi S and Venturi M**. Iodine in evolution of salivary glands and in oral health. *Nutr Health* 20: 119-134, 2009.
437. **Viglietto G, Romano A, Manzo G, Chiappetta G, Paoletti I, Califano D, Galati MG, Mauriello V, Bruni P, Lago CT, Fusco A and Persico MG**. Upregulation of the angiogenic factors PlGF, VEGF and their receptors (Flt-1, Flk-1/KDR) by TSH in cultured thyrocytes and in the thyroid gland of thiouracil-fed rats suggest a TSH-

dependent paracrine mechanism for goiter hypervascularization. *Oncogene* 15: 2687-2698, 1997.

438. **Vivanco M, Dalle JH, Alberti C, Lescoeur B, Yakouben K, Carel JC, Baruchel A and Leger J**. Malignant and benign thyroid nodules after total body irradiation preceding hematopoietic cell transplantation during childhood. *Eur J Endocrinol* 167: 225-233, 2012.
439. **Vlaminck B, Toffoli S, Ghislain B, Demazy C, Raes M and Michiels C**. Dual effect of echinomycin on hypoxia-inducible factor-1 activity under normoxic and hypoxic conditions. *FEBS J* 274: 5533-5542, 2007.
440. **Vleugel MM, Greijer AE, Shvarts A, van der Groep P, van BM, Aarbodem Y, van TH, Harris AL, van Diest PJ and van der Wall E**. Differential prognostic impact of hypoxia induced and diffuse HIF-1alpha expression in invasive breast cancer. *J Clin Pathol* 58: 172-177, 2005.
441. **Waltenberger J, Claesson-Welsh L, Siegbahn A, Shibuya M and Heldin CH**. Different signal transduction properties of KDR and Flt1, two receptors for vascular endothelial growth factor. *J Biol Chem* 269: 26988-26995, 1994.
442. **Wang F, Liu S, Xi S, Yan L, Wang H, Song Y and Sun G**. Arsenic induces the expressions of angiogenesis-related factors through PI3K and MAPK pathways in SV-HUC-1 human uroepithelial cells. *Toxicol Lett* 222: 303-311, 2013.
443. **Wang H and Keiser JA**. Vascular endothelial growth factor upregulates the expression of matrix metalloproteinases in vascular smooth muscle cells: role of flt-1. *Circ Res* 83: 832-840, 1998.
444. **Wang L, Harris TE, Roth RA and Lawrence JC, Jr.** PRAS40 regulates mTORC1 kinase activity by functioning as a direct inhibitor of substrate binding. *J Biol Chem* 282: 20036-20044, 2007.
445. **Wang S, Li X, Parra M, Verdin E, Bassel-Duby R and Olson EN**. Control of endothelial cell proliferation and migration by VEGF signaling to histone deacetylase 7. *Proc Natl Acad Sci U S A* 105: 7738-7743, 2008.
446. **Wang Y, Zang QS, Liu Z, Wu Q, Maass D, Dulan G, Shaul PW, Melito L, Frantz DE, Kilgore JA, Williams NS, Terada LS and Nwariaku FE**. Regulation of VEGF-induced endothelial cell migration by mitochondrial reactive oxygen species. *Am J Physiol Cell Physiol* 301: C695-C704, 2011.
447. **Wapnir IL, Goris M, Yudd A, Dohan O, Adelman D, Nowels K and Carrasco N**. The Na+/I- symporter mediates iodide uptake in breast cancer metastases and can be selectively down-regulated in the thyroid. *Clin Cancer Res* 10: 4294-4302, 2004.
448. **West XZ, Malinin NL, Merkulova AA, Tischenko M, Kerr BA, Borden EC, Podrez EA, Salomon RG and Byzova TV**. Oxidative stress induces angiogenesis by activating TLR2 with novel endogenous ligands. *Nature* 467: 972-976, 2010.
449. **Weyemi U, Redon CE, Aziz T, Choudhuri R, Maeda D, Parekh PR, Bonner MY, Arbiser JL and Bonner WM**. Inactivation of NADPH oxidases NOX4 and NOX5 protects human primary fibroblasts from ionizing radiation-induced DNA damage. *Radiat Res* 183: 262-270, 2015.
450. **Wijkstrom-Frei C, El-Chemaly S, Ali-Rachedi R, Gerson C, Cobas MA, Forteza R, Salathe M and Conner GE**. Lactoperoxidase and human airway host defense. *Am J Respir Cell Mol Biol* 29: 206-212, 2003.

451. **Winkler R**. Iodine—A Potential Antioxidant and the Role of Iodine/Iodide in Health and Disease. *Natural Science* 7: 548-557, 2015.
452. **Winkler R, Griebenow S and Wonisch W**. Effect of iodide on total antioxidant status of human serum. *Cell Biochem Funct* 18: 143-146, 2000.
453. **Winterbourn CC and Kettle AJ**. Biomarkers of myeloperoxidase-derived hypochlorous acid. *Free Radic Biol Med* 29: 403-409, 2000.
454. **Woolard J, Bevan HS, Harper SJ and Bates DO**. Molecular diversity of VEGF-A as a regulator of its biological activity. *Microcirculation* 16: 572-592, 2009.
455. **Woolard J, Wang WY, Bevan HS, Qiu Y, Morbidelli L, Pritchard-Jones RO, Cui TG, Sugiono M, Waine E, Perrin R, Foster R, Digby-Bell J, Shields JD, Whittles CE, Mushens RE, Gillatt DA, Ziche M, Harper SJ and Bates DO**. VEGF165b, an inhibitory vascular endothelial growth factor splice variant: mechanism of action, in vivo effect on angiogenesis and endogenous protein expression. *Cancer Res* 64: 7822-7835, 2004.
456. **World Health Organization**. Iodine status worldwide
WHO Global Database on Iodine Deficiency. *IDD newsletter* 2004.
457. **World Health Organization**. Global Scorecard of Iodine Nutrition 2014-2015. *IDD newsletter* 2016.
458. **Wu J, Brandt S and Hyder SM**. Ligand- and cell-specific effects of signal transduction pathway inhibitors on progestin-induced vascular endothelial growth factor levels in human breast cancer cells. *Mol Endocrinol* 19: 312-326, 2005.
459. **Xu T, Zong Y, Peng L, Kong S, Zhou M, Zou J, Liu J, Miao R, Sun X and Li L**. Overexpression of eIF4E in colorectal cancer patients is associated with liver metastasis. *Onco Targets Ther* 9: 815-822, 2016.
460. **Yamamori T, Yasui H, Yamazumi M, Wada Y, Nakamura Y, Nakamura H and Inanami O**. Ionizing radiation induces mitochondrial reactive oxygen species production accompanied by upregulation of mitochondrial electron transport chain function and mitochondrial content under control of the cell cycle checkpoint. *Free Radic Biol Med* 53: 260-270, 2012.
461. **Yang H, Jager MJ and Grossniklaus HE**. Bevacizumab suppression of establishment of micrometastases in experimental ocular melanoma. *Invest Ophthalmol Vis Sci* 51: 2835-2842, 2010.
462. **Yen L, Benlimame N, Nie ZR, Xiao D, Wang T, Al Moustafa AE, Esumi H, Milanini J, Hynes NE, Pages G and Alaoui-Jamali MA**. Differential regulation of tumor angiogenesis by distinct ErbB homo- and heterodimers. *Mol Biol Cell* 13: 4029-4044, 2002.
463. **Yip CK, Murata K, Walz T, Sabatini DM and Kang SA**. Structure of the human mTOR complex I and its implications for rapamycin inhibition. *Mol Cell* 38: 768-774, 2010.
464. **Yoshida T, Goto S, Kawakatsu M, Urata Y and Li TS**. Mitochondrial dysfunction, a probable cause of persistent oxidative stress after exposure to ionizing radiation. *Free Radic Res* 46: 147-153, 2012.
465. **Yoshimura M, Itasaka S, Harada H and Hiraoka M**. Microenvironment and radiation therapy. *Biomed Res Int* 2013: 685308, 2013.

466. **Yoshinaga S, Mabuchi K, Sigurdson AJ, Doody MM and Ron E**. Cancer risks among radiologists and radiologic technologists: review of epidemiologic studies. *Radiology* 233: 313-321, 2004.
467. **Youson JH and Sower SA**. Theory on the evolutionary history of lamprey metamorphosis: role of reproductive and thyroid axes. *Comp Biochem Physiol B Biochem Mol Biol* 129: 337-345, 2001.
468. **Yu H, Mohan S and Natarajan M**. Radiation-Triggered NF-kappaB Activation is Responsible for the Angiogenic Signaling Pathway and Neovascularization for Breast Cancer Cell Proliferation and Growth. *Breast Cancer (Auckl)* 6: 125-135, 2012.
469. **Yuan L, Moyon D, Pardanaud L, Breant C, Karkkainen MJ, Alitalo K and Eichmann A**. Abnormal lymphatic vessel development in neuropilin 2 mutant mice. *Development* 129: 4797-4806, 2002.
470. **Zablotska LB, Nadyrov EA, Polyanskaya ON, McConnell RJ, O'Kane P, Lubin J, Hatch M, Little MP, Brenner AV, Veyalkin IV, Yauseyenka VV, Bouville A, Drozdovitch VV, Minenko VF, Demidchik YE, Mabuchi K and Rozhko AV**. Risk of thyroid follicular adenoma among children and adolescents in Belarus exposed to iodine-131 after the Chornobyl accident. *Am J Epidemiol* 182: 781-790, 2015.
471. **Zeeshan HM, Lee GH, Kim HR and Chae HJ**. Endoplasmic Reticulum Stress and Associated ROS. *Int J Mol Sci* 17: 327, 2016.
472. **Zhang F, Lau SS and Monks TJ**. The cytoprotective effect of N-acetyl-L-cysteine against ROS-induced cytotoxicity is independent of its ability to enhance glutathione synthesis. *Toxicol Sci* 120: 87-97, 2011.
473. **Zhang YW, Su Y, Volpert OV and Vande Woude GF**. Hepatocyte growth factor/scatter factor mediates angiogenesis through positive VEGF and negative thrombospondin 1 regulation. *Proc Natl Acad Sci U S A* 100: 12718-12723, 2003.
474. **Zhao Y, Hu X, Liu Y, Dong S, Wen Z, He W, Zhang S, Huang Q and Shi M**. ROS signaling under metabolic stress: cross-talk between AMPK and AKT pathway. *Mol Cancer* 16: 79, 2017.
475. **Zhou C, Ziegler C, Birder LA, Stewart AF and Levitan ES**. Angiotensin II and stretch activate NADPH oxidase to destabilize cardiac Kv4.3 channel mRNA. *Circ Res* 98: 1040-1047, 2006.
476. **Ziegler RG, Hoover RN, Pike MC, Hildesheim A, Nomura AM, West DW, Wu-Williams AH, Kolonel LN, Horn-Ross PL, Rosenthal JF and Hyer MB**. Migration patterns and breast cancer risk in Asian-American women. *J Natl Cancer Inst* 85: 1819-1827, 1993.
477. **Zimmermann MB**. Iodine deficiency. *Endocr Rev* 30: 376-408, 2009.
478. **Mauro Costa-Mattioli & Lisa M Monteggia**. mTOR complexes in neurodevelopmental and neuropsychiatric disorders. Nature Neuroscience, 16: 1537–1543, 2013
479. **Anzai K, Ban N, Ozawa T, Tokonami S.** Fukushima Daiichi Nuclear Power Plant accident: facts, environmental contamination, possible biological effects, and countermeasures, J Clin Biochem Nutr. 50(1):2-8, 2012
480. **Sheue-Yann Cheng, Jack L. Leonard, and Paul J. Davis.** Molecular Aspects of Thyroid Hormone Actions. Endocr Rev. 31(2): 139–170, 2010